Discrete Dynamics in Nature and Society

Differential Games and Discrete Dynamics in Applied Sciences

Guest Editors: Massimiliano Ferrara, Gafurjan Ibragimov, and Vincenzo Scalzo

Differential Games and Discrete Dynamics in Applied Sciences

Discrete Dynamics in Nature and Society

Differential Games and Discrete Dynamics in Applied Sciences

Guest Editors: Massimiliano Ferrara, Gafurjan Ibragimov, and Vincenzo Scalzo

Copyright © 2017 Hindawi Publishing Corporation. All rights reserved.

This is a special issue published in "Discrete Dynamics in Nature and Society." All articles are open access articles distributed under the Creative Commons Attribution License, which permits unrestricted use, distribution, and reproduction in any medium, provided the original work is properly cited.

Editorial Board

Douglas R. Anderson, USA
David Arroyo, Spain
Viktor Avrutin, Germany
Stefan Balint, Romania
Kamel Barkaoui, France
Gian I. Bischi, Italy
Gabriele Bonanno, Italy
Driss Boutat, France
Gabriella Bretti, Italy
Filippo Cacace, Italy
Pasquale Candito, Italy
Cengiz Çinar, Turkey
Carmen Coll, Spain
Alicia Cordero, Spain
Daniel Czamanski, Israel
Richard H. Day, USA
Manuel De la Sen, Spain
Luisa Di Paola, Italy
Josef Diblik, Czech Republic
Xiaohua Ding, China
Adam Doliwa, Poland
Elmetwally Elabbasy, Egypt
Hassan A. El-Morshedy, Egypt
Jacques Ferland, Canada
Daniele Fournier-Prunaret, France
Ciprian G. Gal, USA
Gisèle R Goldstein, USA
Vladimir Gontar, Israel
Chris Goodrich, USA
Pilar R. Gordoa, Spain
Kannan Govindan, Denmark
Luca Guerrini, Italy
Giuseppe Izzo, Italy
Sarangapani Jagannathan, USA
Jun Ji, USA
Nikos I. Karachalios, Greece
Eric R. Kaufmann, USA
Victor S. Kozyakin, Russia
Mustafa Kulenović, USA
Jürgen Kurths, Germany
Kousuke Kuto, Japan
Aihua Li, USA
Xiaohui Liu, UK
Jean J. Loiseau, France
Miguel Ángel López, Spain
Ricardo López-Ruiz, Spain
Agustin Martin, Spain
Akio Matsumoto, Japan
Rigoberto Medina, Chile
Vicenç Méndez, Spain
Eleonora Messina, Italy
Ahmad Naimzada, Italy
G. Papashinopoulos, Greece
Juan Pavón, Spain
Allan C. Peterson, USA
Giuseppe Piccardo, Italy
Andrew Pickering, Spain
Chuanxi Qian, USA
Morteza Rafei, Netherlands
Mustapha A. Rami, Spain
Aura Reggiani, Italy
Pavel Rehak, Czech Republic
Paolo Renna, Italy
Marko Robnik, Slovenia
Yuriy Rogovchenko, Norway
Silvia Romanelli, Italy
Leonid Shaikhet, Ukraine
Seenith Sivasundaram, USA
C. Skokos, South Africa
Piergiulio Tempesta, Spain
Tetsuji Tokihiro, Japan
J. R. Torregrosa, Spain
Delfim F. M. Torres, Portugal
Firdaus Udwadia, USA
Antonia Vecchio, Italy
F. R. Villatoro, Spain
Hubertus Von Bremen, USA
Bixiang Wang, USA
Abdul-Aziz Yakubu, USA
Ibrahim Yalcinkaya, Turkey
Bo Yang, USA
Necmettin Yildirim, USA
Guang Zhang, China
Zhengqiu Zhang, China
Lu Zhen, China
Yong Zhou, China
Zhan Zhou, China
Zuonong Zhu, China

Contents

Differential Games and Discrete Dynamics in Applied Sciences
Massimiliano Ferrara, Gafurjan Ibragimov, and Vincenzo Scalzo
Volume 2017, Article ID 6023140, 3 pages

Numerical Approach Based on Two-Dimensional Fractional-Order Legendre Functions for Solving Fractional Differential Equations
Qingxue Huang, Fuqiang Zhao, Jiaquan Xie, Lifeng Ma, Jianmei Wang, and Yugui Li
Volume 2017, Article ID 8630895, 12 pages

New JLS-Factor Model versus the Standard JLS Model: A Case Study on Chinese Stock Bubbles
Zongyi Hu and Chao Li
Volume 2017, Article ID 8017510, 15 pages

Worst-Case Investment and Reinsurance Optimization for an Insurer under Model Uncertainty
Xiangbo Meng, Ximin Rong, Lidong Zhang, and Ziping Du
Volume 2016, Article ID 9693419, 8 pages

Dynamical Analysis of a Computer Virus Model with Delays
Juan Liu, Carlo Bianca, and Luca Guerrini
Volume 2016, Article ID 5649584, 21 pages

A Note on Discrete Multitime Recurrences of Samuelson-Hicks Type
Bruno Antonio Pansera and Francesco Strati
Volume 2016, Article ID 6891302, 4 pages

Topological Entropy of One Type of Nonoriented Lorenz-Type Maps
Guo Feng
Volume 2016, Article ID 6987471, 5 pages

Linear Pursuit Differential Game under Phase Constraint on the State of Evader
Askar Rakhmanov, Gafurjan Ibragimov, and Massimiliano Ferrara
Volume 2016, Article ID 1289456, 6 pages

Dynamic Complexities in 2-Dimensional Discrete-Time Predator-Prey Systems with Allee Effect in the Prey
Jie Yan, Chunli Li, Xueli Chen, and Lishun Ren
Volume 2016, Article ID 4275372, 14 pages

Existence of Nonoscillatory Solutions of Higher-Order Neutral Differential Equations with Distributed Coefficients and Delays
Youjun Liu, Huanhuan Zhao, and Jurang Yan
Volume 2016, Article ID 1026726, 7 pages

Simple Motion Pursuit and Evasion Differential Games with Many Pursuers on Manifolds with Euclidean Metric
Atamurat Kuchkarov, Gafurjan Ibragimov, and Massimiliano Ferrara
Volume 2016, Article ID 1386242, 8 pages

Modeling and Nonlinear Response of the Cam-Follower Oblique-Impact System
Yong-Feng Yang, Yu Lu, Ting-Dong Jiang, and Na Lu
Volume 2016, Article ID 6142501, 8 pages

Risk-Averse Evolutionary Game Model of Aviation Joint Emergency Response
Wei Pan, Ying Guo, and Shujie Liao
Volume 2016, Article ID 9031351, 8 pages

Hindawi Publishing Corporation
Discrete Dynamics in Nature and Society
Volume 2017, Article ID 6023140, 3 pages
http://dx.doi.org/10.1155/2017/6023140

Editorial
Differential Games and Discrete Dynamics in Applied Sciences

Massimiliano Ferrara,[1,2] Gafurjan Ibragimov,[3] and Vincenzo Scalzo[4]

[1] *Department of Law and Economics, University Mediterranea of Reggio Calabria, Via dei Bianchi 2, Palazzo Zani, 89127 Reggio Calabria, Italy*
[2] *The Invernizzi Centre for Research in Innovation, Organization, Strategy and Entrepreneurship (ICRIOS), Bocconi University, Via Sarfatti 25, 20136 Milan, Italy*
[3] *INSPEM and Department of Mathematics, Faculty of Science, Universiti Putra Malaysia, 43400 Serdang, Selangor, Malaysia*
[4] *Department of Economics and Statistics, University of Naples Federico II, Complesso Monte S. Angelo, Via Cintia, 80126 Naples, Italy*

Correspondence should be addressed to Massimiliano Ferrara; massimiliano.ferrara@unirc.it

Received 29 December 2016; Accepted 4 January 2017; Published 24 January 2017

Copyright © 2017 Massimiliano Ferrara et al. This is an open access article distributed under the Creative Commons Attribution License, which permits unrestricted use, distribution, and reproduction in any medium, provided the original work is properly cited.

In many scientific fields, differential games are problems related to the analysis of conflict and strategical interactions in the model of a dynamical system. In particular, in a pursuit-evasion game, one or more pursuers try to capture one or more evaders that try to avoid capture. Contests of pursuit and evasion are among the most widespread, challenging, and important optimization problems that confront mobile agents. But dynamic, stochastic, continuous-space, continuous-time, or discrete-time discrete-space games are usually difficult to handle. Agents that pursue or evade must maintain complex sensory-motor coordination with respect to both a physical environment and a hostile opponent. Because of its extensive applications, such as searching buildings for intruders, traffic control, military strategy, surgical operation, and industrial management, a lot of research has been developed in various directions during the last three decades, not only for that concerns the specific fields of application. In time of these methods, related mathematical tools and models have been intensively studied focusing on all the aspects concerning "dynamics" in a broad sense. In compliance of this aim, by this special issue, we have been interested in articles that explored various aspects of differentiable games and also in dynamics models. This editorial provides a brief review of some concepts related to the subject of the papers published in this *collectanea* devoted to the onset of differential games and discrete dynamics with applications to various branches of research. "Dynamics" is currently an active and fashionable discipline that is having a profound effect on a wide variety of fields, including engineering, physics, biology, economics, finance, and social sciences.

By the present work we are going to present some selected papers which analyze various aspects and applications fall in the "dynamics" following a "discrete" mathematical approach.

The paper entitled "Linear Pursuit Differential Game under Phase Constraint on the State of Evader" by M. Ferrara et al. deals with the linear pursuit differential games where pursuit control is subjected to integral constraints and evasion control is subjected to geometric constraint, with phase constraint being imposed on the state of the evader. For such constraints on controls of players, to obtain solution of pursuit problem for all initial states of phase space is complicated because of boundedness of pursuit resources. By this work, the following technique is proposed to control the phase vector of the pursuer: first-phase vector of the pursuer is brought to a given bounded, convex set, regardless of the behavior of evading player and then, using the evasion control and initial positions of the players, the pursuit control that ensures the completion of pursuit is constructed.

In "Simple Motion Pursuit and Evasion Differential Games with Many Pursuers on Manifolds with Euclidean Metric," M. Ferrara et al. consider pursuit and evasion differential games of a group of pursuers and one evader on manifolds with Euclidean metric. The authors establish that each of the differential games (pursuit or evasion) is equivalent to a differential game of groups of countably many pursuers and one group of countably many evaders in Euclidean space. All the players in any of these groups are

controlled by one controlled parameter. It has been found a condition under which pursuit can be completed, and if this condition is not satisfied, then evasion is possible. Some strategies for the pursuers in pursuit game which ensure completion of the game for a finite time have been given. In the specific case of evasion game, it was given a strategy for the evader.

By the paper entitled "New JLS-Factor Model versus the Standard JLS Model: A Case Study on Chinese Stock Bubbles" Z. Hu and C. Li extend the *Johansen-Ledoit-Sornette* (JLS) model by introducing fundamental economic factors in China (including the interest rate and deposit reserve rate) and the historical volatilities of targeted and US equity indices into the original model, which is a flexible tool to detect bubbles and predict regime changes in financial markets. A general method has been introduced to incorporate these selected factors in addition to the log-periodic power law signature of herding and compare the prediction accuracy of the critical time between the original and the new JLS models (termed the JLS-factor model) by applying these two models to fit two well-known Chinese stock indices in three bubble periods. The results showed that the JLS-factor model with Chinese characteristics successfully depicts the evolutions of bubbles and "antibubbles" as well as constructs efficient end-of-bubble signals for all bubbles in Chinese stock markets. In addition, the results of standard statistical tests demonstrate the excellent explanatory power of these additive factors and confirm that the new JLS model provides useful improvements over the standard JLS model.

X. Meng et al. in the work entitled "Worst-Case Investment and Reinsurance Optimization for an Insurer under Model Uncertainty" study optimal investment-reinsurance strategies for an insurer who faces model uncertainty. The insurer is allowed to acquire new business and invest into a financial market which consists of one risk-free asset and one risky asset whose price process is modeled by a geometric Brownian motion. Minimizing the expected quadratic distance of the terminal wealth to a given benchmark under the "worst-case" scenario, the authors obtain the closed-form expressions of optimal strategies and the corresponding value function by solving the Hamilton-Jacobi-Bellman (HJB) equation. Numerical examples have been presented to show the impact of model parameters on the optimal strategies.

In "Numerical Approach Based on Two-Dimensional Fractional-Order Legendre Functions for Solving Fractional Differential Equations" a robust numerical approach is proposed to obtain the numerical solution of some fractional differential equations. The principal characteristic of the approach proposed by F. Zhao et al. was the new orthogonal functions based on shifted Legendre polynomials to the fractional calculus. Also the fractional differential operational matrix is driven. Then the matrix with the "Tau method" is utilized to transform this problem into a system of linear algebraic equations. By solving the linear algebraic equations, the numerical solution is obtained. The approach is tested via some examples. It is shown that the FLFs yield better results. Finally, error analysis shows that the algorithm is convergent.

In "Dynamical Analysis of a Computer Virus Model with Delays," J. Liu et al. have proposed an SIQR computer virus model with two delays. The linear stability conditions are obtained by using characteristic root method and the developed asymptotic analysis shows the onset of a Hopf bifurcation occurs when the delay parameter reaches a critical value. Moreover the direction of the Hopf bifurcation and stability of the bifurcating period solutions are investigated by using the normal form theory and the center manifold theorem. Finally, numerical investigations are carried out to show the feasibility of the theoretical results.

By "A Note on Discrete Multitime Recurrences of Samuelson-Hicks Type" B. A. Pansera and F. Strati aim at fostering further research on the applications of multitime recurrences in the frame of multitime theory. In particular, the authors apply this method by generalizing the Samuelson-Hicks model so as to make the new concept of time that this method proposes clear. In particular, the multitime approach decomposes a point of time into a vector, taking into account how different coordinates of time referring to the same date can affect the dynamics of a model. Since 1932, the adjective multitime, introduced by Paul Dirac, appears so as to cope with an environment in which there might be more than one dimension of time. The authors make some considerations concerning the physical idea of the multitime notion: they recall that a coordinate space is an index numbering degree of freedom, and the coordinate of time is the usual physical time in which a system evolves. This model is satisfactory, unless the reader turns his attention to relativistic problems. Moreover, some physical phenomena (and social sciences too) are observed in a two-time environment, where the intrinsic time and the observer time are found. In some real phenomena, there is no reason to prefer one coordinate to another. Following these assumptions, the authors refer to multitime as vector parameters of evolution in multitime geometric evolution and multitime optimal control problems.

Constructing a Poincaré map is a method that is often used to study high-dimensional dynamical systems. In "Topological Entropy of One Type of Nonoriented Lorenz-Type Maps," G. Feng has proposed a geometric model of nonoriented Lorenz-type attractor by using this method, and its dynamical property has been described. The topological entropy of one-dimensional nonoriented Lorenz-type maps is also computed in terms of their kneading sequences.

In "Dynamic Complexities in 2-Dimensional Discrete-Time Predator-Prey Systems with Allee Effect in the Prey," L. Ren et al. have presented a study by which the "Allee effect" is incorporated into a predator-prey model with linear functional response. Compared with the predator-prey which only takes the crowding effect and predator partially dependent on prey into consideration, it has been found that the "Allee effect" of the prey species would increase the extinction risk of both the prey and predator. Moreover, by using a center manifold theorem and bifurcation theory, it has been shown that the model with "Allee effect" undergoes the flip bifurcation and Hopf bifurcation in the interior of R_+^2 with different "Allee effect" values. In the two bifurcations, the authors came to the conclusion that different "Allee effects" have different bifurcation value and the increasing of the "Allee effect" increases the value of bifurcation, respectively.

By "Existence of Nonoscillatory Solutions of Higher-Order Neutral Differential Equations with Distributed Coefficients and Delays," Y. Liu et al. have considered the existence of nonoscillatory solutions of higher-order neutral differential equations with distributed coefficients. The authors have used the contraction principle in obtaining new sufficient condition for the existence of nonoscillatory solutions.

In the paper entitled "Modeling and Nonlinear Response of the Cam-Follower Oblique-Impact System" by Y.-F. Yang et al., in order to quickly and accurately analyze the complex behavior of cam-follower oblique-impact system, a mathematical model, which can describe separation, impact, and contact, was established. The transient impact hypothesis was extended, and the oblique collision model was established by considering the tangential slip. "Moreau time-stepping method" was employed to solve the linear complementarity problem transformed by the oblique-impact equations. The simulation results have been organized showing that the cam and follower kept permanent contact when the cam rotational speed was low. With the increase of the cam rotational speed, the cam and follower would be separated and then have impact under the gravity action. The system performance has shown very complex nonlinear characteristics.

In "Risk-Averse Evolutionary Game Model of Aviation Joint Emergency Response," W. Pan et al. have studied effects of risk-averse attitude of both participators in aviation joint emergency response on the coevolution of cooperation mechanisms and individual preferences between airport and nonprofit organization. First, based on the current aviation joint emergency mechanism in China, the authors put forward two mechanisms to select the joint nonprofit organization, including reputation cooperation and bidding competition. Meanwhile, they have considered two preferences including altruism and selfishness. Then "replicator dynamics equations" by using the theory of conditional value-at-risk (CVaR) taking risk aversion attitude into account were built. Finally, the authors show that the risk-averse attitude of the other game participator affects the one participator's decision and the effects subject to some parameters.

The guest editors of this special issue hope that problems discussed and investigated in the papers by the authors of this issue can inspire and motivate researchers in these fields to discover new, innovative, and novel applications in all areas of pure and applied mathematics.

Acknowledgments

We would like to express our great gratitude to all of the authors for their contributions and the reviewers for their serious evaluation of the papers submitted by valuable comments and timely feedback.

Massimiliano Ferrara
Gafurjan Ibragimov
Vincenzo Scalzo

Hindawi Publishing Corporation
Discrete Dynamics in Nature and Society
Volume 2017, Article ID 8630895, 12 pages
http://dx.doi.org/10.1155/2017/8630895

Research Article

Numerical Approach Based on Two-Dimensional Fractional-Order Legendre Functions for Solving Fractional Differential Equations

Qingxue Huang,[1,2,3] Fuqiang Zhao,[1,3] Jiaquan Xie,[1,3] Lifeng Ma,[1,3] Jianmei Wang,[1,3] and Yugui Li[1,3]

[1]*College of Mechanical Engineering, Taiyuan University of Science & Technology, Taiyuan, Shanxi 030024, China*
[2]*College of Mechanical Engineering, Taiyuan University of Technology, Taiyuan, Shanxi 030024, China*
[3]*Shanxi Provincial Key Laboratory of Metallurgical Device Design Theory and Technology, Taiyuan, Shanxi 030024, China*

Correspondence should be addressed to Fuqiang Zhao; zfqgear@163.com

Received 23 August 2016; Revised 2 December 2016; Accepted 18 December 2016; Published 23 January 2017

Academic Editor: Vincenzo Scalzo

Copyright © 2017 Qingxue Huang et al. This is an open access article distributed under the Creative Commons Attribution License, which permits unrestricted use, distribution, and reproduction in any medium, provided the original work is properly cited.

In this paper, a robust, effective, and accurate numerical approach is proposed to obtain the numerical solution of fractional differential equations. The principal characteristic of the approach is the new orthogonal functions based on shifted Legendre polynomials to the fractional calculus. Also the fractional differential operational matrix is driven. Then the matrix with the Tau method is utilized to transform this problem into a system of linear algebraic equations. By solving the linear algebraic equations, the numerical solution is obtained. The approach is tested via some examples. It is shown that the FLF yields better results. Finally, error analysis shows that the algorithm is convergent.

1. Introduction

Fractional-order calculus has a long history. Compared with integer order, fractional differential equations show many advantages over the simulation of physical phenomena [1]. In recent decades, fractional partial differential equations (FPDEs) [2] are widely used to describe engineering processes and dynamical systems; more and more researchers have devoted to study a variety of methods for solving fractional differential equations. The most commonly used methods are generalized differential transform method [3], Adomian decomposition method [4], finite difference method [5], and so on. Recently, the authors have proposed wavelet methods for solving a class of fractional convection-diffusion equations. In [6], different families of wavelets [7–11] have been widely applied for solving problems of partial differential equations. In [12], the authors have obtained the approximate solutions of fractional differential equations using the generalized block pulse operational matrix.

The methods based on the orthogonal functions [13–15] are powerful and wonderful for solving FPDEs and have achieved great success in this field. Now the operational matrices of fractional derivative and integral [14–16] for Bernstein polynomials and Jacobi polynomials [15] have been derived. However, these polynomials use integer power series to approximate fractional ones; it cannot accurately represent properties of fractional integral and differential. Recently, in [17], Rida and Yousef have proposed a fractional extension of classical Legendre polynomials by replacing the integer order derivative in Rodrigues formula [18] with fractional-order derivatives. These functions are complex, so they are not unsuitable for solving FPDEs. Subsequently, Kazem et al. put forward the orthogonal fractional-order Legendre functions based on shifted Legendre polynomials. In [19], they used these functions to obtain the numerical solutions of fractional partial differential equations. Numerical results show that their methods are effective, accurate, and easy to implement. In this paper, FLF is suitable to characterize the properties of fractional partial differential equations; thus we attempt to use fractional-order Legendre functions to acquire numerical solution of the FPDEs.

The article is organized as follows. In Section 2, we introduce some basic definitions of fractional derivatives and integrals. In Section 3, we construct the FLFs and introduce

some properties. In Section 4, the fractional operational matrices of FLFs are obtained. In Section 5, we use the proposed method to solve FPDEs. In Section 6, the proposed method is tested through several numerical examples. In Section 7, the error analysis is given. Finally Section 8 concludes the paper.

2. Preliminaries and Notations

In this section, we recall the essentials of the fractional calculus theory that will be used in this article.

Definition 1. The Riemann-Liouville fractional integral operator of order $\alpha > 0$ is defined as

$$I^{\alpha}u(t) = \frac{1}{\Gamma(\alpha)}\int_0^t (t-s)^{\alpha-1}u(s)\,ds, \quad \alpha > 0,$$
$$I^{0}u(t) = u(t). \tag{1}$$

Definition 2. The Riemann-Liouville definition of fractional differential operator is given as follows:

$$D_*^{\alpha}u(t) = \begin{cases} \dfrac{1}{\Gamma(m-\alpha)}\dfrac{d^m}{dt^m}\displaystyle\int_0^t \frac{u(s)}{(t-s)^{\alpha-m+1}}ds, & \alpha > 0,\ m-1 \le \alpha < m, \\ \dfrac{d^m u(t)}{dt^m}, & \alpha = m. \end{cases} \tag{2}$$

Definition 3. The Caputo definition of fractional differential operator is defined as

$$D^{\alpha}u(t) = \begin{cases} \dfrac{1}{\Gamma(m-\alpha)}\displaystyle\int_0^t \frac{u^{(m)}(\tau)}{(t-\tau)^{\alpha-m+1}}d\tau, & m-1 \le \alpha < m, \\ \dfrac{d^m u(t)}{dt^m}, & \alpha = m. \end{cases} \tag{3}$$

The relation between the Riemann-Liouville operator and Caputo operator is given by the following expressions:

$$D^{\alpha}I^{\alpha}u(t) = u(t),$$
$$I^{\alpha}D^{\alpha}u(t) = u(t) - \sum_{k=0}^{m-1}u^{(k)}(0^+)\frac{t^k}{k!}. \tag{4}$$

For $\alpha \ge 0$, $\nu \ge -1$, and constant C, Caputo fractional derivative has some basic properties which are needed here as follows:

(i) $D^{\alpha}C = 0$,

(ii) $D^{\alpha}t^{\nu} = \begin{cases} 0, & \text{for } \nu \in N_0,\ \nu < \lceil\alpha\rceil, \\ \dfrac{\Gamma(\nu+1)}{\Gamma(\nu+1-\alpha)}t^{\nu-\alpha}, & \text{for } \nu \in N_0,\ \nu \ge \lceil\alpha\rceil \text{ or } \nu \notin N_0,\ \nu > \lfloor\alpha\rfloor. \end{cases}$ (5)

(iii) $D^{\alpha}\left(\sum_{i=0}^{m}c_i u_i(t)\right) = \sum_{i=0}^{m}c_i D^{\alpha}u_i(t)$, where $\{c_i\}_{i=0}^{m}$ are constants.

Definition 4 (generalized Taylor's formula). Suppose that $D^{i\alpha}u(t) \in C[0,1]$ for $i = 0, 1, \ldots, m-1$, then one has

$$u(t) = \sum_{i=0}^{m-1}\frac{t^{i\alpha}}{\Gamma(i\alpha+1)}D^{i\alpha}u(0^+) + \frac{t^{m\alpha}}{\Gamma(m\alpha+1)}D^{m\alpha}u(\xi), \tag{6}$$

where $0 < \xi \le t$, $\forall t \in [0,1]$. Also, one has

$$\left|u(t) - \sum_{i=0}^{m-1}\frac{t^{i\alpha}}{\Gamma(i\alpha+1)}D^{i\alpha}u(0^+)\right| \le M_{\alpha}\frac{t^{m\alpha}}{\Gamma(m\alpha+1)}, \tag{7}$$

where $M_{\alpha} \ge |D^{m\alpha}u(\xi)|$.

In case $\alpha = 1$, the generalized Taylor's formula (6) is the classical Taylors formula.

3. Definitions of Fractional-Order Legendre Definition and Function Approximation

3.1. Shifted Legendre Polynomials. The well-known Legendre polynomials are orthogonal with the weight function $\omega(x) = 1$, which is defined on the interval $[-1, 1]$; namely,

$$\int_{-1}^{1}P_m(x)P_n(x)\omega(x)\,dx = \begin{cases} \dfrac{2}{(2n+1)}, & m = n, \\ 0, & m \ne n. \end{cases} \tag{8}$$

In order to use these polynomials on the interval $[0, 1]$, let $t = 2x - 1$, and then we derived the shifted Legendre polynomials $P_n(2x-1)$ which are denoted by $L_n(t)$. The

shifted Legendre polynomials are orthogonal with the weight function $\omega_l(t) = 1$ over $[0, 1]$, with the orthogonally property

$$\int_0^1 L_i(t) L_j(t) \omega_l(t) dt = \begin{cases} 0, & i \neq j, \\ \dfrac{1}{2i+1}, & i = j. \end{cases} \tag{9}$$

Then $L_i(t)$ can be obtained as follows:

$$\begin{aligned} L_{i+1}(t) &= \frac{(2i+1)}{i+1} L_i(t) - \frac{i}{i+1} L_{i-1}(t), \\ & \qquad i = 1, 2, \ldots, \\ L_0(t) &= 1, \\ L_1(t) &= 2t - 1. \end{aligned} \tag{10}$$

The analytic form of the shifted Legendre polynomial $L_n(t)$ of degree n is given by

$$\begin{aligned} L_n(t) &= \sum_{i=0}^{n} b_{ni} t^i, \\ L_n(0) &= (-1)^n, \\ L_n(1) &= 1, \end{aligned} \tag{11}$$

where $b_{ni} = (-1)^{n+i}((n+i)!/(n-i)!(i!)^2)$.

3.2. Fractional-Order Legendre Definition. We define the fractional-order Legendre functions (FLFs) by introducing the change of variable $t = x^\alpha$ and $\alpha > 0$ on shifted Legendre polynomials. The fractional-order Legendre function $L_i(x^\alpha)$ is denoted by $Fl_i^\alpha(x)$. The fractional-order Legendre functions are a particular solution of the normalized eigenfunctions of the singular Sturm-Liouville problem.

$$\begin{aligned} &\left(\left(x - x^{1+\alpha}\right) Fl_i'^{\alpha}(x)\right)' + \alpha^2 i(i+1) x^{\alpha-1} Fl_i(x) = 0, \\ &\qquad x \in [0, 1]. \end{aligned} \tag{12}$$

Then $Fl_i^\alpha(x)$ can be obtained as follows:

$$\begin{aligned} Fl_{i+1}^\alpha(x) &= \frac{(2i+1)\left(2x^\alpha - 1\right)}{i+1} Fl_i^\alpha(x) - \frac{i}{i+1} Fl_{i-1}^\alpha(x), \\ & \qquad i = 1, 2, \ldots, \\ Fl_0^\alpha(x) &= 1, \\ Fl_1^\alpha(x) &= 2x^\alpha - 1. \end{aligned} \tag{13}$$

We can derive the analytic form of $Fl_i^\alpha(x)$ of degree $i\alpha$ as follows:

$$Fl_i^\alpha(x) = \sum_{s=0}^{i} b_{s,i} x^{s\alpha}, \tag{14}$$

where $b_{s,i} = (-1)^{i+s}(i+s)!/(i-s)!(s!)^2$ and $Fl_i^\alpha(0) = (-1)^i$, $Fl_i^\alpha(1) = 1$.

Theorem 5. *The FLFs are orthogonal with the weight function $\omega_l^\alpha(x) = x^{\alpha-1}$ on the interval $[0, 1]$; then the orthogonally condition is*

$$\int_0^1 Fl_n^\alpha(x) Fl_m^\alpha(x) \omega_l^\alpha(x) dx = \frac{1}{(2n+1)\alpha} \delta_{nm}. \tag{15}$$

Proof. With $\int_0^1 L_n(t) L_m(t) \omega_l(t) dt = (1/(2i+1))\delta_{nm}$, where δ_{nm} is the Kronecker function, let $t = x^\alpha$, and then we have

$$\begin{aligned} &\int_0^1 L_n(t) L_m(t) dt = \int_0^1 L_n\left(x^\alpha\right) L_m\left(x^\alpha\right) \alpha x^{\alpha-1} dx \\ &\quad = \frac{1}{2n+1} \delta_{nm}, \\ &\int_0^1 L_n\left(x^\alpha\right) L_m\left(x^\alpha\right) \alpha x^{\alpha-1} dx \\ &\quad = \int_0^1 Fl_n^\alpha(x) Fl_m^\alpha(x) \alpha x^{\alpha-1} dx = \frac{1}{2n+1} \delta_{nm}, \\ &\int_0^1 Fl_n^\alpha(x) Fl_m^\alpha(x) x^{\alpha-1} dx = \frac{1}{(2n+1)\alpha} \delta_{nm}. \end{aligned} \tag{16}$$

□

3.3. Function Approximation. Suppose $u(x) \in L^2[0, 1]$; it can be expanded in terms of the fractional-order Legendre functions as follows:

$$u(x) = \sum_{i=0}^{\infty} c_i Fl_i^\alpha(x), \tag{17}$$

where the coefficients c_i are obtained by

$$\begin{aligned} c_i &= \alpha(2i+1) \int_0^1 Fl_i^\alpha(x) u(x) \omega_l^\alpha(x) dx, \\ & \qquad i = 0, 1, 2, \ldots. \end{aligned} \tag{18}$$

If we consider truncated series in (17), we obtain

$$u(x) \approx u_m(x) = \sum_{i=0}^{m-1} c_i Fl_i^\alpha(x) = \mathbf{C}^T \mathbf{\Phi}(x), \tag{19}$$

where $\mathbf{C}$ and $\mathbf{\Phi}(x)$ are $m \times 1$ vector given by

$$\begin{aligned} \mathbf{C} &= \left[c_0, c_1, \ldots, c_{m-1}\right]^T, \\ \mathbf{\Phi}(x) &= \left[Fl_0^\alpha(x), Fl_1^\alpha(x), \ldots, Fl_{m-1}^\alpha(x)\right]^T. \end{aligned} \tag{20}$$

Theorem 6. *Suppose $D^{i\alpha} u(x) \in C[0, 1]$ for $i = 0, 1, 2, \ldots, m-1$. $(2m+1)\alpha \geq 1$ and $\mathbf{P}_m^\alpha = \operatorname{span}\{Fl_0^\alpha(x), Fl_1^\alpha(x), \ldots, Fl_{m-1}^\alpha(x)\}$. If $u_m(x) = \mathbf{C}^T \mathbf{\Phi}(x)$ is the best approximation to $u(x)$ from $\mathbf{P}_m^\alpha$, then the error bound is presented as follows:*

$$\left\| u(x) - u_m(x) \right\|_\omega \leq \frac{M_\alpha}{\Gamma(m\alpha + 1)} \sqrt{\frac{1}{(2m+1)\alpha}}, \tag{21}$$

where $M_\alpha \geq |D^{m\alpha} u(x)|$, $x \in [0, 1]$.

Proof. Consider the generalized Taylor's formula

$$u(x) = \sum_{i=0}^{m-1} \frac{x^{i\alpha}}{\Gamma(i\alpha+1)} D^{i\alpha} u(0^+) + \frac{x^{m\alpha}}{\Gamma(m\alpha+1)} D^{m\alpha} u(\xi), \tag{22}$$

where $0 < \xi < x$, $x \in [0,1]$.

With Definition 4

$$\left| u(x) - \sum_{i=0}^{m-1} \frac{x^{i\alpha}}{\Gamma(i\alpha+1)} D^{i\alpha} f(0^+) \right| \le M_\alpha \frac{x^{m\alpha}}{\Gamma(m\alpha+1)}. \tag{23}$$

Since $u_m(x) = \mathbf{C}^T \mathbf{\Phi}(x)$ is the best approximation to u from $\mathbf{P}_m^\alpha$ and $\sum_{i=0}^{m-1} (x^{i\alpha}/\Gamma(i\alpha+1)) D^{i\alpha} f(0^+) \in \mathbf{P}_m^\alpha$, hence

$$\begin{aligned} &\|u(x) - u_m(x)\|_\omega^2 \\ &\le \left\| u(x) - \sum_{i=0}^{m-1} \frac{x^{i\alpha}}{\Gamma(i\alpha+1)} D^{i\alpha} u(0^+) \right\|_\omega^2 \\ &\le \frac{M_\alpha^2}{\Gamma(m\alpha+1)^2} \int_0^1 x^{2m\alpha} x^{\alpha-1} dx, \\ &\|u(x) - u_m(x)\|_\omega^2 \le \frac{M_\alpha^2}{\Gamma(m\alpha+1)^2} \int_0^1 x^{(2m+1)\alpha-1} dx \\ &= \frac{M_\alpha^2}{\Gamma(m\alpha+1)^2 (2m+1)\alpha}. \end{aligned} \tag{24}$$

Now by taking the square roots, then the theorem is proved. □

For arbitrary function $u(x,t) \in L^2([0,1]\times[0,1])$, they can be expanded as the following formula:

$$u(x,t) = \sum_{i=0}^{\infty} \sum_{j=0}^{\infty} u_{ij} Fl_i^a(x) Fl_j^\beta(t), \tag{25}$$

where

$$\begin{aligned} u_{ij} = (2i+1)(2j+1)\alpha\beta \int_0^1 \int_0^1 u(x,t) Fl_i^\alpha(x) Fl_j^\beta(t) \\ \cdot \omega_l^\alpha(x) \omega_l^\beta(t) dx\, dt, \quad i,j = 0,1,\ldots. \end{aligned} \tag{26}$$

Theorem 7. *If the series $\sum_{i=0}^{\infty} \sum_{j=0}^{\infty} u_{ij} Fl_i^a(x) Fl_j^\beta(t)$ converges uniformly to $u(x,t)$ on the square $[0,1]\times[0,1]$, then one has*

$$\begin{aligned} u_{ij} = (2i+1)(2j+1)\alpha\beta \int_0^1 \int_0^1 u(x,t) Fl_i^\alpha(x) Fl_j^\beta(t) \\ \cdot \omega_l^\alpha(x) \omega_l^\beta(t) dx\, dt. \end{aligned} \tag{27}$$

Proof. By multiplying $\omega_l^\alpha(x)\omega_l^\beta(t) Fl_m^\alpha(x) Fl_n^\beta(t)$ on both sides of (25), where i and j are fixed and integrating term wise with regard to x and t on $[0,1]\times[0,1]$, then

$$\begin{aligned} &\int_0^1 \int_0^1 u(x,t) Fl_m^\alpha(x) Fl_n^\beta(t) \omega_l^\alpha(x) \omega_l^\beta(t) dx\, dt = \sum_{i=0}^{\infty} \sum_{j=0}^{\infty} u_{ij} \int_0^1 \int_0^1 Fl_i^\alpha(x) Fl_j^\beta(t) Fl_m^\alpha(x) Fl_n^\beta(t) \omega_l^\alpha(x) \omega_l^\beta(t) dx\, dt \\ &= \sum_{i=0}^{\infty} \sum_{j=0}^{\infty} u_{ij} \int_0^1 \omega_l^\alpha(x) Fl_i^\alpha(x) Fl_m^\alpha(x) dx \int_0^1 \omega_l^\beta(t) Fl_i^\beta(t) Fl_m^\alpha(t) dt = u_{ij} \int_0^1 \omega_l^\alpha(x) \left[Fl_i^\alpha(x)\right]^2 dx \int_0^1 \omega_l^\beta(t) \left[Fl_i^\beta(t)\right]^2 dt \\ &= u_{ij} \frac{1}{(2i+1)\alpha} \frac{1}{(2j+1)\beta}. \end{aligned} \tag{28}$$

□

Theorem 8. *If the function $u(x,t)$ is a continuous function on $[0,1]\times[0,1]$ and the series $\sum_{i=0}^{\infty} \sum_{j=0}^{\infty} u_{ij} Fl_i^a(x) Fl_j^\beta(t)$ converges uniformly to $u(x,t)$, then $\sum_{i=0}^{\infty} \sum_{j=0}^{\infty} u_{ij} Fl_i^a(x) Fl_j^\beta(t)$ is the FLFs expansion of $u(x,t)$.*

Proof. Using contradiction, let

$$\begin{aligned} u(x,t) &= \sum_{i=0}^{\infty} \sum_{j=0}^{\infty} u_{ij} Fl_i^a(x) Fl_j^\beta(t), \\ u(x,t) &\approx \sum_{i=0}^{\infty} \sum_{j=0}^{\infty} g_{ij} Fl_i^a(x) Fl_j^\beta(t). \end{aligned} \tag{29}$$

Then there is at least one coefficient such that $u_{nm} \ne g_{nm}$; however

$$\begin{aligned} u_{nm} = (2m+1)(2n+1)\alpha\beta \int_0^1 \int_0^1 u(x,t) Fl_m^a(x) \\ \cdot Fl_n^\beta(t) \omega_l^\alpha(x) \omega_l^\beta(t) dx\, dt = g_{nm}. \end{aligned} \tag{30}$$

□

Theorem 9. *If two continuous functions defined on $[0,1]\times[0,1]$ have the identical FLFs expansions, then these two functions are identical.*

Proof. Suppose that $u(x,t)$ and $f(x,t)$ can be expended by FLFs as follows:

$$u(x,t) \approx \sum_{i=0}^{\infty}\sum_{j=0}^{\infty} u_{ij} Fl_i^a(x)\, Fl_j^\beta(t),$$
$$f(x,t) \approx \sum_{i=0}^{\infty}\sum_{j=0}^{\infty} u_{ij} Fl_i^a(x)\, Fl_j^\beta(t). \tag{31}$$

By subtracting the above two equations with each other, we have

$$u(x,t) - f(x,t) \approx \sum_{i=0}^{\infty}\sum_{j=0}^{\infty} \left(u_{ij} - u_{ij}\right) Fl_i^a(x)\, Fl_j^\beta(t) = 0 = \sum_{i=0}^{\infty}\sum_{j=0}^{\infty} 0 Fl_i^a(x)\, Fl_j^\beta(t). \tag{32}$$

□

Theorem 10. *If the sum of the absolute values of the FLFs coefficients of a continuous function $u(x,t)$ forms a convergent series, then the FLFs expansion is absolutely uniformly convergent and converges to the function $u(x,t)$.*

Proof. Consider

$$\left|\sum_{i=0}^{\infty}\sum_{j=0}^{\infty} u_{ij} Fl_i^a(x)\, Fl_j^\beta(t)\right| \le \sum_{i=0}^{\infty}\sum_{j=0}^{\infty} \left|u_{ij}\right| \left|Fl_i^a(x)\right| \left|Fl_j^\beta(t)\right| \le \sum_{i=0}^{\infty}\sum_{j=0}^{\infty} \left|u_{ij}\right|. \tag{33}$$

If we consider truncated series in (25), we obtain

$$u(x,t) \approx \sum_{i=0}^{m-1}\sum_{j=0}^{n-1} u_{ij} Fl_i^a(x)\, Fl_j^\beta(t) = \mathbf{\Phi}^T(x)\, \mathbf{U} \mathbf{\Phi}(t), \tag{34}$$

where

$$\mathbf{\Phi}(x) = \left[Fl_0^\alpha(x), Fl_1^\alpha(x), \ldots, Fl_{m-1}^\alpha(x)\right]^T;$$
$$\mathbf{\Phi}(t) = \left[Fl_0^\beta(t), Fl_1^\beta(t), \ldots, Fl_{n-1}^\beta(t)\right]^T, \tag{35}$$
$$\mathbf{U} = \left\{u_{ij}\right\}_{i,j=0}^{m-1,n-1}.$$

In this paper, we use the Tau method [20] to compute the coefficients u_{ij}. □

4. Fractional Differential Operational Matrix of FLFs

The derivative of the $\mathbf{\Phi}(x)$ can be approximated

$$D^\gamma \mathbf{\Phi}(x) \approx \mathbf{D}^\gamma \mathbf{\Phi}(x), \tag{36}$$

where $\mathbf{D}^\gamma$ is called the FLFs operational matrix of derivative.

Theorem 11. *Suppose $\mathbf{D}^\gamma$ is the $m \times m$ operational matrix of Caputo fractional derivatives of order $\gamma > 0$, $\alpha > \gamma/2$, when $\alpha \notin \mathbb{N}$; then the elements of $\mathbf{D}^\gamma$ are obtained as*

$$\left\{d_{ij}\right\}_{i,j}^{m-1;m-1} = (2j+1) \cdot \alpha \sum_{s=0}^{i}\sum_{r=0}^{j} b_{r,j} b'_{s,i} \frac{\Gamma(s\alpha+1)}{\Gamma(s\alpha-\gamma+1)} \frac{1}{(s+r+1)\alpha-\gamma}, \tag{37}$$

where

$$b'_{s,i} = \begin{cases} 0, & s\alpha \in N_0,\ s\alpha < \gamma, \\ b'_{s,i} = b_{s,i} & s\alpha \notin N_0,\ s\alpha \ge [\gamma] \ \text{ or } s\alpha \in N_0,\ s\alpha \ge \gamma. \end{cases} \tag{38}$$

Proof. With the properties of the derivative (ii) and the orthogonally of FLFs, we have

$$D^\gamma Fl_i^\alpha(x) = \sum_{s=0}^{i} b'_{s,i} \frac{\Gamma(s\alpha+1)}{\Gamma(s\alpha-\gamma+1)} x^{s\alpha-\gamma}. \tag{39}$$

Let

$$x^{s\alpha-\gamma} = \sum_{j=0}^{m-1} d_j Fl_j^\alpha(x). \tag{40}$$

Multiplying $\omega_l^\alpha(x) Fl_j^\alpha(x)$ on both sides of (40), we have

$$d_j = (2j+1)\,\alpha \sum_{r=0}^{j} b_{r,j} \frac{1}{(s+r+1)\alpha-\gamma}. \tag{41}$$

Substituting (40) and (41) into (39), we have

$$D^\gamma Fl_i^\alpha(x) = (2j+1) \cdot \alpha \sum_{j=0}^{m-1}\sum_{s=0}^{i}\sum_{r=0}^{j} \frac{b_{r,j} b'_{s,i} \Gamma(s\alpha+1)}{\Gamma(s\alpha-\gamma+1)} \frac{1}{(s+r+1)\alpha-\gamma} \cdot Fl_j^\alpha(x). \tag{42}$$

Hence,

$$d_{ij} = (2j+1) \cdot \alpha \sum_{s=0}^{i}\sum_{r=0}^{j} b_{r,j} b'_{s,i} \frac{\Gamma(s\alpha+1)}{\Gamma(s\alpha-\gamma+1)} \frac{1}{(s+r+1)\alpha-\gamma}, \quad i,j = 0,1,\ldots,m-1. \tag{43}$$

□

5. Description of the Proposed Method

We consider a class of fractional partial differential equations as follows:

$$\frac{\partial^\nu u(x,t)}{\partial x^\nu} + \frac{\partial^\gamma u(x,t)}{\partial t^\gamma} = g(x,t), \tag{44}$$

subject to the initial conditions

$$u(0,t) = u(x,0) = 0, \tag{45}$$

where $0 \le x,t \le 1$, $n-1 < \nu,\gamma \le n$, $\partial^\nu u(x,t)/\partial x^\nu$ and $\partial^\gamma u(x,t)/\partial t^\gamma$ are fractional derivative in Caputo sense, $g(x,t)$ is the known continuous function, and $u(x,t)$ is the unknown function.

If we approximate function $u(x,t)$ by a terms of the FLFs, it can be written as (34). Then we have

$$\begin{aligned}
\frac{\partial^\nu u(x,t)}{\partial x^\nu} &\approx \frac{\partial^\nu \left(\mathbf{\Phi}^T(x)\,\mathbf{U}\mathbf{\Phi}(t)\right)}{\partial x^\nu} \\
&= \frac{\partial^\nu \left(\mathbf{\Phi}^T(x)\right)}{\partial x^\nu}\mathbf{U}\mathbf{\Phi}(t) \\
&= \left(\frac{\partial^\nu \mathbf{\Phi}(x)}{\partial x^\nu}\right)^T \mathbf{U}\mathbf{\Phi}(t) \\
&\approx \mathbf{\Phi}^T(x)\left(\mathbf{D}^\nu\right)^T \mathbf{U}\mathbf{\Phi}(t), \\
\frac{\partial^\gamma u(x,t)}{\partial t^\gamma} &\approx \frac{\partial^\gamma \left(\mathbf{\Phi}^T(x)\,\mathbf{U}\mathbf{\Phi}(t)\right)}{\partial t^\gamma} = \mathbf{\Phi}^T(x)\,\mathbf{U}\frac{\partial^\gamma \mathbf{\Phi}(t)}{\partial t^\gamma} \\
&\approx \mathbf{\Phi}^T(x)\,\mathbf{U}\mathbf{D}^\gamma\mathbf{\Phi}(t), \\
g(x,t) &\approx \mathbf{\Phi}^T(x)\,\mathbf{G}\mathbf{\Phi}(t),
\end{aligned} \tag{46}$$

where

$$\begin{aligned}
&\mathbf{G} = \left\{g_{ij}\right\}_{i,j=0}^{m-1;n-1}, \\
&g_{ij} = (2i+1)(2j+1)\,\alpha\beta \int_0^1\int_0^1 g(x,t)\,Fl_i^\alpha(x)\,Fl_j^\beta(t) \\
&\quad\cdot \omega_l^\alpha(x)\,\omega_l^\beta(t)\,dx\,dt.
\end{aligned} \tag{47}$$

Substituting (46) into (44), we have

$$\begin{aligned}
&\mathbf{\Phi}^T(x)\left(\mathbf{D}^\nu\right)^T \mathbf{U}\mathbf{\Phi}(t) + \mathbf{\Phi}^T(x)\,\mathbf{U}\mathbf{D}^\gamma\mathbf{\Phi}(t) \\
&\quad\approx \mathbf{\Phi}^T(x)\,\mathbf{G}\mathbf{\Phi}(t).
\end{aligned} \tag{48}$$

Similar to the typical Tau method [20], then we generate $mn - n - m + 1$ algebraic equations by multiplying $\omega_l^\alpha(x)\omega_l^\beta(t)Fl_i^\alpha(x)Fl_j^\beta(t)$ (for $i = 0,1,2,\ldots,m-2$; $j = 0,1,2,\ldots,n-2$), integrating from 0 tol and using the orthogonal property, we have

$$\mathbf{H} = \left(\mathbf{D}^\nu\right)^T \mathbf{U} + \mathbf{U}\mathbf{D}^\gamma - \mathbf{G} = 0. \tag{49}$$

For condition. (45), we have

$$\begin{aligned}
u(0,t) &\approx \mathbf{\Phi}^T(0)\,\mathbf{U}\mathbf{\Phi}(t) \approx \mathbf{C}^T\mathbf{\Phi}(t), \\
u(x,0) &\approx \mathbf{\Phi}^T(x)\,\mathbf{U}\mathbf{\Phi}(0) \approx \mathbf{\Phi}^T(x)\,\mathbf{F},
\end{aligned} \tag{50}$$

with

$$\begin{aligned}
&\mathbf{C}^T = \left\{c_i\right\}_{i=0}^{n-1}, \\
&c_i = (2i+1)\,\beta\int_0^1 u(0,t)\,Fl_i^\beta(t)\,\omega_l^\beta(t)\,dt, \\
&\mathbf{F} = \left\{f_j\right\}_{j=0}^{m-1}, \\
&f_j = (2j+1)\,\alpha\int_0^1 u(x,0)\,Fl_j^\alpha(x)\,\omega_l^\alpha(x)\,dx.
\end{aligned} \tag{51}$$

So we obtain

$$\begin{aligned}
\mathbf{\Phi}^T(0)\,\mathbf{U} &\approx \mathbf{C}^T; \\
\mathbf{U}\mathbf{\Phi}(0) &\approx \mathbf{F}.
\end{aligned} \tag{52}$$

Equations (49) and (52) generate $mn + 1$ linear algebraic equations. By solving the linear algebraic equations, the unknown coefficients u_{ij} can be obtained.

6. Error Analysis

We consider $e(x,t) = u(x,t) - u_{mn}(x,t)$ as the error function of the approximate solution $u_{mn}(x,t)$ for $u(x,t)$, where $u(x,t)$ is the exact solution of (44) [21].

Therefore, $u_{mn}(x,t)$ satisfies the following problem:

$$\frac{\partial^\nu u_{mn}(x,t)}{\partial x^\nu} + \frac{\partial^\gamma u_{mn}(x,t)}{\partial t^\gamma} + R_{mn}(x,t) = g(x,t), \tag{53}$$

where $R_{mn}(x,t)$ is the residual function,

$$R_{mn}(x,t) = \frac{\partial^\nu u_{mn}(x,t)}{\partial x^\nu} + \frac{\partial^\gamma u_{mn}(x,t)}{\partial t^\gamma} - g(x,t). \tag{54}$$

We find an approximation $e'_{mn}(x,t)$ to the error function $e_{mn}(x,t)$ in the same way as we did before for the solution of the problem, the error function satisfies the problem

$$\frac{\partial^\nu e_{mn}(x,t)}{\partial x^\nu} + \frac{\partial^\gamma e_{mn}(x,t)}{\partial t^\gamma} = R_{mn}(x,t). \tag{55}$$

We should note that, in order to construct the approximate $e'_{mn}(x,t)$ to $e_{mn}(x,t)$, only (55) needs to be recalculated in the same way as we did before for the solution of (44).

7. Numerical Examples

Example 1. We consider the following FPDE:

$$\begin{aligned}
\frac{\partial^{1/4}u(x,t)}{\partial x^{1/4}} + \frac{\partial^{1/2}u(x,t)}{\partial t^{1/2}} &= g(x,t), \\
u(0,t) &= 0, \\
u(x,0) &= 0,
\end{aligned} \tag{56}$$

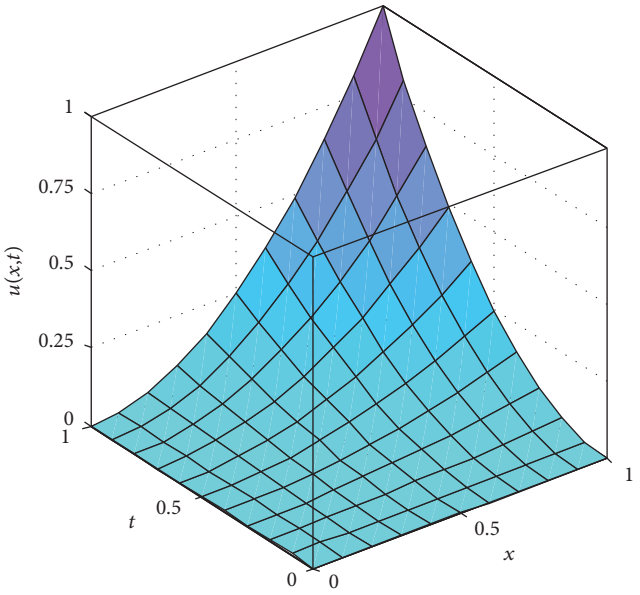

Figure 1: Numerical solution with $m = 6$ for Example 1.

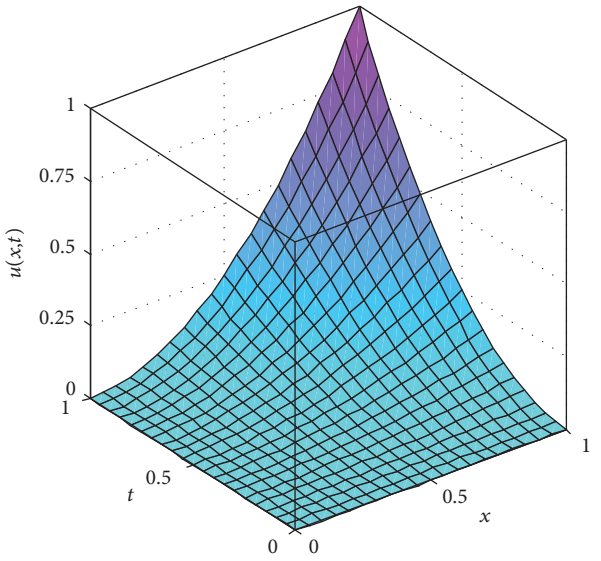

Figure 2: Numerical solution with $m = 8$ for Example 1.

where $g(x,t) = 8x^2t^{3/2}/3\sqrt{\pi} + 32t^2x^{7/4}/21\Gamma(3/4)$; using the method presented in Section 5, the equation is transformed as follows:

$$\left(\mathbf{D}^{1/4}\right)^T \mathbf{U} + \mathbf{U}\mathbf{D}^{1/2} \approx \mathbf{G},$$
$$\mathbf{\Phi}^T(0)\,\mathbf{U} \approx \mathbf{C}^T; \tag{57}$$
$$\mathbf{U}\mathbf{\Phi}(0) \approx \mathbf{F}.$$

By solving (57), we can obtain the numerical solution of the problem.

When $n = 6$, $m = 6$, the matrix $\mathbf{U}$ is get as follows:

$$\mathbf{U} = \begin{bmatrix} 0.0198 & 0.0396 & 0.0282 & 0.0098 & 0.0014 & 0 \\ 0.0486 & 0.0973 & 0.0694 & 0.0242 & 0.0034 & 0 \\ 0.054 & 0.108 & 0.077 & 0.027 & 0.0038 & 0 \\ 0.0412 & 0.0824 & 0.0588 & 0.0206 & 0.0029 & 0 \\ 0.0221 & 0.0443 & 0.0316 & 0.0110 & 0.0015 & 0 \\ 0.0062 & 0.0123 & 0.0087 & 0.0030 & 0 & 0 \end{bmatrix}. \tag{58}$$

When $m = 8$, $n = 6$, the matrix $\mathbf{U}$ is get as follows:

$$\mathbf{U} = \begin{bmatrix} 0.0198 & 0.0396 & 0.0282 & 0.0099 & 0.0013 & 0 \\ 0.0486 & 0.0971 & 0.0693 & 0.0241 & 0.0034 & 0 \\ 0.0540 & 0.1079 & 0.0770 & 0.0269 & 0.0038 & 0 \\ 0.0407 & 0.0814 & 0.0580 & 0.0203 & 0.0029 & 0 \\ 0.0225 & 0.0449 & 0.0320 & 0.0112 & 0.0016 & 0 \\ 0.0092 & 0.0183 & 0.0131 & 0.0046 & 0 & 0 \\ 0.0027 & 0.0054 & 0.0038 & 0.0013 & 0 & 0 \\ 0.0005 & 0.0009 & 0 & 0.0002 & 0 & 0 \end{bmatrix}. \tag{59}$$

When $n = 6$, Figures 1, 2, and 3 show the numerical solution of (56) for $\alpha = 1/4$, $\beta = 1/2$ with $m = 6$, $m = 8$, $m = 10$. The exact solution is x^2t^2 which is shown in Figure 4. We can see clearly that the numerical solutions are very good agreement with the exact solution. Particularly, when $m = 10$ the numerical solution matches the exact solution very well.

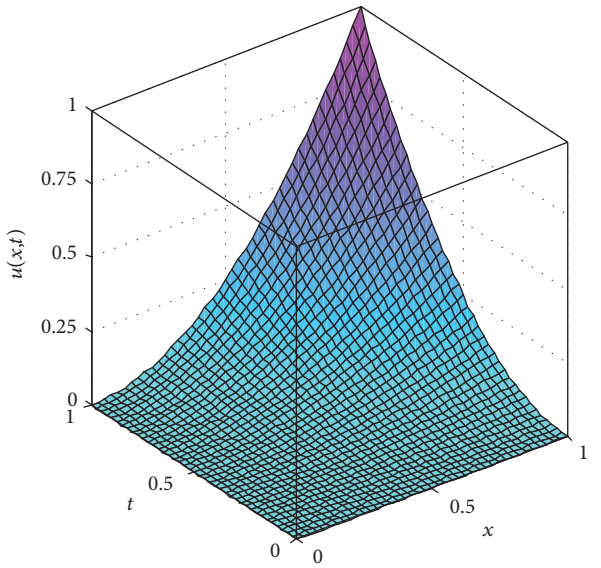

Figure 3: Numerical solution with $m = 10$ for Example 1.

Example 2. We consider the following equation:

$$\frac{\partial^\nu u(x,t)}{\partial x^\nu} + \frac{\partial^\nu u(x,t)}{\partial t^\nu} = g(x,t),$$
$$u(0,t) = 0. \tag{60}$$

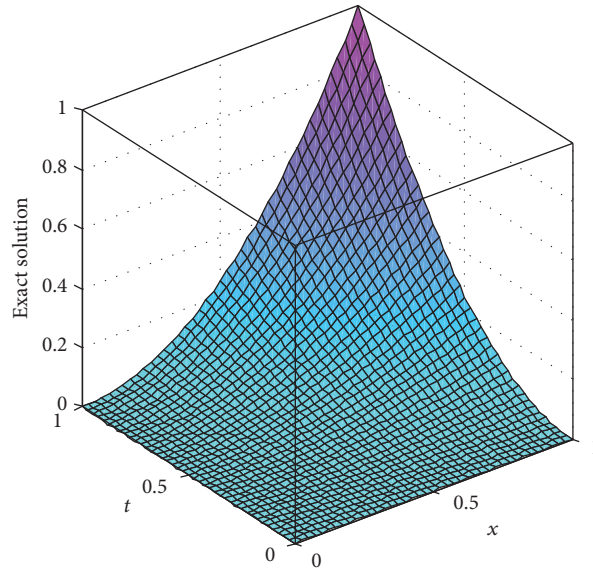

Figure 4: Exact solution for Example 1.

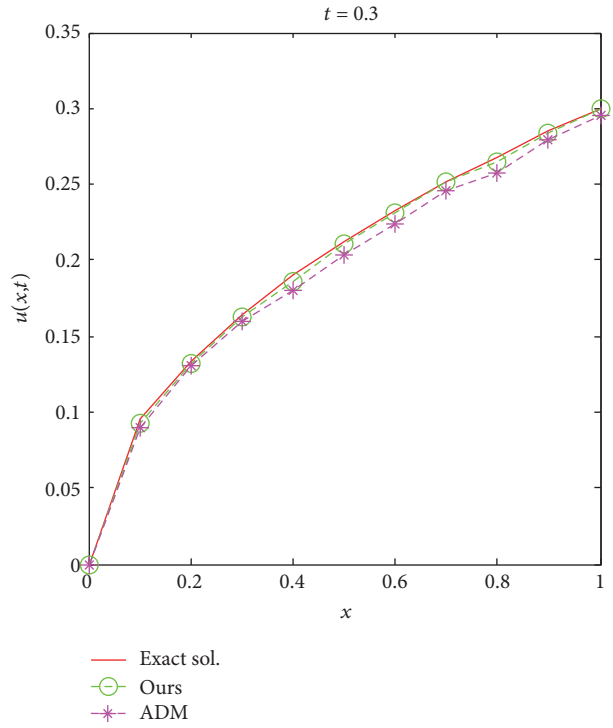

Figure 5: The comparison between FLFM and ADM with $m = 3,\ n = 3$ for Example 2.

The exact solution of this problem is $u(x,t) = x^{1/2}t$, where $\nu = \gamma = 1/2,\ g(x,t) = \sqrt{\pi}t/2 + 2\sqrt{tx}/\sqrt{\pi}$. The equation is transformed as follows:

$$\left(\mathbf{D}^{1/2}\right)^T \mathbf{U} + \mathbf{U}\mathbf{D}^{1/2} \approx \mathbf{G};$$
$$\mathbf{\Phi}^T(0)\,\mathbf{U} \approx \mathbf{C}^T, \tag{61}$$

when $m = 3,\ n = 3$, and $m = 5,\ n = 5$. The results obtained using our proposed method and ADM at $t = 0.3$ are shown in Figures 5 and 6. Comparing the two figures, it can be concluded that the FLFM has a better advantage than ADM for solving fractional partial differential equations and the numerical results have achieved a good convergence precision when small m and n are selected.

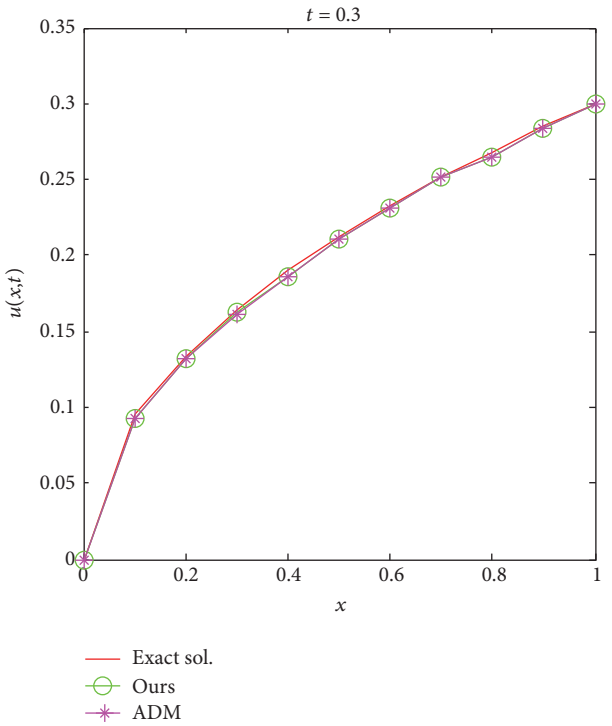

Figure 6: The comparison between FLFM and ADM with $m = 5$, $n = 5$ for Example 2.

Example 3. Consider the following fractional Poisson equation:

$$\frac{\partial^{\nu} u(x,t)}{\partial x^{\nu}} + \frac{\partial^{\gamma} u(x,t)}{\partial t^{\gamma}} = g(x,t), \quad u(0,t) = 0, \quad u(x,0) = 0. \tag{62}$$

(1) When $\nu = \gamma = 5/4$,

$$g(x,t) = \frac{5\Gamma(1/4)}{16} x^{5/2} + \frac{5\Gamma(1/4)}{16} t^{15/4} + \frac{30\sqrt{\pi} x^{5/4} t^{5/4}}{16\Gamma(9/4)} + \frac{2t^{5/2} x^{5/4} \Gamma(15/4)}{\sqrt{\pi}}. \tag{63}$$

The exact solution is $x^{5/2}t^{5/4} + x^{5/4}t^{15/4}$. When $n = 4$, the absolute errors for $m = 5$, $m = 6$, $m = 7$ are shown in Figures 7, 8, and 9.

(2) When $\nu = \gamma = 1/2$, $g(x,t) = \sin(x + t)$. The exact solution is unknown.

Therefore, in order to show the efficiency of the present method, we define the error function as follows:

$$e(x,t) = \mathbf{\Phi}^T(x) \left(\mathbf{D}^{\nu}\right)^T \mathbf{U}\mathbf{\Phi}(t) + \mathbf{\Phi}^T(x)\, \mathbf{U}\mathbf{D}^{\gamma}\mathbf{\Phi}(t) - \mathbf{\Phi}^T(x)\, \mathbf{G}\mathbf{\Phi}(t). \tag{64}$$

Let $\alpha = \beta = 1/2$ with $m = n = 8$, $m = n = 9$, and $m = n = 10$; the absolute error $|e(x,t)|$ is shown in Figures 10, 11, and 12.

When $m = n = 7$, we can have the coefficients matrix $\mathbf{U}$.

$$\mathbf{U} = \begin{bmatrix} 0.1570 & 0.1708 & 0.0198 & 0 & 0.0060 & 0 & 0 \\ 0.1708 & 0.1482 & -0.0152 & 0 & -0.0051 & -0.0001 & 0.0002 \\ 0.0198 & -0.0153 & -0.0381 & -0.0007 & 0.0019 & -0.0004 & 0.0001 \\ -0.0003 & 0.0025 & -0.0007 & -0.0031 & 0.0006 & 0.0001 & -0.0001 \\ -0.0061 & -0.0051 & 0.0018 & 0.0006 & -0.0003 & 0.0001 & 0.0001 \\ 0 & -0.0002 & -0.0003 & 0.0001 & 0.0001 & -0.0001 & -3.029 \\ -0.0002 & 0.0002 & 0.0001 & 0 & 0.0001 & -3.029 & 0 \end{bmatrix}. \tag{65}$$

Then we have the numerical solution $u(x,t) = \mathbf{\Phi}^T(x)\mathbf{U}\mathbf{\Phi}(t)$.

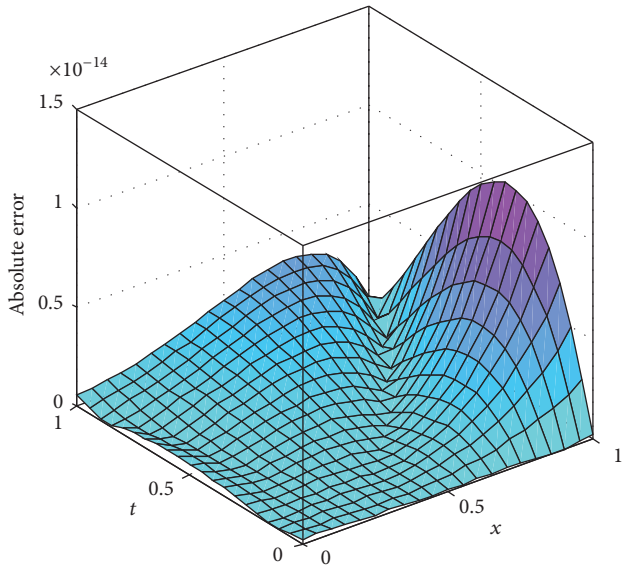

Figure 7: The absolute error for Example 3 with $m = 5$.

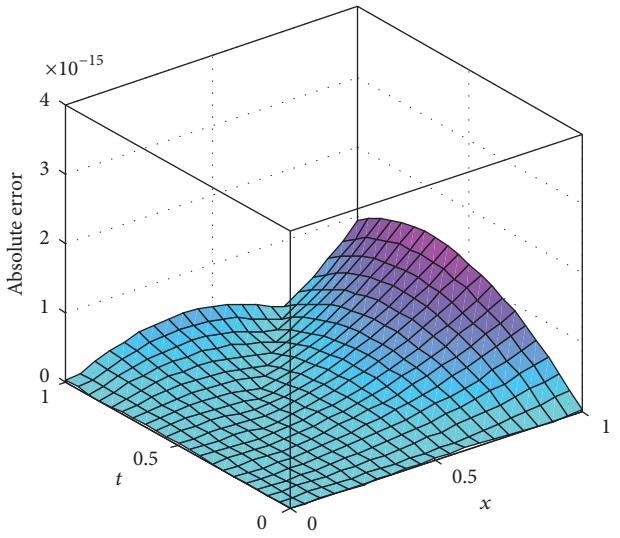

Figure 8: The absolute error for Example 3 with $m = 6$.

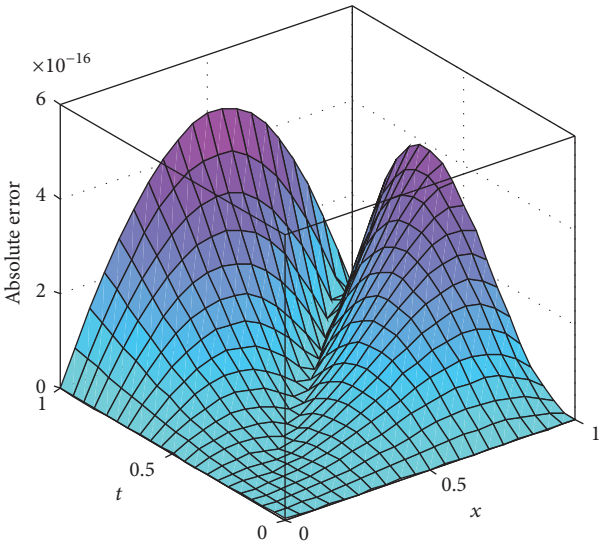

Figure 9: The absolute error for Example 3 with $m = 7$.

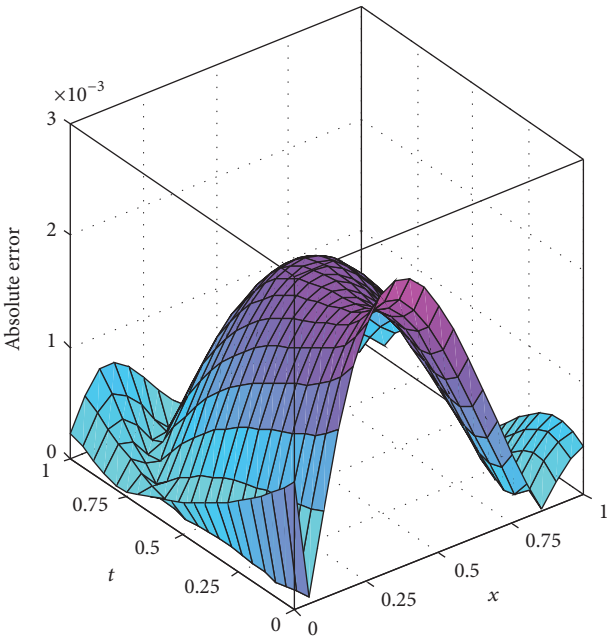

Figure 10: The absolute error for Example 3 with $m = n = 8$.

8. Conclusions

In this paper, we define a basis of FLFs and have derived its fractional differential operational matrix. The fractional derivatives are described in the Caputo sense. The matrix together with Tau method is used to effectively approximate the exact solution of fractional partial differential equations. Compared with other numerical approach, the FLFs-Tau method can accurately represent properties of fractional calculus. Moreover, only a small number of FLFs are needed to obtain a satisfactory result. Numerical results which are given in the previous section demonstrate good accuracy of the algorithm. Finally, error analysis shows that the algorithm is convergent.

Competing Interests

The authors declare that there is no conflict of interests regarding the publication of this paper.

Acknowledgments

This work was supported by Dr. Startup funds of Taiyuan University of Science and Technology (20122054).

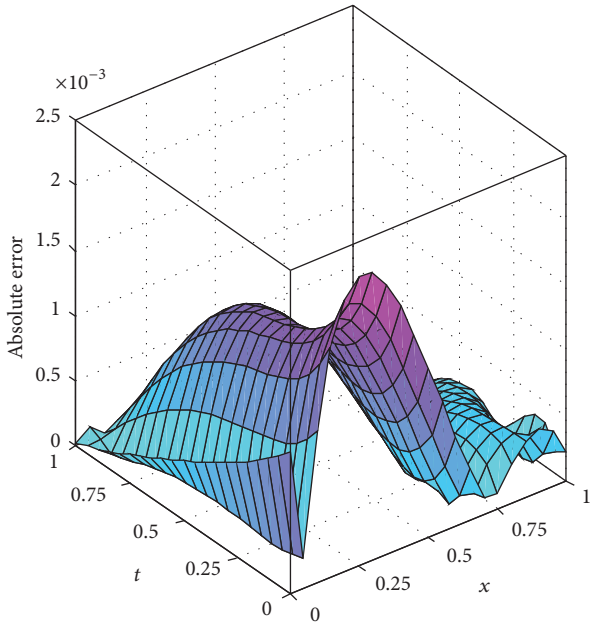

Figure 11: The absolute error for Example 3 with $m = n = 9$.

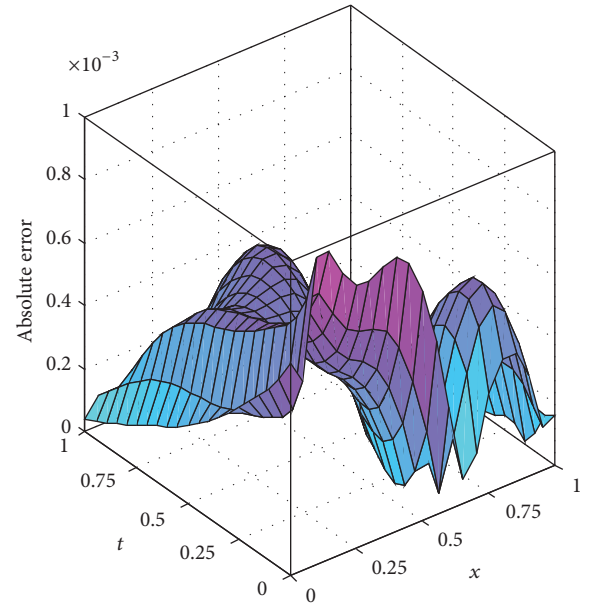

Figure 12: The absolute error for Example 3 with $m = n = 10$.

References

[1] N. Liu and E.-B. Lin, "Legendre wavelet method for numerical solutions of partial differential equations," *Numerical Methods for Partial Differential Equations*, vol. 26, no. 1, pp. 81–94, 2010.

[2] Ü. Lepik, "Solving PDEs with the aid of two-dimensional Haar wavelets," *Computers & Mathematics with Applications*, vol. 61, no. 7, pp. 1873–1879, 2011.

[3] S. Momani, Z. Odibat, and V. S. Erturk, "Generalized differential transform method for solving a space- and time-fractional diffusion-wave equation," *Physics Letters. A*, vol. 370, no. 5-6, pp. 379–387, 2007.

[4] Z. Odibat and S. Momani, "A generalized differential transform method for linear partial differential equations of fractional order," *Applied Mathematics Letters*, vol. 21, no. 2, pp. 194–199, 2008.

[5] W.-C. Tien and C.-K. Chen, "Adomian decomposition method by Legendre polynomials," *Chaos, Solitons and Fractals*, vol. 39, no. 5, pp. 2093–2101, 2009.

[6] Y. Zhang, "A finite difference method for fractional partial differential equation," *Applied Mathematics and Computation*, vol. 215, no. 2, pp. 524–529, 2009.

[7] Y. Chen, Y. Wu, Y. Cui, Z. Wang, and D. Jin, "Wavelet method for a class of fractional convection-diffusion equation with variable coefficients," *Journal of Computational Science*, vol. 1, no. 3, pp. 146–149, 2010.

[8] S. G. Venkatesh, S. K. Ayyaswamy, and S. R. Balachandar, "The Legendre wavelet method for solving initial value problems of Bratu-type," *Computers & Mathematics with Applications*, vol. 63, no. 8, pp. 1287–1295, 2012.

[9] M. Yi and Y. Chen, "Haar wavelet operational matrix method for solving fractional partial differential equations," *CMES. Computer Modeling in Engineering & Sciences*, vol. 88, no. 3, pp. 229–243, 2012.

[10] J. L. Wu, "A wavelet operational method for solving fractional partial differential equations numerically," *Applied Mathematics and Computation*, vol. 214, no. 1, pp. 31–40, 2009.

[11] F. Mohammadi and M. M. Hosseini, "A new Legendre wavelet operational matrix of derivative and its applications in solving the singular ordinary differential equations," *Journal of the Franklin Institute. Engineering and Applied Mathematics*, vol. 348, no. 8, pp. 1787–1796, 2011.

[12] Y. Li and N. Sun, "Numerical solution of fractional differential equations using the generalized block pulse operational matrix," *Computers & Mathematics with Applications*, vol. 62, no. 3, pp. 1046–1054, 2011.

[13] Z. Odibat, "On Legendre polynomial approximation with the VIM or HAM for numerical treatment of nonlinear fractional differential equations," *Journal of Computational and Applied Mathematics*, vol. 235, no. 9, pp. 2956–2968, 2011.

[14] Y. Chen, M. Yi, C. Chen, and C. Yu, "Bernstein polynomials method for fractional convection-diffusion equation with variable coefficients," *CMES. Computer Modeling in Engineering & Sciences*, vol. 83, no. 6, pp. 639–653, 2012.

[15] S. Kazem, "An integral operational matrix based on Jacobi polynomials for solving fractional-order differential equations," *Applied Mathematical Modelling*, vol. 37, no. 3, pp. 1126–1136, 2013.

[16] J. X. Wei, Y. M. Chen, and B. F. Li, "Numerical solution of space-time fractional convection-diffusion equations with variable coefficients using haar wavelets," *CMES: Computer Modeling in Engineering & Sciences*, vol. 89, no. 6, pp. 481–195, 2012.

[17] S. Z. Rida and A. M. Yousef, "On the fractional order Rodrigues formula for the Legendre polynomials," *Advances and Applications in Mathematical Sciences*, vol. 10, no. 5, pp. 509–517, 2011.

[18] M. Klimek and O. P. Agrawal, "Fractional Sturm-Liouville problem," *Computers & Mathematics with Applications*, vol. 66, no. 5, pp. 795–812, 2013.

[19] S. Kazem, S. Abbasbandy, and S. Kumar, "Fractional-order Legendre functions for solving fractional-order differential equations," *Applied Mathematical Modelling*, vol. 37, no. 7, pp. 5498–5510, 2013.

[20] M. Dehghan and A. Saadatmandi, "A tau method for the one-dimensional parabolic inverse problem subject to temperature overspecification," *Computers & Mathematics with Applications*, vol. 52, no. 6-7, pp. 933–940, 2006.

[21] Y. Chen, Y. Sun, and L. Liu, "Numerical solution of fractional partial differential equations with variable coefficients using generalized fractional-order Legendre functions," *Applied Mathematics and Computation*, vol. 244, pp. 847–858, 2014.

Hindawi Publishing Corporation
Discrete Dynamics in Nature and Society
Volume 2017, Article ID 8017510, 15 pages
http://dx.doi.org/10.1155/2017/8017510

Research Article

New JLS-Factor Model versus the Standard JLS Model: A Case Study on Chinese Stock Bubbles

Zongyi Hu and Chao Li

College of Finance and Statistics, Hunan University, Hunan, China

Correspondence should be addressed to Chao Li; 727418702@qq.com

Received 10 September 2016; Revised 30 November 2016; Accepted 14 December 2016; Published 18 January 2017

Academic Editor: Vincenzo Scalzo

Copyright © 2017 Zongyi Hu and Chao Li. This is an open access article distributed under the Creative Commons Attribution License, which permits unrestricted use, distribution, and reproduction in any medium, provided the original work is properly cited.

In this paper, we extend the Johansen-Ledoit-Sornette (JLS) model by introducing fundamental economic factors in China (including the interest rate and deposit reserve rate) and the historical volatilities of targeted and US equity indices into the original model, which is a flexible tool to detect bubbles and predict regime changes in financial markets. We then derive a general method to incorporate these selected factors in addition to the log-periodic power law signature of herding and compare the prediction accuracy of the critical time between the original and the new JLS models (termed the JLS-factor model) by applying these two models to fit two well-known Chinese stock indices in three bubble periods. The results show that the JLS-factor model with Chinese characteristics successfully depicts the evolutions of bubbles and "antibubbles" and constructs efficient end-of-bubble signals for all bubbles in Chinese stock markets. In addition, the results of standard statistical tests demonstrate the excellent explanatory power of these additive factors and confirm that the new JLS model provides useful improvements over the standard JLS model.

1. Introduction

As our understanding of the topic deepens, people are gradually realizing that the stock market is a complex system that has many participants with different characteristics that influence each other. In addition, no stock market is completely independent of another; each connects with others to form a larger system to some extent. For this reason, the stock market shows a nonlinear mechanism in its operation process. Thus, using an equilibrium model to study the stock market is not a suitable approach.

In consideration of the limitations of classical financial theory, more and more researchers are using nonlinear dynamic systems to research financial markets in the new discipline termed "econophysics." For the bubble problem in stock markets, financial physicists combine rational expectations theory in economics with the self-organizing critical phenomenon in statistical physics to diagnose the plausible times at which the bubble burst. Among them, the most representative scholars are Sornette and Johansen and coworkers, who stated that bubbles are not characterized by an exponential increase in prices but rather by a faster-than-exponential growth in prices. They also argued that most financial crashes are the climax of the so-called log-periodic power law signatures (LPPLS) associated with speculative bubbles [1].

The predictive power of LPPLS was first discovered in acoustic emissions prior to rupture and in identifying the precursors of earthquakes [2, 3]. However, the introduction of LPPLS to predict the bursting of speculative bubbles in financial markets goes back to the pioneering works of Feigenbaum and Freund [4] and Sornette et al. [5], who independently of each other disclosed LPPLS structures prior to the crash of the S&P 500 in October 1987. Beyond that, by means of extending the renormalization group approach to the second order of perturbation, Sornette and Johansen [6] proposed the second-order LPPL "Landau" model to capture the evolution of stock prices over a longer precrash period, say seven to eight years, compared with the original LPPL model. Then, they used it to fit the Dow Jones index prior to the 1929 crash and the S&P 500 index prior to the 1987 crash.

Since then, a large body of empirical evidence supporting this proposition has been presented ([7–15] (hereafter the LPPL model is also referred to as the JLS (i.e., Johansen-Ledoit-Sornette) model)). All this research has shown that the time evolutions of the stock market index prior to the 1929, 1987, and 1998 crashes on Wall Street and the 1997 crash in Hong Kong are in very good agreement with the predictions of the LPPL model.

As for the cause of the stock market crash, Johansen and Sornette [13] argued that a large crash is mainly caused by local self-reinforcing imitation between investors and their herding behavior. Under the action of the positive price-to-price feedback mechanism, this self-reinforcing imitation process eventually leads to a bubble. Specifically, if the tendency for traders to "imitate" their "friends" increases up to the "critical" point (or critical time), many traders may place the same order (sell) at the same time, thus causing a crash [13]. However, it is also worth noting that imitation between investors and their herding behavior lead not only to speculative bubbles with accelerating overvaluations of financial markets possibly followed by crashes but also to "antibubbles" with decelerating market devaluations following all-time highs. For this, Johansen and Sornette [16] proposed a third-order Landau expansion in which demand decreases slowly with barriers that progressively reduce, leading to a power law decay of the market price accompanied by decelerating log-periodic oscillations. In addition, they documented this behavior on the Japanese Nikkei stock index from 1990 and on the gold future prices after 1980, both after their all-time highs [16]. Besides, a remarkable similarity in the behavior of the US S&P 500 index from 1996 to August 2002 and of the Japanese Nikkei index from 1985 to 1992 (11-year shift) was presented by Sornette and Zhou [17]. Several other examples have been described in the Russian stock market (Sornette et al., 1999) and in emerging and western markets [17–19]. Among them, authors have analyzed 39 world stock market indices from 2000 to the end of 2002, finding that 22 are in an antibubble regime (owing to the criterion of obtaining at least a solution in the fitting procedure, they have found no evidence of an antibubble in China during that period). However, although this third-order LPPL Landau model is suitable for describing the evolution of bubbles and antibubbles almost twelve years, some deviations may appear when using the second-order LPPL Landau model to calibrate antibubbles, implying that much higher-order Landau models are useless.

In addition to the third-order LPPL Landau model, Sornette and coworkers expanded the original LPPL model, including (a) constructing the Weierstrass-type LPPL model [20, 21], (b) extending the JLS model with second-order harmonics [17], (c) proposing the JLS-factor model in which the LPPL bubble component is augmented by fundamental economic factors [22], (d) inferring the fundamental value of the stock and crash nonlinearity from bubble calibration [23] and detecting market rebounds [24], (e) extending the JLS model to include an additional pricing factor called the "Zipf factor," which describes the diversification risk of stock market portfolio [25], (f) reducing the JLS model to a function of only three nonlinear parameters [26], (g) presenting a volatility-confined LPPL model to describe and diagnose situations when excessive public expectations of future price increases cause prices to be temporarily elevated [27], (h) introducing quantile regression to the LPPLS detection problem and defining the so-called DS LPPLS Confidence and Trust indicators that enrich considerably the diagnosis of bubbles [28] (recently, Zhang et al. [29] added two new indicators (DS LPPLS Bubble Status and End-of-Bubble) into this system), (i) employing a rigorous likelihood approach and providing interval estimates of the parameters, including the most important critical times of market regime changes [30], and (j) presenting a plausible microfounded model for the previously postulated power law finite time singular form of the crash hazard rate in the JLS model of rational expectation bubbles [31]. In addition, the research team at ETH Zurich has further developed an LPPLS-based bubble detection system, as described in Sornette et al. [32] and Zhang et al. [28].

However, although the JLS model has been extended to many different forms, the original model remains a powerful and flexible tool with which to detect financial bubbles and crashes in various markets, especially Chinese stock bubbles. Examples include the antibubble in China's stock market that started in August 2001 [33], two bubbles and subsequent market crashes in two important indices of Chinese stock markets (Shanghai Stock Exchange Composite (SSEC) index and Shenzhen Stock Exchange Component (SZSC) index) between May 2005 and July 2009 [34], two well-known Chinese stock bubbles, from August 2006 to October 2007 (bubble 1) and from October 2008 to August 2009 (bubble 2) [25], and the bubble regime that developed in Chinese stock markets in mid-2014 and started to burst in June 2015 [32].

Unfortunately, the JLS model is based on the assumption that crashes are the outcome of the interactions of market players resulting in herding behavior (i.e., an endogenous origin), while exogenous shocks (due to changes in market fundamentals) rarely play an important role, only serving as trigger factors, which is at odds with standard economy theory [35]. Although Zhou and Sornette [22] presented a general methodology under which to incorporate fundamental economic factors (e.g., interest rate, interest spread, historical volatility, implied volatility, and exchange rates) into the theory of herding to describe bubbles and antibubbles, the most surprising result is that the best model is the second-order LPPL model without any factors. Indeed, the evolution of a complex system is the result of an entangled combination of endogenous organization as well as a response to external news and exogenous shocks, especially for an equity market such as the Chinese stock market that is still immature and heavily influenced by exogenous shocks. Compared with western markets, the Chinese stock market has its own characteristics, including the following: (i) being dominated by individual investors, (ii) being highly volatile, (iii) nontradability of more than two-thirds of the shares, (iv) short sale constraints, (v) response to exogenous information such as government policies, a firm's accounting information, and stock exchange announcements, (vi) stronger imprints of herding, (vii) overspeculation, (viii) overvaluation of markets, (ix) widely taken short-term positions, (x) insider

trading, and (xi) a distempered regulation system [33, 36]. These specific features make the market exhibit strong idiosyncrasies and puzzles in addition to the more common behavior of mature stock markets [37]. Therefore, in addition to the herding behavior between traders, we think that taking into account the influence of government policies and other exogenous shocks on the evolution of Chinese stock bubble may be more advisable, especially the impact from changes in monetary policy and fluctuations in international stock markets.

Given the foregoing, we generalize the standard JLS model by incorporating two fundamental economic factors in China (i.e., the interest rate and deposit reserve rate) and the historical volatility of targeted and US equity indices into the original model. We then present an ex-post analysis of what Jiang et al. [34] and Sornette et al. [32] earlier identified as being the three significant bubbles developing in major Chinese stock markets: the first bubble ran from July 2005 to October 2008, the second one ran from November 2008 to August 2009, and the third one ran from March 2014 to July 2015. We also compare the prediction accuracy of the critical time between the original and the new JLS model (i.e., the JLS-factor model). The empirical results show that the JLS-factor model with Chinese characteristics successfully diagnoses all the well-documented bubbles in Chinese stock markets. Further, by comparing the prediction accuracy of the original and new JLS models, we find that the critical time estimated by the new JLS model for Chinese stock market bubbles during 2005–2015 is closer to the actual time than the original JLS model in general, which demonstrates the excellent explanatory power of our proposed JLS-factor model. In addition, the results of different standard statistical tests show that the new JLS model is superior to the original JLS model. Moreover, the results of significance testing provide indirect evidence on the key role of fundamental economic and exogenous factors in China affecting the evolution of Chinese stock bubbles (except the 2008–2009 bubbles, which were probably punctuated by a vanishingly small change in some endogenous factors).

The remainder of this paper is structured as follows. In Section 2, we summarize the mathematical formulation of the original JLS model, while the extended JLS model is introduced in Section 3. Section 4 presents the construction of the JLS-factor model with Chinese characteristics. Section 5 describes the tests of six documented Chinese stock bubbles by using the new JLS model and the original model and compares their respective predictive power. Section 6 shows the significance test results of the original and new JLS models. Section 7 summarizes our conclusions.

2. Mathematical Formulation of the JLS Model

In this section, we recall the formation of the original JLS model, which provides a flexible framework within which to detect bubbles and predict regime changes in the price time series of a financial asset. It combines (i) the economic theory of rational expectation bubbles, (ii) behavioral finance on imitation and herding of noise traders, and (iii) the mathematical and statistical physics of bifurcations and phase transitions. The model considers the faster-than-exponential (power law with finite time singularity) increase in asset prices accompanied by accelerating oscillations as the main diagnostic of bubbles. It thus embodies a positive feedback loop of higher return anticipations competing with the negative feedback spirals of crash expectations [23].

Within the JLS framework, expected price $p(t)$ conditioned on no crash occurring is obtained as follows (see Zhou and Sornette [22], for the concrete derivation of the model):

$$E_{t_0}\left[p\left(t\right)\right] = p\left(t_0\right) L\left(t\right) \exp\left[\kappa \int_{t_0}^{t} h\left(\tau\right) d\tau\right], \tag{1}$$

where $L(t) = \exp\{\int_{t_0}^{t} [r(\tau) + \sigma(\tau)\varphi(\tau)]d\tau\}$, $r(t)$ is the interest rate, $\sigma(t)$ is the price volatility, $\varphi(t)$ is the market price of risk of the stochastic discount factor, and $h(t)$ is the crash hazard rate, namely, the probability per unit time that the crash will happen in the next instant if it has not yet happened.

For $r(t) = \varphi(t) = 0$ and $L(t) = 1$, we have

$$E_{t_0}\left[p\left(t\right)\right] = p\left(t_0\right) \exp\left[\kappa \int_{t_0}^{t} h\left(\tau\right) d\tau\right]. \tag{2}$$

Johansen et al. [14] proposed that a crash may be caused by local self-reinforcing imitation processes between noise traders that can be quantified by the theory of critical phenomena developed in the physical sciences. Hence, they assumed that the aggregate effect of noise traders can be quantified by the following dynamics of the crash hazard rate:

$$h\left(t\right) = B' x^{m-1} + C' x^{m-1} \cos\left(\omega \ln x - \phi'\right), \tag{3}$$

where $x = |t_c - t|$, t_c is the critical time (i.e., the most probable time for the bursting of the bubble), ω is the angular log-frequency, and $\phi' \in [0,\ 2\pi]$ is an initial phase determining the unit of the time. Generalizing the definition of $t_c - t$ into $|t_c - t|$ allows for the critical time t_c to lie anywhere within the time series, which has the advantage of introducing a degree of flexibility into the search space for t_c with little additional cost [17].

The power law behavior x^{m-1} embodies the mechanisms of positive feedback at the origin of the formation of a bubble, while the cosine term on the RHS of (3) takes into account the existence of a possible hierarchical cascade of panic acceleration punctuating the course of the bubble, resulting from either a preexisting hierarchy in noise trader sizes and/or the interplay between market price impact inertia and nonlinear fundamental value investing [23].

Substituting (3) into (2) and integrating yields the LPPL equation for the price:

$$\ln\left[p\left(t\right)\right] = A + Bx^{m} + Cx^{m} \cos\left(\omega \ln x - \phi\right), \tag{4}$$

where $A = \ln[p(t_c)]$, which gives the terminal log-price at the critical time t_c. $B = -(\kappa/m)B'$ and $C = -(\kappa/\sqrt{m^2 + \omega^2})C'$, respectively, control for the amplitude of the power law acceleration and the log-periodic oscillations. The exponent m quantifies the degree of superexponential growth. ω is the angular log-frequency. ϕ is another phase different to ϕ' that

contains two ingredients: information on the mechanism of the interactions between investors and a rescaling of time. The power law with exponent x^m captures the faster-than-exponential growth in the price and the term $\cos(\omega \ln x - \phi)$ describes the accelerating oscillation decorating the accelerating price. Further, although additional constraints emerge from a compilation of a significant number of historical bubbles that can be summarized as $0.1 \le m \le 0.9$, $6 \le \omega \le 13$ [26], Zhang et al. [28] found larger search ranges $m \in [0, 2]$ and $\omega \in [1, 50]$ from their research on sixteen historical bubbles.

A more general JLS model can be expressed as

$$I(t) = A + Bx^m + Cx^m \cos(\omega \ln x - \phi). \tag{5}$$

Theoretically, the order parameter $I(t)$ can be the price $p(t)$ or the logarithm of price $\ln[p(t)]$, while which one is reasonable to be the dependent variable is dependent on the following criterion. Zhou and Sornette [33] proposed that the observed price is the sum $p(t) = F(t) + M(t)$ of a fundamental price $F(t)$ and of a bubble or an antibubble $M(t)$. They had $I(t) = p(t)$ when $F(t) \ll M(t)$ and $I(t) = \ln[p(t)]$ when $F(t) \sim M(t)$. In fact, based on the rational bubble model of Johansen et al. [14] and Johansen et al. [38], if the magnitude of the crash is proportional to the price increase only associated with the contribution of the bubble, then the correct proxy is the price itself; on the contrary, if the magnitude of the crash is proportional to the price, then the correct proxy is the logarithm of the price [39]. From a theoretical view point, this is unsurprising: the rational expectation model of bubbles and crashes shows that, depending on whether the size of the crash is proportional to the price itself or that of the increase due to the bubble, either the logarithm of the price or the price itself is the correct quantity characterizing the bubble [12].

For the sake of simplicity, let us rewrite (5) in the following form:

$$y(t) = A + Bf(t) + Cg(t), \tag{6}$$

where

$$\begin{aligned} y(t) &= \ln[p(t)] \text{ or } p(t), \\ A &= \ln[p(t_0)], \\ f(t) &= |t_c - t|^m, \\ g(t) &= |t_c - t|^m \cos(\omega \ln|t_c - t| - \phi). \end{aligned} \tag{7}$$

3. Extended JLS Model

The common JLS model is the specific form when $r(t) = \varphi(t) = 0$, as mentioned above. However, $r(t)$ and $\varphi(t)$ do not equal zero in the real world. Thus, we extend the original JLS model locally. Similar to Zhou and Sornette [22], we assume that $\varphi(t)$ is a constant φ, which does not change over time. Moreover, we take the true values of $r(t)$ and $\sigma(t)$ to calibrate the model. Specifically, we specify $r(t)$ as the risk-free interest rate and employ the historical volatility of the targeted asset as a proxy for the volatility factor $\varphi(t)$. All daily data come from the iFinD database.

Through the above extension, the original JLS model can be converted into the following form:

$$y(t) = A + Bf(t) + Cg(t) + \alpha r(t) + \varphi v(t), \tag{8}$$

where

$$\begin{aligned} y(t) &= \ln[p(t)] \text{ or } p(t), \\ A &= \ln[p(t_0)], \\ f(t) &= |t_c - t|^m, \\ g(t) &= |t_c - t|^m \cos(\omega \ln|t_c - t| - \phi), \\ r(t) &= \int_{t_0}^{t} r(\tau)\, d\tau, \\ v(t) &= \int_{t_0}^{t} \sigma(\tau)\, d\tau, \\ \sigma(t) &= \sqrt{\frac{\sum_{t=1}^{n} (p_t - \overline{p})^2}{(n-1)}}, \end{aligned} \tag{9}$$

p_t is the day logarithm yield of the targeted asset, $\overline{p}$ is the average yield, $r(\tau)$ represents the risk-free interest rate, and $\sigma(\tau)$ denotes the historical volatility of the targeted asset.

However, the above model is only a local extension in view of the general JLS model. For Chinese stock markets, the influence of macroeconomic factors, national policy, and the international economic situation on the stock market must be accounted for, except for the impact of the positive feedback effect caused by investors' herding behavior. Therefore, we study the important factors that affect the volatility of Chinese stock indices in the next section and add these to the extended JLS model to construct a new JLS model (i.e., the JLS-factor model), which is suitable for China.

4. JLS-Factor Model with Chinese Characteristics

Owing to their inherent characteristics and drawbacks, Chinese stock markets are more easily affected by changes in monetary policy and fluctuations in international stock markets than mature markets. Hence, in this section, we analyze the impact of these two factors on Chinese stock market volatility and then construct a new JLS-factor model to calibrate the well-known Chinese stock bubbles.

First, the effect of monetary policy, mainly implemented by adjusting the interest rates, deposit reserve rate, and money supply, and so on, on a country's capital market has long been examined in agroscientific research globally. Theoretically, in the context of the transmission mechanism, monetary policy affects stock prices mainly through both the traditional interest rate channel [40] and the credit channel [41]. A number of empirical studies have applied different proxy variables to assess the effects of monetary policy shocks on stock market volatility, including the discount rate [42–45] (Mercer and Johnson, 1996), Federal Funds rate [46–54],

interest rate [55–62] (Octavioet al., 2013), money supply [63–66], and Federal Funds futures [67–75].

Compared with foreign scholars' research, abundant works in China have assessed the relationship between the deposit reserve rate and stock market (e.g., [76–87]). All this research argues that, after changing the supply of money, the variation in the deposit reserve rate causes stock prices to change in the following four ways: (i) the effect of the market interest rate, (ii) the effect of credit scale, (iii) the effect of market structure, and (iv) the effect of stock market announcements. On the one hand, the variation in the deposit reserve rate tends to directly affect the money supply of the whole society and thus changes the capital supply to the stock market and, ultimately, the evolution of stock prices. On the other hand, as a policy signal, the adjustment in the deposit reserve rate significant affects investors' psychological expectations and thus their investment strategies and, ultimately, the evolution of stock prices. Unfortunately, early research into the relationship between swings in the deposit reserve rate and fluctuation in stock prices provided mixed results, finding no consistent relationship between these two variables and that the nature of such dynamics was unstable. From the above, a change in the deposit reserve rate is thus a factor that can affect asset prices. Therefore, we take into account its effect on the evolution of Chinese stock bubbles.

Second, as China has gradually opened up its stock market to foreign investments and cross-border listings, the comovement between the Chinese and the international stock market is increasingly strengthening. Indeed, in extreme cases such as the global financial crisis, such comovement is significantly enhanced given the deterioration of global economic fundamentals and the risk contagion among international financial markets [88, 89]. However, among all international stock markets, domestic research shows that stock price fluctuations in the United States have a more remarkable impact on that in China than others (e.g., [90–96], Hu, 2010). In particular, Zhang et al. [97] and Pan and Liu [98] found that the volatility of US stock indices can be used to predict the trend of Chinese stock prices.

Given the foregoing, we take into account the impact of the deposit reserve rate and US stock index volatility on the evolution of Chinese stock bubbles when constructing the new JLS model. Therefore, we have

$$y(t) = A + Bf(t) + Cg(t) + \alpha r(t) + \beta r_c(t) + \varphi v(t) + \gamma v_a(t), \tag{10}$$

where

$$\begin{aligned} y(t) &= \ln[p(t)] \text{ or } p(t), \\ A &= \ln[p(t_0)], \\ f(t) &= |t_c - t|^m, \\ g(t) &= |t_c - t|^m \cos(\omega \ln|t_c - t| - \phi), \\ r(t) &= \int_{t_0}^{t} r(\tau)\, d\tau, \\ r_c(t) &= \int_{t_0}^{t} r_c(\tau)\, d\tau, \\ v(t) &= \int_{t_0}^{t} \sigma(\tau)\, d\tau, \\ v_a(t) &= \int_{t_0}^{t} \sigma_a(\tau)\, d\tau, \end{aligned} \tag{11}$$

$r(\tau)$ is the risk-free interest rate, $r_c(\tau)$ represents the deposit reserve rate, and $\sigma(\tau)$ and $\sigma_a(\tau)$ are specified as the volatility of the targeted index and NASDAQ, respectively (the NASDAQ Composite Index is a barometer of market value changes in each industrial category, as it includes more than 5000 companies, which is more than any other single securities market. As a result, the NASDAQ Composite Index is more representative than the S&P 500 index and Dow Jones Industrial Average).

Because the specific function forms of $r(\tau)$, $r_c(\tau)$, $\sigma(\tau)$, and $\sigma_a(\tau)$ cannot be determined, we use the trapezoid scheme to integrate $r(t)$, $r_c(t)$, $v(t)$, and $v_a(t)$ in practice, following Zhou and Sornette [22]. That is, we let

$$\begin{aligned} \int_{t_0}^{t} r(\tau)\, d\tau &\approx \sum_{\tau=t_0+1}^{t} \frac{[r(\tau-1) + r(\tau)]}{2}, \\ \int_{t_0}^{t} r_c(\tau)\, d\tau &\approx \sum_{\tau=t_0+1}^{t} \frac{[r_c(\tau-1) + r_c(\tau)]}{2}, \\ \int_{t_0}^{t} \sigma(\tau)\, d\tau &\approx \sum_{\tau=t_0+1}^{t} \frac{[\sigma(\tau-1) + \sigma(\tau)]}{2}, \\ \int_{t_0}^{t} \sigma_a(\tau)\, d\tau &\approx \sum_{\tau=t_0+1}^{t} \frac{[\sigma_a(\tau-1) + \sigma_a(\tau)]}{2}. \end{aligned} \tag{12}$$

5. Results of the Original and New JLS Models

To visually compare the prediction accuracy of the results of the original and new JLS models, in this section, we calibrate the evolutions of two well-known Chinese stock indices (SSEC and SZSC) in three time periods, as selected by two published papers (i.e., [32, 34]) that applied the original JLS model to fit the tendency of these two indices in the corresponding periods. By observing the minimum and maximum values among the targeted indices within the specified periods, we find that the average annual growth rate is 244.55%. This finding implies that the fundamental price $F(t)$ should be much less than the bubble $M(t)$ according to Zhou and Sornette's [33] assumption. In the next step, we employ our JLS-factor model presented in (10) to fit these two indices within the same three periods with $y(t) = p(t)$.

Each calibration uses the algorithm of Universal Global Optimization provided by 1stOpt (First Optimization) software, which has been independently developed by 7D-Soft High Technology Inc. to solve any constrained or unconstrained linear and nonlinear equation(s). This software allows us to estimate all parameters (t_c, ω, m, ϕ, A, B, C, α, β,

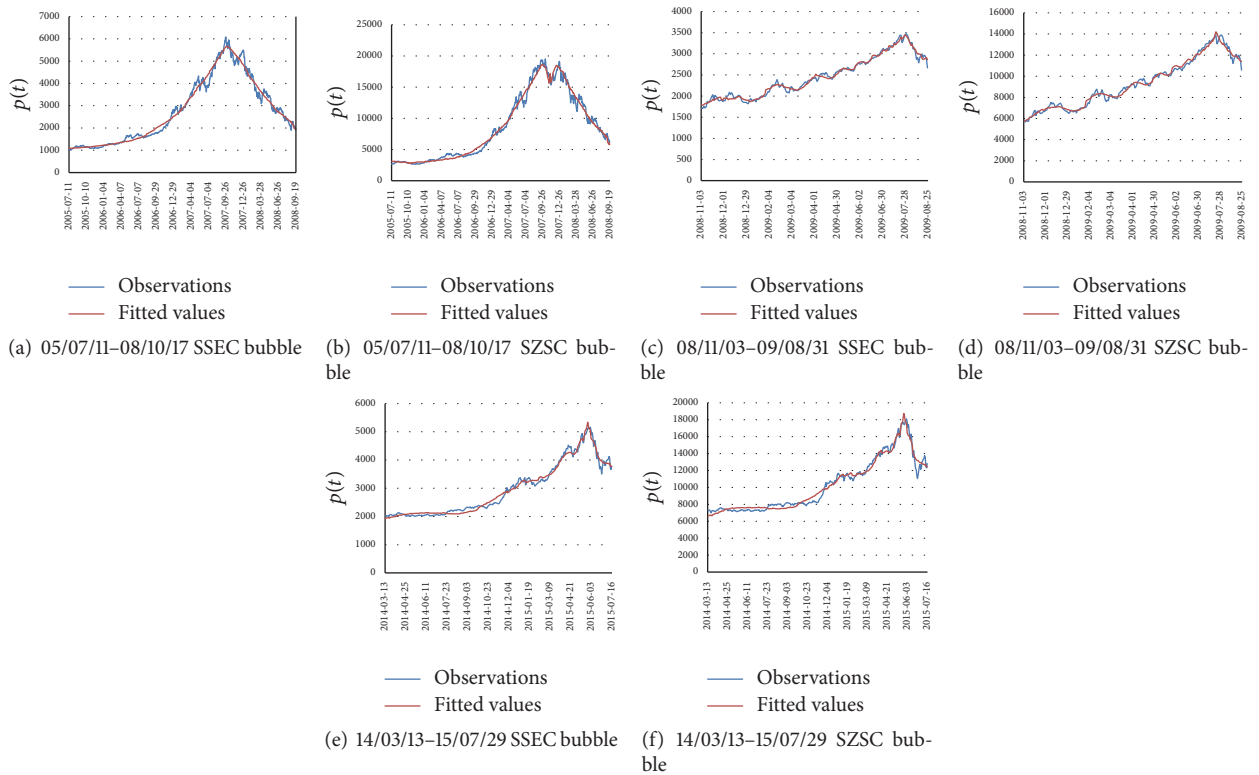

(a) 05/07/11–08/10/17 SSEC bubble

(b) 05/07/11–08/10/17 SZSC bubble

(c) 08/11/03–09/08/31 SSEC bubble

(d) 08/11/03–09/08/31 SZSC bubble

(e) 14/03/13–15/07/29 SSEC bubble

(f) 14/03/13–15/07/29 SZSC bubble

Figure 1: Daily trajectory of the SSEC and SZSC from 2005/07/11 to 2015/07/29 by using the JLS-factor model presented in (10) with $y(t) = p(t)$. The fit of SSEC from 2005/07/11 to 2008/10/17 is illustrated in (a) as a red solid line, whose parameters are $t_c = 2007/10/16$, $\omega = 0.03$, $m = 1.89$, $\phi = 0.03$, $A = 4971.87$, $B = -4809410.22$, $C = 4808854.92$, $\alpha = 215.66$, $\beta = -32.46$, $\varphi = -25.11$, and $\gamma = 0.20$ with an r.m.s. of the fit residuals $\chi = 193.04$. The fit of SZSC from 2005/07/11 to 2008/10/17 is illustrated in (b) as a red solid line, whose parameters are $t_c = 2007/11/26$, $\omega = 1.26$, $m = 0.31$, $\phi = 3.48$, $A = 14926.14$, $B = -7159.59$, $C = 6083.23$, $\alpha = -320.05$, $\beta = 92.46$, $\varphi = 39.43$, and $\gamma = 2.73$ with an r.m.s. of the fit residuals $\chi = 643.26$. The fit of SSEC from 2008/11/03 to 2009/08/31 is illustrated in (c) as a red solid line, whose parameters are $t_c = 2009/08/03$, $\omega = 17.46$, $m = 0.45$, $\phi = 2.14$, $A = 3357.54$, $B = -2150.17$, $C = -122.12$, $\alpha = 74.22$, $\beta = 37.78$, $\varphi = -83.33$, and $\gamma = -0.33$ with an r.m.s. of the fit residuals $\chi = 60.49$. The fit of SZSC from 2008/11/03 to 2009/08/31 is illustrated in (d) as a red solid line, whose parameters are $t_c = 2009/08/03$, $\omega = 17.28$, $m = 0.53$, $\phi = 4.80$, $A = 13437.80$, $B = -10004.44$, $C = 627.84$, $\alpha = 132.05$, $\beta = 66.10$, $\varphi = -56.60$, and $\gamma = -0.25$ with an r.m.s. of the fit residuals $\chi = 282.30$. The fit of SSEC from 2014/03/13 to 2015/07/29 is illustrated in (e) as a red solid line, whose parameters are $t_c = 2015/06/08$, $\omega = 5.50$, $m = 0.39$, $\phi = 1.09$, $A = 5884.95$, $B = -4081.11$, $C = 316.83$, $\alpha = 105.11$, $\beta = 10.50$, $\varphi = -115.53$, and $\gamma = -0.14$ with an r.m.s. of the fit residuals $\chi = 119.37$. The fit of SZSC from 2014/03/13 to 2015/07/29 is illustrated in (f) as a red solid line, whose parameters are $t_c = 2015/06/08$, $\omega = 5.63$, $m = 0.34$, $\phi = 3.99$, $A = 13809.61$, $B = -15604.59$, $C = -1027.34$, $\alpha = -2.62$, $\beta = 535.60$, $\varphi = -392.55$, and $\gamma = -0.84$ with an r.m.s. of the fit residuals $\chi = 486.32$.

φ, and γ) in a given time window of analysis without inputting the initial values. The main results of our calibrations for the evolutions of the 2005–2008, 2008-2009, and 2014-2015 bubbles are illustrated in Figure 1.

As shown in Figure 1, the six fits are very close to the real trajectories of the SSEC and SZSC bubbles, which intuitively shows the superiority of our JLS-factor model. Further, we employ the 1stOpt software again to calibrate the evolutions of the SSEC and SZSC bubbles in the same periods with the original JLS model and compare the estimation accuracies of critical times between the original and new JLS models. The results are shown in Tables 1 and 2.

Tables 1 and 2 show that the estimated accuracy of the critical time by the new JLS model is in general better than that of the original JLS model, except for the 2005–2008 SZSC bubble. In particular, for the 2005–2008 and 2008-2009 SSEC bubbles and the 2008-2009 SZSC bubble, the estimation results of the new JLS model agree well with the actual time at which the bubble burst. Figure 1(b) shows that the 2005–2008 SZSC bubble peaked twice in just two and a half months, which may have been the main cause of the low estimated accuracy.

Recall the setting of $x = |t_c - t|$ above. Two potential problems are associated with this procedure if an antibubble exists during the bubble period. First, it implies that the antibubble is always associated with a bubble which, in addition, has the same t_c. Second, it implies that the bubble and antibubble are symmetric around t_c; that is, the same parameters characterize the index evolution for $t < t_c$ and for $t > t_c$[17]. However, two peaks existed in the evolution of the 2005–2008 SZSC bubble showed in Figure 1(b), and the low estimated accuracy calculated by using both the new and the original JLS models may imply two different t_c during this period: one is the critical time corresponding to the

Table 1: Prediction of the critical time of the SSEC bubbles burst for both models and their differences with the actual times of bubble burst.

Item	Estimated time interval		
	2005/7/11–2008/10/17	2008/11/3–2009/8/31	2014/3/13–2015/7/29
The actual time of bubble burst	2007/10/16 (t_c = 107.79)	2009/8/4 (t_c = 109.59)	2015/6/12 (t_c = 115.45)
The predicted critical time of the original JLS model	2007/10/26 (t_c = 107.82)	2009/7/28 (t_c = 109.57)	2015/5/11 (t_c = 115.36)
The difference between the original JLS model and actual time (days)	−10	7	30
The predicted critical time of the new JLS model	2007/10/16 (t_c = 107.79)	2009/8/3 (t_c = 109.59)	2015/6/8 (t_c = 115.43)
The difference between the new JLS model and actual time (days)	0	1	4

Value in parentheses is the predicted critical time t_c.

Table 2: Prediction of the critical time of the SZSC bubbles burst for both models and their differences with the actual times of bubble burst.

Item	Estimated time interval		
	2005/7/11–2008/10/17	2008/11/3–2009/8/31	2014/3/13–2015/7/29
The actual time of bubble burst	2007/10/31 (t_c = 107.83)	2009/8/4 (t_c = 109.59)	2015/6/12 (t_c = 115.45)
The predicted critical time of the original JLS model	2007/11/22 (t_c = 107.89)	2009/7/28 (t_c = 109.57)	2015/6/3 (t_c = 115.42)
The difference between the original JLS model and actual time (days)	−22	7	9
The predicted critical time of the new JLS model	2007/11/26 (t_c = 107.90)	2009/8/3 (t_c = 109.59)	2015/6/8 (t_c = 115.43)
The difference between the new JLS model and actual time (days)	−26	1	4

Value in parentheses is the predicted critical time t_c.

bursting of a bubble, while the other marks the inception of an antibubble. Hence, we conduct a Lomb analysis, using a parametric detrending approach, to detect the log-periodic oscillations accompanied by the 2007/11/29–2008/10/17 SZSC antibubble (here, we only employ the Lomb analysis to detect the log-periodic oscillations accompanied by an antibubble; the analysis method for a bubble is the same).

Following Zhou and Sornette [33], the assumption that a critical point at the inception of an antibubble exists can be tested by investigating two possible signatures of a critical behavior: a power law relaxation and log-periodic wobbles. Firstly, we test the power law relaxation of the 2007/11/29–2008/10/17 SZSC bubble.

The power law expression for an antibubble reads

$$I(t) = A + B\left|t - t_c\right|^m, \tag{13}$$

where t_c is an estimate of the inception of the antibubble and the order parameter $I(t)$ can be price $p(t)$ or its logarithm $\ln[p(t)]$. If $0 < m < 1$, $I(t)$ is finite; however, its first derivative $I'(t)$ is singular at t_c and B should be negative to ensure that $I(t)$ decreases.

According to the specific characteristics of the 2007/11/29–2008/10/17 SZSC bubble, we only fit it by using the power law formula (13) with $I(t) = p(t)$, whose parameters are t_c = 2008/01/10, m = 0.74, A = 18732, and B = −15108.07 with an r.m.s. of the fit residuals χ = 706.80. According to the fitted values of m and B, we can conclude that the 2007/11/29–2008/10/17 SZSC bubble meets the signature of power law relaxation.

As for the detection of log-periodic oscillations, this is conveniently performed by removing the global trend of the index. One way is to subtract the power law fit (13) from the index and then analyze the wobbles of the obtained residuals $s(t)$ by adopting an adequate spectral analysis. Similarly, we construct the residuals $s(t)$ in the following way:

$$s(t) = \frac{[p(t) - A]}{\left|t - t_c\right|^m}, \tag{14}$$

where A, m, and t_c are obtained from the fit of the pure power law formula (13) to the data.

As implemented in Zhou and Sornette [19, 33], we also use a Lomb periodogram analysis of residuals $s(t)$ to assess the statistical significance level of the extracted log-periodicity. The Lomb periodogram of $s(t)$ is shown in Figure 2.

As shown in Figure 2, the highest peak is at ω = 3.91 with height $P_n(\omega) = 3.05 \times 10^6$. This strong significant peak of the periodogram qualifies the existence of log-periodicity. More precisely, we can employ the false alarm probability P_r (false alarm probability is the chance that we falsely detect log-periodicity in a signal without true log-periodicity) to obtain the statistical significance level of the extracted log-periodicity. Under the null hypothesis of i.i.d. Gaussian fit residuals, P_r is zero [99]. However, assuming an i.i.d. structure is too restrictive as the fit residuals usually have some correlations. If the residuals have long range correlations characterized by a Hurst index H, we can use Zhou and Sornette's [100] computational method of P_r for various values of $H > 1/2$ to obtain the statistical significance

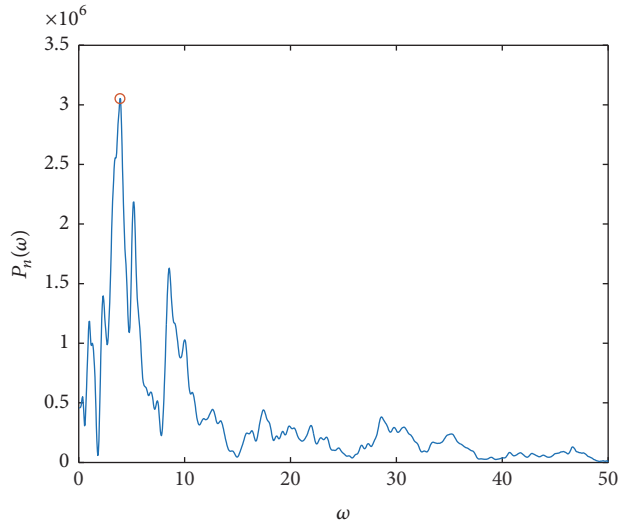

FIGURE 2: The Lomb periodogram analysis of $s(t)$, where $P_n(\omega)$ is a normalized Lomb power (since $P_n(\omega)$ is a normalized Lomb power, $s(t)$ and $[s(t) - \mu_s]/\sigma_s$ have identical Lomb periodogram, where μ_s and σ_s^2, resp., denote the mean and variance of this residuals $s(t)$) and ω is the log-angular frequency.

level of the extracted log-periodicity. For example, if $H = 0.6$, the false alarm probability corresponding to the observed peak $P_n(\omega) = 3.05 \times 10^6$ is $P_r < 10^{-10}$; if $H = 0.7$, it is $P_r < 10^{-8}$; if $H = 0.8$, it is $P_r < 10^{-7}$; and if $H = 0.9$, it is $P_r < 10^{-6}$. All of these mean that the statistical significance of log-periodicity is very high.

From the above, we can conclude that the 2007/11/29–2008/10/17 SZSC bubble is indeed an antibubble. Therefore, we separate the 2005–2008 SZSC bubble into two periods, namely, the 2005/11/15–2007/11/28 SZSC bubble and the 2007/11/29–2008/10/17 SZSC antibubble. Then, we fit these two bubbles by using both the new and original JLS models. The calibrations of these two SZSC bubbles are shown in Figure 3, while the comparison results for both models are shown in Table 3.

Table 3 shows that the prediction result of the 2005–2007 SZSC bubble by using the new JLS model is unsatisfactory; however, it is slightly better than the estimation result of the original JLS model. Meanwhile, the critical time estimated by using the new JLS model for the SZSC antibubble for 2007-2008 is very close to the actual time, which shows that the predictive power of the new JLS model is superior to that of the original model. These results demonstrate that the new JLS model quantifies the time evolution of Chinese stock bubbles remarkably well in terms of the price ending with a crash or a large correction at a time close to the critical time.

Moreover, the corresponding parameters for our calibrations for the evolutions of the 2005–2008, 2008-2009, and 2014-2015 bubbles are listed in Table 4 for comparison purposes.

As shown in Table 4, all the coefficients B are negative, which qualifies that these indices are in the bubble (or antibubble) regime [18]. Among the other parameter values, note that only the power law exponents m of the indices of 05/07/11–08/10/17 SSEC and 05/11/15–07/11/28 SZSC are significantly larger than 1, while the others are between 0 and 1. In the absence of log-periodic oscillations, large values of $m > 1$ imply a relatively steep upward overall acceleration of the index, while $0 < m < 1$ would mean that the overall shape of these indices shows less rapid dynamics. In addition, from the fitting results of 05/07/11–08/10/17 SSEC and 05/11/15–07/11/28 SZSC, we can find that when m are significantly larger than 1 and the angular frequency ω of the log-periodic oscillations is too small, price $p(t)$ will be compensated by a large amplitude of the power law acceleration and log-periodic oscillations; that is, the values $|B|$ and C will be larger. Finally, the effects of the risk-free interest rate, the deposit reserve rate, the volatility of the targeted index, and NASDAQ on price $p(t)$ are by and large inconsistent. This may be because the influences of these exogenous factors on the evolution of bubbles are different in different periods and the reactions of different indices to the same exogenous factors are different as the stock market is a complex system. However, it is interesting to note that this happens to indirectly reflect the instability of the Chinese stock market. Relatively speaking, the effect of the volatility of NASDAQ on price $p(t)$ is smaller than that of the others. Possible reasons for this include the hysteresis of the contagion effect and the lack of synchronicity between the economic cycles of these two countries. By contrast, it also implies that comovements between the Chinese and the US stock markets exist, although this relationship is still weak.

6. Significance Testing of the JLS-Factor Model

In the following, we compare the performances of these fits between the new and original JLS models by using three statistical criteria (i.e., AIC, SC, and HQC). We also test the significance level of the two exogenous factors in the new JLS model, namely, the deposit reserve rate and volatility of NASDAQ. Ideally, these tests require that the fitting residuals are i.i.d. with Gaussian distributions. In reality, the residuals have remaining dependence structures at small scales. As a consequence, the standard statistical significance of the above tests cannot be read from Gaussian statistics tables. Nevertheless, these tests provide useful diagnostics to gauge the relative (rather than absolute) performance of competing models and are thus instructive to identify models [22]. The test results are shown in Tables 5–7.

These tables show that the new JLS model performs better than the original JLS model in all cases according to both the adjusted R-square values and the three test statistics. In addition, according to the significant degree of corresponding coefficients of the deposit reserve rate and volatility of NASDAQ, we find that although the influence of these two factors on the evolution of the 2008-2009 SSEC and SZSC bubbles is not significant, the fitting effect of the whole model is improved after joining these two variables. This finding implies that Chinese stock bubbles are due not only to the exogenous influence of the People's Bank of China and volatility of international stock indices but also to the endogenous self-organization of the markets resulting

Table 3: Prediction of the critical time of the SZSC bubbles burst for both models and their differences with the actual times of bubble burst.

Item	Estimated time interval	
	2005/11/15–2007/11/28	2007/11/29–2008/10/17
The actual time of bubble burst	2007/10/31 (t_c = 107.83)	2008/1/14 (t_c = 108.04)
The predicted critical time of the original JLS model	2007/12/13 (t_c = 107.95)	2008/1/11 (t_c = 108.03)
The difference between the original JLS model and actual time (days)	−43	3
The predicted critical time of the new JLS model	2007/10/8 (t_c = 107.76)	2008/1/15 (t_c = 108.04)
The difference between the new JLS model and actual time (days)	23	−1

Value in parentheses is the predicted critical time t_c.

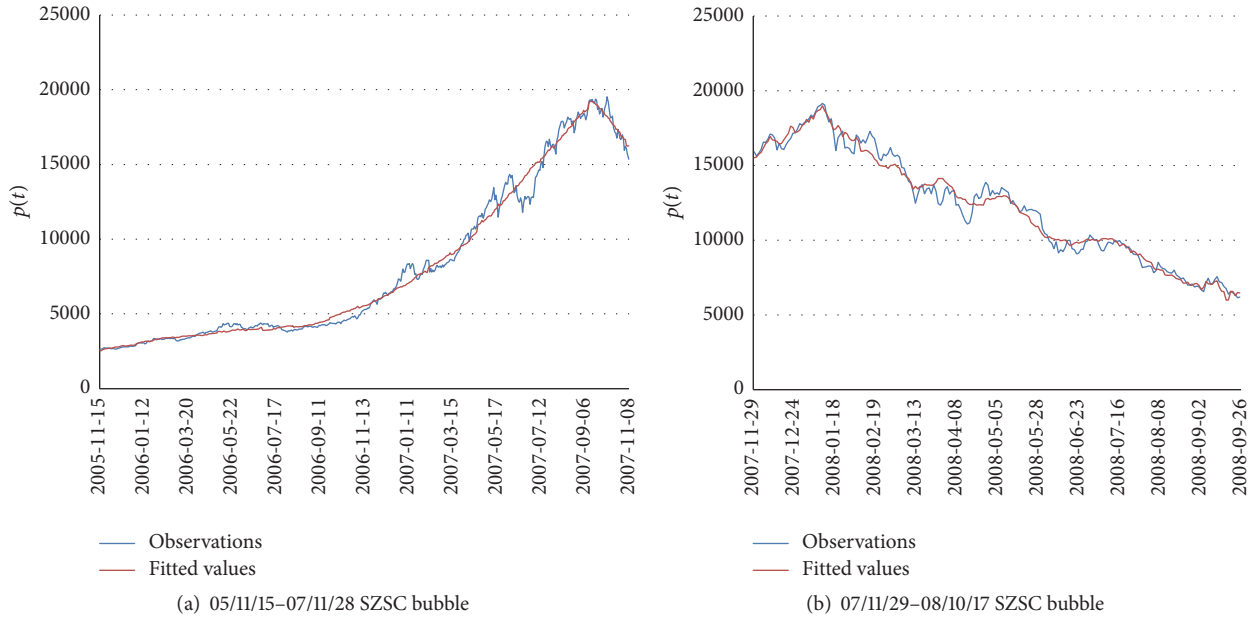

(a) 05/11/15–07/11/28 SZSC bubble

(b) 07/11/29–08/10/17 SZSC bubble

Figure 3: Daily trajectory of the SZSC from 2005/11/15 to 2008/10/17 by using the JLS-factor model presented in (10) with $y(t) = p(t)$. The fit of SZSC from 2005/11/15 to 2007/11/28 is illustrated in (a) as a red solid line, whose parameters are t_c = 2007/10/08, ω = 0.07, m = 1.86, ϕ = 0.07, A = 20506.38, B = −4784674.93, C = 4780598.98, α = −183.50, β = −296.39, φ = 118.94, and γ = 1.87 with an r.m.s. of the fit residuals χ = 523.35. The fit of SZSC from 2007/11/29 to 2008/10/17 is illustrated in (b) as a red solid line, whose parameters are t_c = 2008/01/15, ω = 14.85, m = 0.53, ϕ = 2.82, A = 12998.06, B = −12652.93, C = 1164.16, α = 861.36, β = −275.90, φ = 101.22, and γ = 4.89 with an r.m.s. of the fit residuals χ = 561.68.

from positive feedback between herding investors. For the 2008-2009 Chinese stock bubbles, as in Jiang et al.'s [34] analysis, the regime change in these bubbles occurred in the absence of any significant modification of the economic and financial conditions or any visible driving force. Here, a vanishingly small change in some of the control parameters may have led to a macroscopic bifurcation or phase transition [34]. This means that universal LPPLS sufficiently reflect the fundamental tendency of investors to speculate and herd. Further, the change in the deposit reserve rate and volatility of NASDAQ can dramatically affect the movements of Chinese stock bubbles in the remaining periods in different ways.

7. Conclusion and Discussion

We introduced a new JLS model that combines fundamental economic factors in China (including the interest rate and deposit reserve rate) and the historical volatilities of targeted indices and US equity indices with the original model. The new JLS model not only keeps the dynamic characteristics of a bubble caused by positive feedback but also considers exogenous shocks that trigger the bursting of bubbles. Further, we analyzed in detail six financial bubbles in Chinese stock markets by calibrating the JLS-factor model (see (10)) to two important Chinese stock indices (SSEC and SZSC) from July 2005 to July 2015. We then compared the prediction accuracy of the critical time fitted by the new JLS model with that of the original model. The results of this comparison and the indirect significance tests indicate that all Chinese stock bubbles are a combination of speculative herding behavior and policy-induced reactions as well as international stock index volatility. These results confirm the sensible explanation and superiority of our proposed JLS model.

Table 4: Parameters of the fits of the indices indicated in the first column are calculated by the JLS-factor model (10), where t_c is the most probable time for the bursting of bubble (or the inception of an antibubble), $\omega \in [0.01,\ 40]$ is the angular log-frequency [24], $m \in [0,\ 2]$ quantifies the degree of superexponential growth, $\phi \in [0,\ 2\pi]$ is phase, A gives the terminal price at the critical time t_c, B and C, respectively, control for the amplitude of the power law acceleration and the log-periodic oscillations, α, β, φ, and γ, respectively, measure the effects of the risk-free interest rate, the deposit reserve rate, the volatility of the targeted index, and NASDAQ on the price $p(t)$, and χ denotes the root-mean-square (r.m.s.).

Bubble (antibubble)	t_c	ω	m	ϕ	10^3A	10^4B	10^3C	α	β	φ	γ	χ
05/07/11–08/10/17 SSEC	07/10/16	0.03	1.89	0.03	4.97	−480.94	4808.85	215.66	−32.46	−25.11	0.20	193.04
05/07/11–08/10/17 SZSC	07/11/26	1.26	0.31	3.48	14.93	−0.72	6.08	−320.05	92.46	39.43	2.73	643.26
08/11/03–09/08/31 SSEC	09/08/03	17.46	0.45	2.14	3.36	−0.21	−0.12	74.22	37.78	−83.33	−0.33	60.49
08/11/03–09/08/31 SZSC	09/08/03	17.28	0.53	4.80	13.44	−1.00	0.63	132.05	66.10	−56.60	−0.25	282.30
14/03/13–15/07/29 SSEC	15/06/08	5.50	0.39	1.09	5.88	−0.41	0.32	105.11	10.50	−115.53	−0.14	119.37
14/03/13–15/07/29 SZSC	15/06/08	5.63	0.34	3.99	13.81	−1.56	−1.03	−2.62	535.60	−392.55	−0.84	486.32
05/11/15–07/11/28 SZSC	07/10/08	0.07	1.86	0.07	20.51	−478.47	4780.60	−183.50	−296.39	118.94	1.87	523.35
07/11/29–08/10/17 SZSC	08/01/15	14.85	0.53	2.82	12.00	−1.27	1.16	861.36	−275.90	101.22	4.89	561.68

Table 5: The significance test results of the new and the original JLS model for the SSEC bubbles.

Independent variable	2005/7/11–2008/10/17		2008/11/3–2009/8/31		2014/3/13–2015/7/29	
	JLS model	New JLS model	JLS model	New JLS model	JLS model	New JLS model
A	5731.247	4992.469	2825.911	4653.301	4792.062	7704.706
	(280.536)***	(91.959)***	(61.353)***	(24.645)***	(212.031)***	(48.030)***
B	−442310.7	−441176.2	−880.458	−3444.690	−2954.052	−5275.828
	(−104.248)***	(−62.898)***	(−10.370)***	(−15.337)***	(−88.287)***	(−40.295)***
C	441796.9	440839.6	−0.518	−154.749	−362.186	−365.562
	(104.014)***	(62.763)***	(−48.883)***	(−12.484)***	(−17.492)***	(−19.400)***
α		8.616		−1.487		−13.058
		(11.445)***		(−0.852)		(−4.771)***
β		−1.437		−0.203		2.568
		(−6.260)***		(−0.724)		(6.028)***
φ		−2.214		−0.439		−2.669
		(−3.491)***		(−0.257)		(−2.855)***
γ		−5.284		0.650		−22.477
		(−4.733)***		(0.693)		(−9.467)***
N	796	796	340	340	340	340
$\overline{R}^2$	0.978	0.983	0.913	0.984	0.961	0.986
F-statistic	17320.70***	7531.207***	1784.438***	2089.920***	4146.165***	3995.439***
AIC	13.593	13.337	14.674	11.066	13.273	12.249
SC	13.610	13.378	14.708	11.180	13.307	12.328
HQC	13.599	13.353	14.688	11.112	13.286	12.280

The regression coefficients, adjusted R-squares ($\overline{R}^2$), and three statistical criteria are presented. The t-statistics are reported in the parentheses. ***Significance at the 1% confidence level.

Table 6: The significance test results of the new and the original JLS model for the SZSC bubbles.

Independent variable	2005/7/11–2008/10/17		2008/11/3–2009/8/31		2014/3/13–2015/7/29	
	JLS model	New JLS model	JLS model	New JLS model	JLS model	New JLS model
A	18490.62	20234.73	2827.723	4643.542	17060.47	28286.88
	(79.333)***	(65.072)***	(61.104)***	(24.763)***	(184.250)***	(49.029)***
B	−7103.479	−8099.557	−879.179	−3427.315	−10429.75	−19848.04
	(−23.023)***	(−29.957)***	(−10.349)***	(−15.398)***	(−78.527)***	(−41.031)***
C	6244.976	6196.875	−0.519	−154.527	−1126.786	−1288.108
	(52.350)***	(57.204)***	(−48.751)***	(−12.533)***	(−14.849)***	(−17.401)***
α		3.127		−1.639		50.255
		(1.095)		(−0.941)		(4.384)***
β		1.877		−0.192		−5.513
		(2.234)*		(−0.686)		(−3.137)**
φ		5.347		−0.349		14.983
		(3.076)**		(−0.204)		(3.927)***
γ		−39.379		0.685		−98.284
		(−11.916)***		(0.734)		(−9.908)***
N	796	796	340	340	340	340
$\overline{R}^2$	0.978	0.987	0.913	0.984	0.951	0.979
F-statistic	17954.89***	10329.40***	1782.521***	2089.289***	3271.277***	2673.850***
AIC	16.174	15.643	14.675	11.067	15.902	15.046
SC	16.192	15.684	14.709	11.180	15.936	15.125
HQC	16.181	15.658	14.689	11.113	15.916	15.078

The regression coefficients, adjusted R-squares ($\overline{R}^2$), and three statistical criteria are presented. The t-statistics are reported in the parentheses. *Significance at the 10% confidence level. **Significance at the 5% confidence level. ***Significance at the 1% confidence level.

Table 7: The significance test results of the new and the original JLS model for the 2005–2008 SZSC bubbles.

Independent variable	2005/11/15–2007/11/28		2007/11/29–2008/10/17	
	JLS model	New JLS model	JLS model	New JLS model
A	17692.97	41967.41	15512.45	19841.75
	(260.833)***	(30.219)***	(72.230)***	(130.481)***
B	−39857.89	−98196.21	−10840.88	−40897.70
	(−115.809)***	(−32.662)***	(−20.378)***	(−21.170)***
C	−36775.25	−89665.52	−2.800	1885.201
	(−105.480)***	(−33.281)***	(−54.535)***	(7.814)***
α		290.262		−140.944
		(20.157)***		(−14.366)***
β		−90.608		23.000
		(−20.270)***		(13.351)***
φ		8.009		107.469
		(2.782)***		(15.265)***
γ		7.62		−17.028
		(1.419)		(−1.587)
N	495	495	340	340
$\overline{R}^2$	0.983	0.993	0.904	0.980
F-statistic	14598.80***	10925.42***	1594.129***	1731.150***
AIC	15.899	15.108	18.096	15.380
SC	15.925	15.167	18.130	15.490
HQC	15.909	15.131	18.109	15.424

The regression coefficients, adjusted R-squares ($\overline{R}^2$), and three statistical criteria are presented. The t-statistics are reported in the parentheses. ***Significance at the 1% confidence level.

However, it is interesting to find that there is no obvious reason to believe that there is any critical difference between SSEC and SZSC, while the crucial fitting parameters are very different during the bubble time 2005–2008. In reality, the evolutions of the standardized 2005–2008 SSEC bubble and the standardized 2005–2008 SZSC bubble are similar and their correlation coefficient is as high as 0.99. However, these few differences might lead to significantly different fitting results.

The word "critical" is used in science with different meanings. Sornette and Johansen [101] used it in the context of the critical phenomena studied in statistical physics in connection with phase transitions. Here, however, it describes a system at the border between order and disorder, which is characterized by an extremely large susceptibility to external factors and a strong correlation between different parts of the system. Examples of such systems are liquids and magnets, where the system will progressively become orderly under small external changes. In particular, this helps address the question of what is/are the cause(s) of bubbles and crashes. The crucial insight is that a system made of competing investors subjected to the myriad of influences, both exogenous news and endogenous interactions and reflexivity, can develop into endogenously self-organized self-reinforcing regimes that would qualify as bubbles; moreover, crashes occur as a global self-organized transition. The implication of modeling a market crash as a bifurcation is to solve the question of what makes a crash: in the framework of bifurcation theory (or phase transitions), sudden shifts in behavior arise from small changes in circumstances, with qualitative changes in the nature of the solutions that can occur abruptly when the parameters change smoothly. That is, a minor change of circumstances, interaction strength, or heterogeneity may lead to a sudden and dramatic change, such as during an earthquake and a financial crash. Note that, according to this "critical" point of view, the specific manner by which prices collapse is not the most important problem: a crash occurs because the market has entered an unstable phase and any small disturbance or process may have triggered the existence of this instability [102]. For example, think of a ruler held up vertically on your finger: this unstable position will lead eventually to its collapse as a result of a small (or an absence of adequate) motion of your hand or due to any tiny whiff of air. The collapse is fundamentally due to the unstable position; the instantaneous cause of the collapse is secondary [1].

From the above, we know that if the bubble state is unstable, a small disturbance will trigger the bursting of the bubble. Hence, although there are few differences between the 2005–2008 SSEC bubble and the 2005–2008 SZSC bubble, as long as the trigger factors (exogenous or endogenous) show small differences, the burst time of the bubble will

be strikingly different, as will the results of the other JLS model parameters. Thus, the crucial fitting parameters are very different during the bubble time of 2005–2008.

Competing Interests

The authors declare that there is no conflict of interests regarding the publication of this paper.

References

[1] D. Sornette, *Why Stock Markets Crash (Critical Events In Complex Financial Systems)*, Princeton University Press, 2003.

[2] J. Anifrani, C. Le Floc'h, D. Sornette, and B. Souillard, "Universal log-periodic correction to renormalization group scaling for rupture stress prediction from acoustic emissions," *Journal De Physique I*, vol. 5, no. 6, pp. 631–638, 1995.

[3] A. Johansen, D. Sornette, J. H. Wakita, U. Tsunogai, W. I. Newman, and H. Saleur, "Descrete scaling in earthquake precursory phenomena: evidence in the Kobe earthquake, Japan," *Journal de Physique I*, vol. 6, no. 10, pp. 1391–1402, 1996.

[4] J. A. Feigenbaum and P. G. O. Freund, "Discrete scale invariance in stock markets before crashes," *International Journal of Modern Physics B*, vol. 10, no. 27, pp. 3737–3745, 1996.

[5] D. Sornette, A. Johansen, and J.-P. Bouchaud, "Stock market crashes, precursors and replicas," *Journal De Physique I*, vol. 6, no. 1, pp. 167–175, 1996.

[6] D. Sornette and A. Johansen, "Large financial crashes," *Physica A: Statistical Mechanics and its Applicationss*, vol. 245, no. 3-4, pp. 411–422, 1997.

[7] J. A. Feigenbaum and P. G. O. Freund, "Discrete scale invariance and the 'second black Monday'," *Modern Physics Letters B*, vol. 12, no. 2-3, pp. 57–60, 1998.

[8] S. Gluzman and V. I. Yukalov, "Renormalization group analysis of October market crashes," *Modern Physics Letters B*, vol. 12, no. 2-3, pp. 75–84, 1998.

[9] N. Vandewalle, P. Boveroux, A. Minguet, and M. Ausloos, "The crash of October 1987 seen as a phase transition: amplitude and universality," *Physica A: Statistical Mechanics and Its Applications*, vol. 255, no. 1-2, pp. 201–210, 1998.

[10] L. Laloux, M. Potters, R. Cont, J.-P. Aguilar, and J.-P. Bouchaud, "Are financial crashes predictable?" *Europhysics Letters*, vol. 45, no. 1, pp. 1–5, 1999.

[11] S. Drozdz, F. Ruf, J. Speth, and M. Wójcik, "Imprints of log-periodic self-similarity in the stock market," *European Physical Journal B*, vol. 10, no. 3, pp. 589–593, 1999.

[12] A. Johansen and D. Sornette, "Predicting financial crashes using discrete scale invariance," *SSRN Electronic Journal*, 26 pages, 1999.

[13] A. Johansen and D. Sornette, "Modeling the stock market prior to large crashes," *The European Physical Journal B*, vol. 9, no. 1, pp. 167–174, 1999.

[14] A. Johansen, D. Sornette, and O. Ledoit, "Predicting financial crashes using discrete scale invariance," *The Journal of Risk*, vol. 1, no. 4, pp. 5–32, 1999.

[15] N. Vandewalle, M. Ausloos, P. Boveroux, and A. Minguet, "How the financial crash of October 1997 could have been predicted," *The European Physical Journal B*, vol. 4, no. 2, pp. 139–141, 1998.

[16] A. Johansen and D. Sornette, "Financial "anti-bubbles": log-periodicity in gold and nikkei collapses," *International Journal of Modern Physics C*, vol. 10, no. 4, pp. 563–575, 1999.

[17] D. Sornette and W. Zhou, "The US 2000–2002 market descent: how much longer and deeper?" *Quantitative Finance*, vol. 2, no. 6, pp. 468–481, 2002.

[18] A. Johansen and D. Sornette, "Bubbles and anti-bubbles in latin-american, asian and western stock markets: An Empirical Study," *International Journal of Theoretical and Applied Finance*, vol. 4, no. 6, p. 853, 2001.

[19] W.-X. Zhou and D. Sornette, "Evidence of a worldwide stock market log-periodic anti-bubble since mid-2000," *Physica A: Statistical Mechanics and its Applications*, vol. 330, no. 3-4, pp. 543–583, 2003.

[20] S. Gluzman and D. Sornette, "Log-periodic route to fractal functions," *Physical Review E*, vol. 65, no. 3, Article ID 036142, 2002.

[21] W.-X. Zhou and D. Sornette, "Renormalization group analysis of the 2000–2002 anti-bubble in the US S&P500 index: Explanation of the hierarchy of five crashes and prediction," *Physica A: Statistical Mechanics and Its Applications*, vol. 330, no. 3-4, pp. 584–604, 2003.

[22] W.-X. Zhou and D. Sornette, "Fundamental factors versus herding in the 2000–2005 US stock market and prediction," *Physica A: Statistical Mechanics and its Applications*, vol. 360, no. 2, pp. 459–482, 2006.

[23] W. Yan, R. Woodard, and D. Sornette, "Inferring fundamental value and crash nonlinearity from bubble calibration," *Quantitative Finance*, vol. 14, no. 7, pp. 1273–1282, 2010.

[24] W. Yan, R. Woodard, and D. Sornette, "Diagnosis and prediction of tipping points in financial markets: crashes and rebounds," *Physics Procedia*, vol. 3, no. 5, pp. 1641–1657, 2010.

[25] W. Yan, R. Woodard, and D. Sornette, "The role of diversification risk in financial bubbles," *The Journal of Investment Strategies*, vol. 1, no. 4, pp. 63–83, 2012.

[26] V. Filimonov and D. Sornette, "A stable and robust calibration scheme of the log-periodic power law model," *Physica A*, vol. 392, no. 17, pp. 3698–3707, 2013.

[27] L. Lin, R. E. Ren, and D. Sornette, "The volatility-confined LPPL model: a consistent model of 'explosive' financial bubbles with mean-reverting residuals," *International Review of Financial Analysis*, vol. 33, pp. 210–225, 2014.

[28] Q. Zhang, Q. Zhang, and D. Sornette, "Early warning signals of financial crises with multi-scale quantile regressions of log-periodic power law singularities," *PLoS ONE*, vol. 11, no. 11, Article ID e0165819, 2016.

[29] Q. Zhang, D. Sornette, M. Balcilar, R. Gupta, Z. A. Ozdemir, and I. H. Yetkiner, "LPPLS bubble indicators over two centuries of the S&P 500 index," *SSRN Electronic Journal*, pp. 126–139, 2016.

[30] V. Filimonov, G. Demos, and D. Sornette, "Modified profile likelihood inference and interval forecast of the burst of financial bubbles," *SSRN Electronic Journal*, 40 pages, 2016.

[31] M. Seyrich and D. Sornette, "Micro-foundation using percolation theory of the finite time singular behavior of the crash hazard rate in a class of rational expectation bubbles," *International Journal of Modern Physics C. Computational Physics and Physical Computation*, vol. 27, no. 10, Article ID 1650113, 20 pages, 2016.

[32] D. Sornette, G. Demos, Q. Zhang, P. Cauwels, and Q. Zhang, "Real-time prediction and post-mortem analysis of the Shanghai 2015 stock market bubble and crash," *The Journal of Investment Strategies*, vol. 4, no. 4, pp. 77–95, 2015.

[33] W.-X. Zhou and D. Sornette, "Antibubble and prediction of China's stock market and real-estate," *Physica A: Statistical*

Mechanics and its Applications, vol. 337, no. 1-2, pp. 243–268, 2004.

[34] Z.-Q. Jiang, W.-X. Zhou, D. Sornette, R. Woodard, K. Bastiaensen, and P. Cauwels, "Bubble diagnosis and prediction of the 2005–2007 and 2008-2009 Chinese stock market bubbles," *Journal of Economic Behavior and Organization*, vol. 74, no. 3, pp. 149–162, 2010.

[35] D. Sornette and W.-X. Zhou, "Predictability of large future changes in major financial indices," *International Journal of Forecasting*, vol. 22, no. 1, pp. 153–168, 2006.

[36] S.-W. Cheng, Ed., *Diagnoses and Prescription: Unveiling The Chinese Stock Market*, Economic Science Press, Beijing, China, 2003 (Chinese).

[37] J. G. Fernald and J. H. Rogers, "Puzzles in the Chinese stock market," Federal Reserve Bank International Finance Discussion Paper 619, 1998, http://ssrn.com/abstract=124268.

[38] A. Johansen, O. Ledoit, and D. Sornette, "Crashes as critical points," *International Journal of Theoretical and Applied Finance*, vol. 3, no. 2, pp. 219–255, 2000.

[39] A. Johansen and D. Sornette, "Shocks, crashes and bubbles in financial markets," *Brussels Economic Review*, vol. 53, no. 2, pp. 201–253, 2010.

[40] B. S. Bernanke and A. S. Blinder, "The federal funds rate and the channels of monetary transmission," *American Economic Review*, vol. 82, no. 4, pp. 901–921, 1992.

[41] B. S. Bernanke and M. Gertler, "Inside the black box: the credit channel of the monetary policy transmission," *Journal of Economic Perspectives*, vol. 9, pp. 27–48, 1995.

[42] G. R. Jensen and R. R. Johnson, "Discount rate changes and security returns in the U.S., 1962-1991," *Journal of Banking and Finance*, vol. 19, no. 1, pp. 79–95, 1995.

[43] A. D. Patelis, "Stock return predictability and the role of monetary policy," *Journal of Finance*, vol. 52, no. 5, pp. 1951–1972, 1997.

[44] C. M. Conover, G. R. Jensen, and R. R. Johnson, "Monetary environments and international stock returns," *Journal of Banking and Finance*, vol. 23, no. 9, pp. 1357–1381, 1999.

[45] I. Christos and K. Alexandros, "The impact of monetary policy on stock price," *Journal of Policy Modeling*, vol. 30, no. 1, pp. 33–53, 2008.

[46] P. Maio, "Another look at the stock return response to monetary policy actions," *Review of Finance*, vol. 18, no. 1, pp. 321–371, 2014.

[47] G. R. Jensen and J. M. Mercer, "Monetary policy and the cross-section of expected stock returns," *Journal of Financial Research*, vol. 25, no. 1, pp. 125–139, 2002.

[48] R. Rigobon and B. Sack, "The impact of monetary policy on asset prices," *Journal of Monetary Economics*, vol. 51, no. 8, pp. 1553–1575, 2004.

[49] R. S. Gurkaynak, B. P. Sack, and E. T. Swanson, "Do actions speak louder than words? The response of asset prices to monetary policy actions and statements," *SSRN Electronic Journal*, vol. 1, no. 1, pp. 55–93, 2005.

[50] T. Davig and J. Gerlach, "State-dependent stock market reactions to monetary policy," *SSRN Electronic Journal*, vol. 2, no. 4, pp. 65–83, 2006.

[51] Y. D. Li, T. B. Işcan, and K. Xu, "The impact of monetary policy shocks on stock prices: evidence from Canada and the United States," *Journal of International Money & Finance*, vol. 29, no. 5, pp. 876–896, 2010.

[52] E. Castelnuovo and S. Nistico, "Stock market conditions and monetary policy in a DSGE model for the U.S.," *Journal of Economic Dynamics & Control*, vol. 34, no. 9, pp. 1700–1731, 2010.

[53] A. Kontonikas and A. Kostakis, "On monetary policy and stock market anomalies," *Journal of Business Finance and Accounting*, vol. 40, no. 7-8, pp. 1009–1042, 2013.

[54] L. A. Gallo, R. N. Hann, and C. Li, "Aggregate earnings surprises, monetary policy, and stock returns," *Journal of Accounting and Economics*, vol. 62, no. 1, pp. 103–120, 2016.

[55] B. J. Lobo, "Interest rate surprises and stock prices," *The Financial Review*, vol. 37, no. 1, pp. 73–91, 2002.

[56] N. Cassola and C. Morana, "Monetary policy and the stock market in the euro area," *Journal of Policy Modeling*, vol. 26, no. 3, pp. 387–399, 2004.

[57] D. Bredin, S. Hyde, D. Nitzsche, and G. O'Reilly, "UK stock returns and the impact of domestic monetary policy shocks," *Journal of Business Finance and Accounting*, vol. 34, no. 5-6, pp. 872–888, 2007.

[58] C. Ioannidis and A. Kontonikas, "The impact of monetary policy on stock prices," *Journal of Policy Modeling*, vol. 30, no. 1, pp. 33–53, 2008.

[59] B. Mohamadpour, N. Behravan, S. Espahbodi, and R. Karimi, "An empirical study of relationship between monetary policy and stock market performance in Malaysia," *Australian Journal of Basic & Applied Sciences*, vol. 6, no. 12, pp. 142–148, 2012.

[60] J. Ruiz, "Response of Spanish stock market to ECB monetary policy during financial crisis," *Spanish Review of Financial Economics*, vol. 13, no. 2, pp. 41–47, 2015.

[61] J. Galí and L. Gambetti, "The effects of monetary policy on stock market bubbles: some evidence," *American Economic Journal: Macroeconomics*, vol. 7, no. 1, pp. 233–257, 2015.

[62] S. Bashiri, M. Pahlavani, and R. Boostani, "Optimal monetary policy and stock market fluctuations," *Applied Economics & Finance*, vol. 3, no. 2, pp. 157–178, 2016.

[63] W. K. Wong, H. Khan, and J. Du, "Money, interest rate and stock prices: new evidence from Singapore and the United States," 2005, http://ssrn.com/abstract=1607605.

[64] F. Lippi and S. Neri, "Information variables for monetary policy in an estimated structural model of the Euro area," *Journal of Monetary Economics*, vol. 54, no. 4, pp. 1256–1270, 2007.

[65] D. Pilinkus, "Stock market and macroeconomic variables: evidences from Lithuania," *Economics and Management Journal*, vol. 14, pp. 884–891, 2009.

[66] E. H. Thabet, "Examining the long run relationship between the U.S. money supply (M2) and The Canadian Stock Market," *International Journal of Economics & Finance*, vol. 6, no. 10, pp. 180–190, 2014.

[67] K. N. Kuttner, "Monetary policy surprises and interest rates: evidence from the Fed funds futures market," *Journal of Monetary Economics*, vol. 47, no. 3, pp. 523–544, 2001.

[68] B. S. Bernanke and K. N. Kuttner, "What explains the stock market's reaction to federal reserve policy?" *Journal of Finance*, vol. 60, no. 3, pp. 1221–1257, 2005.

[69] A. Basistha and A. Kurov, "Macroeconomic cycles and the stock market's reaction to monetary policy," *Journal of Banking & Finance*, vol. 32, no. 12, pp. 2606–2616, 2008.

[70] M. Farka, "The effect of monetary policy shocks on stock prices accounting for endogeneity and omitted variable biases," *Review of Financial Economics*, vol. 18, no. 1, pp. 47–55, 2009.

[71] H. Chuliá, M. Martens, and D. V. Dijk, "Asymmetric effects of federal funds target rate changes on S&P100 stock returns, volatilities and correlations," *Journal of Banking & Finance*, vol. 34, no. 4, pp. 834–839, 2010.

[72] S. Vähämaa and J. Äijö, "The Fed's policy decisions and implied volatility," *The Journal of Futures Markets*, vol. 31, no. 10, pp. 995–1010, 2011.

[73] A. Kurov, "What determines the stock market's reaction to monetary policy statements?" *Review of Financial Economics*, vol. 21, no. 4, pp. 175–187, 2012.

[74] A. Kontonikas, R. MacDonald, and A. Saggu, "Stock market reaction to fed funds rate surprises: state dependence and the financial crisis," *Journal of Banking and Finance*, vol. 37, no. 11, pp. 4025–4037, 2013.

[75] N. Gospodinov and I. Jamali, "The response of stock market volatility to futures-based measures of monetary policy shocks," *International Review of Economics and Finance*, vol. 37, pp. 42–54, 2015.

[76] Y. Li, "Causes and expected effects of continual increasing deposit reserve of PBC," *Finance & Economics*, vol. 2, pp. 1–6, 2007 (Chinese).

[77] Y. Liu, "Impact of deposit reserve rate adjustment on Chinese security market," *Statistical Research*, vol. 3, pp. 42–45, 2008 (Chinese).

[78] J.-Y. Zuo and W. Wang, "Research on announcement effect of the compulsory reserve policy in China," *South China Finance*, vol. 7, pp. 20–23, 2009 (Chinese).

[79] Y. Yu and Y. Hou, "The impact of monetary policy change on stock price trend in China," *Research on Economics and Management*, vol. 11, pp. 88–91, 2010 (Chinese).

[80] X.-M. Wen, H. Jiang, and Z. Liu, "Empirical research on the impact of changes in deposit reserve ratio on stock market," *Systems Engineering*, vol. 4, pp. 18–24, 2012 (Chinese).

[81] D.-H. Liu and R. Zhang, "The stock market portfolio with the deposit reserve rate shifts: evidence from China," *Pakistan Journal of Statistics*, vol. 29, no. 6, pp. 1129–1140, 2013.

[82] F. Guo, J. Hu, and M. Jiang, "Monetary shocks and asymmetric effects in an emerging stock market: the case of China," *Economic Modelling*, vol. 32, no. 1, pp. 532–538, 2013.

[83] Y. Tang, Y. Luo, J. Xiong, F. Zhao, and Y.-C. Zhang, "Impact of monetary policy changes on the Chinese monetary and stock markets," *Physica A: Statistical Mechanics and its Applications*, vol. 392, no. 19, pp. 4435–4449, 2013.

[84] H.-F. Yue, W.-J. Dong, and L.-V. Xin, "The asymmetric impact analysis on the stock market of the deposit reserve adjustment rate in China," *Journal of Central University of Finance & Economics*, vol. 1, pp. 30–35, 2013 (Chinese).

[85] P. Li, J. Gao, and J. Liao, "The impact of adjustment of deposit reserve requirement ratio on stock market: the empirical study of high frequency data in China market," *Securities Market Herald*, vol. 10, pp. 24–33, 2014 (Chinese).

[86] J.-B. Chen and L. Xu, "The short period reaction of stock market to interest rate and deposit-reserve ratio adjustments in China," *Journal of Applied Statistics and Management*, vol. 2, pp. 355–362, 2014 (Chinese).

[87] H. Kim, J. Kim, J. Lee, and D. Ryu, "The impact of monetary policy on banking and finance stock prices in China," *Applied Economics Letters*, vol. 21, no. 18, pp. 1257–1261, 2014.

[88] H. Cheng and J. L. Glascock, "Stock market linkages before and after the asian financial crisis: evidence from three Greater China economic area stock markets and the US," *Review of Pacific Basin Financial Markets & Policies*, vol. 9, no. 2, pp. 297–315, 2006.

[89] W. Chen, Y. Wei, Q. Lang, Y. Lin, and M. Liu, "Financial market volatility and contagion effect: a copula-multifractal volatility approach," *Physica A: Statistical Mechanics & Its Applications*, vol. 398, pp. 289–300, 2014.

[90] K. Fan, Z. Lu, and S. Wang, "Dynamic linkages between the China and international stock markets," *Asia-Pacific Financial Markets*, vol. 16, no. 3, pp. 211–230, 2009.

[91] L.-G. Chen, P.-F. Wu, and N. Liu, "The empirical study on the degree of international stock market co-movements," *Journal of Quantitative & Technical Economics*, vol. 23, no. 11, pp. 124–132, 2006 (Chinese).

[92] Z.-G. Ding, Z. Su, and X.-Y. Du, "Study on correlation between business cycle and volatility of security markets in China based on bivariate SWARCH Model," *Journal of Quantitative & Technical Economics*, vol. 24, no. 3, pp. 61–71, 2007 (Chinese).

[93] Y. Shen, X.-F. Zhang, and Y.-B. Liu, "Empirical analysis on the co-movement effects Inter-Asia-Pacific regional capital markets—case study on the stock market of mainland China, HK," *Japan and the U.S. On Economic Problems*, vol. 4, pp. 83–86, 2011 (Chinese).

[94] C. Li, J.-X. Wang, and B. Wang, "Theoretical comprehension and empirical study of linkage effect of international capital market," *Journal of Xi'an Jiaotong University (Social Sciences)*, vol. 9, pp. 1–8, 2012 (Chinese).

[95] X. Luo, "Analysis of the co-movement between China's and U.S. stock markets: based on the CSI 300 and the Dow Jones Industrial Average Index," *Journal of Chengdu University of Technology (Social Sciences)*, vol. 1, pp. 67–72, 2014 (Chinese).

[96] T. C. Chiang and X. Chen, "Empirical analysis of dynamic linkages between China and international stock markets," *Journal of Mathematical Finance*, vol. 6, no. 1, pp. 189–212, 2016.

[97] B.-A. Zhang, Z. Fan, and X. Li, "Comovement between China and U.S.'s stock markets," *Economic Research Journal*, vol. 11, pp. 141–151, 2010 (Chinese).

[98] W.-R. Pan and J.-X. Liu, "The study on the stock market co-movement between China and America after the introduction of QFII and QDII," *Journal of Jiangxi University of Finance & Economics*, vol. 1, pp. 5–10, 2010 (Chinese).

[99] W. H. Press, S. A. Teukolsky, B. P. Flannery, and W. T. Vetterling, *Numerical Recipes in FORTRAN: The Art of Scientific Computing*, Cambridge University, Cambridge, UK, 1996.

[100] W.-X. Zhou and D. Sornette, "Statistical significance of periodicity and log-periodicity with heavy-tailed correlated noise," *International Journal of Modern Physics C*, vol. 13, no. 2, pp. 137–170, 2002.

[101] D. Sornette and A. Johansen, "A hierarchical model of financial crashes," *Physica A: Statistical Mechanics and Its Applications*, vol. 261, no. 3-4, pp. 581–598, 1998.

[102] T. Kaizoji and D. Sornette, "Market bubbles and crashes," *Quantitative Finance*, vol. 71, no. 1, pp. 173–204, 2008.

Hindawi Publishing Corporation
Discrete Dynamics in Nature and Society
Volume 2016, Article ID 9693419, 8 pages
http://dx.doi.org/10.1155/2016/9693419

Research Article

Worst-Case Investment and Reinsurance Optimization for an Insurer under Model Uncertainty

Xiangbo Meng,[1,2] Ximin Rong,[1] Lidong Zhang,[2] and Ziping Du[3,4]

[1]*School of Science, Tianjin University, Tianjin 300072, China*
[2]*School of Science, Tianjin University of Science & Technology, Tianjin 300457, China*
[3]*School of Economics and Management, Tianjin University of Science & Technology, Tianjin 300222, China*
[4]*Financial Engineering and Risk Management Research Center, Tianjin University of Science & Technology, Tianjin 300222, China*

Correspondence should be addressed to Ximin Rong; rongximin@tju.edu.cn

Received 5 September 2016; Revised 6 November 2016; Accepted 28 November 2016

Academic Editor: Gafurjan Ibragimov

Copyright © 2016 Xiangbo Meng et al. This is an open access article distributed under the Creative Commons Attribution License, which permits unrestricted use, distribution, and reproduction in any medium, provided the original work is properly cited.

In this paper, we study optimal investment-reinsurance strategies for an insurer who faces model uncertainty. The insurer is allowed to acquire new business and invest into a financial market which consists of one risk-free asset and one risky asset whose price process is modeled by a Geometric Brownian motion. Minimizing the expected quadratic distance of the terminal wealth to a given benchmark under the "worst-case" scenario, we obtain the closed-form expressions of optimal strategies and the corresponding value function by solving the Hamilton-Jacobi-Bellman (HJB) equation. Numerical examples are presented to show the impact of model parameters on the optimal strategies.

1. Introduction

In recent years, insurance companies are playing the more active role in the financial market. To avoid their risk, insurers are apt to invest in the financial market, purchase reinsurance from the reinsurer and acquire new business (acting as a reinsurer for other insurers). Tremendous literature on optimal investment and/or reinsurance problem for insurers has been investigated. For example, Browne [1] studied the optimal investment problem for an insurer whose surplus is described by a drifted Brownian motion under the criterion of maximizing the expected exponential utility of the terminal wealth or minimizing the ruin probability. To the same question, Hipp and Plum [2] showed a different result when insurance business is modeled by a compound Poisson process. Schmidli [3, 4] investigated optimal strategies under the criterion of minimizing the ruin probability.

Mean-variance portfolio selection theory was first proposed by Markowitz [5] and it has been used to investigate optimal investment and reinsurance problems in the actuarial literature [6–13].

In addition, it is important to consider model uncertainty due to the uncertainties in the global economy and the debit crisis exiting in financial markets and insurance industries. Meanwhile a growing number of scholars have paid attention to incorporating model uncertainty into optimization problems. For example, Talay and Zheng [14] viewed the Trader and the Market as two players and formulated the model risk control problem as a zero-sum stochastic differential game problem. Mataramvura and Øksendal [15] investigated the risk-minimizing portfolio selection problem in a jump diffusion market. Zhang and Siu [16] studied optimal investment and reinsurance problems via the game theoretic approach and derived closed-form solutions when the objective function is the expected exponential utility of terminal wealth and the expected discounted penalty of ruin, respectively. Lin et al. [17] discussed an optimal portfolio selection problem of an insurer who faces model uncertainty and obtained closed-form solutions to the game problems in both the jump diffusion risk process and its diffusion approximation for the case of an exponential utility by using techniques of stochastic linear-quadratic control.

In this paper, we are concerned about optimal investment and reinsurance strategies for an insurer with model uncertainty. Suppose that the insurer can purchase proportional reinsurance/acquire new business and invest in a simplified continuous-time financial market with a bank account and a risky stock. We measure the risk faced by the insurer by means of the deviation of the surplus to a fixed terminal target (a given benchmark). The insurer's objective is to find an optimal investment-reinsurance strategy under the criterion of minimizing the expected quadratic distance of the terminal wealth to the given benchmark in the "worst-case" scenario. Different from those in Zhang and Siu [16], we propose here a mean-variance portfolio optimization problem under model uncertainty.

The rest of this paper is organized as follows. In Section 2, we give the assumptions and formulate the model dynamics. In Section 3, we derive optimal investment-reinsurance strategy and the corresponding value function with the help of stochastic control theory. In Section 4, we provide some numerical analyses to demonstrate our results. Section 5 concludes the paper.

2. Model Formulation

Throughout this paper, we work on a filtered complete probability space $(\Omega, \mathcal{F}, \mathcal{P}, \{\mathcal{F}_t\}_{0\le t\le T})$, where $\mathcal{P}$ is a reference probability measure from which a family of real-world probability measures absolutely continuous with respect to $\mathcal{P}$ are generated; $\{\mathcal{F}_t\}_{0\le t\le T}$ is the filtration generated by all Brownian motions standing for the information available up to time t. The finite constant $T > 0$ is a final time horizon.

2.1. Surplus Process. In what follows, we consider an insurer whose surplus process $\{R(t), t \in [0,T]\}$ is approximated by a diffusion model. We firstly go back to the classical risk model as follows:

$$R(t) = x_0 + ct - \sum_{i=1}^{N_t} Y_i. \tag{1}$$

Here $\{Y_i\}$ is the size of the ith claim and $\{Y_i,\ i = 1, 2, \ldots\}$ are independent and identically distributed (i.i.d.) nonnegative random variables with finite first-order moment μ_∞ and second-order moment σ_∞^2; $\{N_t\}$, independent of $\{Y_i,\ i = 1, 2, \ldots\}$, is a homogeneous Poisson process with intensity λ; $c > 0$ is the premium rate which is assumed to be calculated by the expected value principle, that is, $c = (1+\delta)\lambda\mu_\infty$, where δ is the safety loading of the insurer and x_0 is the initial capital.

According to Grandell [18] or Schmidli [19], the insurer's surplus process can be approximated by the following diffusion model:

$$R(t) = x_0 + qt + \sigma_0 W_0(t), \tag{2}$$

where $q = \delta\lambda\mu_\infty$ is the premium return rate of the insurer; $\sigma_0^2 = \lambda\sigma_\infty^2$ represents the volatility of the insurer's surplus; $\{W_0(t)\}$ is a standard Brownian motion.

2.2. Financial Market. The insurance company is allowed to invest the money into a financial market with a riskless asset and a risky asset. Without loss of generality we assume any fractional units of assets can be traded continuously and no taxes or transaction costs are involved in our model.

The price process of the riskless asset $\{S_0(t) \mid t \in [0,T]\}$ is modeled by

$$dS_0(t) = r_0 S_0(t)\, dt, \quad S_0(0) = 1, \tag{3}$$

where $r_0 > 0$ represents the riskless interest rate.

The price process of the risky asset $\{S_1(t) \mid t \in [0,T]\}$ follows the geometric Brownian process

$$dS_1(t) = S_1(t)\left[r_1 dt + \sigma_1 dW_1(t)\right], \quad S_1(0) = s_1 > 0, \tag{4}$$

where $r_1 > r_0$ is the appreciation rate of the risky asset and $\sigma_1 > 0$ is the volatility of the risky asset; $\{W_1(t) \mid t \in [0,T]\}$ is another one-dimensional standard Brownian motion. For convenience, we assume $\{W_0(t) \mid t \in [0,T]\}$ and $\{W_1(t) \mid t \in [0,T]\}$ are independent Brownian motions.

2.3. Wealth Process. As mentioned before, the insurer is allowed to invest in the financial market and purchase proportional reinsurance or acquire new business as described in Bäuerle [6]. We denote by $\pi(t)$ the money amount invested in the risky asset and by $a(t)$ the retention level of reinsurance. For each $t \in [0,T]$, $\vartheta(t) := (\pi(t), a(t))$ represents the strategy adopted by the insurance company and denote by $\{X^\vartheta(t) \mid t \in [0,T]\}$ the surplus of the insurance company with the above notation ϑ. Thus the wealth process $X^\vartheta(t)$ of the insurer can be described as

$$\begin{aligned} dX^\vartheta(t) &= \left[\lambda\mu_\infty(\eta a(t) - (\eta - \delta)) + r_0 X^\vartheta(t) + r\pi(t)\right] dt \\ &\quad + \sigma_0 a(t)\, dW_0(t) + \sigma_1 \pi(t)\, dW_1(t), \\ X^\vartheta(0) &= x_0, \end{aligned} \tag{5}$$

where $r = r_1 - r_0 > 0$, $\eta > \delta$ is the safety loading of the reinsurance/new business.

A strategy $\vartheta = \{(\pi(t), a(t)),\ t \in [0,T]\}$ is said to be admissible if it is $\mathcal{F}_t$-progressively measurable, $a(t) \ge 0$, $E[\int_0^T (\sigma_0^2 a^2(t) + \sigma_1^2 \pi^2(t))ds] < +\infty$, and (5) has a unique strong solution. Denote by $\mathcal{A}$ the set of all admissible strategies.

2.4. Model Uncertainty. For each $t \in [0,T]$, define the enlarged σ-field $\mathcal{G}(t)$, the minimal σ-field generated by $\mathcal{F}^{W_0}(t)$ and $\mathcal{F}^{W_1}(t)$. Denote $\mathcal{G}(t) := \mathcal{F}^{W_0}(t) \vee \mathcal{F}^{W_1}(t)$ and denote $\mathbf{G} := \{\mathcal{G}(t) \mid t \in [0,T]\}$.

Now specify the space of admissible controls by the market. Define $\{\theta(t) \mid t \in [0,T]\}$, which is satisfying the following conditions:

(1) $\{\theta(t) \mid t \in [0,T]\}$ is $\mathbf{G}$-progressively measurable;

(2) $\theta(t) := \theta(t,\omega) < 1$, for a.a. $(t,\omega) \in [0,T] \times \Omega$;

(3) $\int_0^T \theta^2(t)dt < \infty$, $\mathcal{P}$-a.s..

Write Θ for the space of all processes satisfying the above three conditions.

For each $\theta \in \Theta$, define a real-valued, $\mathbf{G}$-adapted process $\{\Lambda^{\theta}(t) \mid t \geq 0\}$ on $(\Omega, \mathscr{F}, \mathscr{P})$ by

$$\Lambda^{\theta}(t) \coloneqq \exp\left\{-\int_0^t \theta(u)\, dW_0(u) - \int_0^t \theta(u)\, dW_1(u) - \int_0^t \theta^2(u)\, du\right\}. \tag{6}$$

By Ito's differentiation rule,

$$d\Lambda^{\theta}(t) = \Lambda^{\theta}(t)\left[-\theta(t)\, dW_0(t) - \theta(t)\, dW_1(t)\right], \quad \Lambda^{\theta}(0) = 1, \ \mathscr{P}\text{-a.s.} \tag{7}$$

So, Λ^{θ} is a $(\mathbf{G}, \mathscr{P})$-(local)-martingale. Hence,

$$\mathrm{E}\left[\Lambda^{\theta}(T)\right] = 1. \tag{8}$$

For each $\theta \in \Theta$, a new (real-world) probability measure $\mathscr{P}^{\theta}$ absolutely continuous with respect to $\mathscr{P}$ on $\mathscr{G}(T)$ is defined by

$$\left.\frac{d\mathscr{P}^{\theta}}{d\mathscr{P}}\right|_{\mathscr{G}(T)} \coloneqq \Lambda^{\theta}(T). \tag{9}$$

Then the family $\mathscr{P}(\Theta)$ of real-world probability measures with index set Θ is generated.

3. The Basic Problem (MV)

As in Mataramvura and Øksendal [15], we define $\{U(t) \mid t \in [0,T]\}$, a vector process, by

$$\begin{aligned} dU(t) &= \left(dU_0(t), dU_1(t), dU_2(t)\right)' \\ &= \left(dU_0(t), dU_1^{\vartheta}(t), dU_2^{\theta}(t)\right)' \\ &= \left(dt, dX^{\vartheta}(t), d\Lambda^{\theta}(t)\right)', \\ U(0) &= u = (s, u_1, u_2)' = (s, x, \Lambda)'. \end{aligned} \tag{10}$$

Suppose the market is the leader of the game and aims to select an admissible strategy $\{\theta(t) \mid t \in [0,T]\}$ which represents the "worst-case" scenario of the minimal expected quadratic deviation between the terminal surplus and some preset targets. That leads to the Min-Max problem

$$\begin{aligned} \Psi(u) &= \inf_{\vartheta \in \mathscr{A}} \sup_{\theta \in \Theta} \left\{\mathrm{E}_{\theta}^{u}\left[\left(X^{\vartheta}(T) - k\right)^2\right]\right\} \\ &= \mathrm{E}_{\theta^*}^{u}\left[\left(X^{\vartheta^*}(T) - k\right)^2\right], \end{aligned} \tag{11}$$

where $k \in \mathscr{R}_+$ is a certain predefined benchmark. Here it is reasonable to assume $k \geq x_0 e^{r_0 T}$, which states that the insurer's terminal wealth k cannot be less than the amount earned by the insurer if all the wealth was invested in the risk-free asset. The market selects an optimal probability scenario $\{\theta^*(t) \mid t \in [0,T]\}$ to maximize the minimal expected quadratic deviation and the insurer reacts antagonistically by choosing an optimal portfolio processes $\{\vartheta^*(t) \mid t \in [0,T]\}$ to minimize the expected quadratic deviation of $X^{\vartheta}(T)$ to k.

For each u and $(\theta, \vartheta) \in \Theta \times \mathscr{A}$, we define

$$\begin{aligned} J^{\theta,\vartheta}(u) &= \mathrm{E}_{\theta}^{u}\left[\left(X^{\vartheta}(T) - k\right)^2\right] \\ &= \mathrm{E}^{u}\left[\Lambda^{\theta}(T)\left(X^{\vartheta}(T) - k\right)^2\right]. \end{aligned} \tag{12}$$

Then we can get another statement of the above Min-Max problem (11) by the version of Bayes' rule: to solve the problem, we must find $\Psi(u)$, $\theta^* \in \Theta$, and $\vartheta^* = (\pi^*, a^*) \in \mathscr{A}$ such that

$$\Psi(u) = \inf_{\vartheta \in \mathscr{A}} \sup_{\theta \in \Theta} J^{\theta,\vartheta}(u) = J^{\theta^*,\vartheta^*}(u). \tag{13}$$

Similar to the handling in Øksendal [20] and Øksendal and Sulem [21], we could consider feedback Markov controls and, for some functions, $\theta_0 : [0,T] \times (0,\infty) \times (0,\infty) \to \mathscr{R}$ and $\vartheta_0 : [0,T] \times (0,\infty) \times (0,\infty)$, assume that for each $t \in [0,T]$, $\theta(t) \coloneqq \theta_0(U(t))$ and $\vartheta(t) \coloneqq \vartheta_0(U(t))$ under some mild conditions. Then, for each pair $(\theta, \vartheta) \in (\Theta, \mathscr{A})$, the generator of the process $U(\cdot)$ is a partial differential operator $\mathscr{L}^{\theta,\vartheta}(h(u))$.

$$\begin{aligned} &\mathscr{L}^{\theta,\vartheta}(h(u)) \\ &= \frac{\partial h}{\partial t} + \left\{\lambda\mu_{\infty}\left[\eta a - (\eta - \delta)\right] + r_0 u_1 + r\pi\right\}\frac{\partial h}{\partial u_1} \\ &\quad + \frac{1}{2}\left(\sigma_0^2 a^2 + \sigma_1^2 \pi^2\right)\frac{\partial^2 h}{\partial u_1^2} + u_2^2 \theta^2 \frac{\partial^2 h}{\partial u_2^2} \\ &\quad - \left(\sigma_0 a + \sigma_1 \pi\right)\theta u_2 \frac{\partial^2 h}{\partial u_1 \partial u_2}, \end{aligned} \tag{14}$$

where $h(u) \coloneqq h(\cdot,\cdot,\cdot) \in \mathscr{C}^{1,2,2}([0,T] \times (0,\infty) \times (0,\infty))$.

Theorem 1 (verification theorem). *For the Min-Max problem, if there exist three real value functions ϕ, θ^*, and ϑ^* satisfying the following HJB system:*

$$\begin{aligned} \inf_{\vartheta \in \mathscr{A}} \sup_{\theta \in \Theta} \mathscr{L}^{\theta,\vartheta}\left[\phi(t, u_1, u_2)\right] &= 0, \\ \phi(T, u_1, u_2) &= u_2\left(u_1 - k\right)^2, \end{aligned} \tag{15}$$

then $\Psi(u) = \phi(t, u_1, u_2)$, θ^* corresponds to the "worst-case" scenario, and $\vartheta^* = (\pi^*, a^*)$ is the optimal investment-reinsurance strategy.

The proof of Theorem 1 is similar to the proof of Theorem 3.2 in Mataramvura and Øksendal [15]. So we do not repeat it here.

In order to solve problem (11), we only need to solve the HJB equation (15). Motivated by the terminal boundary

condition, we try the following parametric form of the value function:

$$\phi(t,u_1,u_2) = u_2\left[A(t)u_1^2 + B(t)u_1 + C(t)\right], \quad (16)$$

where $A(\cdot)$, $B(\cdot)$, and $C(\cdot)$ are three suitable functions, and the boundary condition in Theorem 1 implies that $A(T) = 1$, $B(T) = -2k$, and $C(T) = k^2$. The corresponding partial derivatives are

$$\begin{aligned}
\frac{\partial\phi}{\partial t} &= u_2\left[\dot{A}(t)u_1^2 + \dot{B}(t)u_1 + \dot{C}(t)\right],\\
\frac{\partial\phi}{\partial u_1} &= u_2\left[2A(t)u_1 + B(t)\right],\\
\frac{\partial^2\phi}{\partial u_1^2} &= 2A(t)u_2,\\
\frac{\partial\phi}{\partial u_2} &= A(t)u_1^2 + B(t)u_1 + C(t), \quad \frac{\partial^2\phi}{\partial u_2^2} = 0,\\
\frac{\partial^2\phi}{\partial u_1\partial u_2} &= 2A(t)u_1 + B(t).
\end{aligned} \quad (17)$$

Substituting the above derivatives into $\mathscr{L}^{\theta,\vartheta}(\phi(u))$, we have

$$\begin{aligned}
\mathscr{L}^{\theta,\vartheta}(\phi(u)) = u_2\Big\{&\dot{A}(t)u_1^2 + \dot{B}(t)u_1 + \dot{C}(t)\\
&+\left[r_0u_1 - \lambda\mu_\infty(\eta-\delta)\right]\left[2A(t)u_1 + B(t)\right]\\
&+\left(\lambda\mu_\infty\eta - \sigma_0\theta\right)\left[2A(t)u_1 + B(t)\right]a + \sigma_0^2A(t)a^2\\
&+\left(r - \sigma_1\theta\right)\left[2A(t)u_1 + B(t)\right]\pi + \sigma_1^2A(t)\pi^2\Big\}.
\end{aligned} \quad (18)$$

For fixed θ, by the first-order condition, we can get

$$\widehat{\pi}(\theta) = \frac{\sigma_1\theta - r}{2\sigma_1^2}\left[2u_1 + \frac{B(t)}{A(t)}\right], \quad (19)$$

$$\widehat{a}(\theta) = \frac{\sigma_0\theta - \lambda\mu_\infty\eta}{2\sigma_0^2}\left[2u_1 + \frac{B(t)}{A(t)}\right]. \quad (20)$$

Substituting $\widehat{\vartheta} = (\widehat{\pi}(\theta), \widehat{a}(\theta))$ into $\mathscr{L}^{\theta,\vartheta}(\phi(u))$, we have

$$\begin{aligned}
\mathscr{L}^{\theta,\widehat{\vartheta}}(\phi(u)) = u_2\Big\{&\dot{A}(t)u_1^2 + \dot{B}(t)u_1 + \dot{C}(t)\\
&+\left[r_0u_1 - \lambda\mu_\infty(\eta-\delta)\right]\left[2A(t)u_1 + B(t)\right]\\
&-\left[\sigma_0\theta - \lambda\mu_\infty\eta\right]^2\frac{\left[2A(t)u_1 + B(t)\right]^2}{4\sigma_0^2A(t)}\\
&-\left[\sigma_1\theta - r\right]^2\frac{\left[2A(t)u_1 + B(t)\right]^2}{4\sigma_1^2A(t)}\Big\}.
\end{aligned} \quad (21)$$

Maximizing over θ gives the first-order condition for the maximum point $\theta = \widehat{\theta}$ as follows:

$$\widehat{\theta} = \frac{1}{2}\left(\frac{\lambda\mu_\infty\eta}{\sigma_0} + \frac{r}{\sigma_1}\right) = \frac{r\sigma_0 + \lambda\mu_\infty\eta\sigma_1}{2\sigma_0\sigma_1}. \quad (22)$$

So,

$$\begin{aligned}
\widehat{\pi}(t) &= \widehat{\pi}\left(\widehat{\theta}\right) = \frac{\lambda\mu_\infty\eta\sigma_1 - r\sigma_0}{4\sigma_0\sigma_1^2}\left[2u_1 + \frac{B(t)}{A(t)}\right],\\
\widehat{a}(t) &= \widehat{a}\left(\widehat{\theta}\right) = \frac{r\sigma_0 - \lambda\mu_\infty\eta\sigma_1}{4\sigma_0^2\sigma_1}\left[2u_1 + \frac{B(t)}{A(t)}\right].
\end{aligned} \quad (23)$$

We rewrite $\mathscr{L}^{\widehat{\theta},\widehat{\vartheta}}(\phi(u))$ as follows:

$$\begin{aligned}
\mathscr{L}^{\widehat{\theta},\widehat{\vartheta}}(\phi(u)) = u_2\Big\{&\left[\dot{A}(t) + \left(2r_0 - \mathscr{D}\right)A(t)\right]u_1^2\\
&+\left[\dot{B}(t) + \left(r_0 - \mathscr{D}\right)B(t) - 2\Gamma A(t)\right]u_1 + \dot{C}(t)\\
&-\Gamma B(t) - \frac{\mathscr{D}B^2(t)}{4A(t)}\Big\},
\end{aligned} \quad (24)$$

where $\mathscr{D} = (r\sigma_0 - \lambda\mu_\infty\eta\sigma_1)^2/4\sigma_0^2\sigma_1^2$ and $\Gamma = \lambda\mu_\infty(\eta - \delta)$.

To ensure $\mathscr{L}^{\widehat{\theta},\widehat{\vartheta}}(\phi(u)) = 0$ holds, we require

$$\begin{aligned}
&\dot{A}(t) + \left(2r_0 - \mathscr{D}\right)A(t) = 0, \quad A(T) = 1,\\
&\dot{B}(t) + \left(r_0 - \mathscr{D}\right)B(t) - 2\Gamma A(t) = 0, \quad B(T) = -2k,\\
&\dot{C}(t) - \Gamma B(t) - \frac{\mathscr{D}B^2(t)}{4A(t)} = 0, \quad C(T) = k^2.
\end{aligned} \quad (25)$$

Then it is easy to obtain

$$\begin{aligned}
A(t) &= e^{(2r_0 - \mathscr{D})(T-t)},\\
B(t) &= -2\left[\frac{\Gamma}{r_0}\left(e^{r_0(T-t)} - 1\right) + k\right]e^{(r_0 - \mathscr{D})(T-t)},\\
C(t) &= \left[\frac{\Gamma}{r_0}\left(e^{r_0(T-t)} - 1\right) + k\right]^2 e^{-\mathscr{D}(T-t)}.
\end{aligned} \quad (26)$$

So, for $s \le t \le T$, we have

$$\begin{aligned}
\widehat{\pi}(t) &= \frac{r\sigma_0 - \lambda\mu_\infty\eta\sigma_1}{2\sigma_0\sigma_1^2}\left[\left(k - \frac{\Gamma}{r_0}\right)e^{-r_0(T-t)} - \left(u_1 - \frac{\Gamma}{r_0}\right)\right] = \frac{r\sigma_0 - \lambda\mu_\infty\eta\sigma_1}{2\sigma_0\sigma_1^2e^{r_0(T-t)}}\left[\left(k - xe^{r_0(T-t)}\right) + \frac{\Gamma}{r_0}\left(e^{r_0(T-t)} - 1\right)\right],\\
\widehat{a}(t) &= \frac{\lambda\mu_\infty\eta\sigma_1 - r\sigma_0}{2\sigma_0^2\sigma_1}\left[\left(k - \frac{\Gamma}{r_0}\right)e^{-r_0(T-t)} - \left(u_1 - \frac{\Gamma}{r_0}\right)\right] = \frac{\lambda\mu_\infty\eta\sigma_1 - r\sigma_0}{2\sigma_0^2\sigma_1e^{r_0(T-t)}}\left[\left(k - xe^{r_0(T-t)}\right) + \frac{\Gamma}{r_0}\left(e^{r_0(T-t)} - 1\right)\right].
\end{aligned} \quad (27)$$

Note that the reinsurance strategy a must be nonnegative. Denote

$$\Delta = \lambda\mu_\infty\eta\sigma_1 - r\sigma_0,$$
$$H(t) = \left(k - xe^{r_0(T-t)}\right) + \frac{\Gamma}{r_0}\left(e^{r_0(T-t)} - 1\right). \tag{28}$$

Then for $t \in [0, T]$,

(i) when $\Delta \geq 0, H(t) \geq 0$ or $\Delta \leq 0, H(t) \leq 0$, it is easy to get $\widehat{a}(t) \geq 0$, which can be a candidate of the optimal strategy;

(ii) when $\Delta \leq 0, H(t) \geq 0$ or $\Delta \geq 0, H(t) \leq 0$, we may choose $\widehat{a} = 0$ as the optimal reinsurance strategy since (18) is a second-order polynomial in a. Thus the operator $\mathscr{L}^{\theta,\vartheta}(h(v))$ in (14) can be changed as

$$\begin{aligned}\mathscr{L}^{\theta,\vartheta}(h(u)) = {} & \frac{\partial h}{\partial t} + \left\{\lambda\mu_\infty(\delta - \eta) + r_0u_1 + r\pi\right\}\frac{\partial h}{\partial u_1} \\ & + \frac{1}{2}\sigma_1^2\pi^2\frac{\partial^2 h}{\partial u_1^2} + u_2^2\theta^2\frac{\partial^2 h}{\partial u_2^2} \\ & - \sigma_1\pi\theta u_2\frac{\partial^2 h}{\partial u_1\partial u_2}.\end{aligned} \tag{29}$$

Parallel to the proof of Theorem 1, we can obtain the same form of expression of the investment strategy $\widehat{\pi}$ in (19) for fixed $\widehat{\theta} = r/\sigma_1$. Then the minimum point $\widehat{\pi}$ is given by $\widehat{\pi} = 0$.

Combining with Theorem 1, the above analyses are summarized as the following theorem.

Theorem 2. *The optimal investment-reinsurance strategy of the Min-Max problem (11) is*

$$\begin{aligned}&(\pi^*, a^*) \\ &= \begin{cases}\left(-\dfrac{H(t)\Delta}{2\sigma_0\sigma_1^2e^{r_0(T-t)}}, \dfrac{H(t)\Delta}{2\sigma_0^2\sigma_1e^{r_0(T-t)}}\right), & \text{if } H(t)\Delta \geq 0, \\ (0,0), & \text{if } H(t)\Delta \leq 0.\end{cases}\end{aligned} \tag{30}$$

Moreover, the corresponding value function is given by

$$\begin{aligned}\Psi(u) = u_2\Bigg\{e^{-\mathscr{D}(T-s)}\Bigg[u_1e^{r_0(T-s)} - \frac{\Gamma}{r_0}\left(e^{r_0(T-s)} - 1\right) \\ - k\Bigg]^2\Bigg\}.\end{aligned} \tag{31}$$

Remark 3. We find that (i) under model uncertainty the optimal policy $\vartheta^* = (\pi^*, a^*)$ depends on the volatility of both the insurer's surplus and the risky asset; (ii) if we do not take account of the model risk, the corresponding optimal investment-reinsurance strategies (see Appendix) are different: the volatility of the insurer's surplus has no influence on the investment strategy $\widetilde{\pi}(t)$ (see Appendix (A.11)), and the volatility of the risky asset has no influence on the reinsurance strategy $\widetilde{a}(t)$ (see Appendix (A.12)).

4. Numerical Results

In this section, we present some numerical illustrations and sensitivity analysis of optimal investment-reinsurance strategies. Throughout the numerical analysis, unless otherwise stated, the basic parameters are given by $x_0 = 10$, $\lambda = 1$, $u_1 = 1$, $\eta = 1.5$, $\delta = 1.1$, $r_0 = 0.04$, $r_1 = 0.2$, $\sigma_0 = 1.5$, $\sigma_1 = 1.15$, $k = 15$, $T = 5$, and $N = 300$. In the following numerical examples, we illustrate the effect of different parameters on the optimal strategies by varying the value of one parameter with others fixed each time.

Figure 1 shows the effect of the riskless rate of interest r_0, the appreciation rate of the risky asset r_1, the volatility of the insurer's surplus σ_0, and the volatility of the risky asset σ_1 on the optimal investment strategy $\pi^*(t)$. We compare the investment strategies in Figure 1(a) when $r_0 = 0.01$ and $r_0 = 0.06$ for fixed $t \in [0, 5]$. It is shown that as the risk-free interest rate r_0 increases, the optimal investment strategy $\pi^*(t)$ moves up in any time. And when t is near time 0, the trend is very obvious. From Figures 1(b) and 1(c), we find that $\pi^*(t)$ increases with respect to r_1 and σ_0 for fixed $t \in [0, 5]$ where we compare the investment strategies when $r_1 = 0.05$ and $r_1 = 0.35$ and $\sigma_0 = 1.15$ and $\sigma_0 = 1.5$. It is a different case as in Figure 1(d), where we compare the investment strategies when $\sigma_1 = 0.55$ and $\sigma_1 = 1.65$ for fixed $t \in [0, 5]$.

Figure 2 shows the effect of different parameters on the optimal reinsurance strategy. In Figure 2(a), we compare the reinsurance strategies when $r_0 = 0.01$ and $r_0 = 0.06$ for fixed $t \in [0, 5]$. It is shown that as the risk-free interest rate r_0 increases, the optimal investment strategy $\pi^*(t)$ moves down. In Figure 2(b), we compare the reinsurance strategies when $r_1 = 0.05$ and $r_1 = 0.35$ for fixed $t \in [0, 5]$. In Figure 2(c), we compare the reinsurance strategies when $\sigma_0 = 1.15$ and $\sigma_0 = 1.55$ for fixed $t \in [0, 5]$. In Figure 2(d), we compare the reinsurance strategies when $\sigma_1 = 0.55$ and $\sigma_1 = 1.65$ for fixed $t \in [0, 5]$.

We can find from the above two groups of Figures that, while keeping other parameters unchanged:

(i) The insurer is inclined to invest in the market (compared with buying reinsurance) when the riskless rate of interest r_0 increases.

(ii) When the appreciation rate of the risky asset r_1 increases, the insurer is inclined to invest in the market (compared with buying reinsurance) during the first half of the horizon and to buy reinsurance (compared with investing in the market) during the second half of the horizon.

(iii) As the volatility of the insurers surplus σ_0 increases, the insurer seems to be willing to invest in the market during the first half of the horizon and buy reinsurance during the second half of the horizon.

(iv) The insurer is inclined to invest in the market (compared with buying reinsurance) when the volatility of the risky asset σ_1 increases.

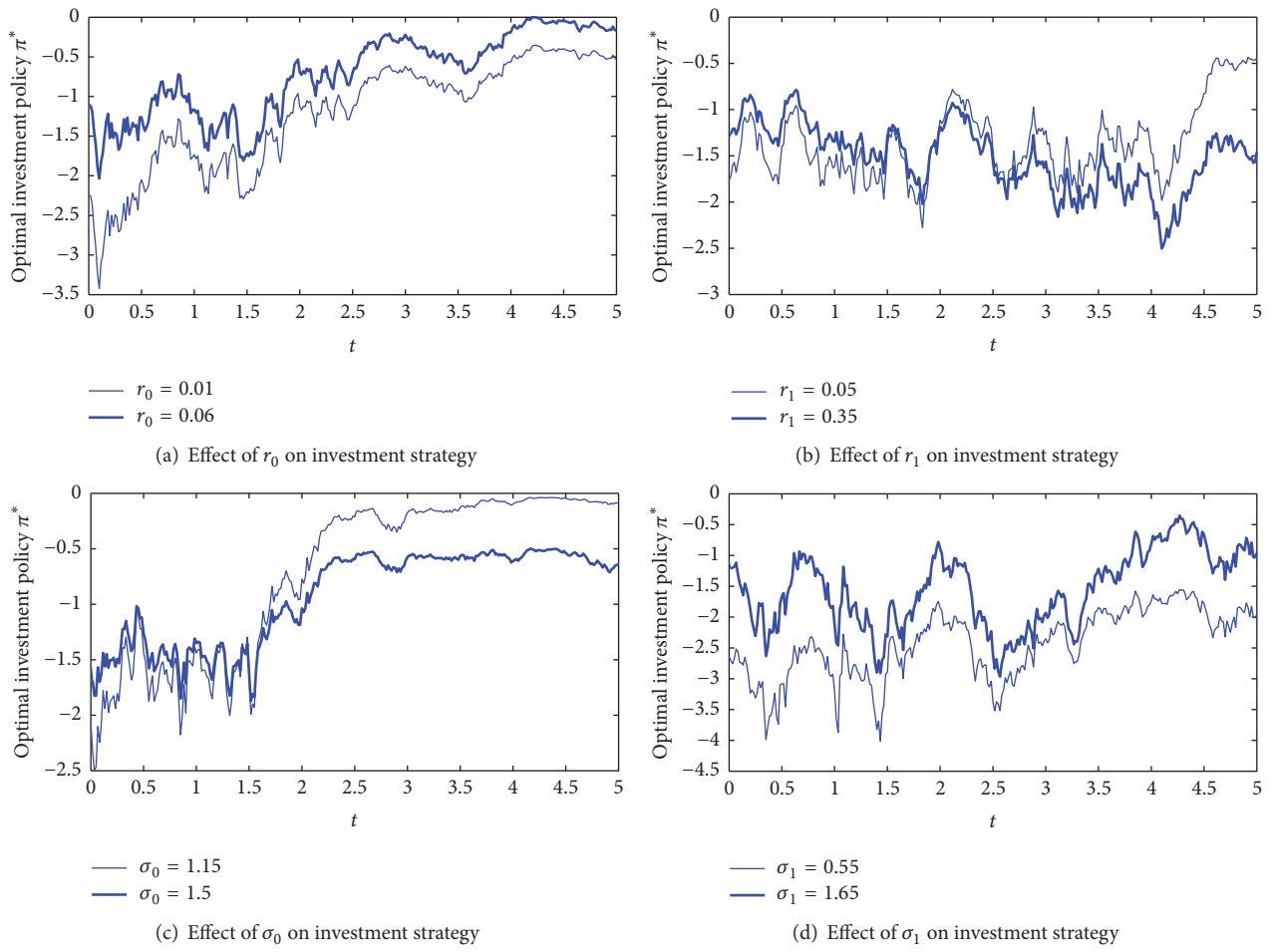

(a) Effect of r_0 on investment strategy

(b) Effect of r_1 on investment strategy

(c) Effect of σ_0 on investment strategy

(d) Effect of σ_1 on investment strategy

FIGURE 1: The effect of parameters on optimal investment strategy.

5. Conclusion

In this paper, we study an optimization problem for an insurer when facing uncertainties. The insurer is allowed to invest into a financial market and purchase proportional reinsurance/acquire new business. The model uncertainty is described by a family of probability measures equivalent to the original probability measure. Compared with Zhang and Siu [16] and Lin et al. [17], we focus on the criterion of minimizing the expected quadratic distance of the insurer's terminal wealth to a given benchmark. Under the "worst-case" scenario, we have derived the optimal investment-reinsurance strategy and the corresponding value function explicitly. In addition, we have presented some numerical illustrations and sensitivity analysis to show the effect of parameters on optimal strategies.

Appendix

Optimal Strategies without Model Risk

The insurer aims to select an optimal investment and reinsurance strategy ϑ which minimizes the expected quadratic distance of the terminal wealth to a given benchmark. That is to find

$$V(x) = \inf_{\vartheta \in \mathcal{A}} \left\{ \mathrm{E}^x \left[\left(X^{\vartheta}(T) - k \right)^2 \right] \right\}. \tag{A.1}$$

Here we also assume $k \geq x_0 e^{r_0 T}$.

Then the generator of the process $V(\cdot)$ is a partial differential operator.

$$\begin{aligned} \widetilde{\mathscr{L}}(h(u)) = {} & \frac{\partial h}{\partial t} \\ & + \left\{ \lambda \mu_{\infty} \left[\eta a - (\eta - \delta) \right] + r_0 u_1 + r\pi \right\} \frac{\partial h}{\partial x} \\ & + \frac{1}{2} \left(\sigma_0^2 a^2 + \sigma_1^2 \pi^2 \right) \frac{\partial^2 h}{\partial x^2}. \end{aligned} \tag{A.2}$$

Thus we can obtain the following HJB equation:

$$\inf_{\vartheta \in \mathcal{A}} \widetilde{\mathscr{L}} \left[\varphi(t,x) \right] = 0, \quad \varphi(T,x) = (x-k)^2. \tag{A.3}$$

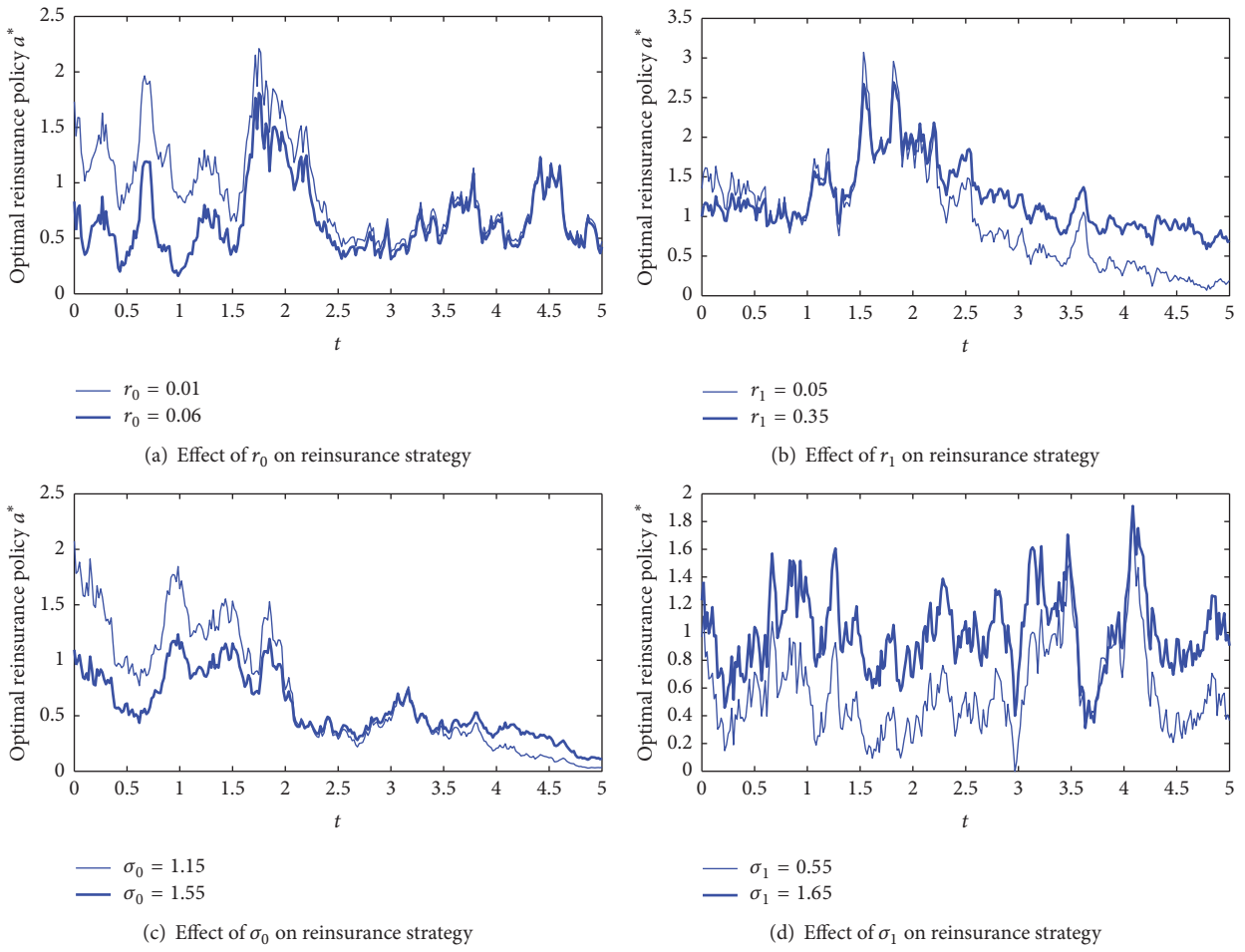

(a) Effect of r_0 on reinsurance strategy

(b) Effect of r_1 on reinsurance strategy

(c) Effect of σ_0 on reinsurance strategy

(d) Effect of σ_1 on reinsurance strategy

Figure 2: The effect of parameters on optimal reinsurance strategy.

Motivated by the terminal boundary condition, we try the following parametric form of the value function:

$$\varphi(t,x) = m(t)x^2 + n(t)x + l(t), \tag{A.4}$$

with $m(T) = 1, n(T) = -2k, l(T) = k^2$. The corresponding partial derivatives are

$$\begin{aligned}\frac{\partial\varphi}{\partial t} &= \dot{m}(t)x^2 + \dot{n}(t)x + \dot{l}(t),\\ \frac{\partial\varphi}{\partial x} &= 2m(t)x + n(t),\\ \frac{\partial^2\varphi}{\partial x^2} &= 2m(t)x.\end{aligned} \tag{A.5}$$

Substituting the above derivatives into $\widetilde{\mathscr{L}}(\varphi(x))$, we have

$$\begin{aligned}&\widetilde{\mathscr{L}}(\varphi(x))\\ &= \dot{m}(t)x^2 + \dot{n}(t)x + \dot{l}(t)\\ &\quad + [r_0 x - \lambda\mu_\infty(\eta-\delta)][2m(t)x + n(t)]\\ &\quad + \lambda\mu_\infty\eta[2m(t)x + n(t)]a + \sigma_0^2 m(t)a^2\\ &\quad + r[2m(t)u_1 + n(t)]\pi + \sigma_1^2 m(t)\pi^2.\end{aligned} \tag{A.6}$$

For fixed θ, by the first-order condition, we can get

$$\begin{aligned}\widetilde{\pi}(\theta) &= -\frac{r}{2\sigma_1^2}\left[2x + \frac{n(t)}{m(t)}\right],\\ \widetilde{a}(\theta) &= -\frac{\lambda\mu_\infty\eta}{2\sigma_0^2}\left[2x + \frac{n(t)}{m(t)}\right].\end{aligned} \tag{A.7}$$

Substituting $\widetilde{\vartheta} = (\widetilde{\pi}(\theta), \widetilde{a}(\theta))$ into $\widetilde{\mathscr{L}}(\varphi(x))$, we have

$$\begin{aligned}\widetilde{\mathscr{L}}(\varphi(x)) &= [\dot{m}(t) + (2r_0 - \mathscr{E})m(t)]x^2\\ &\quad + [\dot{n}(t) + (r_0 - \mathscr{E})n(t) - 2\Gamma m(t)]x\\ &\quad + \dot{l}(t) - \Gamma n(t) - \frac{\mathscr{E}n^2(t)}{4m(t)},\end{aligned} \tag{A.8}$$

where $\mathscr{E} = (r^2\sigma_0^2 + \lambda^2\mu_\infty^2\eta^2\sigma_1^2)/\sigma_0^2\sigma_1^2$ and $\Gamma = \lambda\mu_\infty(\eta - \delta)$.

To ensure $\widetilde{\mathscr{L}}(\varphi(x)) = 0$ holds, we require

$$\begin{aligned}&\dot{m}(t) + (2r_0 - \mathscr{E})m(t) = 0, \quad m(T) = 1,\\ &\dot{n}(t) + (r_0 - \mathscr{E})n(t) - 2\Gamma m(t) = 0, \quad n(T) = -2k,\\ &\dot{l}(t) - \Gamma n(t) - \frac{\mathscr{E}n^2(t)}{4m(t)} = 0, \quad l(T) = k^2.\end{aligned} \tag{A.9}$$

Then it is easy to obtain

$$m(t) = e^{(2r_0-\mathscr{E})(T-t)},$$
$$n(t) = -2\left[\frac{\Gamma}{r_0}\left(e^{r_0(T-t)}-1\right)+k\right]e^{(r_0-\mathscr{E})(T-t)}, \tag{A.10}$$
$$l(t) = \left[\frac{\Gamma}{r_0}\left(e^{r_0(T-t)}-1\right)+k\right]^2 e^{-\mathscr{E}(T-t)}.$$

So, for $s \le t \le T$, we get the optimal strategies

$$\begin{aligned}\widetilde{\pi}(t) &= \frac{r}{\sigma_1^2}\left[\left(k-\frac{\Gamma}{r_0}\right)e^{-r_0(T-t)}-\left(x-\frac{\Gamma}{r_0}\right)\right] \\ &= \frac{r}{\sigma_1^2 e^{r_0(T-t)}}\left[\left(k-xe^{r_0(T-t)}\right)+\frac{\Gamma}{r_0}\left(e^{r_0(T-t)}-1\right)\right]\end{aligned} \tag{A.11}$$

$$\begin{aligned}\widetilde{a}(t) &= \frac{\lambda\mu_\infty\eta}{\sigma_0^2}\left[\left(k-\frac{\Gamma}{r_0}\right)e^{-r_0(T-t)}-\left(x-\frac{\Gamma}{r_0}\right)\right] \\ &= \frac{\lambda\mu_\infty\eta}{\sigma_0^2 e^{r_0(T-t)}}\left[\left(k-xe^{r_0(T-t)}\right)+\frac{\Gamma}{r_0}\left(e^{r_0(T-t)}-1\right)\right]\end{aligned} \tag{A.12}$$

and the value function

$$V(x) = e^{-\mathscr{E}(T-s)}\left[xe^{r_0(T-s)}-\frac{\Gamma}{r_0}\left(e^{r_0(T-s)}-1\right)-k\right]^2. \tag{A.13}$$

Competing Interests

The authors declare that there are no competing interests regarding the publication of this paper.

Acknowledgments

The authors acknowledge the support from the National Natural Science Foundation of China (Grants nos. 11201335 and 11301376).

References

[1] S. Browne, "Optimal investment policies for a firm with a random risk process: exponential utility and minimizing the probability of ruin," *Mathematics of Operations Research*, vol. 20, no. 4, pp. 937–958, 1995.

[2] C. Hipp and M. Plum, "Optimal investment for insurers," *Insurance: Mathematics & Economics*, vol. 27, no. 2, pp. 215–228, 2000.

[3] H. Schmidli, "Optimal proportional reinsurance policies in a dynamic setting," *Scandinavian Actuarial Journal*, vol. 1, pp. 55–68, 2001.

[4] H. Schmidli, "On minimizing the ruin probability by investment and reinsurance," *The Annals of Applied Probability*, vol. 12, no. 3, pp. 890–907, 2002.

[5] H. Markowitz, "Portfolio selection," *The Journal of Finance*, vol. 7, no. 1, pp. 77–91, 1952.

[6] N. Bäuerle, "Benchmark and mean-variance problems for insurers," *Mathematical Methods of Operations Research*, vol. 62, no. 1, pp. 159–165, 2005.

[7] L. Bai and H. Zhang, "Dynamic mean-variance problem with constrained risk control for the insurers," *Mathematical Methods of Operations Research*, vol. 68, no. 1, pp. 181–205, 2008.

[8] Y. Zeng, Z. Li, and J. Liu, "Optimal strategies of benchmark and mean-variance portfolio selection problems for insurers," *Journal of Industrial and Management Optimization*, vol. 6, no. 3, pp. 483–496, 2010.

[9] Y. Zeng and Z. Li, "Optimal time-consistent investment and reinsurance policies for mean-variance insurers," *Insurance: Mathematics and Economics*, vol. 49, no. 1, pp. 145–154, 2011.

[10] M. C. Chiu and H. Y. Wong, "Mean-variance asset-liability management: cointegrated assets and insurance liability," *European Journal of Operational Research*, vol. 223, no. 3, pp. 785–793, 2012.

[11] M. C. Chiu and H. Y. Wong, "Mean–variance asset–liability management with asset correlation risk and insurance liabilities," *Insurance: Mathematics and Economics*, vol. 59, pp. 300–310, 2014.

[12] Y. Zeng, Z. Li, and Y. Lai, "Time-consistent investment and reinsurance strategies for mean–variance insurers with jumps," *Insurance: Mathematics & Economics*, vol. 52, no. 3, pp. 498–507, 2013.

[13] Y. Shen and Y. Zeng, "Optimal investment-reinsurance strategy for mean-variance insurers with square-root factor process," *Insurance: Mathematics & Economics*, vol. 62, pp. 118–137, 2015.

[14] D. Talay and Z. Zheng, "Worst case model risk management," *Finance and Stochastics*, vol. 6, no. 4, pp. 517–537, 2002.

[15] S. Mataramvura and B. Øksendal, "Risk minimizing portfolios and HJBI equations for stochastic differential games," *Stochastics*, vol. 80, no. 4, pp. 317–337, 2008.

[16] X. Zhang and T. K. Siu, "Optimal investment and reinsurance of an insurer with model uncertainty," *Insurance: Mathematics and Economics*, vol. 45, no. 1, pp. 81–88, 2009.

[17] X. Lin, C. Zhang, and T. K. Siu, "Stochastic differential portfolio games for an insurer in a jump-diffusion risk process," *Mathematical Methods of Operations Research*, vol. 75, no. 1, pp. 83–100, 2012.

[18] J. Grandell, *Aspects of Risk Theory*, Springer, 1991.

[19] H. Schmidli, *Stochastic Control in Insurance*, Probability and Its Applications (New York), Springer, London, UK, 2008.

[20] B. Øksendal, *Stochastic Differential Equations*, Springer, 2003.

[21] B. Øksendal and A. Sulem, *Applied stochastic control of jump diffusions*, Universitext, Springer, Berlin, Germany, 2005.

Hindawi Publishing Corporation
Discrete Dynamics in Nature and Society
Volume 2016, Article ID 5649584, 21 pages
http://dx.doi.org/10.1155/2016/5649584

Research Article

Dynamical Analysis of a Computer Virus Model with Delays

Juan Liu,[1] Carlo Bianca,[2] and Luca Guerrini[3]

[1]*Department of Mathematics and Physics, Bengbu University, Bengbu 233030, China*
[2]*Laboratoire de Physique Statistique, Ecole Normale Supérieure, PSL Research University, Université Paris Diderot Sorbonne Paris-Cité, Sorbonne Universités, UPMC Univ Paris 06, CNRS, 24 rue Lhomond, 75005 Paris, France*
[3]*Department of Management, Polytechnic University of Marche, 60121 Ancona, Italy*

Correspondence should be addressed to Juan Liu; liujuan7216@163.com

Received 5 August 2016; Accepted 29 September 2016

Academic Editor: Vincenzo Scalzo

Copyright © 2016 Juan Liu et al. This is an open access article distributed under the Creative Commons Attribution License, which permits unrestricted use, distribution, and reproduction in any medium, provided the original work is properly cited.

An SIQR computer virus model with two delays is investigated in the present paper. The linear stability conditions are obtained by using characteristic root method and the developed asymptotic analysis shows the onset of a Hopf bifurcation occurs when the delay parameter reaches a critical value. Moreover the direction of the Hopf bifurcation and stability of the bifurcating period solutions are investigated by using the normal form theory and the center manifold theorem. Finally, numerical investigations are carried out to show the feasibility of the theoretical results.

1. Introduction

The advances of information technology and the widespread popularity of computer networks have increased the interest in the computer viruses. In the past decades, many epidemic models such as SIR model [1, 2], SIRS model [3, 4], SEIR model [5–7], SEIRS model [8] and SEIQRS model [9] characterizing the spread of computer viruses in networks were investigated by many scholars. It is worthwhile to note that the dynamical models above neglect the time delay in the spreading process of computer viruses. To our knowledge, there have been some computer virus models with time delay proposed to depict the spread of a computer virus. In [10, 11], Muroya et al. studied the global stability of a delayed SIRS computer virus propagation model, respectively. In [12], Feng et al. investigated the Hopf bifurcation of a delayed SIRS viral infection model in computer networks by regarding the delay due to temporary immune period of the recovered computers as a bifurcation parameter. In [13], Dong et al. analyzed the Hopf bifurcation of a delayed SEIR computer virus model with multistate antivirus by regarding the time delay due to the period that the computers use antivirus software to clean the viruses as the bifurcation parameter. In [14], Zhang and Yang studied the Hopf bifurcation of the following SIQR computer virus model with time delay:

$$\begin{aligned}
\frac{dS(t)}{dt} &= (1-p)b - \beta S(t-\tau) I(t-\tau) - dS(t), \\
\frac{dI(t)}{dt} &= \beta S(t-\tau) I(t-\tau) - (\delta + d + \alpha_1 + \gamma) I(t), \\
\frac{dQ(t)}{dt} &= \delta I(t) - (\varepsilon + d + \alpha_2) Q(t), \\
\frac{dR(t)}{dt} &= \gamma I(t) + pb + \varepsilon Q(t) - dR(t),
\end{aligned} \tag{1}$$

where $S(t)$, $I(t)$, $Q(t)$, and $R(t)$ denote the numbers of nodes in states susceptible, infectious, quarantined, and recovered at time t, respectively. b, p, α_1, α_2, β, γ, δ, and ε are the parameters of system (1) and τ is the time delay due to the latent period of the computer virus. Zhang and Yang obtained the sufficient conditions for the local stability and existence of local Hopf bifurcation by regarding the delay as a bifurcation parameter and investigated the properties of the Hopf bifurcation by using the normal form method and center manifold theory. As stated in [13], it usually takes

a period to clean the viruses in the computers infected by viruses for antivirus software. Therefore, it is reasonable to incorporate the time delay due to the period that antivirus software uses to clean viruses in the infectious and the quarantined computers into system (1). Bearing all above in mind, this paper deals with the analysis of the Hopf bifurcation of the following system with two delays:

$$\begin{aligned}
\frac{dS(t)}{dt} &= (1-p)\,b - \beta S(t-\tau_1)\,I(t-\tau_1) - dS(t),\\
\frac{dI(t)}{dt} &= \beta S(t-\tau_1)\,I(t-\tau_1) - (\delta + d + \alpha_1)\,I(t)\\
&\quad - \gamma I(t-\tau_2),\\
\frac{dQ(t)}{dt} &= \delta I(t) - (d+\alpha_2)\,Q(t) - \varepsilon Q(t-\tau_2),\\
\frac{dR(t)}{dt} &= \gamma I(t-\tau_2) + pb + \varepsilon Q(t-\tau_2) - dR(t),
\end{aligned} \tag{2}$$

where τ_1 is the time delay due to the latent period of the computer virus and τ_2 is the time delay due to the period that the antivirus software uses to clean the computer viruses in the infectious and the quarantined nodes.

This paper mainly investigates the effect of the two delays on system (2). The remainder of this paper is organized as follows. The local stability of the positive equilibrium and existence of local Hopf bifurcation are analyzed in Section 2 by choosing different combination of the two delays as a bifurcation parameter. Direction of the Hopf bifurcation, stability, and period of the bifurcating periodic solutions on the center manifold are determined in Section 3. Some numerical simulations are presented to illustrate the validity of the main results in Section 4. Finally a critical analysis and further research directions are contained in Section 5.

2. Local Stability of the Positive Equilibrium and Existence of Local Hopf Bifurcation

According to the analysis in [14] we know that if $R_0 = (1-p)b\beta/d(\delta + d\alpha_1 + \gamma) > 1$, system (2) has a unique positive equilibrium $D_*(S_*, I_*, Q_*, R_*)$, where

$$\begin{aligned}
S_* &= \frac{\delta + d + \alpha_1 + \gamma}{\beta},\\
I_* &= \frac{(1-p)\,b\beta - d(\delta + d + \alpha_1 + \gamma)}{\beta(\delta + d + \alpha_1 + \gamma)},\\
Q_* &= \frac{\delta I_*}{\varepsilon + d + \alpha_2},\\
R_* &= \frac{pb + \gamma I_* + \varepsilon Q_*}{d}.
\end{aligned} \tag{3}$$

The characteristic equation of system (2) at D_* is

$$\begin{vmatrix}
\lambda - a_{11} - b_{11}e^{-\lambda\tau_1} & -b_{12}e^{-\lambda\tau_1} & 0 & 0\\
-b_{21}e^{-\lambda\tau_1} & \lambda - a_{22} - b_{22}e^{-\lambda\tau_1} - c_{22}e^{-\lambda\tau_2} & 0 & 0\\
0 & -a_{32} & \lambda - a_{33} - c_{33}e^{-\lambda\tau_2} & 0\\
0 & -c_{42}e^{-\lambda\tau_2} & -c_{43}e^{-\lambda\tau_2} & \lambda - a_{44}
\end{vmatrix} = 0, \tag{4}$$

from which we obtain

$$\begin{aligned}
&\lambda^4 + A_3\lambda^3 + A_2\lambda^2 + A_1\lambda + A_0\\
&\quad + \left(B_3\lambda^3 + B_2\lambda^2 + B_1\lambda + B_0\right)e^{-\lambda\tau_1}\\
&\quad + \left(C_3\lambda^3 + C_2\lambda^2 + C_1\lambda + C_0\right)e^{-\lambda\tau_2}\\
&\quad + \left(D_2\lambda^2 + D_1\lambda + D_0\right)e^{-\lambda(\tau_1+\tau_2)}\\
&\quad + \left(E_2\lambda^2 + E_1\lambda + E_0\right)e^{-2\lambda\tau_2}\\
&\quad + (F_1\lambda + F_0)\,e^{-\lambda(\tau_1+2\tau_2)} = 0,
\end{aligned} \tag{5}$$

where

$$\begin{aligned}
A_0 &= a_{11}a_{22}a_{33}a_{44},\\
A_1 &= -\left(a_{11}a_{22}(a_{33}+a_{44}) + a_{33}a_{44}(a_{11}+a_{22})\right),\\
A_2 &= a_{11}a_{22} + a_{33}a_{44} + (a_{11}+a_{22})(a_{33}+a_{44}),\\
A_3 &= -(a_{11}+a_{22}+a_{33}+a_{44}),\\
B_0 &= a_{33}a_{44}(a_{11}b_{22} + a_{22}b_{11}),\\
B_2 &= a_{11}b_{22} + a_{22}b_{11} + (a_{33}+a_{44})(b_{11}+b_{22}),\\
B_1 &= -\left(a_{33}a_{44}(b_{11}+b_{22})\right.\\
&\quad \left. + (a_{33}+a_{44})(a_{11}b_{22} + a_{22}b_{11})\right),\\
B_3 &= -(b_{11}+b_{22}),\\
C_0 &= a_{11}a_{44}(a_{22}c_{33} + a_{33}c_{22}),\\
C_1 &= -\left(c_{22}(a_{11}a_{33} + a_{11}a_{44} + a_{33}a_{44})\right.\\
&\quad \left. + c_{33}(a_{11}a_{22} + a_{11}a_{44} + a_{22}a_{44})\right),\\
C_2 &= c_{22}(a_{11}+a_{33}+a_{44}) + c_{33}(a_{11}+a_{22}+a_{44}),\\
C_3 &= -(c_{22}+c_{33}),\\
D_0 &= a_{33}a_{44}b_{11}c_{22} + a_{44}c_{33}(a_{11}b_{22} + a_{22}b_{11}),
\end{aligned}$$

$$
\begin{aligned}
D_1 &= -(a_{33}+a_{44})b_{11}b_{22} - (a_{11}+a_{44})b_{22}c_{33} - (a_{22}\\
&\quad + a_{44})b_{11}c_{33},\\
D_2 &= b_{11}c_{22} + b_{11}c_{33} + b_{22}c_{33},\\
E_0 &= a_{11}a_{44}c_{22}c_{33},\\
E_1 &= -(a_{11}+a_{44})c_{22}c_{33},\\
E_2 &= c_{22}c_{33},\\
F_0 &= a_{44}b_{11}c_{22}c_{33},\\
F_1 &= -b_{11}c_{22}c_{33},
\end{aligned}
\tag{6}
$$

with

$$
\begin{aligned}
a_{11} &= -d,\\
a_{22} &= -(d+\alpha_1+\delta),\\
a_{32} &= \delta,\\
a_{33} &= -(d+\alpha_2),\\
a_{44} &= -d,\\
b_{11} &= -\beta I_*,\\
b_{12} &= -\beta S_*,\\
b_{21} &= \beta I_*,\\
b_{22} &= \beta S_*,\\
c_{22} &= -\gamma,\\
c_{33} &= -\varepsilon,\\
c_{42} &= \gamma,\\
c_{43} &= \varepsilon.
\end{aligned}
\tag{7}
$$

Case 1 ($\tau_1 = \tau_2 = 0$). When $\tau_1 = \tau_2 = 0$, (5) becomes

$$
\begin{aligned}
&\lambda^4 + A_{13}\lambda^3 + A_{12}\lambda^2 + A_{11}\lambda + A_{10} = 0,\\
&A_{10} = A_0 + B_0 + C_0 + D_0 + E_0 + F_0,\\
&A_{11} = A_1 + B_1 + C_1 + D_1 + E_1 + F_1,\\
&A_{12} = A_2 + B_2 + C_2 + D_2 + E_2,\\
&A_{13} = A_3 + B_3 + C_3 = 3d + \alpha_2 + \varepsilon + \beta I_*.
\end{aligned}
\tag{8}
$$

Thus, if the condition (H_{11}) (9) holds, then the positive equilibrium D_* of system (2) is locally asymptotically stable when $\tau_1 = \tau_2 = 0$.

$$
\begin{aligned}
\mathrm{Det}_2 &= \begin{vmatrix} A_{13} & 1 \\ A_{11} & A_{12} \end{vmatrix} > 0,\\
\mathrm{Det}_3 &= \begin{vmatrix} A_{13} & 1 & 0 \\ A_{11} & A_{12} & A_{13} \\ 0 & A_{10} & A_{11} \end{vmatrix} > 0,\\
\mathrm{Det}_4 &= \begin{vmatrix} A_{13} & 1 & 0 & 0 \\ A_{11} & A_{12} & A_{13} & 1 \\ 0 & A_{10} & A_{11} & A_{12} \\ 0 & 0 & 0 & A_{10} \end{vmatrix} > 0.
\end{aligned}
\tag{9}
$$

Case 2 ($\tau_1 > 0, \tau_2 = 0$). When $\tau_1 > 0, \tau_2 = 0$, (5) becomes

$$
\begin{aligned}
&\lambda^4 + A_{23}\lambda^3 + A_{22}\lambda^2 + A_{21}\lambda + A_{20}\\
&\quad + \left(B_{23}\lambda^3 + B_{22}\lambda^2 + B_{21}\lambda + B_{20}\right)e^{-\lambda\tau_1} = 0,
\end{aligned}
\tag{10}
$$

where

$$
\begin{aligned}
A_{20} &= A_0 + C_0 + E_0,\\
A_{21} &= A_1 + C_1 + E_1,\\
A_{22} &= A_2 + C_2 + E_2,\\
A_{23} &= A_3 + C_3,\\
B_{20} &= B_0 + D_0 + F_0,\\
B_{21} &= B_1 + D_1 + F_1,\\
B_{22} &= B_2 + D_2.
\end{aligned}
\tag{11}
$$

Let $\lambda = i\omega_1$ $(\omega_1 > 0)$ be the root of (10); we get

$$
\begin{aligned}
&\left(B_{21}\omega_1 - B_{23}\omega_1^3\right)\sin\tau_1\omega_1 + \left(B_{20} - B_{22}\omega_1^2\right)\cos\tau_1\omega_1\\
&\quad = A_{22}\omega_1^2 - \omega_1^4 - B_{20},\\
&\left(B_{21}\omega_1 - B_{23}\omega_1^3\right)\cos\tau_1\omega_1 - \left(B_{20} - B_{22}\omega_1^2\right)\sin\tau_1\omega_1\\
&\quad = A_{23}\omega_1^3 - A_{21}\omega_1,
\end{aligned}
\tag{12}
$$

from which one can obtain

$$
\omega_1^8 + e_{23}\omega_1^6 + e_{22}\omega_1^4 + e_{21}\omega_1^2 + e_{20} = 0,
\tag{13}
$$

where

$$
\begin{aligned}
e_{20} &= A_{20}^2 - B_{20}^2,\\
e_{21} &= A_{21}^2 - B_{21}^2 - 2A_{20}A_{22} + 2B_{20}B_{22},\\
e_{22} &= A_{22}^2 - B_{22}^2 + 2A_{20} - 2A_{21}A_{23} + 2B_{21}B_{23},\\
c_{23} &= A_{23}^2 - B_{23}^2 - 2A_{22}.
\end{aligned}
\tag{14}
$$

Let $\omega_1^2 = v_1$; then (13) becomes

$$
v_1^4 + e_{23}v_1^3 + e_{22}^2v_1^2 + e_{21}v_1 + e_{20} = 0.
\tag{15}
$$

Obviously, if all the coefficients of system (2) are given, then we can obtain all the roots of (15) by Matlab software package easily. Thus, we make the following assumption.

(H_{21}) (15) has at least one positive root.

If the condition (H_{21}) holds, then there exists a positive root v_{10} for (15) such that (10) has a pair of purely imaginary roots $\pm i\omega_{10} = \pm i\sqrt{v_{10}}$. For ω_{10},

$$
\begin{aligned}
\tau_{10} &= \frac{1}{\omega_{10}}\\
&\quad \times \arccos\frac{n_{26}\omega_{10}^6 + n_{24}\omega_{10}^4 + n_{22}\omega_{10}^2 + n_{20}}{m_{26}\omega_{10}^6 + m_{24}\omega_{10}^4 + m_{22}\omega_{10}^2 + m_{20}},
\end{aligned}
\tag{16}
$$

where

$$\begin{aligned} m_{20} &= B_{20}^2, \\ m_{22} &= B_{21}^2 - 2B_{20}B_{22}, \\ m_{24} &= B_{22}^2 - 2B_{21}B_{23}, \\ m_{26} &= B_{23}^2, \\ n_{20} &= -A_{20}B_{20}, \\ n_{22} &= A_{20}B_{22} - A_{21}B_{21} + A_{22}B_{20}, \\ n_{24} &= A_{21}B_{23} - A_{22}B_{22} + A_{23}B_{21} - B_{20}, \\ n_{26} &= B_{22} - A_{23}B_{23}. \end{aligned} \tag{17}$$

Substituting $\lambda(\tau_1)$ into the left side of (10) and taking the derivative with respect to τ_1, one can obtain

$$\begin{aligned} \left[\frac{d\lambda}{d\tau_1}\right]^{-1} &= -\frac{4\lambda^3 + 3A_{23}\lambda^2 + 2A_{22}\lambda + A_{21}}{\lambda\left(\lambda^4 + A_{23}\lambda^3 + A_{22}\lambda^2 + A_{21}\lambda + A_{20}\right)} \\ &\quad + \frac{3B_{23}\lambda^2 + 2B_{22}\lambda + B_{21}}{\lambda\left(B_{23}\lambda^3 + B_{22}\lambda^2 + B_{21}\lambda + B_{20}\right)} - \frac{\tau_1}{\lambda}. \end{aligned} \tag{18}$$

Thus,

$$\begin{aligned} &\operatorname{Re}\left[\frac{d\lambda}{d\tau_1}\right]^{-1}_{\lambda=i\omega_{10}} \\ &= \frac{f_1'(v_{1*})}{B_{23}^2\omega_{10}^6 + \left(B_{22}^2 - 2B_{21}B_{23}\right)\omega_{10}^4 + \left(B_{21}^2 - 2B_{20}B_{22}\right)\omega_{10}^2 + B_{20}^2}, \end{aligned} \tag{19}$$

where $v_{1*} = \omega_{10}^2$ and $f_1(v_1) = v_1^4 + e_{23}v_1^3 + e_{22}^2v_1^2 + e_{21}v_1 + e_{20}$.

Thus, if the condition (H_{22}) $f_1'(v_{1*}) \neq 0$ holds, then $\operatorname{Re}[d\lambda/d\tau_1]^{-1}_{\lambda=i\omega_{10}} \neq 0$. According to the Hopf bifurcation theorem in [15], we have the following results.

Theorem 1. *If the conditions (H_{21})-(H_{22}) hold, then the positive equilibrium $D_*(S_*, I_*, Q_*, R_*)$ is asymptotically stable for $\tau_1 \in [0, \tau_{10})$ and system (2) undergoes a Hopf bifurcation at the positive equilibrium $D_*(S_*, I_*, Q_*, R_*)$ when $\tau_1 = \tau_{10}$.*

Case 3 ($\tau_1 = 0, \tau_2 > 0$). When $\tau_1 = 0, \tau_2 > 0$, (5) becomes

$$\begin{aligned} &\lambda^4 + A_{33}\lambda^3 + A_{32}\lambda^2 + A_{31}\lambda + A_{30} \\ &\quad + \left(C_{33}\lambda^3 + C_{32}\lambda^2 + C_{31}\lambda + C_{30}\right)e^{-\lambda\tau_2} \\ &\quad + \left(E_{32}\lambda^2 + E_{31}\lambda + E_{30}\right)e^{-2\lambda\tau_2} = 0, \end{aligned} \tag{20}$$

where

$$\begin{aligned} A_{30} &= A_0 + B_0, \\ A_{31} &= A_1 + B_1, \\ A_{32} &= A_2 + B_2, \\ A_{33} &= A_3 + B_3, \\ C_{30} &= C_0 + D_0, \\ C_{31} &= C_1 + D_1, \\ C_{32} &= C_2 + D_2, \\ C_{33} &= C_3, \\ E_{30} &= E_0 + F_0, \\ E_{31} &= E_1 + F_1, \\ E_{32} &= E_2. \end{aligned} \tag{21}$$

Multiplying by $e^{\lambda\tau_2}$, (20) becomes

$$\begin{aligned} &C_{33}\lambda^3 + C_{32}\lambda^2 + C_{31}\lambda + C_{30} \\ &\quad + \left(\lambda^4 + A_{33}\lambda^3 + A_{32}\lambda^2 + A_{31}\lambda + A_{30}\right)e^{\lambda\tau_2} \\ &\quad + \left(E_{32}\lambda^2 + E_{31}\lambda + E_{30}\right)e^{-\lambda\tau_2} = 0. \end{aligned} \tag{22}$$

Let $\lambda = i\omega_2$ ($\omega_2 > 0$) be the root of (22); then

$$\begin{aligned} &\left(\omega_2^4 - \left(A_{32} + E_{32}\right)\omega_2^2 + A_{30} - E_{30}\right)\sin\tau_2\omega_2 \\ &\quad + \left(\left(A_{31} + E_{31}\right)\omega_2 - A_{33}\omega_2^3\right)\cos\tau_2\omega_2 = C_{33}\omega_2^3 \\ &\quad - C_{31}\omega_2, \\ &\left(\omega_2^4 - \left(A_{32} + E_{32}\right)\omega_2^2 + A_{30} + E_{30}\right)\cos\tau_2\omega_2 \\ &\quad - \left(\left(A_{31} - E_{31}\right)\omega_2 - A_{33}\omega_2^3\right)\sin\tau_2\omega_2 = C_{32}\omega_2^2 \\ &\quad - A_{30}. \end{aligned} \tag{23}$$

It follows that

$$\begin{aligned} \cos\tau_2\omega_2 &= \frac{n_{36}\omega_2^6 + n_{34}\omega_2^4 + n_{32}\omega_2^2 + n_{30}}{\omega_2^8 + m_{36}\omega_2^6 + m_{34}\omega_2^4 + m_{32}\omega_2^2 + m_{30}}, \\ \sin\tau_2\omega_2 &= \frac{n_{37}\omega_2^7 + n_{35}\omega_2^5 + n_{33}\omega_2^3 + n_{31}\omega_2}{\omega_2^8 + m_{36}\omega_2^6 + m_{34}\omega_2^4 + m_{32}\omega_2^2 + m_{30}}, \end{aligned} \tag{24}$$

where

$$\begin{aligned} m_{30} &= A_{30}^2 - E_{30}^2, \\ m_{32} &= A_{31}^2 - E_{31}^2 - 2A_{30}\left(A_{32} + E_{32}\right), \\ m_{34} &= \left(A_{32} + E_{32}\right)^2 - 2A_{31}A_{33} + 2A_{30}, \\ m_{36} &= A_{33}^2 - 2\left(A_{32} + E_{32}\right), \\ n_{30} &= \left(E_{30} - A_{30}\right)C_{30}, \\ n_{31} &= \left(A_{31} + E_{31}\right)C_{30} - \left(A_{30} + E_{30}\right)C_{31}, \\ n_{32} &= \left(A_{32} + E_{32}\right)C_{30} - \left(A_{31} - E_{31}\right)C_{31} \\ &\quad + \left(A_{30} - E_{30}\right)C_{32}, \end{aligned}$$

$$
\begin{aligned}
n_{33} &= (A_{30} + E_{30}) C_{33} - (A_{31} + E_{31}) C_{32} \\
&\quad + (A_{32} + E_{32}) C_{31} - A_{33} C_{30}, \\
n_{34} &= (A_{31} - E_{31}) C_{33} - (A_{32} + E_{32}) C_{32} - A_{33} C_{31} \\
&\quad - C_{30}, \\
n_{35} &= A_{33} C_{32} - C_{31} - (A_{32} + E_{32}) C_{33}, \\
n_{36} &= C_{32} - A_{33} C_{33}, \\
n_{37} &= C_{33}.
\end{aligned} \tag{25}
$$

Then, we can get

$$
\begin{aligned}
&\omega_2^{16} + e_{37}\omega_2^{14} + e_{36}\omega_2^{12} + e_{35}\omega_2^{10} + e_{34}\omega_2^8 + e_{33}\omega_2^6 \\
&\quad + e_{32}\omega_2^4 + e_{31}\omega_2^2 + e_{30} = 0,
\end{aligned} \tag{26}
$$

with

$$
\begin{aligned}
e_{30} &= m_{30}^2 - n_{30}^2, \\
e_{31} &= 2m_{30}m_{32} - 2n_{30}n_{32} - n_{31}^2, \\
e_{32} &= m_{32}^2 - n_{32}^2 + 2m_{30}m_{34} - 2n_{30}n_{34} - 2n_{31}n_{33}, \\
e_{33} &= 2m_{30}m_{36} + 2m_{32}m_{34} - 2n_{30}n_{36} - 2n_{31}n_{35} \\
&\quad - 2n_{32}n_{34} - n_{33}^2, \\
e_{34} &= m_{34}^2 - n_{34}^2 + 2m_{30} + 2m_{32}m_{36} - 2n_{31}n_{37} \\
&\quad - 2n_{32}n_{36} - 2n_{33}n_{35}, \\
e_{35} &= 2m_{32} + 2m_{34}m_{36} - 2n_{33}n_{37} - 2n_{34}n_{36} - n_{35}^2, \\
e_{36} &= m_{36}^2 - n_{36}^2 + 2m_{34} - 2n_{35}n_{37}, \\
e_{37} &= 2m_{36} - n_{37}^2.
\end{aligned} \tag{27}
$$

Let $\omega_2^2 = \nu_2$; (26) becomes

$$
\begin{aligned}
&\nu_2^8 + e_{37}\nu_2^7 + e_{36}\nu_2^6 + e_{35}\nu_2^5 + e_{34}\nu_2^4 + e_{33}\nu_2^3 + e_{32}\nu_2^2 \\
&\quad + e_{31}\nu_2 + e_{30} = 0.
\end{aligned} \tag{28}
$$

Similar as in Case 2, we make the following assumption.

(H_{31}) (28) has at least one positive root.

If condition (H_{31}) holds, there exists a positive root ν_{20} for (22) such that (22) has a pair of purely imaginary root $\pm i\omega_{20} = \pm i\sqrt{\nu_{20}}$. For ω_{20},

$$
\begin{aligned}
\tau_{20} &= \frac{1}{\omega_{20}} \\
&\quad \times \arccos \frac{n_{36}\omega_{20}^6 + n_{34}\omega_{20}^4 + n_{32}\omega_{20}^2 + n_{30}}{\omega_{20}^8 + m_{36}\omega_{20}^6 + m_{34}\omega_{20}^4 + m_{32}\omega_{20}^2 + m_{30}}.
\end{aligned} \tag{29}
$$

Differentiating the two sides of (22) regarding τ_2, we obtain

$$
\left[\frac{d\lambda}{d\tau_2}\right]^{-1} = \frac{P_{30}(\lambda)}{Q_{30}(\lambda)} - \frac{\tau_2}{\lambda}, \tag{30}
$$

where

$$
\begin{aligned}
&P_{30}(\lambda) \\
&\quad = 3C_{33}\lambda^2 + 2C_{32}\lambda + C_{31} + (2E_{32} + E_{31}) e^{-\lambda\tau_2} \\
&\qquad + \left(4\lambda^3 + 3A_{33}\lambda^2 + 2A_{32}\lambda + A_{31}\right) e^{\lambda\tau_2}, \\
&Q_{30}(\lambda) \\
&\quad = \left(E_{32}\lambda^3 + E_{31}\lambda^2 + E_{30}\lambda\right) e^{-\lambda\tau_2} \\
&\qquad - \left(\lambda^5 + A_{33}\lambda^4 + A_{32}\lambda^3 + A_{31}\lambda^2 + A_{30}\lambda\right) e^{\lambda\tau_2},
\end{aligned} \tag{31}
$$

where

$$
\begin{aligned}
P_{3R} &= \left(A_{31} + E_{31} - 3A_{33}\omega_{20}^2\right) \cos\tau_{20}\omega_{20} \\
&\quad - 2\left((A_{32} - E_{32})\omega_{20} - 2\omega_{20}^3\right) \sin\tau_{20}\omega_{20} + C_{31} \\
&\quad - 3C_{33}\omega_{20}^2, \\
P_{3I} &= \left(A_{31} - E_{31} - 3A_{33}\omega_{20}^2\right) \sin\tau_{20}\omega_{20} \\
&\quad - 2\left((A_{32} + E_{32})\omega_{20} - 2\omega_{20}^3\right) \cos\tau_{20}\omega_{20} \\
&\quad + 2C_{32}\omega_{20}, \\
Q_{3R} &= \left((A_{31} - E_{31})\omega_{20}^2 - A_{33}\omega_{20}^4\right) \cos\tau_{20}\omega_{20} \\
&\quad + \left(\omega_{20}^5 - (A_{32} + E_{32})\omega_{20}^3 + (A_{30} + E_{30})\omega_{20}\right) \\
&\quad \cdot \sin\tau_{20}\omega_{20}, \\
Q_{3I} &= \left((A_{31} + E_{31})\omega_{20}^2 - A_{33}\omega_{20}^4\right) \sin\tau_{20}\omega_{20} \\
&\quad - \left(\omega_{20}^5 + (A_{32} - E_{32})\omega_{20}^3 + (A_{30} - E_{30})\omega_{20}\right) \\
&\quad \cdot \cos\tau_{20}\omega_{20}.
\end{aligned} \tag{32}
$$

Therefore, if condition (H_{32}) $P_{3R}Q_{3R} + P_{3I}Q_{3I} \neq 0$ holds, then $\mathrm{Re}[d\lambda/d\tau_2]^{-1}_{\lambda=i\omega_{20}}$. Thus, we have the following results according to the Hopf bifurcation theorem in [15].

Theorem 2. *If conditions (H_{31})-(H_{32}) hold, then the positive equilibrium $D_*(S_*, I_*, Q_*, R_*)$ is asymptotically stable for $\tau_2 \in [0, \tau_{20})$ and system (2) undergoes a Hopf bifurcation at the positive equilibrium $D_*(S_*, I_*, Q_*, R_*)$ when $\tau_2 = \tau_{20}$.*

Case 4 ($\tau_1 > 0, \tau_2 > 0$ and $\tau_2 \in (0, \tau_{20})$). Let $\lambda = i\omega_1'$ ($\omega_1' > 0$) be the root of (5); then we obtain

$$
\begin{aligned}
G_{41}\left(\omega_1'\right) \sin\tau_1\omega_1' + G_{42}\left(\omega_1'\right) \cos\tau_1\omega_1' &= G_{43}\left(\omega_1'\right), \\
G_{41}\left(\omega_1'\right) \cos\tau_1\omega_1' - G_{42}\left(\omega_1'\right) \sin\tau_1\omega_1' &= G_{44}\left(\omega_1'\right),
\end{aligned} \tag{33}
$$

where

$$\begin{aligned}
G_{41}\left(\omega_1'\right) &= B_1\omega_1' - B_3\left(\omega_1'\right)^3 + D_1\omega_1'\cos\tau_2\omega_1' \\
&\quad - \left(D_0 - D_2\left(\omega_1'\right)^2\right)\sin\tau_2\omega_1' \\
&\quad + F_1\omega_1'\cos 2\tau_2\omega_1' - F_0\sin 2\tau_2\tau_2\omega_1', \\
G_{42}\left(\omega_1'\right) &= B_0 - B_2\left(\omega_1'\right)^2 + D_1\omega_1'\sin\tau_2\omega_1' \\
&\quad + \left(D_0 - D_2\left(\omega_1'\right)^2\right)\cos\tau_2\omega_1' \\
&\quad + F_1\omega_1'\sin 2\tau_2\omega_1' - F_0\cos 2\tau_2\tau_2\omega_1', \\
G_{43}\left(\omega_1'\right) &= A_2\left(\omega_1'\right)^2 - \left(\omega_1'\right)^4 - A_0 \\
&\quad - \left(C_1\omega_1' - C_3\left(\omega_1'\right)^3\right)\sin\tau_2\omega_1' \\
&\quad - \left(C_0 - C_2\left(\omega_1'\right)^2\right)\cos\tau_2\omega_1' \\
&\quad - E_1\omega_1'\sin 2\tau_2\omega_1' \\
&\quad - \left(E_0 - E_2\left(\omega_1'\right)^2\right)\cos 2\tau_2\omega_1', \\
G_{44}\left(\omega_1'\right) &= A_3\left(\omega_1'\right)^3 - A_1\omega_1' \\
&\quad - \left(C_1\omega_1' - C_3\left(\omega_1'\right)^3\right)\cos\tau_2\omega_1' \\
&\quad + \left(C_0 - C_2\left(\omega_1'\right)^2\right)\sin\tau_2\omega_1' \\
&\quad - E_1\omega_1'\cos 2\tau_2\omega_1' \\
&\quad + \left(E_0 - E_2\left(\omega_1'\right)^2\right)\sin 2\tau_2\omega_1'.
\end{aligned} \tag{34}$$

Then, we can obtain the following equation with respect to ω_1':

$$\begin{aligned}
&f_{40}\left(\omega_1'\right) + 2f_{41}\left(\omega_1'\right)\cos\tau_2\omega_1' + 2f_{42}\left(\omega_1'\right)\sin\tau_2\omega_1' \\
&\quad + 2f_{43}\left(\omega_1'\right)\cos 2\tau_2\omega_1' + 2f_{44}\left(\omega_1'\right)\sin 2\tau_2\omega_1' \\
&= 0,
\end{aligned} \tag{35}$$

where

$$\begin{aligned}
f_{40}\left(\omega_1'\right) &= \left(\omega_1'\right)^8 + \left(A_3^2 - B_3^2 + C_3^2 - 2A_2\right)\left(\omega_1'\right)^6 \\
&\quad + \left(A_2^2 - B_2^2 + C_2^2 - D_2^2 + E_2^2 - 2A_1A_3 + 2B_1B_3\right. \\
&\quad \left. - 2C_1C_3 + 2A_0\right)\left(\omega_1'\right)^4 + \left(A_1^2 - B_1^2 + C_1^2 - D_1^2\right. \\
&\quad \left. + E_1^2 - F_1^2 - 2A_0A_2 + 2B_0B_2 - 2C_0C_2 + 2D_0D_2\right. \\
&\quad \left. - 2E_0E_2\right)\left(\omega_1'\right)^2 + A_0^2 - B_0^2 + C_0^2 - D_0^2 + E_0^2 - F_0^2, \\
f_{41}\left(\omega_1'\right) &= \left(A_3C_3 - C_2\right)\left(\omega_1'\right)^6 + \left(A_2C_2 - A_1C_3\right. \\
&\quad \left. - A_3C_1 - B_2D_2 + B_3D_1 + C_2E_2 - C_3E_1 + C_0\right) \\
&\quad \cdot \left(\omega_1'\right)^4 + \left(A_1C_1 - A_0C_2 - A_2C_0 + B_0D_2 - B_1D_1\right. \\
&\quad \left. + B_2D_0 - C_0E_2 + C_1E_1 - C_2E_0 - D_1F_1 + D_2F_0\right) \\
&\quad \cdot \left(\omega_1'\right)^2 + A_0C_0 - B_0F_0 - D_0F_0, \\
f_{42}\left(\omega_1'\right) &= -C_3\left(\omega_1'\right)^7 + \left(A_2C_3 - A_3C_2 + B_3D_2\right. \\
&\quad \left. - C_3E_2 + C_1\right)\left(\omega_1'\right)^5 + \left(A_1C_2 - A_0C_3 - A_2C_1\right. \\
&\quad \left. + A_3C_0 - B_1D_2 + B_2D_1 - B_3D_0 + C_1E_2 - C_2E_1\right. \\
&\quad \left. + C_3E_0 + D_2F_1\right)\left(\omega_1'\right)^3 + \left(A_0E_1 - A_1E_0 - B_0D_1\right. \\
&\quad \left. + B_1D_0 - C_0E_1 + C_1E_0 - D_0F_1 + D_1F_0\right)\omega_1', \\
f_{43}\left(\omega_1'\right) &= -E_2\left(\omega_1'\right)^6 + \left(A_2E_2 + B_3F_1 + E_0\right)\left(\omega_1'\right)^4 \\
&\quad - \left(A_0E_2 + A_2E_0 + B_1F_1 - B_2F_0\right)\left(\omega_1'\right)^2 + B_0F_0 \\
&\quad - A_0E_0, \\
f_{44}\left(\omega_1'\right) &= \left(E_1 - A_3E_2\right)\left(\omega_1'\right)^5 + \left(A_1E_2 - A_2E_1\right. \\
&\quad \left. + A_3E_0 + B_2F_1 - B_3F_0\right)\left(\omega_1'\right)^3\left(A_0E_1 - A_1E_0\right. \\
&\quad \left. - B_0F_1 + B_1F_0\right)\omega_1'.
\end{aligned} \tag{36}$$

In order to give the main results in this paper, we make the following assumption.

(H_{41}) (35) has at least one positive root.

If the condition (H_{41}) holds, then there exists a positive root ω_{10}' for (35) such that (5) has a pair of purely imaginary root $\pm i\omega_{10}'$. For ω_{10}',

$$\begin{aligned}
\tau_{10}' &= \frac{1}{\omega_{10}'} \\
&\quad \times \arccos\frac{G_{42}\left(\omega_{10}'\right)\times G_{43}\left(\omega_{10}'\right) + G_{41}\left(\omega_{10}'\right)\times G_{44}\left(\omega_{10}'\right)}{G_{41}^2\left(\omega_{10}'\right) + G_{42}^2\left(\omega_{10}'\right)}.
\end{aligned} \tag{37}$$

Substituting $\lambda(\tau_1)$ into (5) and differentiating both sides of it with respect to τ_1, then

$$\left[\frac{d\lambda}{d\tau_1}\right]^{-1} = \frac{P_{40}(\lambda)}{Q_{40}(\lambda)} - \frac{\tau_1}{\lambda}, \tag{38}$$

where

$$\begin{aligned}
P_{40}(\lambda) &= 4\lambda^3 + 3A_3\lambda^2 + 2A_2\lambda + A_1 + \left(3B_3\lambda^2\right. \\
&\quad \left. + 2B_2\lambda + B_1\right)e^{-\lambda\tau_1} - \left(\tau_2C_3\lambda^3 + \left(\tau_2C_2 - 3C_3\right)\lambda^2\right.
\end{aligned}$$

$$
\begin{aligned}
&+\left(\tau_2 C_1 - 2C_2\right)\lambda + \tau_2 C_0 - C_1\Big) e^{-\lambda\tau_2} - \Big(\tau_2 D_2\lambda^2 \\
&+\left(\tau_2 D_1 - 2D_2\right)\lambda + \tau_2 D_0 - D_1\Big) e^{-\lambda(\tau_1+\tau_2)} \\
&-\Big(2\tau_2 E_2\lambda^2 + 2\left(\tau_2 E_1 - E_2\right)\lambda + 2\tau_2 E_0 - E_1\Big) e^{-2\lambda\tau_2} \\
&-\left(2\tau_2 F_1\lambda + 2\tau_2 F_0 - F_1\right) e^{-\lambda(\tau_1+2\tau_2)}, \\
Q_{40}(\lambda) &= \Big(B_3\lambda^4 + B_2\lambda^3 + B_1\lambda^2 + B_0\lambda\Big) e^{-\lambda\tau_1} + \Big(D_2\lambda^3 \\
&+ D_1\lambda^2 + D_0\Big) e^{-\lambda(\tau_1+\tau_2)} + \Big(F_1\lambda^2 + F_0\lambda\Big) e^{-\lambda(\tau_1+2\tau_2)}.
\end{aligned} \tag{39}
$$

We therefore derive that

$$
\mathrm{Re}\left[\frac{d\lambda}{d\tau_1}\right]^{-1}_{\lambda=i\omega'_{10}} = \frac{P_{4R}Q_{4R} + P_{4I}Q_{4I}}{Q_{4R}^2 + Q_{4I}^2}, \tag{40}
$$

where

$$
\begin{aligned}
P_{4R} &= A_1 - 3A_3\left(\omega'_{10}\right)^2 + \Big[\left(2C_2 - \tau_2 C_1\right)\omega'_{10} \\
&+ \tau_2 C_3\left(\omega'_{10}\right)^3\Big]\sin\tau_2\omega'_{10}\Big[\left(\tau_2 C_2 - 3C_3\right)\left(\omega'_{10}\right)^2 \\
&+ C_1 - \tau_2 C_0\Big]\cos\tau_2\omega'_{10} + 2\left(E_2 - \tau_2 E_1\right)\omega'_{10} \\
&\cdot \sin 2\tau_2\omega'_{10} + \Big(2\tau_2 E_2\left(\omega'_{10}\right)^2 + E_1 - 2\tau_2 E_0\Big) \\
&\cdot \cos 2\tau_2\omega'_{10} + \Big[\left(2D_2 - \tau_2 D_1\right)\omega'_{10}\cos\tau_2\omega'_{10} \\
&- \Big(\tau_2 D_2\left(\omega'_{10}\right)^2 + D_1 - \tau_2 D_0\Big)\sin\tau_2\omega'_{10} \\
&- \left(F_1 - 2\tau_2 F_0\right)\sin 2\tau_2\omega'_{10} + 2\tau_2 F_1\omega'_{10}\cos 2\tau_2\omega'_{10} \\
&+ 2B_2\omega'_{10}\Big]\sin\tau'_{10}\omega'_{10} \\
&+ \Big[\left(2D_2 - \tau_2 D_1\right)\omega'_{10}\sin\tau_2\omega'_{10} \\
&+ \Big(\tau_2 D_2\left(\omega'_{10}\right)^2 + D_1 - \tau_2 D_0\Big)\cos\tau_2\omega'_{10} \\
&+ \left(F_1 - 2\tau_2 F_0\right)\cos 2\tau_2\omega'_{10} - 2\tau_2 F_1\omega'_{10}\sin 2\tau_2\omega'_{10} \\
&+ B_1 - 3B_3\left(\omega'_{10}\right)^2\Big]\cos\tau'_{10}\omega'_{10}, \\
P_{4I} &= 2A_2\omega'_{10} - 4\left(\omega'_{10}\right)^3 + \Big[\Big(2C_2 - \tau_2 C_1\omega'_{10}\Big)\omega'_{10} \\
&+ \tau_2 C_3\left(\omega'_{10}\right)^3\Big]\cos\tau_2\omega'_{10} - \Big[\left(\tau_2 C_2 - 3C_3\right)\left(\omega'_{10}\right)^2 \\
&+ C_1 - \tau_2 C_0\Big]\sin\tau_2\omega'_{10} + 2\left(E_2 - \tau_2 E_1\right)\omega'_{10} \\
&\cdot \cos 2\tau_2\omega'_{10} - \Big(2\tau_2 E_2\left(\omega'_{10}\right)^2 + E_1 - 2\tau_2 E_0\Big) \\
&\cdot \sin 2\tau_2\omega'_{10}\Big[\left(2D_2 - \tau_2 D_1\right)\omega'_{10}\cos\tau_2\omega'_{10} \\
&- \Big(\tau_2 D_2\left(\omega'_{10}\right)^2 + D_1 - \tau_2 D_0\Big)\sin\tau_2\omega'_{10} \\
&- \left(F_1 - 2\tau_2 F_0\right)\sin 2\tau_2\omega'_{10} + 2\tau_2 F_1\omega'_{10}\cos 2\tau_2\omega'_{10} \\
&+ 2B_2\omega'_{10}\Big]\cos\tau'_{10}\omega'_{10} \\
&- \Big[\left(2D_2 - \tau_2 D_1\right)\omega'_{10}\sin\tau_2\omega'_{10} \\
&+ \Big(\tau_2 D_2\left(\omega'_{10}\right)^2 + D_1 - \tau_2 D_0\Big)\cos\tau_2\omega'_{10} \\
&+ \left(F_1 - 2\tau_2 F_0\right)\cos 2\tau_2\omega'_{10} 2\tau_2 F_1\omega'_{10}\sin 2\tau_2\omega'_{10} + B_1 \\
&- 3B_3\left(\omega'_{10}\right)^2\Big]\sin\tau'_{10}\omega'_{10}, \\
Q_{4R} &= \Big[\Big(D_0\omega'_{10} - D_2\left(\omega'_{10}\right)^3\Big)\sin\tau_2\omega'_{10} \\
&- D_1\left(\omega'_{10}\right)^2\cos\tau_2\omega'_{10} + F_0\omega'_{10}\sin 2\tau_2\omega'_{10} \\
&- F_1\left(\omega'_{10}\right)^2\cos 2\tau_2\omega'_{10} + B_3\left(\omega'_{10}\right)^4 - B_1\left(\omega'_{10}\right)^2\Big] \\
&\cdot \cos\tau'_{10}\omega'_{10} + \Big[\Big(D_0\omega'_{10} - D_2\left(\omega'_{10}\right)^3\Big)\cos\tau_2\omega'_{10} \\
&+ D_1\left(\omega'_{10}\right)^2\sin\tau_2\omega'_{10} + F_0\omega'_{10}\cos 2\tau_2\omega'_{10} \\
&+ F_1\left(\omega'_{10}\right)^2\sin 2\tau_2\omega'_{10} + B_0\omega'_{10} - B_2\left(\omega'_{10}\right)^3\Big] \\
&\cdot \sin\tau'_{10}\omega'_{10}, \\
Q_{4I} &= \Big[\Big(D_0\omega'_{10} - D_2\left(\omega'_{10}\right)^3\Big)\cos\tau_2\omega'_{10} \\
&+ D_1\left(\omega'_{10}\right)^2\sin\tau_2\omega'_{10} + F_0\omega'_{10}\cos 2\tau_2\omega'_{10} \\
&+ F_1\left(\omega'_{10}\right)^2\sin 2\tau_2\omega'_{10} + B_0\omega'_{10} - B_2\left(\omega'_{10}\right)^3\Big] \\
&\cdot \cos\tau'_{10}\omega'_{10} - \Big[\Big(D_0\omega'_{10} - D_2\left(\omega'_{10}\right)^3\Big)\sin\tau_2\omega'_{10} \\
&- D_1\left(\omega'_{10}\right)^2\cos\tau_2\omega'_{10} + F_0\omega'_{10}\sin 2\tau_2\omega'_{10} \\
&- F_1\left(\omega'_{10}\right)^2\cos 2\tau_2\omega'_{10} + B_3\left(\omega'_{10}\right)^4 - B_1\left(\omega'_{10}\right)^2\Big] \\
&\cdot \sin\tau'_{10}\omega'_{10}.
\end{aligned} \tag{41}
$$

Therefore, if condition (H_{42}) $P_{4R}Q_{4R} + P_{4I}Q_{4I} \neq 0$ holds, then $\mathrm{Re}[d\lambda/d\tau_1]^{-1}_{\lambda=i\omega'_{10}} \neq 0$. Thus, we have the following results according to the Hopf bifurcation theorem in [15].

Theorem 3. *For system (2), if conditions (H_{41})-(H_{42}) hold and $\tau_2 \in (0, \tau_{20})$, then the positive equilibrium $D_*(S_*, I_*, Q_*, R_*)$ is asymptotically stable for $\tau_1 \in [0, \tau'_{10})$ and system (2) undergoes a Hopf bifurcation at the positive equilibrium $D_*(S_*, I_*, Q_*, R_*)$ when $\tau_1 = \tau'_{10}$ and a family of periodic solutions bifurcate from $D_*(S_*, I_*, Q_*, R_*)$ near $\tau_1 = \tau'_{10}$.*

Case 5 ($\tau_1 > 0$, $\tau_2 > 0$ and $\tau_1 \in (0, \tau_{10})$). Multiplying by $e^{\lambda\tau_2}$, (5) becomes

$$\begin{aligned} &C_3\lambda^3 + C_2\lambda^2 + C_1\lambda + C_0 \\ &\quad + \left(\lambda^4 + A_3\lambda^3 + A_2\lambda^2 + A_1\lambda + A_0\right)e^{\lambda\tau_2} \\ &\quad + \left(B_3\lambda^3 + B_2\lambda^2 + B_1\lambda + B_0\right)e^{\lambda(\tau_2-\tau_1)} \\ &\quad + \left(D_2\lambda^2 + D_1\lambda + D_0\right)e^{-\lambda\tau_1} \\ &\quad + \left(E_2\lambda^2 + E_1\lambda + E_0\right)e^{-\lambda\tau_2} \\ &\quad + \left(F_1\lambda + F_0\right)e^{-\lambda(\tau_1+\tau_2)} = 0. \end{aligned} \tag{42}$$

Let $\lambda = i\omega_2'$ ($\omega_2' > 0$) be the root of (42); then we get

$$\begin{aligned} G_{51}\left(\omega_2'\right)\cos\tau_2\omega_2' - G_{52}\left(\omega_2'\right)\sin\tau_2\omega_2' &= G_{55}\left(\omega_2'\right), \\ G_{53}\left(\omega_2'\right)\sin\tau_2\omega_2' + G_{54}\left(\omega_2'\right)\cos\tau_2\omega_2' &= G_{56}\left(\omega_2'\right), \end{aligned} \tag{43}$$

where

$$\begin{aligned} G_{51}\left(\omega_2'\right) &= \left(\omega_2'\right)^4 - \left(A_2 + E_2\right)\left(\omega_2'\right)^2 + A_0 + E_0 \\ &\quad + \left(B_0 + F_0 - B_2\left(\omega_2'\right)^2\right)\cos\tau_1\omega_2' \\ &\quad + \left(\left(B_1 + F_1\right)\omega_2' - B_3\left(\omega_2'\right)^3\right)\sin\tau_1\omega_2', \\ G_{52}\left(\omega_2'\right) &= \left(A_1 - E_1\right)\omega_2' - A_3\left(\omega_2'\right)^3 \\ &\quad - \left(B_0 - F_0 - B_2\left(\omega_2'\right)^2\right)\sin\tau_1\omega_2' \\ &\quad + \left(\left(B_1 - F_1\right)\omega_2' - B_3\left(\omega_2'\right)^3\right)\cos\tau_1\omega_2', \\ G_{53}\left(\omega_2'\right) &= \left(\omega_2'\right)^4 - \left(A_2 - E_2\right)\left(\omega_2'\right)^2 + A_0 - E_0 \\ &\quad + \left(B_0 - F_0 - B_2\left(\omega_2'\right)^2\right)\cos\tau_1\omega_2' \\ &\quad + \left(\left(B_1 - F_1\right)\omega_2' - B_3\left(\omega_2'\right)^3\right)\sin\tau_1\omega_2', \\ G_{54}\left(\omega_2'\right) &= \left(A_1 + E_1\right)\omega_2' - A_3\left(\omega_2'\right)^3 \\ &\quad - \left(B_0 + F_0 - B_2\left(\omega_2'\right)^2\right)\sin\tau_1\omega_2' \\ &\quad + \left(\left(B_1 + F_1\right)\omega_2' - B_3\left(\omega_2'\right)^3\right)\cos\tau_1\omega_2', \\ G_{55}\left(\omega_2'\right) &= C_2\left(\omega_2'\right)^2 - C_0 - D_1\omega_2\sin\tau_1\omega_2' \\ &\quad - \left(D_0 - D_2\left(\omega_2'\right)^2\right)\cos\tau_1\omega_2', \\ G_{56}\left(\omega_2'\right) &= C_3\left(\omega_2'\right)^3 - C_1\omega_2' - D_1\omega_2'\cos\tau_1\omega_2' \\ &\quad + \left(D_0 - D_2\left(\omega_2'\right)^2\right)\sin\tau_1\omega_2'. \end{aligned} \tag{44}$$

Then, we get

$$\begin{aligned} &\cos\tau_2\omega_2' \\ &\quad = \frac{G_{52}\left(\omega_2'\right)\times G_{56}\left(\omega_2'\right) + G_{53}\left(\omega_2'\right)\times G_{55}\left(\omega_2'\right)}{G_{51}\left(\omega_2'\right)\times G_{53}\left(\omega_2'\right) + G_{52}\left(\omega_2'\right)\times G_{54}\left(\omega_2'\right)}, \\ &\sin\tau_2\omega_2' \\ &\quad = \frac{G_{51}\left(\omega_2'\right)\times G_{56}\left(\omega_2'\right) - G_{54}\left(\omega_2'\right)\times G_{55}\left(\omega_2'\right)}{G_{51}\left(\omega_2'\right)\times G_{53}\left(\omega_2'\right) + G_{52}\left(\omega_2'\right)\times G_{54}\left(\omega_2'\right)}. \end{aligned} \tag{45}$$

Thus, we can obtain the following function with respect to ω_2':

$$\cos^2\tau_2\omega_2' + \sin^2\tau_2\omega_2' = 1. \tag{46}$$

Suppose that (H_{51}) (46) has at least one positive root.

If condition (H_{51}) holds, there exists a positive root $\omega_2' > 0$ of (46) such that (46) has a pair of purely imaginary roots $\pm i\omega_2'$. For ω_2',

$$\begin{aligned} \tau_{20}' &= \frac{1}{\omega_{20}'} \\ &\quad \times \arccos\frac{G_{52}\left(\omega_{20}'\right)\times G_{56}\left(\omega_{20}'\right) + G_{53}\left(\omega_{20}'\right)\times G_{55}\left(\omega_{20}'\right)}{G_{51}\left(\omega_{20}'\right)\times G_{53}\left(\omega_{20}'\right) + G_{52}\left(\omega_{20}'\right)\times G_{54}\left(\omega_{20}'\right)}. \end{aligned} \tag{47}$$

Taking the derivative with respect to τ_2 in (42), we can obtain

$$\left[\frac{d\lambda}{d\tau_2}\right]^{-1} = \frac{P_{50}(\lambda)}{Q_{50}(\lambda)} - \frac{\tau_2}{\lambda}, \tag{48}$$

where

$$\begin{aligned} P_{50}(\lambda) &= 3C_3\lambda^2 + 2C_2\lambda + C_1 + \left(4\lambda^3 + 3A_3\lambda^2\right. \\ &\quad \left. + 2A_2\lambda + A_1\right)e^{\lambda\tau_2} + \left(2E_2\lambda + E_1\right)e^{-\lambda\tau_2} - \left(\tau_1D_2\lambda^2\right. \\ &\quad \left. + \left(\tau_1D_1 - 2D_2\right)\lambda + \tau_1D_0 - D_1\right)e^{-\lambda\tau_1} - \left(\tau_1F_1\lambda\right. \\ &\quad \left. + \tau_1F_0 - F_1\right)e^{-\lambda(\tau_1+\tau_2)} - \left(\tau_1B_3\lambda^3 + \left(\tau_1B_2 - 3B_3\right)\lambda^2\right. \\ &\quad \left. + \left(\tau_1B_1 - 2B_2\right)\lambda + \tau_1B_0 - B_1\right)e^{\lambda(\tau_2-\tau_1)}, \\ Q_{50}(\lambda) &= \left(E_2\lambda^3 + E_1\lambda^2 + E_0\lambda\right)e^{-\lambda\tau_2} + \left(F_1\lambda^2 + F_0\lambda\right) \\ &\quad \cdot e^{-\lambda(\tau_1+\tau_2)} - \left(\lambda^5 + A_3\lambda^4 + A_2\lambda^3 + A_1\lambda^2 + A_0\lambda\right) \\ &\quad \cdot e^{\lambda\tau_2} - \left(B_3\lambda^4 + B_2\lambda^3 + B_1\lambda^2 + B_0\lambda\right)e^{\lambda(\tau_2-\tau_1)}. \end{aligned} \tag{49}$$

Define

$$\operatorname{Re}\left[\frac{d\lambda}{d\tau_2}\right]^{-1}_{\lambda=i\omega_{20}'} = \frac{P_{5R}Q_{5R} + P_{5I}Q_{5I}}{Q_{5R}^2 + Q_{5I}^2}. \tag{50}$$

Obviously, if the condition (H_{52}) $P_{5R}Q_{5R} + P_{5I}Q_{5I} \neq 0$, then $\operatorname{Re}[d\lambda/d\tau_2]^{-1}_{\lambda=i\omega_{20}'} \neq 0$. Thus, we have the following results according to the Hopf bifurcation theorem in [15].

Theorem 4. *For system (2), if the conditions* (H_{51})-(H_{52}) *hold and* $\tau_1 \in (0, \tau_{10})$*, then the positive equilibrium* $D_*(S_*, I_*, Q_*, R_*)$ *is asymptotically stable for* $\tau_2 \in [0, \tau_{20}')$ *and system (2) undergoes a Hopf bifurcation at the positive equilibrium* $D_*(S_*, I_*, Q_*, R_*)$ *when* $\tau_2 = \tau_{20}'$ *and a family of periodic solutions bifurcate from* $D_*(S_*, I_*, Q_*, R_*)$ *near* $\tau_2 = \tau_{20}'$.

3. Properties of the Hopf Bifurcation

In this section, we investigate the direction of the Hopf bifurcation and the stability of the Hopf bifurcation of system (2) when $\tau_2 > 0$ and $\tau_1 = \tau_{1*} \in (0, \tau_{10})$ by using the normal form theory and the center manifold theorem in [15]. Throughout this section, we assume that $\tau_{1*} < \tau_{20}'$.

Let $u_1(t) = S(t) - S_*$, $u_2(t) = I(t) - I_*$, $u_3(t) = Q(t) - Q_*$, $u_4(t) = R(t) - R_*$, and $\tau_2 = \tau_{20}' + \mu$, $\mu \in R$ and normalize the time delay by $t \to (t/\tau_2)$. Then system (1) can be transformed into as

$$\dot{u}(t) = L_\mu u_t + F(\mu, u_t), \tag{51}$$

where

$$\begin{aligned}
&u(t) = (u_1(t), u_2(t), u_3(t), u_4(t))^T \in R^4,\\
&L_\mu\phi = (\tau_{20}' + \mu)\\
&\quad\cdot\left(A_{\text{trix}}\phi(0) + B_{\text{trix}}\phi\left(-\frac{\tau_{1*}}{\tau_{20}^*}\right) + C_{\text{trix}}\phi(-1)\right),\\
&F(\mu, \phi) = (\tau_{10}^* + \mu)\\
&\quad\cdot\begin{pmatrix} -\beta\phi_1\left(-\frac{\tau_{1*}}{\tau_{20}^*}\right)\phi_2\left(-\frac{\tau_{1*}}{\tau_{20}^*}\right)\\ \beta\phi_1\left(-\frac{\tau_{1*}}{\tau_{20}^*}\right)\phi_2\left(-\frac{\tau_{1*}}{\tau_{20}^*}\right)\\ 0\\ 0\end{pmatrix},\\
&A_{\text{trix}} = \begin{pmatrix} a_{11} & 0 & 0 & 0\\ 0 & a_{12} & 0 & 0\\ 0 & a_{32} & a_{33} & 0\\ 0 & 0 & 0 & a_{44}\end{pmatrix},\\
&B_{\text{trix}} = \begin{pmatrix} b_{11} & b_{12} & 0 & 0\\ b_{21} & b_{22} & 0 & 0\\ 0 & 0 & 0 & 0\\ 0 & 0 & 0 & 0\end{pmatrix},\\
&C_{\text{trix}} = \begin{pmatrix} 0 & 0 & 0 & 0\\ 0 & c_{22} & 0 & 0\\ 0 & 0 & c_{33} & 0\\ 0 & c_{42} & c_{43} & 0\end{pmatrix}.
\end{aligned} \tag{52}$$

By the Riesz representation theorem, there is a 4×4 matrix function with bounded variation components $\eta(\theta, \mu)$, $\theta \in [-1, 0]$ such that

$$L_\mu\phi = \int_{-1}^{0} d\eta(\theta, \mu)\phi(\theta), \quad \phi \in C([-1, 0], R^4). \tag{53}$$

In fact, we choose

$$\begin{aligned}
&\eta(\theta, \mu)\\
&= \begin{cases} (\tau_{20}' + \mu)(A_{\text{trix}} + B_{\text{trix}} + C_{\text{trix}}), & \theta = 0,\\ (\tau_{20}' + \mu)(B_{\text{trix}} + C_{\text{trix}}), & \theta \in \left[-\frac{\tau_{1*}}{\tau_{20}'}, 0\right),\\ (\tau_{20}' + \mu)C_{\text{trix}}, & \theta \in \left(-1, -\frac{\tau_{1*}}{\tau_{20}'}\right),\\ 0, & \theta = -1.\end{cases}
\end{aligned} \tag{54}$$

For $\phi \in C([-1, 0], R^4)$, we define

$$\begin{aligned}
A(\mu)\phi &= \begin{cases} \frac{d\phi(\theta)}{d\theta}, & -1 \le \theta < 0,\\ \int_{-1}^{0} d\eta(\theta, \mu)\phi(\theta), & \theta = 0,\end{cases}\\
R(\mu)\phi &= \begin{cases} 0, & -1 \le \theta < 0,\\ F(\mu, \phi), & \theta = 0.\end{cases}
\end{aligned} \tag{55}$$

Then system (51) is equivalent to the following operator equation:

$$\dot{u}(t) = A(\mu)u_t + R(\mu)u_t. \tag{56}$$

Next, we define the adjoint operator A^* of A

$$A^*(\varphi) = \begin{cases} -\frac{d\varphi(s)}{ds}, & 0 < s \le 1,\\ \int_{-1}^{0} d\eta^T(s, 0)\varphi(-s), & s = 0,\end{cases} \tag{57}$$

and a bilinear inner product

$$\begin{aligned}
\langle\varphi(s), \phi(\theta)\rangle &= \overline{\varphi}(0)\phi(0)\\
&\quad - \int_{\theta=-1}^{0}\int_{\xi=0}^{\theta}\overline{\varphi}(\xi - \theta)\, d\eta(\theta)\phi(\xi)\, d\xi,
\end{aligned} \tag{58}$$

where $\eta(\theta) = \eta(\theta, 0)$.

Let $\rho(\theta) = (1, \rho_2, \rho_3, \rho_4)^T e^{i\omega'_{20}\tau'_{20}\theta}$ be the eigenvectors of $A(0)$ corresponding to $+i\omega'_{20}\tau'_{20}$ and $\rho'(s) = (1/K)(1, \rho'_2, \rho'_3, \rho'_4)e^{i\omega'_{20}\tau'_{20}s}$ be the eigenvectors of A^* corresponding to $-i\omega'_{20}\tau'_{20}$. Then, we obtain

$$\begin{aligned}
\rho_2 &= \frac{i\omega'_{20} - a_{11} - b_{11}e^{-i\tau_{1*}\omega'_{20}}}{b_{12}e^{-i\tau_{1*}\omega'_{20}}},\\
\rho_3 &= \frac{a_{32}\left(i\omega'_{20} - a_{11} - b_{11}e^{-i\tau_{1*}\omega'_{20}}\right)}{\left(i\omega'_{20} - a_{33} - c_{33}e^{-i\tau'_{20}\omega'_{20}}\right)b_{12}e^{-i\tau_{1*}\omega'_{20}}},\\
\rho_4 &= \frac{c_{42}\rho_2 + c_{43}\rho_3}{\left(i\omega'_{20} - a_{44}\right)e^{i\tau'_{20}\omega'_{20}}},\\
\rho'_2 &= -\frac{i\omega'_{20} + a_{11} + b_{11}e^{i\tau_{1*}\omega'_{20}}}{b_{21}e^{i\tau_{1*}\omega'_{20}}},\\
\rho'_4 &= -\frac{i\omega'_{20} + a_{33} + c_{33}e^{i\tau'_{20}\omega'_{20}}}{c_{43}e^{i\tau'_{20}\omega'_{20}}},\\
\rho'_3 &= -\left[\left(i\omega'_{20} + a_{22} + b_{22}e^{i\tau_{1*}\omega'_{20}}\right)\rho'_2 + b_{12}e^{i\tau_{1*}\omega'_{20}}\right]\\
&\quad\times\left(c_{42}e^{i\tau'_{20}\omega'_{20}} - \frac{a_{32}c_{43}e^{i\tau'_{20}\omega'_{20}}}{i\omega'_{20} + c_{33}e^{i\tau'_{20}\omega'_{20}}}\right)^{-1}.
\end{aligned} \tag{59}$$

From (58), we can obtain

$$\begin{aligned}
\overline{K} &= 1 + \rho_2\overline{\rho}'_2 + \rho_3\overline{\rho}'_3 + \rho_4\overline{\rho}'_4 + \tau_{1*}e^{-i\omega'_{20}\tau_{1*}}\left(b_{11}\right.\\
&\quad\left. + b_{21}\overline{\rho}'_2 + \rho_2\left(b_{12} + b_{22}\overline{\rho}'_2\right)\right)\\
&\quad + \tau'_{20}e^{-i\omega'_{20}\tau'_{20}}\left(\rho_2\left(c_{22}\overline{\rho}'_2 + c_{42}\overline{\rho}'_4\right)\right.\\
&\quad\left. + \rho_3\left(c_{33}\overline{\rho}'_3 + c_{43}\overline{\rho}'_4\right)\right)
\end{aligned} \tag{60}$$

such that $\langle\rho^*, \rho\rangle = 1$, $\langle\rho^*, \overline{\rho}\rangle = 0$.

Following the algorithms given in [15] and using similar computation process in [16], we can get the coefficients which determine the properties of the Hopf bifurcation:

$$\begin{aligned}
g_{20} &= 2\beta\tau'_{20}\overline{K}\left(\overline{\rho}'_2 - 1\right)\rho^{(1)}\left(-\frac{\tau_{1*}}{\tau'_{20}}\right)\rho^{(2)}\left(-\frac{\tau_{1*}}{\tau'_{20}}\right),\\
g_{11} &= \beta\tau'_{20}\overline{K}\left(\overline{\rho}'_2 - 1\right)\left(\rho^{(1)}\left(-\frac{\tau_{1*}}{\tau'_{20}}\right)\overline{\rho}^{(2)}\left(-\frac{\tau_{1*}}{\tau'_{20}}\right)\right.\\
&\quad\left. + \overline{\rho}^{(1)}\left(-\frac{\tau_{1*}}{\tau'_{20}}\right)\rho^{(1)}\left(-\frac{\tau_{1*}}{\tau'_{20}}\right)\right),\\
g_{02} &= 2\beta\tau'_{20}\overline{K}\left(\overline{\rho}'_2 - 1\right)\overline{\rho}^{(1)}\left(-\frac{\tau_{1*}}{\tau'_{20}}\right)\overline{\rho}^{(2)}\left(-\frac{\tau_{1*}}{\tau'_{20}}\right),\\
g_{21} &= 2\beta\tau'_{20}\overline{K}\left(\overline{\rho}'_2 - 1\right)\left(W_{11}^{(1)}\left(-\frac{\tau_{1*}}{\tau'_{20}}\right)\rho^{(2)}\left(-\frac{\tau_{1*}}{\tau'_{20}}\right)\right.\\
&\quad + \frac{1}{2}W_{20}^{(1)}\left(-\frac{\tau_{1*}}{\tau'_{20}}\right)\overline{\rho}^{(2)}\left(-\frac{\tau_{1*}}{\tau'_{20}}\right)\\
&\quad + W_{11}^{(2)}\left(-\frac{\tau_{1*}}{\tau'_{20}}\right)\rho^{(1)}\left(-\frac{\tau_{1*}}{\tau'_{20}}\right)\\
&\quad\left. + \frac{1}{2}W_{20}^{(2)}\left(-\frac{\tau_{1*}}{\tau'_{20}}\right)\overline{\rho}^{(1)}\left(-\frac{\tau_{1*}}{\tau'_{20}}\right)\right),
\end{aligned} \tag{61}$$

with

$$\begin{aligned}
W_{20}(\theta) &= \frac{ig_{20}\rho(0)}{\tau'_{20}\omega'_{20}}e^{i\tau'_{20}\omega'_{20}\theta} + \frac{i\overline{g}_{02}\overline{\rho}(0)}{3\tau'_{20}\omega'_{20}}e^{-i\tau'_{20}\omega'_{20}\theta}\\
&\quad + E_1e^{2i\tau'_{20}\omega'_{20}\theta},\\
W_{11}(\theta) &= -\frac{ig_{11}\rho(0)}{\tau'_{20}\omega'_{20}}e^{i\tau'_{20}\omega'_{20}} + \frac{i\overline{g}_{11}\overline{\rho}(0)}{\tau'_{20}\omega'_{20}}e^{-i\tau'_{20}\omega'_{20}\theta}\\
&\quad + E_2,
\end{aligned} \tag{62}$$

where E_1 and E_2 can be determined by the following equations, respectively,

$$\begin{aligned}
&\begin{pmatrix}
a'_{11} & -b_{12}e^{-2i\tau_{1*}\omega'_{20}} & 0 & 0\\
-b_{21}e^{-2i\tau_{1*}\omega'_{20}} & a'_{22} & 0 & 0\\
0 & -a_{32} & a'_{33} & 0\\
0 & -c_{42}e^{-2i\tau'_{20}\omega'_{20}} & -c_{43}e^{-2i\tau'_{20}\omega'_{20}} & 2i\omega'_{20} - a_{44}
\end{pmatrix}E_1 = 2\begin{pmatrix}
E_{11}\\ E_{12}\\ 0\\ 0
\end{pmatrix},\\
&\begin{pmatrix}
a_{11} + b_{11} & b_{21} & 0 & 0\\
b_{21} & a_{22} + b_{22} + c_{22} & 0 & 0\\
0 & a_{32} & a_{33} + a_{44} & 0\\
0 & c_{42} & c_{43} & a_{44}
\end{pmatrix}E_2 = \begin{pmatrix}
E_{21}\\ E_{22}\\ 0\\ 0
\end{pmatrix},
\end{aligned} \tag{63}$$

with

$$
\begin{aligned}
a_{11}' &= 2i\omega_{20}' - a_{11} - b_{11}e^{-2i\tau_{1*}\omega_{20}'},\\
a_{22}' &= 2i\omega_{20}' - a_{22} - b_{22}e^{-2i\tau_{1*}\omega_{20}'} - c_{22}e^{-2i\tau_{20}'\omega_{20}'},\\
a_{33}' &= 2i\omega_{20}' - a_{33} - c_{33}e^{-2i\tau_{20}'\omega_{20}'},\\
E_{11} &= -\beta\rho^{(1)}\left(-\frac{\tau_{1*}}{\tau_{20}'}\right)\rho^{(2)}\left(-\frac{\tau_{1*}}{\tau_{20}'}\right),\\
E_{12} &= \beta\rho^{(1)}\left(-\frac{\tau_{1*}}{\tau_{20}'}\right)\rho^{(2)}\left(-\frac{\tau_{1*}}{\tau_{20}'}\right),\\
E_{21} &= -\beta\left(\rho^{(1)}\left(-\frac{\tau_{1*}}{\tau_{20}'}\right)\overline{\rho}^{(2)}\left(-\frac{\tau_{1*}}{\tau_{20}'}\right)\right.\\
&\quad \left.+\,\overline{\rho}^{(1)}\left(-\frac{\tau_{1*}}{\tau_{20}'}\right)\rho^{(1)}\left(-\frac{\tau_{1*}}{\tau_{20}'}\right)\right),\\
E_{22} &= \beta\left(\rho^{(1)}\left(-\frac{\tau_{1*}}{\tau_{20}'}\right)\overline{\rho}^{(2)}\left(-\frac{\tau_{1*}}{\tau_{20}'}\right)\right.\\
&\quad \left.+\,\overline{\rho}^{(1)}\left(-\frac{\tau_{1*}}{\tau_{20}'}\right)\rho^{(1)}\left(-\frac{\tau_{1*}}{\tau_{20}'}\right)\right).
\end{aligned}
\tag{64}
$$

Then, we can get the following coefficients:

$$
\begin{aligned}
C_1(0) &= \frac{i}{2\tau_{20}'\omega_{20}'}\left(g_{11}g_{20} - 2\left|g_{11}\right|^2 - \frac{\left|g_{02}\right|^2}{3}\right)\\
&\quad + \frac{g_{21}}{2},\\
\mu_2 &= -\frac{\operatorname{Re}\left\{C_1(0)\right\}}{\operatorname{Re}\left\{\lambda'\left(\tau_{20}'\right)\right\}},\\
\beta_2 &= 2\operatorname{Re}\left\{C_1(0)\right\},\\
T_2 &= -\frac{\operatorname{Im}\left\{C_1(0)\right\} + \mu_2\operatorname{Im}\left\{\lambda'\left(\tau_{20}'\right)\right\}}{\tau_{20}'\omega_{20}'},
\end{aligned}
\tag{65}
$$

in which μ_2 determines the direction of the Hopf bifurcation; β_2 determines the stability of the bifurcation periodic solutions and T_2 determines the period of the bifurcation periodic solutions. From the conclusion of [15], we have the main results in this section.

Theorem 5. *For system (2), μ_2 determines the direction of the Hopf bifurcation: if $\mu_2 > 0$ ($\mu_2 < 0$), the Hopf bifurcation is supercritical (subcritical). β_2 determines the stability of the bifurcating periodic solution: if $\beta_2 < 0$ ($\beta_2 > 0$) the bifurcating periodic solutions are stable (unstable). T_2 determines the period of the bifurcating periodic solution: if $T_2 > 0$ ($T_2 < 0$), the period of the bifurcating periodic solutions increases (decreases).*

4. Numerical Investigations

In this section, a numerical example is given to support the theoretical results in Sections 2 and 3. We choose the same values of the parameters as in [14] and let $p = 0.2$, $\beta = 0.1$, $d = 0.01$, $\alpha_1 = 0.01$, $\gamma = 0.5$, $\delta = 0.1$, $\varepsilon = 0.1$, $\alpha_2 = 0.02$, and $b = 10$. Then, we get the following system:

$$
\begin{aligned}
\frac{dS(t)}{dt} &= 8 - 0.1S\left(t-\tau_1\right)I\left(t-\tau_1\right) - 0.01S(t),\\
\frac{dI(t)}{dt} &= 0.1S\left(t-\tau_1\right)I\left(t-\tau_1\right) - 0.12I(t)\\
&\quad - 0.5I\left(t-\tau_2\right),\\
\frac{dQ(t)}{dt} &= 0.1I(t) - 0.03Q(t) - 0.1 * Q\left(t-\tau_2\right),\\
\frac{dR(t)}{dt} &= 0.5I\left(t-\tau_2\right) + 2 + 0.1Q\left(t-\tau_2\right)\\
&\quad - 0.01R(t).
\end{aligned}
\tag{66}
$$

Then, we can get $R_0 = 129.0323 > 1$ and the unique positive equilibrium $D_*(6.2, 12.8032, 9.8486, 938.646)$ of system (66) and condition (H_{11}) holds.

For $\tau_1 > 0$, $\tau_2 = 0$, we obtain $\omega_{10} = 0.4107$, $\tau_{10} = 1.3265$. By Theorem 1, we can conclude that the positive equilibrium D_* is locally asymptotically stable when $\tau_1 \in [0, 1.3265)$. In this case, the propagation of computer viruses can be predicted and controlled easily. This property can be illustrated by Figures 1–3. However, if we choose $\tau_1 = 1.3625 > \tau_{10} = 1.3265$, the positive equilibrium D_* becomes unstable and a Hopf bifurcation occurs, which can be illustrated by Figures 4–6. When a Hopf bifurcation occurs, the state of computer viruses propagation changes from an equilibrium point to a limit cycle and it means that the propagation of computer viruses is out of control. Similarly, we have $\omega_{20} = 1.6022$, $\tau_{20} = 1.7852$ when $\tau_1 = 0$, $\tau_2 > 0$. The corresponding waveforms and phase plots are shown as in Figures 7–12.

For $\tau_1 > 0$, $\tau_2 > 0$ and $\tau_2 = 1.05 \in (0, \tau_{20})$. We can obtain $\omega_1' = 1.9403$ and then we obtain $\tau_{10}' = 0.8903$. Figures 13–15 show that the positive equilibrium D_* of system (66) is asymptotically stable when $\tau_1 = 0.785 < 0.8903 = \tau_{10}'$ and Figures 16–18 show that there is a Hopf bifurcation occurs at the positive equilibrium D_* of system (66) and a family of periodic solutions bifurcate from D_* when $\tau_1 = 0.9755 > \tau_{10}' = 0.8903$. Similarly, we have $\omega_2' = 2.0411$ and $\tau_{20}' = 1.3485$ when $\tau_2 > 0$, $\tau_1 = 0.65 \in (0, \tau_{10})$. The corresponding waveforms and plots are shown in Figures 19–24. In addition, we can obtain $\mu_2 = 1.3987$, $\beta_2 = -2.2318 < 0$, $T_2 = 8.4012 > 0$. Thus, we can conclude that the Hopf bifurcation is supercritical, the bifurcating periodic solutions are stable, and the period of the periodic solutions increases according to Theorem 5.

5. Critical Analysis and Research Perspectives

In this paper, an SIQR computer virus model with two delays is investigated. Compared with the system considered in [14],

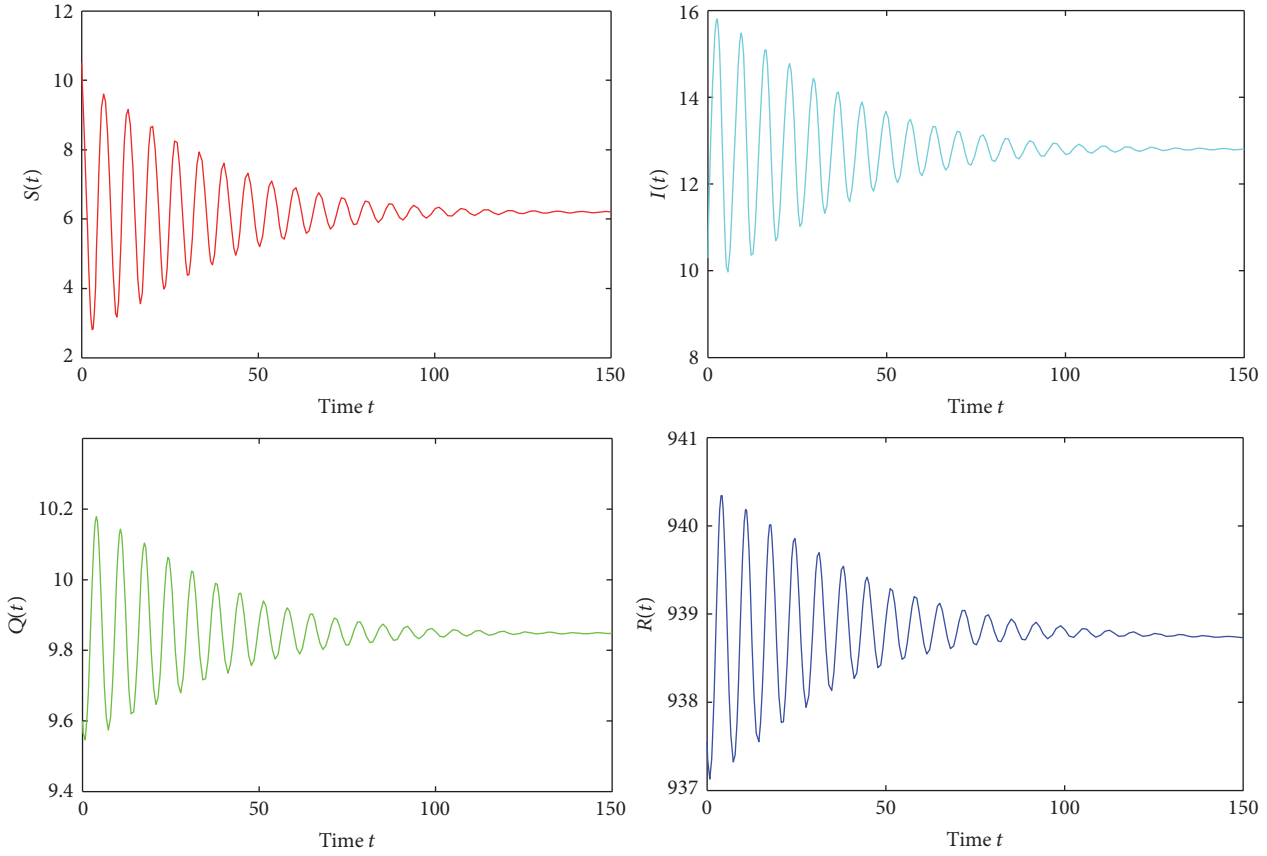

Figure 1: The trajectory of S, I, Q, and R when $\tau_1 = 1.3025 < 1.3265 = \tau_{10}$.

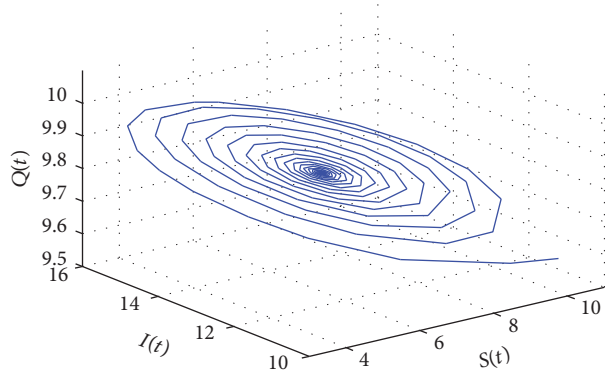

Figure 2: The phase plot of S, I, and Q when $\tau_1 = 1.3025 < 1.3265 = \tau_{10}$.

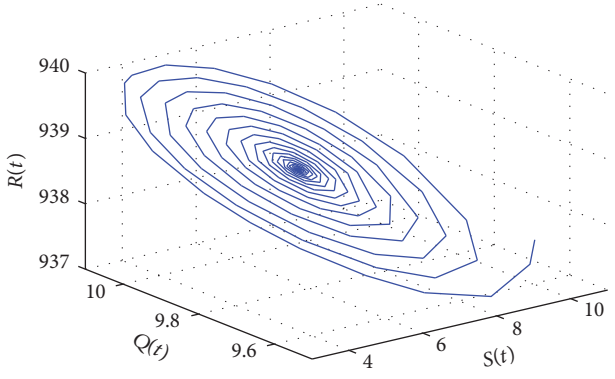

Figure 3: The phase plot of S, Q, and R when $\tau_1 = 1.3025 < 1.3265 = \tau_{10}$.

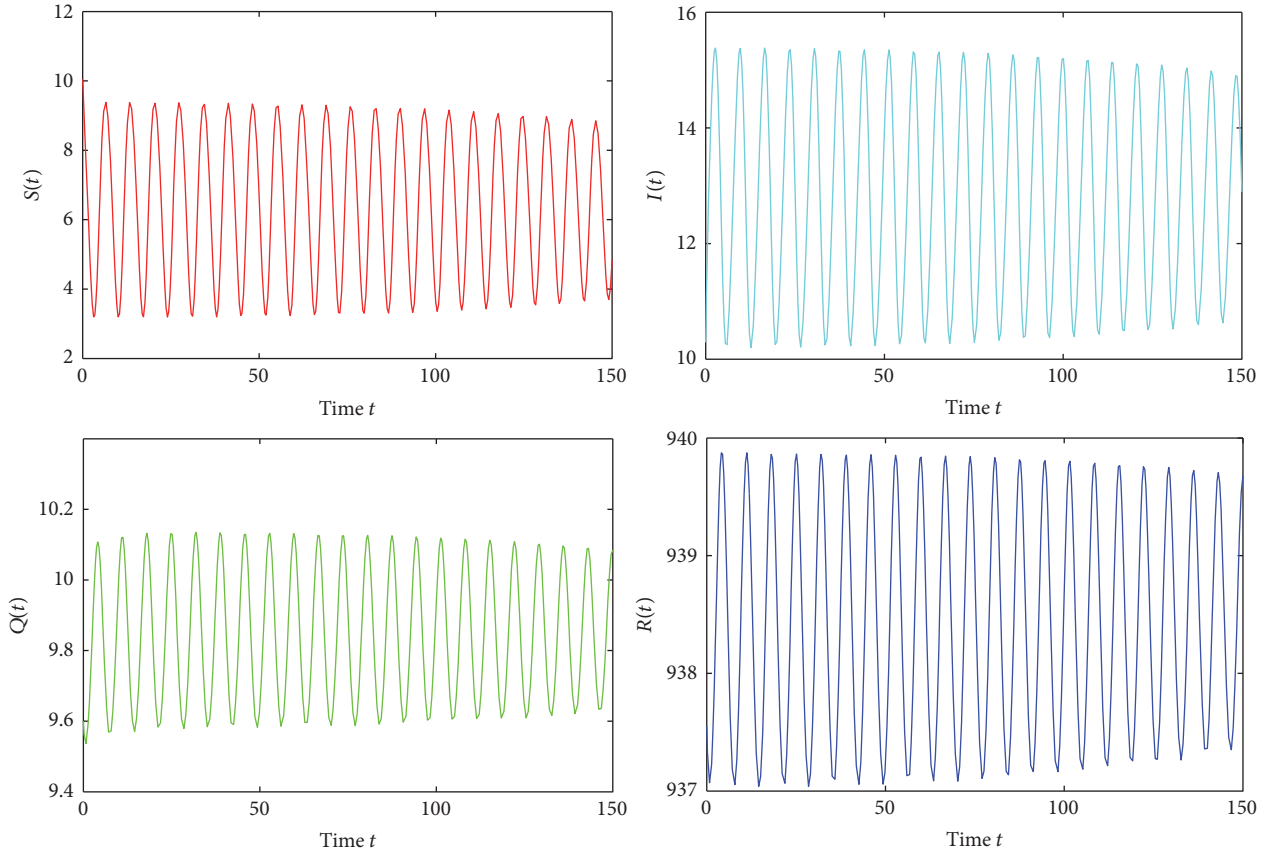

Figure 4: The trajectory of S, I, Q, and R when $\tau_1 = 1.3625 > 1.3265 = \tau_{10}$.

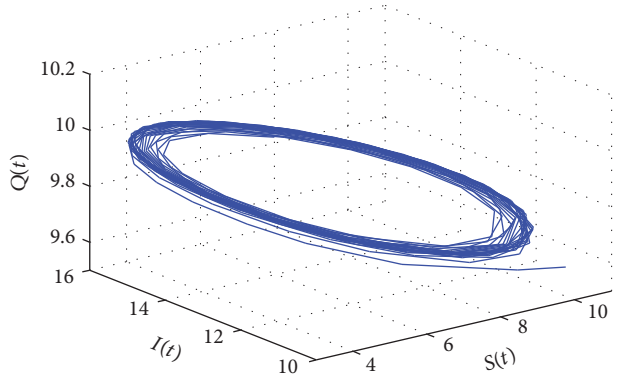

Figure 5: The phase plot of S, I, and Q when $\tau_1 = 1.3625 > 1.3265 = \tau_{10}$.

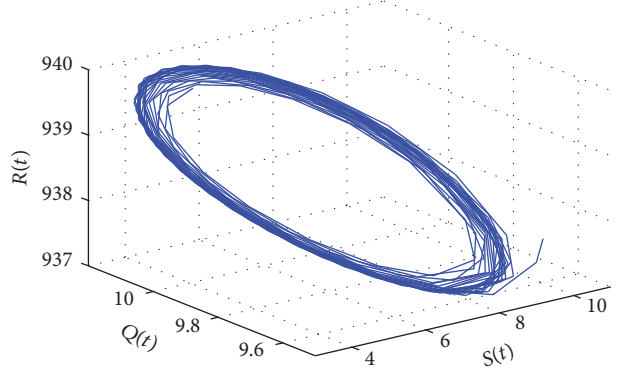

Figure 6: The phase plot of S, Q, and R when $\tau_1 = 1.3625 > 1.3265 = \tau_{10}$.

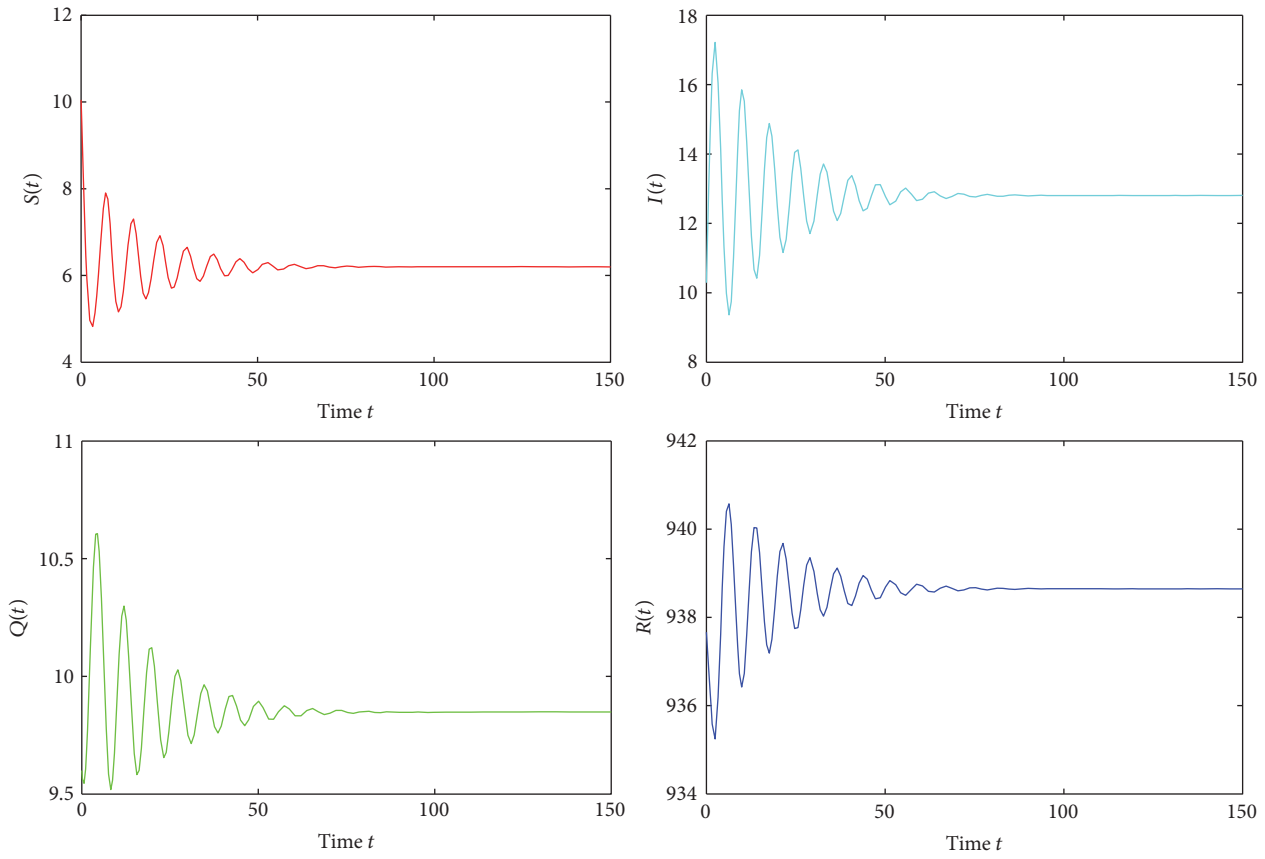

Figure 7: The trajectory of S, I, Q, and R when $\tau_2 = 1.65 < 1.7852 = \tau_{20}$.

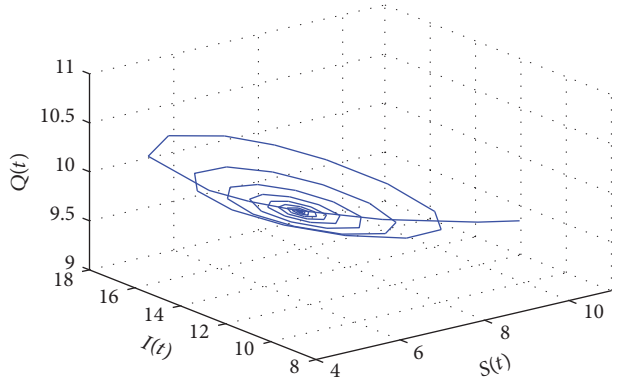

Figure 8: The phase plot of S, I, and Q when $\tau_2 = 1.65 < 1.7852 = \tau_{20}$.

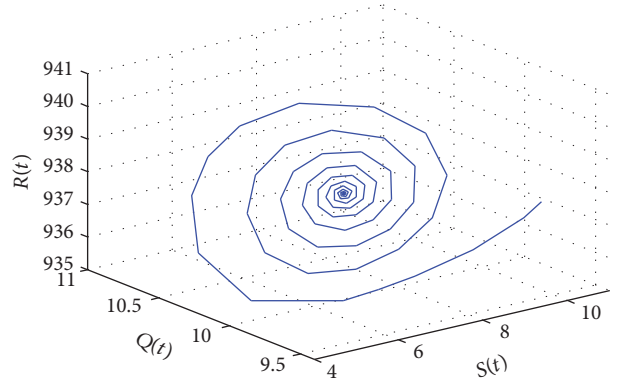

Figure 9: The phase plot of S, Q, and R when $\tau_2 = 1.65 < 1.7852 = \tau_{20}$.

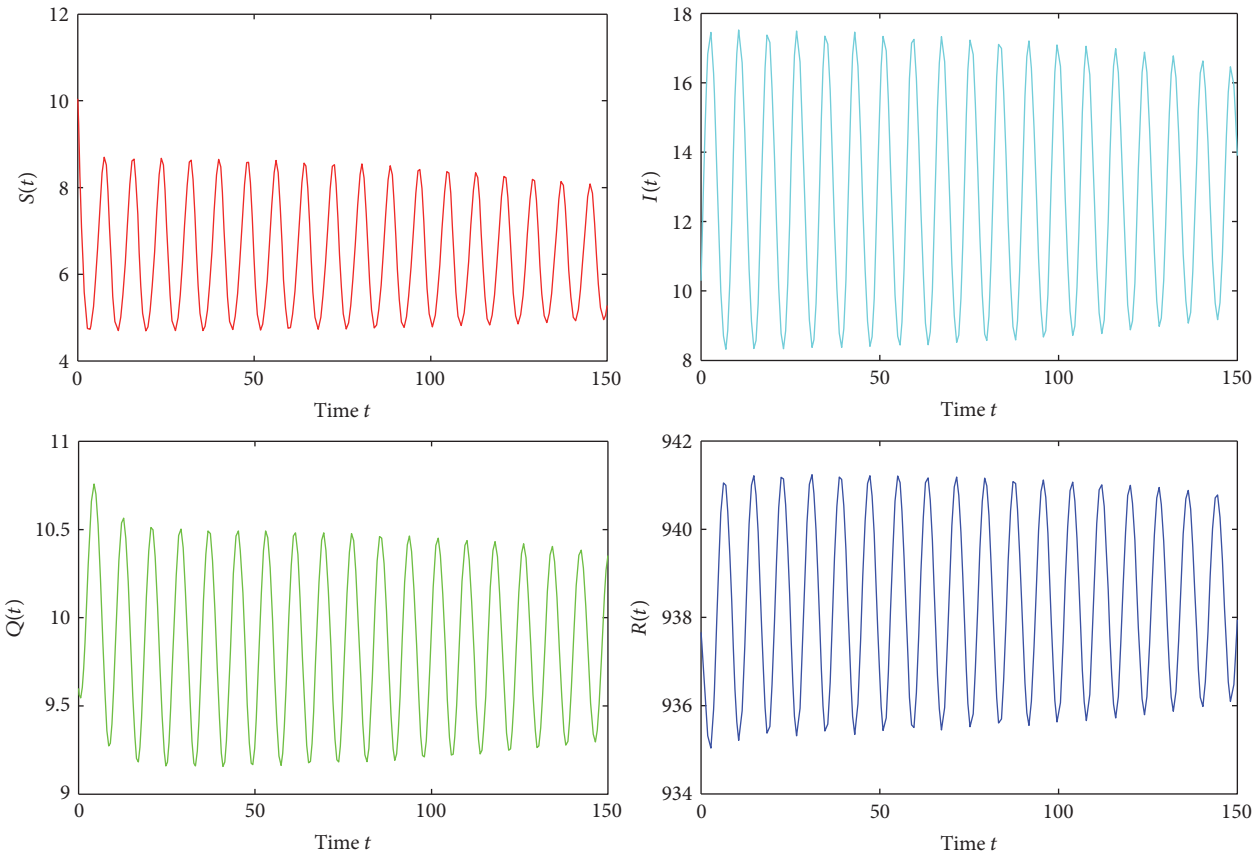

Figure 10: The trajectory of S, I, Q, and R when $\tau_2 = 1.8625 > 1.7852 = \tau_{20}$.

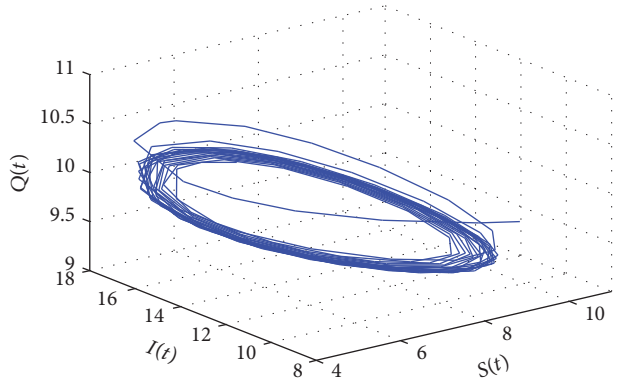

Figure 11: The phase plot of S, I, and Q when $\tau_2 = 1.86251.7852 = \tau_{20}$.

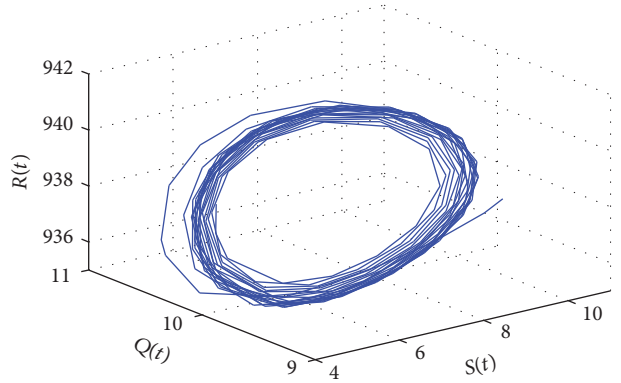

Figure 12: The phase plot of S, Q, and R when $\tau_2 = 1.8625 > 1.7852 = \tau_{20}$.

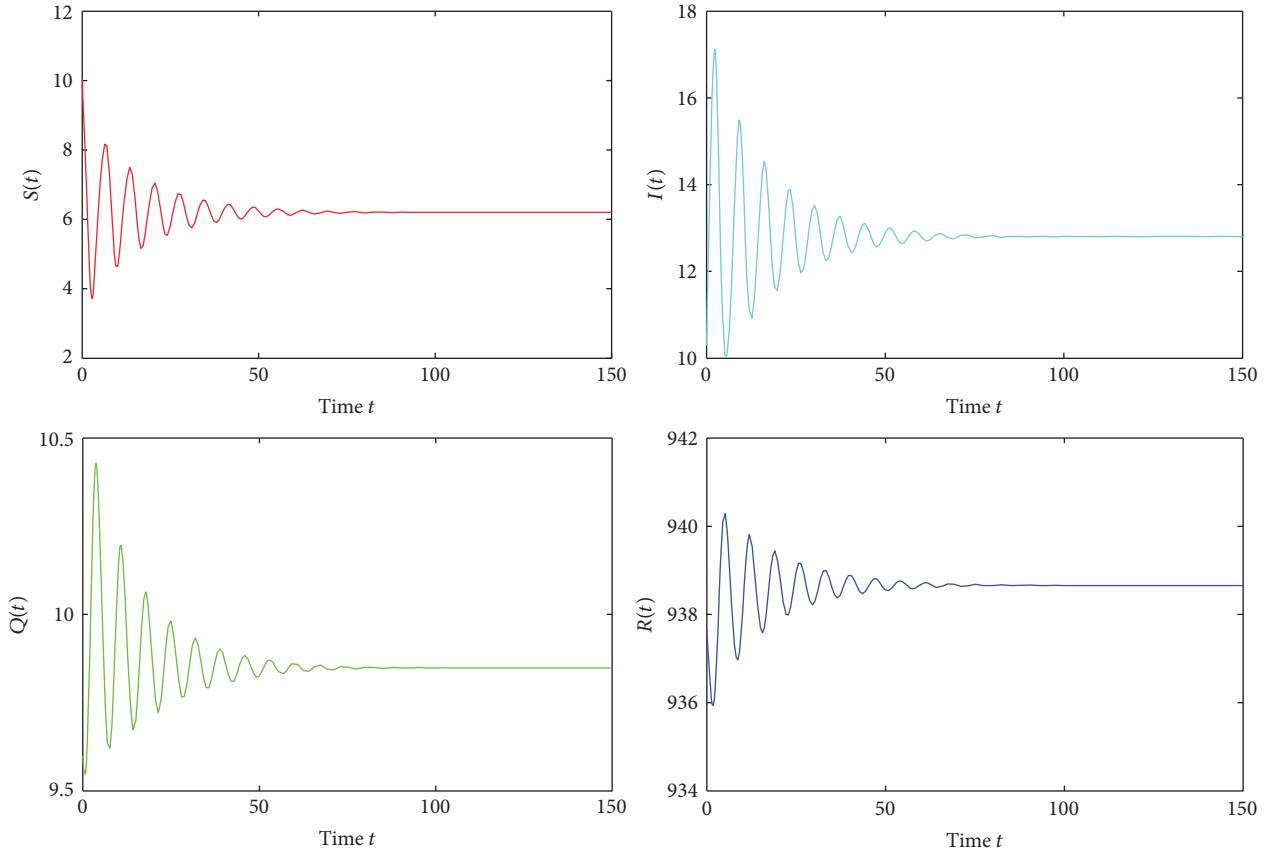

Figure 13: The trajectory of S, I, Q, and R when $\tau_1 = 0.785 < 0.8903 = \tau'_{10}$ and $\tau_2 = 1.05$.

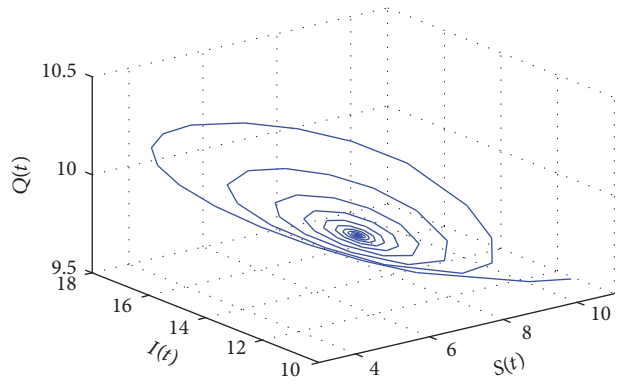

Figure 14: The phase plot of S, I, and Q when $\tau_1 = 0.785 < 0.8903 = \tau'_{10}$ and $\tau_2 = 1.05$.

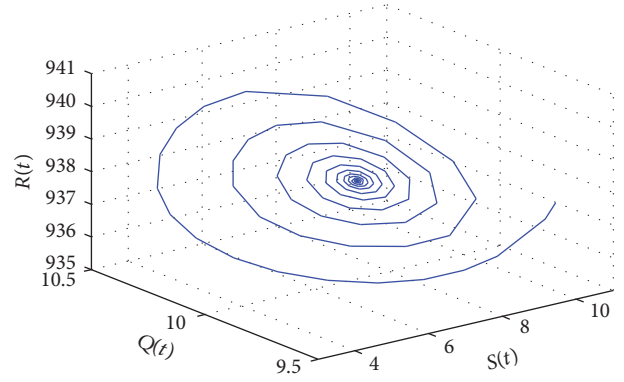

Figure 15: The phase plot of S, Q, and R when $\tau_1 = 0.785 < 0.8903 = \tau'_{10}$ and $\tau_2 = 1.05$.

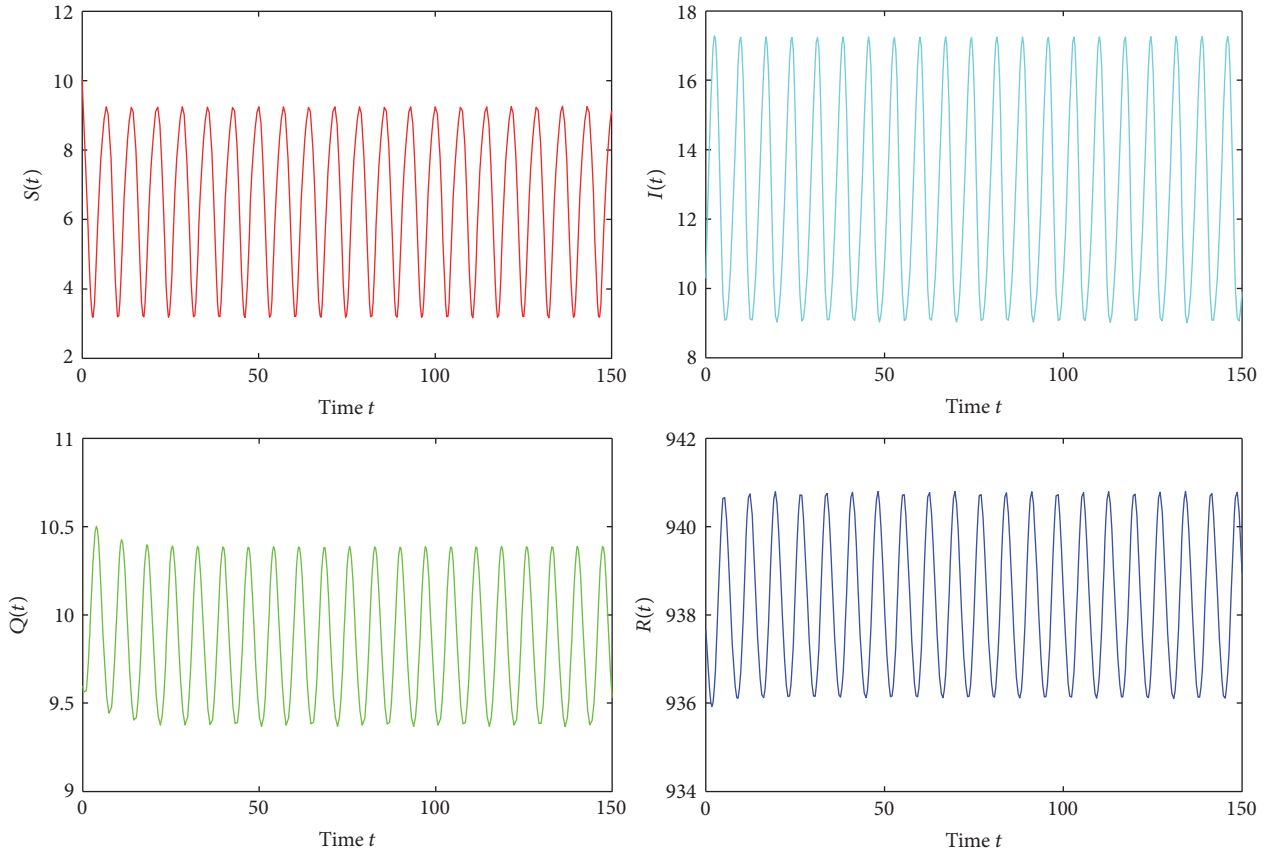

Figure 16: The trajectory of S, I, Q, and R when $\tau_1 = 0.9755 > 0.8903 = \tau'_{10}$ and $\tau_2 = 1.05$.

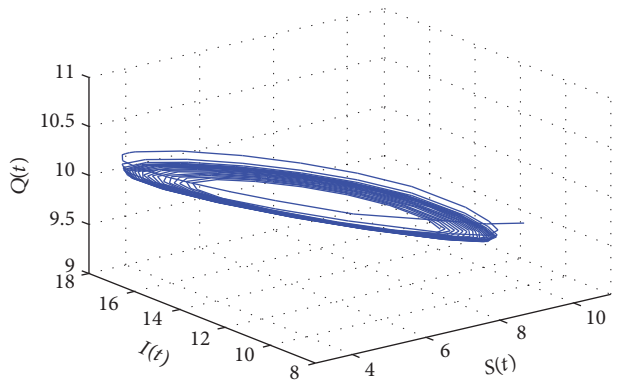

Figure 17: The phase plot of S, I, and Q when $\tau_1 = 0.9755 > 0.8903 = \tau'_{10}$ and $\tau_2 = 1.05$.

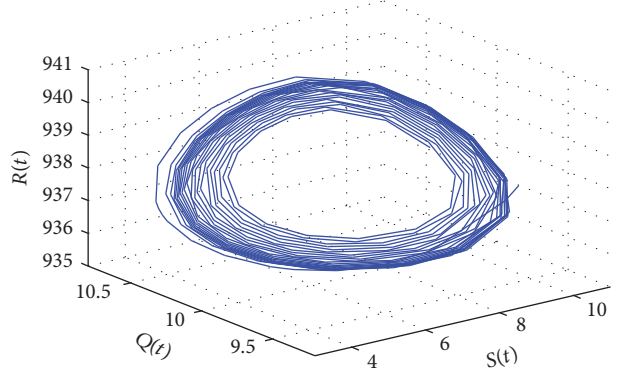

Figure 18: The phase plot of S, Q, and R when $\tau_2 = 0.9755 > 0.8903 = \tau'_{20}$ and $\tau_2 = 1.05$.

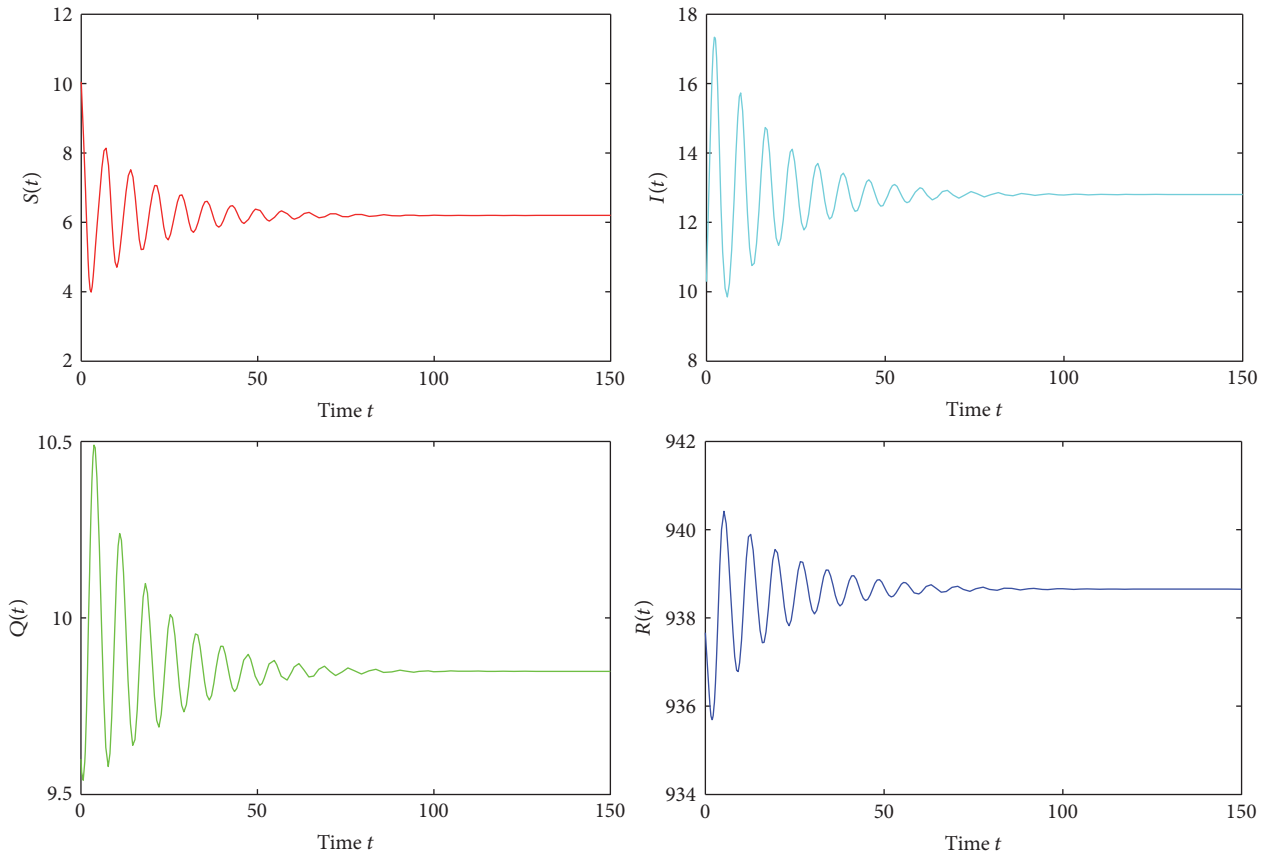

Figure 19: The trajectory of S, I, Q, and R when $\tau_2 = 1.235 < 1.3485 = \tau'_{20}$ and $\tau_1 = 0.65$.

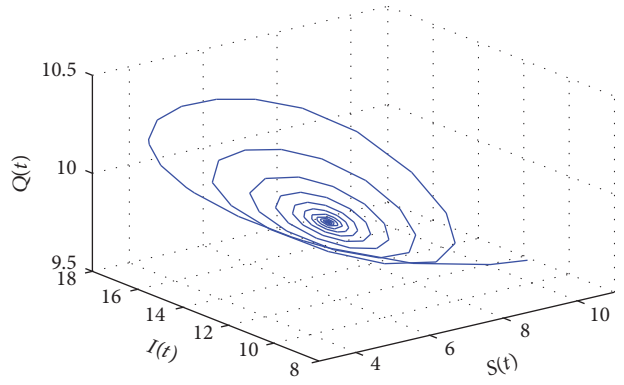

Figure 20: The phase plot of S, I, and Q when $\tau_2 = 1.235 < 1.3485 = \tau'_{20}$ and $\tau_1 = 0.65$.

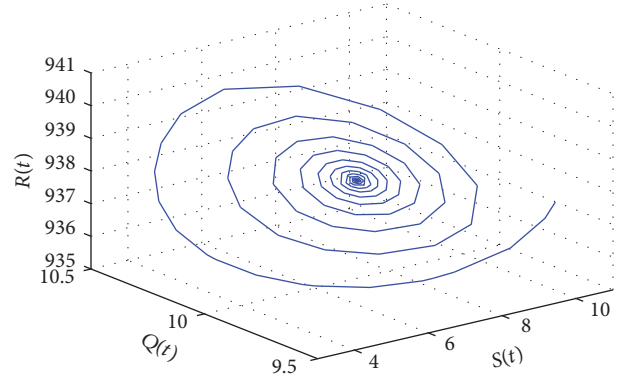

Figure 21: The phase plot of S, Q, and R when $\tau_2 = 1.235 < 1.3485 = \tau'_{20}$ and $\tau_1 = 0.65$.

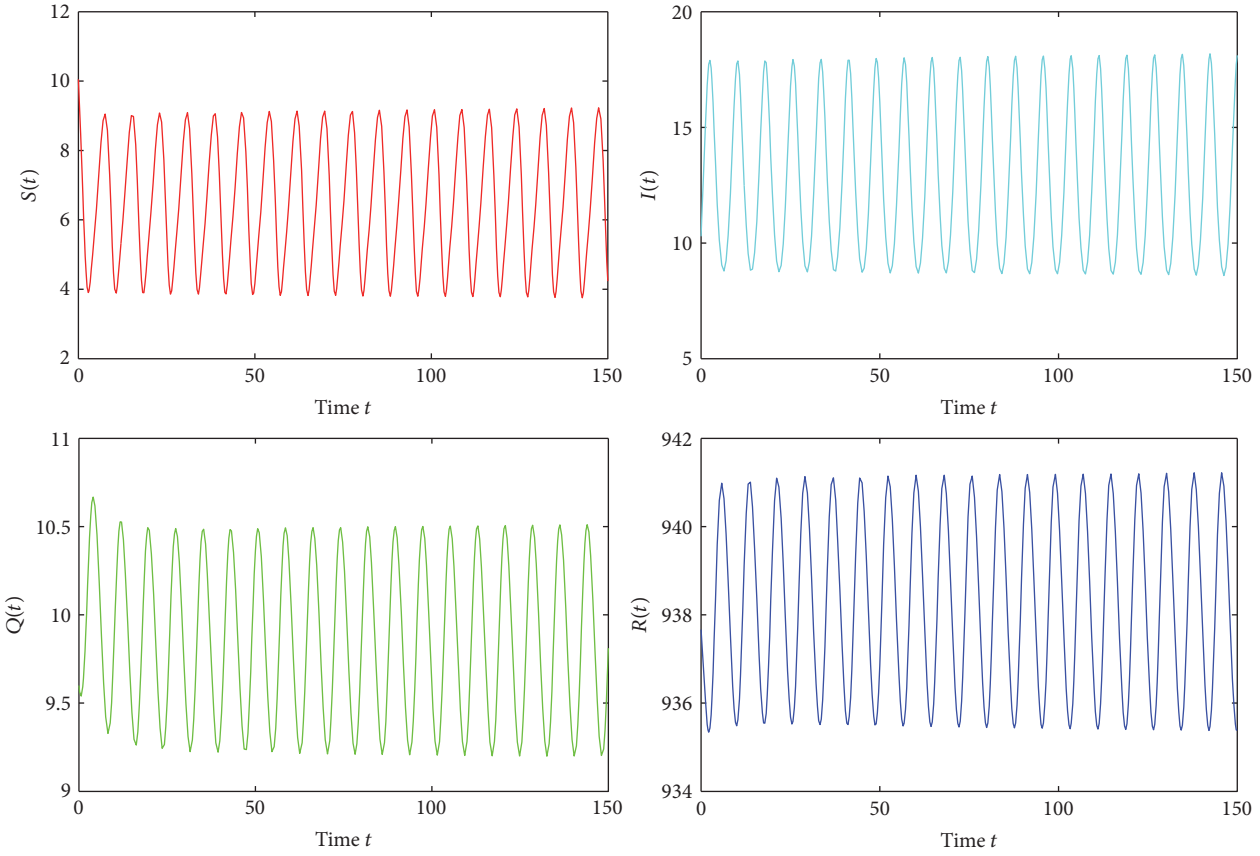

Figure 22: The trajectory of S, I, Q, and R when $\tau_2 = 1.52 > 1.3485 = \tau'_{20}$ and $\tau_1 = 0.65$.

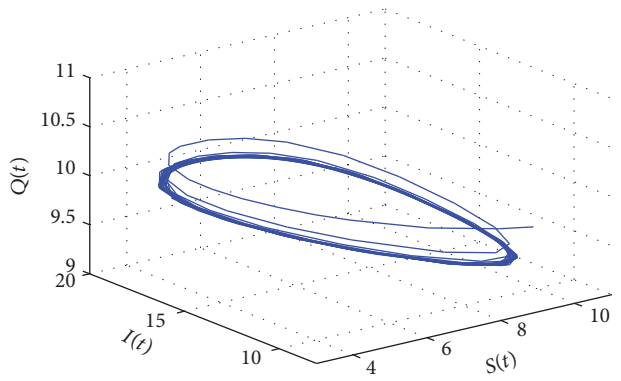

Figure 23: The phase plot of S, I, and Q when $\tau_2 = 1.52 > 1.3485 = \tau'_{20}$ and $\tau_1 = 0.65$.

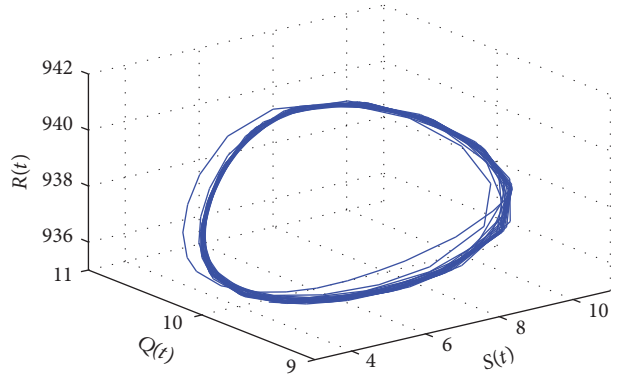

Figure 24: The phase plot of S, Q, and R when $\tau_2 = 1.52 > 1.3485 = \tau'_{20}$ and $\tau_1 = 0.65$.

the system in this paper is more general because it accounts for not only the time delay due to the latent period of the computer virus but also the time delay due to the period that the antivirus software uses to clean the computer viruses in the infectious and the quarantined nodes. The sufficient conditions for the stability of the positive equilibrium and existence of the Hopf bifurcation for the possible combinations of two delays are obtained. When the conditions are satisfied, then there exists a critical value of the delay below which system (2) is locally asymptotically stable and above which system (2) is unstable. The direction and the stability of the bifurcating periodic solutions are determined by applying the normal theory and the center manifold theorem. Numerical simulations show that the computer viruses may be controlled by shortening the time delay due to the latent period of the computer viruses and the time delay due to the period that the antivirus software uses to clean the computer viruses in the infectious and the quarantined nodes.

However, it should be pointed out that we suppose that the recovered computers have a permanent immunization period and they can no longer be infected. This is not consistent with real situation. In order to overcome this limitation and considering that the recovered computers may be infected again after a temporary immunity period, it is definitely an interesting work to investigate the following more general SIQRS model with multiple delays:

$$\begin{aligned}
\frac{dS(t)}{dt} &= (1-p)\,b - \beta S(t-\tau_1)\,I(t-\tau_1) - dS(t) \\
&\quad + \sigma R(t-\tau_3), \\
\frac{dI(t)}{dt} &= \beta S(t-\tau_1)\,I(t-\tau_1) - (\delta + d + \alpha_1)\,I(t) \\
&\quad - \gamma I(t-\tau_2), \\
\frac{dQ(t)}{dt} &= \delta I(t) - (d+\alpha_2)\,Q(t) - \varepsilon Q(t-\tau_2), \\
\frac{dR(t)}{dt} &= \gamma I(t-\tau_2) + pb + \varepsilon Q(t-\tau_2) - dR(t) \\
&\quad - \sigma R(t-\tau_3),
\end{aligned} \tag{67}$$

where σ is the transition rate from the recovered computers to the susceptible computers. τ_3 is the temporary immunity period after which a recovered computer may be infected again. We leave the analysis of the more complicated bifurcations of system (67) as the future work.

Further research directions include the possibility of linking the results obtained with the model proposed in the present paper with the results coming from the networks theory; see the recent review paper [17]. Specifically, the interest focuses on the possibility to gain a deep understanding of the impact of the network topology on the viral prevalence; see [18, 19]. In this context, the model proposed in this paper, which is a coarse-grained compartment-level model, can be considered as a network where all nodes are classified into a few compartments according to their states and whose degree distribution takes into account the rule of interactions proposed in the present paper.

Competing Interests

The authors declare that there are no competing interests regarding the publication of this paper.

Acknowledgments

This work was supported by Natural Science Foundation of the Higher Education Institutions of Anhui Province (KJ2015A144).

References

[1] J. R. C. Piqueira and V. O. Araujo, "A modified epidemiological model for computer viruses," *Applied Mathematics and Computation*, vol. 213, no. 2, pp. 355–360, 2009.

[2] J. G. Ren, X. F. Yang, Q. Y. Zhu, L.-X. Yang, and C. M. Zhang, "A novel computer virus model and its dynamics," *Nonlinear Analysis: Real World Applications*, vol. 13, no. 1, pp. 376–384, 2012.

[3] C. Gan, X. Yang, W. Liu, Q. Zhu, and X. Zhang, "Propagation of computer virus under human intervention: a dynamical model," *Discrete Dynamics in Nature and Society*, vol. 2012, Article ID 106950, 8 pages, 2012.

[4] C. Gan, X. Yang, and Q. Zhu, "Propagation of computer virus under the influences of infected external computers and removable storage media: modeling and analysis," *Nonlinear Dynamics*, vol. 78, no. 2, pp. 1349–1356, 2014.

[5] H. Yuan and G. Q. Chen, "Network virus-epidemic model with the point-to-group information propagation," *Applied Mathematics and Computation*, vol. 206, no. 1, pp. 357–367, 2008.

[6] H. Yuan, G. Chen, J. Wu, and H. Xiong, "Towards controlling virus propagation in information systems with point-to-group information sharing," *Decision Support Systems*, vol. 48, no. 1, pp. 57–68, 2009.

[7] M. Peng, X. He, J. Huang, and T. Dong, "Modeling computer virus and its dynamics," *Mathematical Problems in Engineering*, vol. 2013, Article ID 842614, 5 pages, 2013.

[8] B. K. Mishra and S. K. Pandey, "Dynamic model of worms with vertical transmission in computer network," *Applied Mathematics and Computation*, vol. 217, no. 21, pp. 8438–8446, 2011.

[9] B. K. Mishra and N. Jha, "SEIQRS model for the transmission of malicious objects in computer network," *Applied Mathematical Modelling*, vol. 34, no. 3, pp. 710–715, 2010.

[10] Y. Muroya, Y. Enatsu, and H. X. Li, "Global stability of a delayed SIRS computer virus propagation model," *International Journal of Computer Mathematics*, vol. 91, no. 3, pp. 347–367, 2014.

[11] J. Ren, X. Yang, L.-X. Yang, Y. Xu, and F. Yang, "A delayed computer virus propagation model and its dynamics," *Chaos, Solitons & Fractals*, vol. 45, no. 1, pp. 74–79, 2012.

[12] L. P. Feng, X. F. Liao, H. Q. Li, and Q. Han, "Hopf bifurcation analysis of a delayed viral infection model in computer networks," *Mathematical and Computer Modelling*, vol. 56, no. 7-8, pp. 167–179, 2012.

[13] T. Dong, X. Liao, and H. Li, "Stability and Hopf bifurcation in a computer virus model with multistate antivirus," *Abstract and Applied Analysis*, vol. 2012, Article ID 841987, 16 pages, 2012.

[14] Z. Z. Zhang and H. Z. Yang, "Hopf bifurcation of an SIQR computer virus model with time delay," *Discrete Dynamics in Nature and Society*, vol. 2015, Article ID 101874, 8 pages, 2015.

[15] B. D. Hassard, N. D. Kazarinoff, and Y. H. Wan, *Theory and applications of Hopf bifurcation*, vol. 41, Cambridge University Press, Cambridge, Uk, 1981.

[16] M. Ferrara, L. Guerrini, and G. M. Bisci, "Center manifold reduction and perturbation method in a delayed model with a mound-shaped Cobb-Douglas production function," *Abstract and Applied Analysis*, vol. 2013, Article ID 738460, 6 pages, 2013.

[17] R. Pastor-Satorras, C. Castellano, P. Van Mieghem, and A. Vespignani, "Epidemic processes in complex networks," *Reviews of Modern Physics*, vol. 87, no. 3, pp. 925–979, 2015.

[18] L.-X. Yang, M. Draief, and X. Yang, "The impact of the network topology on the viral prevalence: a node-based approach," *PLoS ONE*, vol. 10, no. 7, article e0134507, 2015.

[19] L. X. Yang, M. Draief, and X. Yang, "Heterogeneous virus propagation in networks: a theoretical study," *Mathematical Methods in the Applied Sciences*, 2016.

Hindawi Publishing Corporation
Discrete Dynamics in Nature and Society
Volume 2016, Article ID 6891302, 4 pages
http://dx.doi.org/10.1155/2016/6891302

Research Article

A Note on Discrete Multitime Recurrences of Samuelson-Hicks Type

Bruno Antonio Pansera[1,2] and Francesco Strati[1,2,3]

[1]*Department of Law and Economics, University Mediterranea of Reggio Calabria, Reggio Calabria, Italy*
[2]*Decisions Lab, University Mediterranea of Reggio Calabria, Reggio Calabria, Italy*
[3]*Department of Economics and Statistics, University of Siena, Siena, Italy*

Correspondence should be addressed to Francesco Strati; francesco.strati@unisi.it

Received 11 August 2016; Accepted 5 October 2016

Academic Editor: Gafurjan Ibragimov

Copyright © 2016 B. A. Pansera and F. Strati. This is an open access article distributed under the Creative Commons Attribution License, which permits unrestricted use, distribution, and reproduction in any medium, provided the original work is properly cited.

By this work, we aim at fostering further research on the applications of multitime recurrences. In particular, we shall apply this method by generalizing the Samuelson-Hicks model so as to make the new concept of time that this method proposes clear. In particular, the multitime approach decomposes a point of time into a vector, taking into account how different coordinates of time referring to the same date can affect the dynamics of a model.

1. Introduction

This work belongs to a series of papers (see [1–4]) which explore the notion of *multitime* in different branches of mathematical analysis, such as economics and physics. Since 1932, the adjective *multitime*, introduced by Paul Dirac, appears so as to cope with an environment in which there might be more than one dimension of time.

We make some considerations concerning the physical idea of the multitime notion: we recall that a *coordinate space* is an index numbering degrees of freedom, and the coordinate of time is the usual physical time in which a system evolves. This model is satisfactory, unless we turn our attention to relativistic problems. Moreover, some physical phenomena (and social sciences too) are observed in a two-time environment $t = (t^1, t^2)$, in which t^1 is the *intrinsic time* and t^2 is the *observer time*. In some real phenomena, there is no reason to prefer one coordinate to another. Following these assumptions, we refer to multitime as *vector parameters of evolution* in *multitime geometric evolution* and *multitime optimal control problems*.

The second relevant aspect to analyze is the multitime wave functions considered by Paul Dirac in 1932 via m-time evolution equations $ih(\partial\psi/\partial t^\alpha) = H_\alpha\psi$. The Dirac PDEs system is consistent (completely integrable) if and only if $[H_\alpha, H_\beta] = 0$ for $\alpha \neq \beta$. The consistency condition is easy to achieve for noninteracting particles, while it turns out to be harder in the presence of interactions. All of these laws cannot be applied to relevant problems, if one aims at a plain covariant formulation of relativistic quantum mechanics.

Eventually, following the literature, we can divide the laws of evolution of physical theories into two branches: the *single-time evolution laws* (ODEs) and the *multitime evolution laws* (PDEs). It is clear that, in order to turn a single-time evolution into a multitime evolution, changing the ODEs into PDEs is enough by accepting that time t is C^∞ function of certain parameters; let us say that $t = t(s^1, \ldots, s^m)$.

Many authors studied the different applications of these notions: we recall some significative papers as [4–10] in which the PDEs constraints usually show significant challenges for optimization principles. The multivariable maximum principle was studied in the presence of PDE constraints (see [1]).

The multivariate recurrences are based on multiple sequences; they come from areas like analysis of algorithms, computational biology, information theory, queueing theory, filters theory, statistical physics, and so forth. We consider a lattice of points with positive integer coordinates in $\mathbb{R}^n$. A

multivariate recurrence is a set of rules which transfer a point to another, together with initial conditions, which is capable of covering the hole lattice.

A multivariate recurrence relation is an equation that recursively defines a multivariate sequence, once one or more initial terms are given: each further term of the sequence is defined as a function of the preceding terms. Some defined recurrence relations can have very complex (chaotic) behaviors, and they are part of a field of mathematics known as nonlinear analysis.

We shall extend the *Floquet theory* which had been firstly utilized for periodic linear ODEs [11] and then extended to difference equations [12–15]. In [3, 16], the authors have extended this theory to the multitemporal first-order PDEs. In Floquet theory, it is necessary to find the associated monodromy matrix and its eigenvalues (called Floquet multipliers) in order to pass from a constant coefficient state to a periodic one. It can be crucial in a recurrence formulation (as noted in [14]) in which time-independent coefficients are unrealistic. An application of the Floquet theory can be found in [14]; here, we shall discuss a further possible extension. In this case, there is a generalization of the periodicity to a *sheet of time* rather than a point of time approach. In few words, it can be stated that, by a multitime approach, a point of time opens up to a vector of multiple times at that date (see Figure 1).

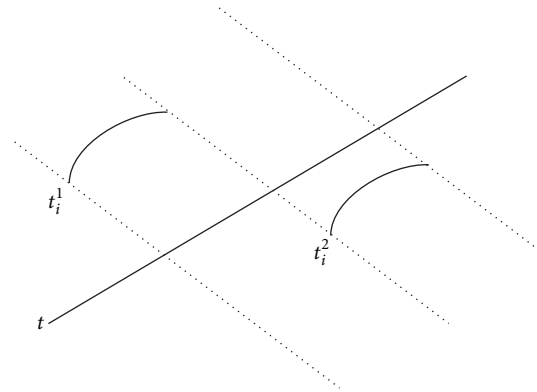

Figure 1: An example of multitime sheet.

2. The Model

2.1. A Hint on the Samuelson-Hicks Model. The standard Samuelson-Hicks model has been made of two crucial components: γ, the propensity to consume, for which amount $C_t = \gamma Y_{t-1}$ is consumed, in which Y_{t-1} is the income at $t-1$, and the rest is saved. The second component is that productive capital needs to aggregate production in fixed proportion α: $K_t = \alpha Y_{t-1}$. Defining the investment as a change in capital stock $I_t = K_t - K_{t-1}$, then $I_t = \alpha(Y_{t-1} - Y_{t-2})$, that is, the standard principle of acceleration. Furthermore, since $Y_t = C_t + I_t$, then a single recurrence equation in income is

$$Y_t = (\alpha + \gamma) Y_{t-1} - \alpha Y_{t-2}. \tag{1}$$

In [17], Samuelson applied the accelerator to consumption only, while, in [18], Hicks described its application to all expenditures including floors to depreciation levels and ceilings to incomes growth.

The equations of the model encompass autonomous factors $\overline{C}$ (consumption independent from income) and $\overline{I}$ (investment not dependent on business cycles): $C_t = \gamma Y_{t-1} + \overline{C}$ and $I_t = \alpha(Y_{t-1} - Y_{t-2}) + \overline{I}$. Notice that these autonomous components are crucial for the determination of the cycle. The *induced* investment depends on the change in output (on the cycle), while the autonomous part depends on technological progress, innovation, or population growth. If the autonomous investment increases at a regular rate, then the economy is in a progressive equilibrium.

A problem may arise: autonomous components grow at a constant rate, and α and γ do not depend upon the cycle and are assumed to be constant too. In [14], these constant factors become periodic and then they are *floquetized* in the sense of the following section (even if they, and we, detrended the model since growing autonomous investments have been removed). Moreover, we shall discuss a further generalization of the Floquet periodicity in which every period is decomposed into a vector of times rather than a simple point.

2.2. From Floquetizations to Multitime. Define element $t = (t^1, \ldots, t^m) \in \mathbb{N}^m$ as a *discrete multitime* and function $x : \mathbb{N}^m \to \mathbb{R}^n$ as a *multivariate sequence*. Moreover, denote $\mu(t) = \min\{t^1, \ldots, t^m\}$ and $\mathbf{1} = (1, \ldots, 1) \in \mathbb{N}^m$. It seems intuitive to see the discrete multitime as a series of vectors in which the time is not seen as a simple straight line in $\mathbb{R}$ and every time as a point on that line; with the multitime approach, every point of time is turned into a vector. In general, in economics, a model is defined in either discrete or continuous time: in the former case, it is usual to say that a generic event happens at $t = 1$ and spreads its effects at $t = 2$ and so forth. For a multitime approach, an event does not come into being at $t = i \in \mathbb{N}$ but at $t = t^i \equiv (t_1^i, t_2^i, t_3^i, \ldots, t_m^i)$; it can be thought of as a *sheet of time* instead of a *point* (see Figure 1). An event that occurred on a sheet of time t^1 spreads its effects on the subsequent sheet of time t^2 and so on.

Periodic coefficients are a proper generalization of constant ones, since the former take into account the periodical characteristic. This generalization can be applied to the Samuelson-Hicks model with constant coefficient and try to understand if generalizing it to a periodic coefficient model may be of some interest. This approach is called *floquetization*, in particular for coefficient h_t

$$h_{t+\theta} = z h_t; \tag{2}$$

then it can be defined as a *floquetian* of type (θ, z), in which when $z = 1$, it is nothing more than θ-periodicity. If $z \neq 1$, then floquetian coefficiencies are a straightforward generalization of the θ-periodic ones. The discrete multitime

periodic coefficient model is a further generalization to a multitime approach, where

$$h(t+\theta) = A(t)\,h(t), \tag{3}$$

$$h(t+\mathbf{1}) = A(t)\,h(t) \quad \text{with } \theta \equiv \mathbf{1}, \tag{4}$$

where, in case of $m \geqslant 2$, $A : \mathbb{N}^m \to \mathscr{M}_n(\mathbb{R})$. In general, for any $T \in \mathbb{N}$, the form

$$A(t + T\cdot\mathbf{1}) = A(t) \tag{5}$$

is called *T-diagonal periodic*.

2.3. Samuelson-Hicks Meets Multitime. The discrete multitime periodic coefficient Samuelson-Hicks model can be written as a first order diagonal recurrence system of the form of (4)

$$\begin{pmatrix} Y(t+\mathbf{1}) \\ C(t+\mathbf{1}) \end{pmatrix} = \begin{pmatrix} \gamma(t)+\alpha(t) & -\dfrac{\alpha(t)}{\gamma(t-\mathbf{1})} \\ \gamma(t) & 0 \end{pmatrix} \begin{pmatrix} Y(t) \\ C(t) \end{pmatrix}, \quad t \in \mathbb{N}^m \tag{6}$$

that satisfies the following conditions:

$$\begin{aligned} &Y(t)|_{t^\alpha=0} = Y_{0\alpha}\left(t^1,\ldots,\widehat{t^\alpha},\ldots,t^m\right), \\ &C(t)|_{t^\alpha=0} = C_{0\alpha}\left(t^1,\ldots,\widehat{t^\alpha},\ldots,t^m\right), \\ &Y_{0\alpha}\left(t^1,\ldots,\widehat{t^\alpha},\ldots,t^m\right)\Big|_{t^\beta=0} \\ &\quad = Y_{0\beta}\left(t^1,\ldots,\widehat{t^\beta},\ldots,t^m\right)\Big|_{t^\alpha=0}, \\ &C_{0\alpha}\left(t^1,\ldots,\widehat{t^\alpha},\ldots,t^m\right)\Big|_{t^\beta=0} \\ &\quad = C_{0\beta}\left(t^1,\ldots,\widehat{t^\beta},\ldots,t^m\right)\Big|_{t^\alpha=0}. \end{aligned} \tag{7}$$

The marginal propensity to consume $0 < \gamma < 1$; moreover, α can be defined as decelerator if $0 < \alpha < 1$, keeper if $\alpha = 1$, and accelerator if $\alpha > 1$. National income Y and its endogenous variable C (consumption) are assumed as strictly positive multitime sequences $Y(t)$ and $C(t)$. Notice that, in the original model, γ and α are constant factors. In [14], they have been used as (θ, z)-periodic parameters γ_t and α_t as the autonomous consumption $\overline{C}$ turned into C_t. This periodicity has been extended to (θ, A)-periodic parameters $\gamma(t)$, $\alpha(t)$, $Y(t)$, $C(t)$.

The model may be written as the second order homogeneous diagonal recurrence equation:

$$\begin{aligned} &Y(t+\mathbf{2}) - \left(\gamma(t+\mathbf{1}) + \alpha(t+\mathbf{1})\right) Y(t+\mathbf{1}) \\ &\quad + \alpha(t+\mathbf{1})\,Y(t) = 0, \quad t \in \mathbb{N}^m, \end{aligned} \tag{8}$$

satisfying the following conditions:

$$\begin{aligned} &Y(t+2) - (\gamma+\alpha)\,Y(t+1) + \alpha Y(t) = 0, \quad t \in \mathbb{N}^m, \\ &Y(t)|_{t^\alpha=0} = Y_{0\alpha}\left(t^1,\ldots,\widehat{t^\alpha},\ldots,t^m\right), \\ &Y(t)|_{t^\alpha=1} = Y_{1\alpha}\left(t^1,\ldots,\widehat{t^\alpha},\ldots,t^m\right), \\ &Y_{0\alpha}\left(t^1,\ldots,\widehat{t^\alpha},\ldots,t^m\right)\Big|_{t^\beta=0} \\ &\quad = Y_{0\beta}\left(t^1,\ldots,\widehat{t^\beta},\ldots,t^m\right)\Big|_{t^\alpha=0}, \\ &Y_{1\alpha}\left(t^1,\ldots,\widehat{t^\alpha},\ldots,t^m\right)\Big|_{t^\beta=1} \\ &\quad = Y_{1\beta}\left(t^1,\ldots,\widehat{t^\beta},\ldots,t^m\right)\Big|_{t^\alpha=1}, \\ &Y_{0\alpha}\left(t^1,\ldots,\widehat{t^\alpha},\ldots,t^m\right)\Big|_{t^\beta=1} \\ &\quad = Y_{1\beta}\left(t^1,\ldots,\widehat{t^\beta},\ldots,t^m\right)\Big|_{t^\alpha=0}. \end{aligned} \tag{9}$$

A prominent role is played by the so-called *Floquet multiplier* of (8), that is, first reconverting (8) into an equivalent diagonal recurrence system:

$$\begin{pmatrix} Y(t+\mathbf{1}) \\ Z(t+\mathbf{1}) \end{pmatrix} = \underbrace{\begin{pmatrix} 0 & 1 \\ -\alpha(t+\mathbf{1}) & \gamma(t+\mathbf{1})+\alpha(t+\mathbf{1}) \end{pmatrix}}_{=A(t+\mathbf{1})} \begin{pmatrix} Y(t) \\ Z(t) \end{pmatrix}, \quad t \in \mathbb{N}^m, \tag{10}$$

where $A(t+\mathbf{1})$ is T-periodic matrix. Then, find the *Floquet multiplier*, which is an eigenvalue of the matrix:

$$C(t) = \prod_{k=0}^{T-1} A\left(t + \left(T - k - \mu(t)\cdot\mathbf{1}\right)\right), \tag{11}$$

that is called the *monodromy matrix*. It is a 2×2 matrix with determinant

$$\begin{aligned} \det C(t) = {} & \alpha\left(t + \left(T - \mu(t)\right)\cdot\mathbf{1}\right) \times \cdots \\ & \times \alpha\left(t + \left(1 - \mu(t)\right)\cdot\mathbf{1}\right). \end{aligned} \tag{12}$$

Thus, the multipliers are the roots of the quadratic equation:

$$z^2 - z\,(\operatorname{Tr} C) + \det C = 0 \tag{13}$$

and these multipliers will depend on $t^1 - \mu(t), \ldots, t^m - \mu(t)$.

3. Discussion and Conclusions

The multiplier-accelerator model shows how cycles can occur in economics. The Floquet theory can be used to

generalize the constant coefficient framework of the standard Samuelson-Hicks model. By *floquetizing* this model, the behavior of the system around their constant value can be studied and thus it is possible to study the periodic cycle. This can happen by the use of the *monodromy matrix* which is the link between the coefficients and their periodic generalization. These kind of matrices study the behavior of a dynamic system around a singularity, in this case a constant coefficient.

It can be stated that each motion of national income Y is bounded in (8) if and only if this motion is bounded and $\alpha \leqslant 1$ in (12). For $\alpha > 1$, it is unbounded and, moreover, each motion of Y vanishes if $\alpha < 1$.

The *floquetized* Samuelson-Hicks model has been further generalized by taking into account a discrete multitime model generalizing the point of time to a *sheet* of time, as mentioned above. By a *sheet* of time, the dynamic system may be decomposed into different summable time vectors in which it is possible to study the effect of each coefficient separately. It can be possible to *explode* the model into different current times, like those paintings from the analytical cubism. It is important to apply the model so as to study recursively the effect of lagged coefficients to the subsequent ones, but the new effect which may become crucial is that in each sheet one can observe a decomposed model: on every time encompassed by a sheet, one can see how modifications of a coefficient affect the coefficients in the same current time *sheet* and so how this vector affects the model in the other sheet by understanding that model thoroughly.

Competing Interests

The authors declare that there are no competing interests regarding the publication of this paper.

Acknowledgments

The authors thank Massimiliano Ferrara for his invaluable advice and guidance. This research was partially supported by a grant of the Department of Law and Economics of the University Mediterranea of Reggio Calabria.

References

[1] C. Udrişte, "Multitime controllability, observability and bang-bang principle," *Journal of Optimization Theory and Applications*, vol. 139, no. 1, pp. 141–157, 2008.

[2] C. Udriste and M. Ferrara, "Multitime models of optimal growth," *WSEAS Transactions on Mathematics*, vol. 7, no. 1, pp. 51–55, 2008.

[3] C. Udrişte, M. Ferrara, and D. Opris, *Economic Geometric Dynamics*, vol. 6 of *Mono-Graphs and Textbooks*, Geometry Balkan Press, Bucharest, Romania, 2004.

[4] C. Udrişte, M. Ferrara, D. Zugrăvescu, and F. Munteanu, "Controllability of a nonholonomic macroeconomic system," *Journal of Optimization Theory and Applications*, vol. 154, no. 3, pp. 1036–1054, 2012.

[5] V. Barbu, I. Lasiecka, D. Tiba, and C. Varsan, "Analysis and optimization of differential systems, IFIP TC7/WG7.2," in *Proceedings of the International Working Conference on Analysis and Optimization of Differential Systems*, Kluwer Academic, Constanta, Romania, September 2002.

[6] G. Barles and A. Tourin, "Commutation properties of semigroups for first-order Hamilton-Jacobi equations and application to multi-time equations," *Indiana University Mathematics Journal*, vol. 50, no. 4, pp. 1523–1544, 2001.

[7] A. M. Bayen, R. L. Raffard, and C. J. Tomlin, "Adjoint-based constrained control of Eulerian transportation networks: application to air traffic control," in *Proceedings of the American Control Conference (AAC '04)*, pp. 5539–5545, Boston, Mass, USA, July 2004.

[8] F. Cardin and C. Viterbo, "Commuting Hamiltonians and Hamilton-Jacobi multi-time equations," *Duke Mathematical Journal*, vol. 144, no. 2, pp. 235–284, 2008.

[9] M. Motta and F. Rampazzo, "Nonsmooth multi-time Hamilton-Jacobi systems," *Indiana University Mathematics Journal*, vol. 55, no. 5, pp. 1573–1614, 2006.

[10] S. Pickenhain and M. Wagner, "Piecewise continuous controls in Dieudonné-Rashevsky type problems," *Journal of Optimization Theory and Applications*, vol. 127, no. 1, pp. 145–163, 2005.

[11] G. Floquet, "Sur les èquations diffèrentielles linèaires á coefficients pèriodiques," *Annales Scientifiques de l'École Normale Supérieure*, vol. 12, pp. 47–88, 1883.

[12] P. A. Kuchment, *Floquet Theory for Partial Differential Equations*, Birkhauser, 1993.

[13] N. G. Markley, *Principles of Differential Equations*, Pure and Applied Mathematics (New York), John Wiley & Sons, New York, NY, USA, 2004.

[14] P. V. Mouche and W. Heijman, *Floquet Theory and Economic Dynamics (Extended version)*, Wageningen Economic Papers, Wageningen, The Netherlands, 1996.

[15] V. A. Yakubovich and V. M. Starzhinskii, *Linear Differential Equations with Periodic Coefficients*, vol. 1, John Wiley & Sons, New York, NY, USA, 1975.

[16] C. Udrişte, "Multitime floquet theory," *Atti della Accademia Peloritana dei Pericolanti—Classe di Scienze Fisiche, Matematiche e Naturali*, vol. 91, no. 2, article A5, 2013.

[17] P. A. Samuelson, "Interactions between the multiplier analysis and the principle of acceleration," *Review of Economic Statistics*, vol. 21, no. 2, pp. 75–78, 1939.

[18] J. R. Hicks, *A Contribution to the Theory of the Trade Cycle*, Oxford University Press, Oxford, UK, 1950.

Hindawi Publishing Corporation
Discrete Dynamics in Nature and Society
Volume 2016, Article ID 6987471, 5 pages
http://dx.doi.org/10.1155/2016/6987471

Research Article

Topological Entropy of One Type of Nonoriented Lorenz-Type Maps

Guo Feng

Basic Subject Department, Shandong Women's University, Jinan 250300, China

Correspondence should be addressed to Guo Feng; sdwugf@163.com

Received 16 June 2016; Accepted 29 September 2016

Academic Editor: Massimiliano Ferrara

Copyright © 2016 Guo Feng. This is an open access article distributed under the Creative Commons Attribution License, which permits unrestricted use, distribution, and reproduction in any medium, provided the original work is properly cited.

Constructing a Poincaré map is a method that is often used to study high-dimensional dynamical systems. In this paper, a geometric model of nonoriented Lorenz-type attractor is studied using this method, and its dynamical property is described. The topological entropy of one-dimensional nonoriented Lorenz-type maps is also computed in terms of their kneading sequences.

1. Introduction

The Lorenz attractor is usually divided into three types, which are called oriented, semioriented, and nonoriented Lorenz attractor, respectively, and the existence condition of Lorenz attractor of planar map is given in [1]. The oriented dynamical property is studied in detail in [2–4]. In this paper, the nonoriented situation is discussed. Lorenz system is approximated by the Shimizu-Morioka model ($\dot{x} = y$, $\dot{y} = x - ay - xz$, $\dot{z} = -bz + x^2$) when the parameter r is large. This model has nonoriented Lorenz attractors for certain parameters, (e.g., $a \approx 0.59$ and $b \approx 0.45$). The bifurcations and chaos of the model are discussed using numerical method in [5, 6]. In this paper, a geometric model of the type attractor is described, and a formula for computation of the topological entropy of one-dimensional nonoriented Lorenz maps is given.

2. A Geometric Model of the Nonoriented Lorenz-Type Attractors

The differential equation with a single parameter $\dot{X} = f(\mu, X)$, $X \in R^3$, is considered, and it is symmetric about z-axis. The butterfly homoclinic orbit exists when the parameter μ is zero and the equilibrium point is $O = (0, 0, 0)$. The eigenvalue of the linearization matrix at O satisfies $0 < c \leq a < b$. Through simple coordinate transformations, the equation can be reduced to

$$\begin{aligned} \dot{x} &= ax + P(\mu, x, y, z) \\ \dot{y} &= -by + Q(\mu, x, y, z) \\ \dot{z} &= -cz + R(\mu, x, y, z), \end{aligned} \tag{1}$$

where P, Q, and R are high-order items. In the neighborhood of O, the dynamical property of the equations can be described by its linear part. Due to the symmetry of the system, we only discuss the situation $x \geq 0$. The sections $\Sigma_0 : z = d$ and $\Sigma_1 : x = d$ (where $d > 0$) are taken near the equilibrium O. The sections are shown in Figure 1(a). The solution of the linear equations $\dot{x} = ax$, $\dot{y} = -by$, and $\dot{z} = -cz$ are $x = x_0 e^{at}$, $y = y_0 e^{-bt}$, and $z = de^{-ct}$ with the initial point (x_0, y_0, d) on Σ_0. The time of the flow with the initial point from Σ_0 to Σ_1 is $\tau = (1/a)\ln(d/x_0)$ with $d = x_0 e^{a\tau}$. Then the map $T_0 : \Sigma_0 \to \Sigma_1 T_0$ is defined by

$$\begin{aligned} y_1 &= y_0 e^{-b\tau} \\ z_1 &= de^{-c\tau}; \end{aligned} \tag{2}$$

that is,

$$\begin{aligned} y_1 &= y_0 x_0^{\gamma} d^{-\gamma} \\ z_1 &= x_0^{\gamma} d^{1-\gamma}, \end{aligned} \tag{3}$$

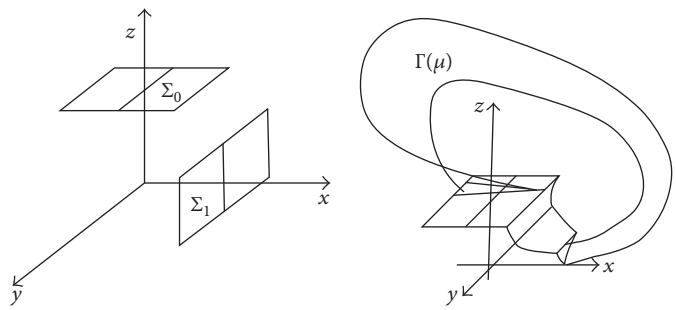

(a) (b)

Figure 1: Poincaré map of the Lorenz.

where $\nu = c/a$ is called the saddle point index and $\gamma = b/a$. Let $\Gamma(0)$ be the homoclinic orbit of the unperturbed system (when $\mu = 0$), and let $\Gamma(\mu)$ be its perturbed solution; see Figure 1(b). Then the flows adjacent $\Gamma(\mu)$ determine a map $T_1 : \Sigma_1 \to \Sigma_0$. In the small neighborhood of the origin M on Σ_1, the map $T_1 : \Sigma_1 \to \Sigma_0$ can be written as

$$\begin{aligned} \overline{x}_0 &= \mu + a_{11} z_1 + a_{12} y_1 + \cdots \\ \overline{y}_0 &= u(\mu) + a_{21} z_1 + a_{22} y_1 + \cdots . \end{aligned} \tag{4}$$

When the determinant of a matrix $\left(\begin{smallmatrix} a_{11} & a_{12} \\ a_{21} & a_{22} \end{smallmatrix}\right)$ is less than zero, the manifold by the map T_1 defined is nonoriented. μ is a splitting parameter, and the coordinate of $M_0(\mu) = \Gamma(\mu) \cap \Sigma_0$ is $(\mu, u(\mu))$. The map $T = T_1 \circ T_0$ is obtained on Σ_0:

$$\begin{aligned} \overline{x}_0 &= \mu + a_{11} d^{1-\nu} x_0^{\nu} + a_{12} d^{-\gamma} y_0 x_0^{\gamma} + \cdots \\ \overline{y}_0 &= u(\mu) + a_{21} d^{1-\nu} x_0^{\nu} + a_{22} d^{-\gamma} y_0 x_0^{\gamma} + \cdots . \end{aligned} \tag{5}$$

Let $d = 1$ by scaling variable, and remove the under index zero. Thus, we can obtain

$$\begin{aligned} \overline{x} &= \mu + A x^{\nu} + a_{12} y x^{\gamma} + \cdots \\ \overline{y} &= u(\mu) + a_{21} x^{\nu} + a_{22} y x^{\gamma} + \cdots , \end{aligned} \tag{6}$$

where $A = a_{11}$ is called the boundary line. This paper discusses the nonoriented Lorenz-type map corresponding to the situation $A < 0$ and $\mu > 0$, and let a_{12}, a_{21}, and a_{22} be all greater than zero.

Because the system is symmetric, we consider the case of $x \le 0$ and obtain the map

$$\begin{aligned} \overline{x} &= \left(\mu + A|x|^{\nu} + a_{12} y |x|^{\gamma} + \cdots\right) \operatorname{sign}(x) \\ \overline{y} &= \left(u(\mu) + a_{21}|x|^{\nu} + a_{22} y |x|^{\gamma} + \cdots\right) \operatorname{sign}(x) . \end{aligned} \tag{7}$$

Considering the truncated map,

$$\begin{aligned} \overline{x} &= \left(\mu + A|x|^{\nu}\right) \operatorname{sign}(x) \\ \overline{y} &= \left(u(\mu) + a_{21}|x|^{\nu} + a_{22} y |x|^{\gamma}\right) \operatorname{sign}(x) . \end{aligned} \tag{8}$$

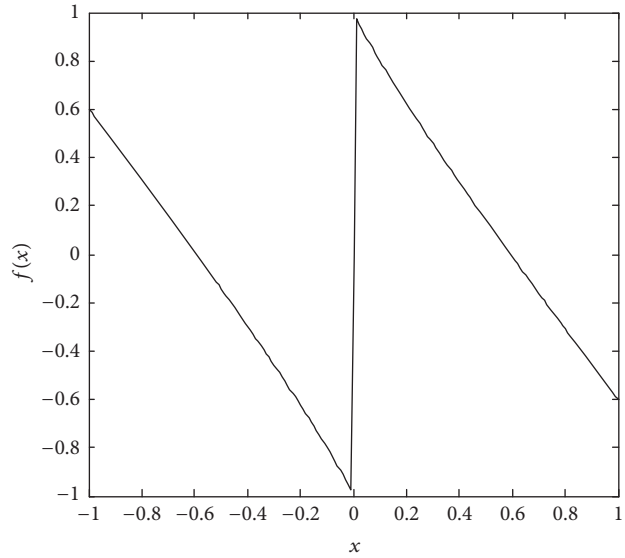

Figure 2: Graph of $f(x)$ while $\mu = 1$, $A = -1.6$, and $\nu = 0.9$.

The above formula is the Lorenz Poincaré map as shown in Figure 1(b).

For simplicity, we write the above map as $(\overline{x}, \overline{y}) = F(x, y) = (f(x), g(x, y))$. Taking $\mu = 1$, $u(\mu) = 0.5$, and $U = (-1 \le x \le 1, -1 \le y \le 1)$ on Σ_0, as $|1 + A| < 1$, $|0.5 + a_{21} + a_{22}| < 1$. The graph of $f(x)$ is shown in Figure 2. The region U is the contraction region of the map $F(x, y)$ as shown in Figure 3.

It is similar to the condition of an existing strange attractor about oriented Lorenz map in [2]. When $|\partial f/\partial x| > \sqrt{2}$, $|\partial g/\partial y| < 1/2$; that is, $A\nu > \sqrt{2}$ and $a_{22}\gamma < 1/2$; the invariant set $\bigcap_{n \ge 0} T^n(U) = \Lambda$ is a nonoriented Lorenz attractor as shown in Figure 4. Obviously, if $\mu \le 1$, then $|\partial f/\partial x| > \sqrt{2}$ in the set $[-1, 1] \setminus \{0\}$.

Being similar to [2], the dynamical property of $T|_{\Lambda}$ can be described by the shift map of the inverse limit pace of the map $f|_I$. So it is very important to study the dynamic behavior of this kind of attractor by studying the one-dimensional map $f(x)$.

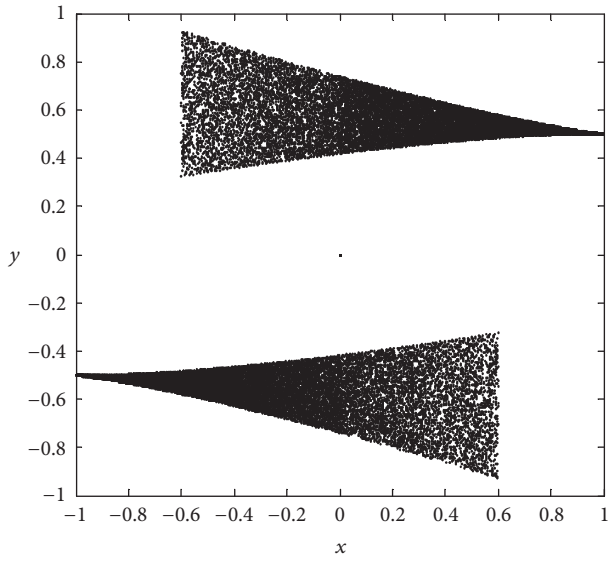

FIGURE 3: Graph of $F(U)$ while $\mu = 1$, $u(\mu) = 0.5$, $A = -1.6$, $\nu = 0.9$, $a_{21} = 0.1$, $a_{22} = 0.3$, and $\gamma = 1.2$.

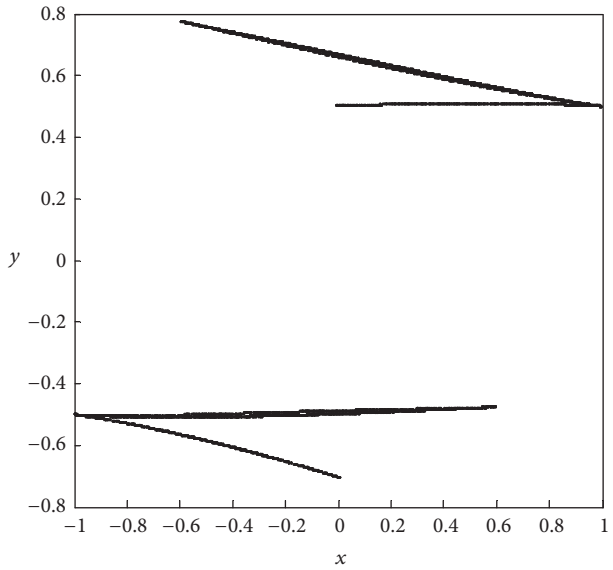

FIGURE 4: The strange attractor of $F(x, y)$ (the parameters are the same as Figure 3).

3. The Calculation of the Topological Entropy of Nonoriented Lorenz-Type Map

As $I = [-1, 1]$, if the map $f(x) : I \to I$ satisfies the condition where

(1) $[-1, 0)$ and $(0, 1]$ are continuous and monotone,

(2) $\lim_{x\to 0-} f(x) = -1$ and $\lim_{x\to 0+} f(x) = 1$, $f(0) = 0$,

(3) the set $D(f) = \bigcup_{n\geq 0} f^{-n}(0)$ is dense on the interval I,

then $f(x) : I \to I$ is called a nonoriented Lorenz-type map.

The topological entropy of one-dimensional Lorenz-type map is defined in [7].

$$h_f = \lim_{n\to\infty} \ln \frac{N_n}{n} = \lim_{n\to\infty} \ln \sqrt[n]{N_n}, \tag{9}$$

where N_n is the number of discontinuous points of $f^n(x)$. The definition in (9) is similar to the one about piecewise monotone continuous map given by de Melo and van Strien [8]. Here, the discontinuous points correspond to the critical points in [8]. This paper will calculate topological entropy of the map f. In order to facilitate the calculation, for a sequence $N_1, N_2, N_3, \ldots$, we consider the power series

$$N(t) = N_1 + N_2 t + N_3 t^2 + \cdots, \tag{10}$$

where $t \in C$.

Lemma 1. *As $n \to \infty$, the sequence $\sqrt[n]{N_n} = \sqrt[n]{N(f^n)}$ is convergent.*

Proof. Firstly, we show that

$$N(g \circ f) \leq N(g) N(f), \tag{11}$$

where f and g are Lorenz-type maps; $N(f)$ is the number of discontinuous points of f. Because, in each interval on which f is continuous, the number of the discontinuous points of g is at most $N(g)$, the inequality $N(g \circ f) \leq N(g)N(f)$ holds. Let k be a fixed natural number; for $\forall n \in \mathbf{Z}$, $\exists p, q \in \mathbf{Z}$ such that $n = pk + q$, where $0 \leq q < k$. By the formula,

$$N(f^n) \leq \left(N\left(f^k\right)\right)^p N\left(f^q\right), \tag{12}$$

we have

$$\left(N\left(f^n\right)\right)^{1/n} \leq \left(N\left(f^k\right)\right)^{p/pk+q} N(f)^{p/pk+q}. \tag{13}$$

If $n \to \infty$, then $p \to \infty$, and q is bounded. Thus, we have $p/(pk + q) \to 1/k$ and $p/(pk + q) \to 0$. Therefore,

$$\lim_{n\to\infty} \sup\left(\left(N\left(f^n\right)\right)^{1/n}\right) \leq \left(N\left(f^k\right)\right)^{1/k}. \tag{14}$$

Since k is arbitrary,

$$\begin{aligned} \lim_{n\to\infty} \sup\left(\left(N\left(f^n\right)\right)^{1/n}\right) &\leq \inf\left(\left(N\left(f^k\right)\right)^{1/k}\right) \\ &\leq \lim_{k\to\infty} \inf\left(\left(N\left(f^k\right)\right)^{1/k}\right); \end{aligned} \tag{15}$$

we can prove the sequence $\sqrt[n]{N_n}$ is convergent.

Let $\widetilde{N}_n$ be the number of points which fall at the discontinuous points firstly when $f^n(x_0) = 0$ and $f^k(x_0) \neq 0$, $k = 0, 1, \ldots, n-1$. □

Lemma 2. $\lim_{n\to\infty} \sqrt[n]{\widetilde{N}_n} = \lim_{n\to\infty} \sqrt[n]{N_n}$.

Proof. It is clear that

$$\widehat{N}_n \le N_n \le n\widehat{N}_n \tag{16}$$

and that $\lim_{n\to\infty}\sqrt[n]{N_n}$ exists; this also holds for $\lim_{n\to\infty}\sqrt[n]{\widehat{N}_n}$. Besides, $\lim_{n\to\infty}\sqrt[n]{\widehat{N}_n} = \lim_{n\to\infty}\sqrt[n]{n\widehat{N}_n}$. Thus, we have $\lim_{n\to\infty}\sqrt[n]{\widehat{N}_n} = \lim_{n\to\infty}\sqrt[n]{N_n}$.

Let $\widehat{N}(t) = \widehat{N}_1 + \widehat{N}_2 t + \widehat{N}_3 t^2 + \cdots$ denote the power series associated with the sequence $N_1, N_2, N_3, \ldots$. By Lemma 2, the convergence radius of the series $1+t\widehat{N}(t)$ and $1+tN(t)$ is equal to $\lim_{n\to\infty} 1/\sqrt[n]{\widehat{N}_n} = \lim_{n\to\infty} 1/\sqrt[n]{N_n}$.

Now, we give the symbolic dynamics model of the one-dimensional nonoriented Lorenz maps. For $x \in I$, Let $\varphi(x) = \varphi_0\varphi_1\varphi_2\cdots$ denote its symbol sequence, where

$$\varphi_n = \begin{cases} -1 & f^n(x) < 0, \\ 0 & f^n(x) = 0, \\ 1 & f^n(x) > 0. \end{cases} \tag{17}$$

There is also a sequence $\varepsilon(x) = \varepsilon_0\varepsilon_1\varepsilon_2\cdots$, where

$$\varepsilon_n = \begin{cases} -1, & \text{if } f^n(x) \ne 0, \\ 0, & \text{if } f^n(x) = 0. \end{cases} \tag{18}$$

Thus, we can obtain a sequence

$$k(x) = k_0k_1k_2\cdots, \tag{19}$$

which is called the invariant coordinates of x, where

$$\begin{aligned} k_0 &= \varphi_0, \\ k_1 &= \varepsilon_0\varphi_1, \\ k_2 &= \varepsilon_0\varepsilon_1\varphi_2, \\ &\vdots \end{aligned} \tag{20}$$

Therefore, we obtain a map $k : I \to \Omega_3^+$, where Ω_3^+ is a one-sided symbol space associated with the symbols -1, 0, and 1. It is clear that $k(f(x)) = \sigma(k(x))$, where $\sigma : \Omega_3^+ \to \Omega_3^+$ is the shift map. The order of invariant coordinates is as follows: if $k_0 = k_0', \ldots, k_{n-1} = k_{n-1}', k_n < k_n'$, then $k < k'$. □

Lemma 3. *For $x, y \in I$, if $x < y$, then $k(x) \le k(y)$; that is, $k : I \to \Omega_3^+$ is a monotone increasing function on the interval I.*

Proof. If x and y lie in the left-hand side and right-hand side of the discontinuous point 0, respectively, then the conclusion is obvious. Suppose that $k_k(x) = k_k(y)$ for $k < n$. Let J be the interval $[x, y]$. Then there is $f^n(x) < f^n(y)$ or $f^n(x) > f^n(y)$ determined by increasing or decreasing of $f^n|_J$. When $k \le n$, J is a monotone interval of f^k. For $z \in J$, by the chain rule, $\operatorname{sign}(Df^n(z)) = \varepsilon_0\varepsilon_1\cdots\varepsilon_{n-1}$. If $\varepsilon_0\varepsilon_1\cdots\varepsilon_{n-1} > 0$, then $f^n(x) < f^n(y)$; that is, $\varphi_n(x) < \varphi_n(y)$.

If $\varepsilon_0\varepsilon_1\cdots\varepsilon_{n-1} < 0$, then $f^n(x) > f^n(y)$; that is, $\varphi_n(x) > \varphi_n(y)$. For both cases, we have

$$\begin{aligned} k_n(x) &= \varepsilon_0\varepsilon_1\cdots\varepsilon_{n-1}\varphi\left(f^n(x)\right) \\ &\le \varepsilon_0\varepsilon_1\cdots\varepsilon_{n-1}\varphi\left(f^n(y)\right) = k_n(y), \end{aligned} \tag{21}$$

when $\varphi_n(x) = \varphi_n(y) = 0$; the above equal signs hold. Obviously, if $x, y \in I \setminus D$, then $k(x) < k(y)$. Let $x+$ and $x-$ denote the left and right limit points of x, respectively. By Lemma 1, $k(x-)$ and $k(x+)$ exist. For discussion, the sequence of point x is signed by a power series in complex field; that is, $k(x,t) = k_0 + k_1t + k_2t^2 + \cdots$. □

Lemma 4. $k(1-,t) - k(-1+,t) = \sum_{x\in\operatorname{in}(I)}[k(x+,t) - k(x-,t)]$.

Proof. The function $k(x,t) \bmod (t^n)$ is the series $k(x,t)$, which is to be truncated from t^n. For fixed t, $k(x,t) \bmod (t^n)$ is a step function with a finite number of discontinuous points; then the statement of the lemma follows.

We call $\alpha = k(0-) = \lim_{x\to 0-}k(x)$ and $\beta = k(0+) = \lim_{x\to 0+}k(x)$ the kneading sequences of the map f. The result of Lemma 4 can be simplified by kneading sequences. □

Theorem 5. $k(1-,t) - k(-1+,t) = \widehat{N}(t)[\beta(t) - \alpha(t)]$.

Proof. If $f^n(x_0) = 0$ and $f^k(x_0) \ne 0$, $k = 0, 1, \ldots, n-1$, then

$$\begin{aligned} k\left(x_0+,t\right) &= k\left(x_0,t\right) + t^n\beta(t), \\ k\left(x_0-,t\right) &= k\left(x_0,t\right) + t^n\alpha(t). \end{aligned} \tag{22}$$

Substituting the above two equations into Lemma 4, we can obtain

$$k(1-,t) - k(-1+,t) = \sum_{n=0}^{\infty}\widehat{N}_n t^n\left[\beta(t) - \alpha(t)\right]. \tag{23}$$

For one-dimensional nonoriented Lorenz-type maps,

$$\begin{aligned} \sigma(\beta) &= k(1-), \\ \sigma(\alpha) &= k(-1+); \end{aligned} \tag{24}$$

that is,

$$\begin{aligned} \beta(t) &= 1 - k(1-,t)\,t, \\ \alpha(t) &= -1 - k(-1+,t)\,t. \end{aligned} \tag{25}$$

Substituting (24) and (25) into (23),

$$\left[\beta(t) - \alpha(t)\right]\left[1 + t\widehat{N}(t)\right] = 2. \tag{26}$$

Because the series $1 + t\widehat{N}(t)$ is absolutely convergent, when $|t| < \lim_{n\to\infty} 1/\sqrt[n]{\widehat{N}_n}$, the series $1 + t\widehat{N}(t)$ is an analytic function in convergent circle $|t| = \lim_{n\to\infty} 1/\sqrt[n]{\widehat{N}_n}$.

The series $1 + t\widehat{N}(t)$ has poles in convergent circle. The series of $1 + t\widehat{N}(t)$ is positive, so $|1 + t\widehat{N}(t)| \le 1 + |t|\widehat{N}(|t|)$ and the point $t_0 = \lim_{n\to\infty} 1/\sqrt[n]{\widehat{N}_n} = \lim_{n\to\infty} 1/\sqrt[n]{N_n}$ in

convergent circle is the pole of the series $1 + t\widehat{N}(t)$. By (26), t_0 is the minimum positive zero of the polynomial function $\beta(t) - \alpha(t)$; that is, t_0 is the minimum positive root of the model of the equation

$$\beta(t) - \alpha(t) = 0. \tag{27}$$

Substituting t_0 into (9), we obtain a formula of topological entropy of the map:

$$h_f = -\ln t_0. \tag{28}$$

□

Example 6. Calculate the topological entropy of the map:

$$g(x) = \begin{cases} 1 - \sqrt{2}x, & 0 < x \le 1 \\ -1 - \sqrt{2}x, & -1 \le x < 0. \end{cases} \tag{29}$$

$\beta = (1, -1, -1, 1, -1, 1, \ldots)$ is an eventually periodic sequence; then $\beta(t) = 1 - t - t^2/(1+t)$. By the symmetry of the map $g(x)$, we have $\alpha = -\beta$, Substituting the expressions of $\alpha(t)$ and $\beta(t)$ into (27), we obtain $2(1 - t - t^2/(1+t)) = 0$ and $t_0 = 1/\sqrt{2}$. Thus, $h_g = -\ln|t_0| = \ln\sqrt{2}$.

4. Conclusion

For the dynamic systems described by differential equations, the Lorenz Poincaré map is a mostly used method to study the structure of strange attractors of the systems. The dynamical behavior of the Lorenz-type attractor can be described by one-dimensional Lorenz-type map. The topological entropy of the Lorenz map can be calculated by using the symbol sequence of the boundary points of the invariant interval, and we can know the system is chaos or not.

Competing Interests

The author declares that there are no competing interests regarding the publication of this paper.

References

[1] V. S. Afraimovich, V. V. Bykov, and L. P. Shil'nikov, "On structurally unstable attracting limit sets of Lorenz attractor type," *Transactions of the Moscow Mathematical Society*, vol. 44, no. 2, pp. 153–216, 1982.

[2] J. Guckenheimer and R. Williams, "Structural stability of the Lorenz attractor," *Publ. Math. IEHS*, vol. 50, pp. 59–72, 1980.

[3] R. Williams, "The structure of Lorenz attractors," *Publications Mathématiques de l'IHÉS*, vol. 50, pp. 101–152, 1979.

[4] J. Guckenheimer, "A strange, strange attractor," in *Hopf Bifurcation and Its Applications*, pp. 368–381, Springer, Berlin, Germany, 1976.

[5] A. L. Shil'nikov, "On bifurcations of the Lorenz attractor in the Shimizu-Morioka model," *Physica D*, vol. 62, no. 1–4, pp. 338–346, 1993.

[6] A. L. Shil'nikov, "Bifurcation and chaos in the Shimizu-Morioka model system," *Selecta Mathematica Sovietica*, vol. 10, no. 2, pp. 455–568, 1991.

[7] V. Afraimovich and S.-B. Hsu, *Lectures on Chaotic Dynamical Systems*, American Mathematical Society and International Press, 2003.

[8] W. de Melo and S. van Strien, *One-Dimensional Dynamics*, Springer, Berlin, Germany, 1993.

Hindawi Publishing Corporation
Discrete Dynamics in Nature and Society
Volume 2016, Article ID 1289456, 6 pages
http://dx.doi.org/10.1155/2016/1289456

Research Article

Linear Pursuit Differential Game under Phase Constraint on the State of Evader

Askar Rakhmanov,[1] Gafurjan Ibragimov,[2] and Massimiliano Ferrara[3,4]

[1]*Department of Informatics, Tashkent University of Information Technologies, TUIT, Amir Temur Str. 108, 100202 Tashkent, Uzbekistan*
[2]*Department of Mathematics & Institute for Mathematical Research, Universiti Putra Malaysia, Serdang, Malaysia*
[3]*Department of Law and Economics, University Mediterranea of Reggio Calabria, Reggio Calabria, Italy*
[4]*ICRIOS, Bocconi University, Milan, Italy*

Correspondence should be addressed to Massimiliano Ferrara; massimiliano.ferrara@unirc.it

Received 22 June 2016; Accepted 14 September 2016

Academic Editor: Rigoberto Medina

Copyright © 2016 Askar Rakhmanov et al. This is an open access article distributed under the Creative Commons Attribution License, which permits unrestricted use, distribution, and reproduction in any medium, provided the original work is properly cited.

We consider a linear pursuit differential game of one pursuer and one evader. Controls of the pursuer and evader are subjected to integral and geometric constraints, respectively. In addition, phase constraint is imposed on the state of evader, whereas pursuer moves throughout the space. We say that pursuit is completed, if inclusion $y(t_1) - x(t_1) \in M$ is satisfied at some $t_1 > 0$, where $x(t)$ and $y(t)$ are states of pursuer and evader, respectively, and M is terminal set. Conditions of completion of pursuit in the game from all initial points of players are obtained. Strategy of the pursuer is constructed so that the phase vector of the pursuer first is brought to a given set, and then pursuit is completed.

1. Introduction

Pursuit and evasion differential game problems under different type of constraints on controls of players were studied by many researchers, for example, [1–24]. In [11, 16], main approaches of solution of pursuit and evasion differential games were given and fundamental results were obtained. In [2–5, 7, 10, 13, 15, 17–19, 22, 24], various pursuit and evasion differential game problems were investigated under phase constraints. Sufficient conditions of completion of pursuit were obtained in [4, 5, 19], when controls of both players are subjected to geometric constraints [19] or integral constraints [4], and phase constraint is being imposed on the state of the evader. The objectives of the researches [8, 9, 12] are to find value of the game and construct optimal strategies of players. The paper [5] is devoted to discrete pursuit games with phase constraints.

The present paper is continuation of [4, 5, 19] and deals with the linear pursuit differential games where pursuit control is subjected to integral constraints and evasion control is subjected to geometric constraint, with phase constraint being imposed on the state of the evader. For such constraints on controls of players, to obtain solution of pursuit problem for all initial states of phase space is complicated because of boundedness of pursuit resources.

In the present paper, the following technique is proposed to control the phase vector of the pursuer: first-phase vector of the pursuer is brought to a given bounded, convex set, regardless of the behavior of evading player and then, using the evasion control and initial positions of the players, the pursuit control that ensures the completion of pursuit is constructed.

New sufficient conditions of completion of pursuit from all initial positions for a finite time have been obtained and results have been illustrated on a model example. This paper is closely related to [4, 5, 19, 20, 23].

2. Statement of Problem

Consider a linear differential game of one pursuer and one evader described by

$$\begin{aligned} \dot{x} &= Ax + u, \\ \dot{y} &= By + v, \end{aligned} \tag{1}$$

where $x, y \in R^n$ are state vectors of pursuer and evader, respectively, A, B are $n \times n$ matrices, and $u, v \in R^n$ are control parameters of pursuer and evader, respectively.

The terminal set has the form $M = M_0 + M_1$, where M_0 is a linear subspace of R^n and M_1 is a subset of L, which is orthogonal complement of M_0 to R^n. It is assumed that relative interior of M_0 with respect to L is not empty. Pursuer moves throughout the space, but evader is subjected to state constraint and it moves only within given bounded convex set D.

Definition 1. Measurable functions $u = u(t)$ and $v = v(t)$, $t \geq 0$, that satisfy constraints

$$\int_0^\infty |u(t)|^2 \, dt \leq \rho^2, \qquad v \in Q \subset R^n, \tag{2}$$

are called admissible controls of pursuer and evader, respectively, where $\rho > 0$ is a given number and Q is a compact subset of R^n.

Definition 2. One says that pursuit can be completed from initial points $x_0, y_0 \in R^n$, $y_0 \in D$, $y_0 - x_0 \notin M$, for time t_1; if, for any admissible control of evader $v = v(t)$, $0 \leq t \leq t_1$, one can construct an admissible control of pursuer $u = u(t)$, $0 \leq t \leq t_1$, such that, for solutions $x(t)$, $y(t)$, $0 \leq t \leq t_1$, of initial value problems,

$$\dot{x} = Ax + u(t), \quad x(0) = x_0, \qquad \dot{y} = By + v(t), \quad y(0) = y_0. \tag{3}$$

Inclusion $y(t_1) - x(t_1) \in M$ is satisfied and $y(t) \in D$ for all $0 \leq t \leq t_1$. It is assumed that, to construct pursuit control $u(t)$, it is allowed to use values $v(t)$, $x(t)$, $y(t)$ at any time $t \geq 0$.

As it is known, if $u = u(t)$ and $v = v(t)$, $t \geq 0$, are any admissible controls of players, then, for the initial value problems (3), we have

$$x(t) = \Psi(t) x_0 + \int_0^t \Psi(t-\tau) u(\tau) \, d\tau, \qquad y(t) = \Phi(t) y_0 + \int_0^t \Phi(t-\tau) v(\tau) \, d\tau, \tag{4}$$

where $\Psi(t) = \exp(At)$, $\Phi(t) = \exp(Bt)$, $t \geq 0$.

Problem 3. Find conditions of completion of pursuit in game (1)-(2) from all initial points of players.

3. Main Result

Let π denote the operator of orthogonal projection of R^n onto L. Since $\operatorname{int} M_1 \neq \emptyset$, set D is convex and bounded, Q is compact set, and then there exist numbers $\ell > 0, R > 0, \sigma > 0$, and vector $m \in M_1$, such that $D \subset RS \subset R^n$, $\ell S_1 \subset -m + M_1$, $Q \subset \sigma S$, where S and S_1 are closed unit balls of spaces R^n and L and centered at the origins of these spaces, respectively. It is clear that, in the case of $R \leq \ell$, solution of pursuit problem is straightforward, and, therefore, from now on, we assume that $R \gg \ell$.

Assumption 4. There exist numbers $d > 0, \ell_1, \ell_2 \geq 0, \ell_1 + \ell_2 = \ell$, $\alpha, 1 < \alpha \leq R/(R - \ell_2)$ and a linear measurable mapping $F(t, \tau) : R^n \to R^n$ in τ, $0 \leq \tau \leq t$, such that

(i) $\|F(t, \tau)\| \leq d, 0 \leq \tau \leq t$,

(ii) $(1/\alpha) \int_0^t [\pi\Phi(t-\tau) - \pi\Psi(t-\tau)F(t,\tau)] Q \, d\tau \subset \ell_1 S_1$.

Assumption 5. There exist continuous function $T : (0, \rho) \to [0, \infty)$ and number $\rho_1, 0 < \rho_1 < \rho$, such that

(i) $(\rho - \rho_1)^2 / T(\rho_1) > d^2\sigma^2/\alpha^2$,

(ii) for each pair of points (x_*, y), $y - x_* \notin M$, $y \in D$, $x_* \in D$, there is time $t = t(x_*, y) \leq T(\rho_1)$ for

$$-m + \frac{1}{\alpha}\pi\Phi(t) y - \pi\Psi(t) x_* \in \int_0^t \pi\Psi(t-\tau) \left(\frac{\rho_1}{\sqrt{t}} S \right) d\tau, \tag{5}$$

where $x_* \in D$ and this point can be, in particular, the center of the ball of minimal radius containing D.

It follows from Assumption 5(i) that there is number ε, $0 < \varepsilon < \rho - \rho_1$, such that

$$\frac{(\rho - \rho_1 - \varepsilon)^2}{T(\rho_1)} > \frac{d^2\sigma^2}{\alpha^2}. \tag{6}$$

Assumption 6. For any $x \in R^n$, there is finite number $r = r(x) > 0$ such that

$$-x_* + \Psi(r) x \in \int_0^r \Psi(r-\tau) \left(\sqrt{\frac{2\rho\varepsilon - \varepsilon^2}{r}} \right) S \, d\tau. \tag{7}$$

Theorem 7. *Let Assumptions 4–6 hold true. Then, pursuit can be completed in game (1)-(2) from all points (x_0, y_0), $y_0 - x_0 \notin M$, $y_0 \in D$, for a finite time.*

Proof. Let (x_0, y_0), $y_0 - x_0 \notin M$, $y_0 \in D$ be any point. Consider two cases: (i) $x_0 \in D$ and (ii) $x_0 \notin D$. Let $x_0 \in D$. According to Assumption 5(ii), for pair (x_0, y_0), $y_0 - x_0 \notin M$, $x_0 \in D$, specify time $t_1 = t_1(x_0, y_0) \leq T(\rho_1)$, satisfying

$$-m + \frac{1}{\alpha}\pi\Phi(t_1) y_0 - \pi\Psi(t_1) x_0 \in \int_0^{t_1} \pi\Psi(t_1 - \tau) \left(\frac{\rho_1}{\sqrt{t_1}} S \right) d\tau. \tag{8}$$

It follows from (8) that there exists measurable selection $w(t)$, $0 \leq t \leq t_1$, of multivalued mapping $\pi\Psi(t_1 - \tau)((\rho_1/\sqrt{t_1})S)$, $0 \leq \tau \leq t_1$, such that

$$-m + \frac{1}{\alpha}\pi\Phi(t_1) y_0 - \pi\Psi(t_1) x_0 = \int_0^{t_1} w(t) \, dt. \tag{9}$$

Now, we consider

$$w(t) = \pi\Psi(t_1 - t)\,\omega(t), \quad 0 \le t \le t_1, \tag{10}$$

with respect to unknown vector-function $\omega(t) \in (\rho_1/\sqrt{t_1})S$, $0 \le t \le t_1$. Then, we can apply Filippov's Lemma [6] on existence of measurable solution of (10).

Therefore,

$$\begin{aligned} &-m + \frac{1}{\alpha}\pi\Phi(t_1)\,y_0 - \pi\Psi(t_1)\,x_0 \\ &\quad = \int_0^{t_1} \pi\Psi(t_1 - t)\,\omega(t)\,dt, \end{aligned} \tag{11}$$

with respect to unknown vector-function $\omega(t) \in (\rho_1/\sqrt{t_1})S$, $0 \le t \le t_1$, has measurable solution $\omega = \omega_1^0(t)$, $0 \le t \le t_1$.

Next, assuming that $v = v(t)$, $0 \le t \le t_1$, is any admissible control of the evader, we construct pursuit control as follows:

$$u(t) = u_1(t) = \frac{1}{\alpha}F(t_1, t)\,v(t) + \omega_1^0(t), \quad 0 \le t \le t_1. \tag{12}$$

Then, using (4) yields

$$\begin{aligned} &\frac{1}{\alpha}\pi y(t_1) - \pi x(t_1) = \frac{1}{\alpha}\pi\Phi(t_1)\,y_0 - \pi\Psi(t_1)\,x_0 + \frac{1}{\alpha} \\ &\cdot \int_0^{t_1} \left[\pi\Phi(t_1 - \tau) - \pi\Psi(t_1 - \tau)\,F(t_1, \tau)\right] v(\tau)\,d\tau \\ &- \int_0^{t_1} \pi\Psi(t_1 - \tau)\,\omega_1^0(\tau)\,d\tau = \frac{1}{\alpha} \\ &\cdot \int_0^{t_1} \left[\pi\Phi(t_1 - \tau) - \pi\Psi(t_1 - \tau)\,F(t_1, \tau)\right] v(\tau)\,d\tau \\ &+ \frac{1}{\alpha}\pi\Phi(t_1)\,y_0 - \pi\Psi(t_1)\,x_0 \\ &- \int_0^{t_1} \pi\Psi(t_1 - \tau)\,\omega_1^0(\tau)\,d\tau. \end{aligned} \tag{13}$$

Next, adding vector $-m$ to both sides of (13) and then using Assumption 4(ii) and (12) yield

$$\begin{aligned} &-m + \frac{1}{\alpha}\pi y(t_1) - \pi x(t_1) = -m + \frac{1}{\alpha}\pi\Phi(t_1)\,y_0 \\ &- \pi\Psi(t_1)\,x_0 - \int_0^{t_1} \pi\Psi(t_1 - t)\,\omega_1^0(t)\,dt + \frac{1}{\alpha} \\ &\cdot \int_0^{t_1} \left[\pi\Phi(t_1 - \tau) - \pi\Psi(t_1 - \tau)\,F(t_1, \tau)\right] v(\tau)\,d\tau \\ &= \frac{1}{\alpha}\int_0^{t_1} \left[\pi\Phi(t_1 - t) - \pi\Psi(t_1 - t)\,F(t_1, t)\right] v(t)\,dt \\ &\in \frac{1}{\alpha}\int_0^{t_1} \left[\pi\Phi(t_1 - \tau) - \pi\Psi(t_1 - \tau)\,F(t_1, \tau)\right] Q\,d\tau \\ &\subset \ell_1 S_1. \end{aligned} \tag{14}$$

Therefore,

$$\left|-m + \frac{1}{\alpha}\pi y(t_1) - \pi x(t_1)\right| \le \ell_1. \tag{15}$$

Now, we use inclusion $y(T) \in D \subset RS$, inequality (15), and definition of numbers α, ℓ_1, ℓ_2 to obtain

$$\begin{aligned} &\left|-m + \pi y(t_1) - \pi x(t_1)\right| \\ &\quad = \left|\pi y(t_1) - \frac{1}{\alpha}\pi y(t_1) - m + \frac{1}{\alpha}\pi y(t_1) - \pi x(t_1)\right| \\ &\quad \le \frac{\alpha - 1}{\alpha}\left|\pi y(t_1)\right| + \left|-m + \frac{1}{\alpha}\pi y(t_1) - \pi x(t_1)\right| \\ &\quad \le \frac{\alpha - 1}{\alpha}R + \ell_1 \le \ell_2 + \ell_1 = \ell. \end{aligned} \tag{16}$$

Therefore,

$$\pi y(t_1) - \pi x(t_1) \in m + \ell S_1 \subset M_1, \tag{17}$$

which implies that

$$y(t_1) - x(t_1) \in M. \tag{18}$$

Thus, we have proven that, in case (i), game (1)-(2) is completed at time t_1.

Let us turn to case (ii). By Assumption 6, for point $x_0 \in R^n$, the following inclusion is satisfied at some time $r_1 = r_1(x_0) > 0$:

$$-x_* + \Psi(r_1)\,x_0 \in \int_0^{r_1} \Psi(r_1 - \tau)\left(\sqrt{\frac{2\rho\varepsilon - \varepsilon^2}{r_1}}\right) S\,d\tau. \tag{19}$$

Consider

$$-x_* + \Psi(r_1)\,x_0 = \int_0^{r_1} \Psi(r_1 - \tau)\,u(\tau)\,d\tau, \tag{20}$$

with respect to unknown vector-function $u(t) \in (\sqrt{(2\rho\varepsilon - \varepsilon^2)/r_1})S$, $0 \le t \le r_1$. Using Filippov's lemma [6], we obtain from inclusion (19) existence of measurable solution of (20). Denote it by $u_0(t)$, $0 \le t \le r_1$. Let $t = r_1$, $u(t) = -u_0(t)$, $0 \le t \le r_1$, in (3) and use (20) with $u(t) = u_0(t)$, $0 \le t \le r_1$, to obtain

$$\begin{aligned} x(r_1) &= x_* - x_* + \Psi(r_1)\,x_0 \\ &\quad - \int_0^{r_1} \Psi(r_1 - \tau)\,u_0(\tau)\,d\tau = x_* \in D. \end{aligned} \tag{21}$$

Now, take $t = r_1$ as the initial time and let $x_0 = x(r_1) = x_*$, $y_0 = y(r_1)$. Assume that $y_0 - x_0 \notin M$, since game (1)-(2) is completed at $t = r_1$. Then, conditions of case (i) are satisfied and the rest of the proof runs as before. It should be noted that, in case (ii), pursuit is completed at the time $r_1 + t_1$.

Next, we show admissibility of control (12). Indeed, using the Minkowski inequality gives

$$\begin{aligned} \int_0^{t_1} \left|u_1(t)\right|^2 dt &= \int_0^{t_1} \left|\frac{1}{\alpha}F(t_1, t)\,v(t) + \omega_1^0(t)\right|^2 dt \\ &\le \left[\left(\int_0^{t_1} \left|\frac{1}{\alpha}F(t_1, t)\,v(t)\right|^2 dt\right)^{1/2} \right. \\ &\quad \left. + \left(\int_0^{t_1} \left|\omega_1^0(t)\right|^2 dt\right)^{1/2}\right]^2. \end{aligned} \tag{22}$$

Then, by Assumptions 4(i) and 5, according to $\omega_1^0(t) \in (\rho_1/\sqrt{t_1})S$, $Q \subset \sigma S$, we have, in case (i), that

$$\begin{aligned}\int_0^{t_1} |u_1(t)|^2\, dt &\le \left[\frac{d\sigma}{\alpha}\sqrt{t_1} + \left(\frac{\rho_1}{t_1}\right)t_1\right]^2 \\ &\le \left[\frac{d\sigma}{\alpha}\sqrt{T(\rho_1)} + \rho_1\right]^2 \\ &< (\rho - \rho_1 + \rho_1)^2 = \rho^2,\end{aligned} \tag{23}$$

and, in case (ii),

$$\begin{aligned}\int_0^{t_1} |u_1(t)|^2\, dt &\le \left[\frac{d\sigma}{\alpha}\sqrt{t_1} + \left(\frac{\rho_1}{t_1}\right)t_1\right]^2 \\ &\le \left[\frac{d\sigma}{\alpha}\sqrt{T(\rho_1)} + \rho_1\right]^2 \\ &< (\rho - \varepsilon - \rho_1 + \rho_1)^2 = (\rho - \varepsilon)^2.\end{aligned} \tag{24}$$

Since, by construction $|u_0(t)| \le \sqrt{\varepsilon(2\rho - \varepsilon)/r_1}$, $0 \le t \le r_1$,

$$\begin{aligned}&\int_0^{r_1} |u_0(t)|^2\, dt \le \varepsilon(2\rho - \varepsilon), \\ &\int_0^{r_1+t_1} |u(t)|^2\, dt = \int_0^{r_1} |u_0(t)|^2\, dt + \int_{r_1}^{r_1+t_1} |u_1(t)|^2\, dt \\ &\qquad = \varepsilon(2\rho - \varepsilon) + (\rho - \varepsilon)^2 = \rho^2,\end{aligned} \tag{25}$$

which implies admissibility of pursuit control in case (ii). Theorem 7 has been proven. □

Assumption 8. There exist numbers $d_1 > 0$, α_1, $1 < \alpha_1 \le R/(R-\ell)$ and a linear measurable mapping $F_1(t,\tau) : R^n \to R^n$ in τ, $0 \le \tau \le t$, such that

(i) $\pi\Psi(t-\tau)F_1(t,\tau) = \pi\Phi(t-\tau)$, $0 \le \tau \le t$,

(ii) Assumptions 4(i) and 5 are satisfied at $\alpha = \alpha_1$, $d = d_1$.

Theorem 9. *Let Assumptions 6 and 8 hold true. Then, pursuit can be completed in game (1)-(2) from any point (x_0, y_0), $y_0 - x_0 \notin M$, $y_0 \in D$ for a finite time.*

Proof. Let (x_0, y_0), $y_0 - x_0 \notin M$, $y_0 \in D$ be an arbitrary point. As in the proof of Theorem 7, there are two cases: (i) $x_0 \in D$, and (ii) $x_0 \notin D$. Let $x_0 \in D$. Using Assumption 5(ii), we define time $t_2 = t_2(x_0, y_0) \le T(\rho_1)$ for point (x_0, y_0), $y_0 - x_0 \notin M$, that satisfies

$$\begin{aligned}&-m + \frac{1}{\alpha_1}\pi\Phi(t_2)\, y_0 - \pi\Psi(t_2)\, x_0 \\ &\quad \in \int_0^{t_2} \pi\Psi(t_2 - \tau)\left(\frac{\rho_1}{\sqrt{t_2}}S\right)d\tau.\end{aligned} \tag{26}$$

Consider

$$\begin{aligned}&-m + \frac{1}{\alpha_1}\pi\Phi(t_2)\, y_0 - \pi\Psi(t_2)\, x_0 \\ &\quad = \int_0^{t_2} \pi\Psi(t_2 - t)\,\omega(t)\, dt,\end{aligned} \tag{27}$$

with respect to unknown vector-function $\omega(t) \in (\rho_1/\sqrt{t_2})S$, $0 \le t \le t_2$. Using Filippov's lemma [6], we obtain from (26) that there exists a measurable solution of (27). Denote it by $\omega_2^0(t)$, $0 \le t \le t_2$.

Let $v = v(t)$, $0 \le t \le t_2$, be any admissible control of the evader. For each $t \in [0, t_2]$, we construct pursuit control as follows:

$$u(t) = u_2(t) = \frac{1}{\alpha_1}F(t_2, t)\, v(t) + \omega_2^0(t), \quad 0 \le t \le t_2. \tag{28}$$

Then, using Assumption 8(i) and the fact that $\omega_2^0(t)$, $0 \le t \le t_2$, is a solution of (27), we obtain, for solution (4) of initial value problem (3) at $t = t_2$,

$$\begin{aligned}&-m + \pi y(t_2) - \pi x(t_2) = -m + \pi\Phi(t_2)\, y_0 - \pi\Psi(t_2) \\ &\quad \cdot x_0 + \int_0^{t_2}\left(\pi\Phi(t_2 - t) - \frac{1}{\alpha_1}\pi\Psi(t_2 - t)\, F_1(t_2, t)\right) \\ &\quad \cdot v(t)\, dt - \int_0^{t_2} \pi\Psi(t_2 - t)\,\omega_2^0(t)\, dt = -m + \frac{1}{\alpha_1} \\ &\quad \cdot \pi\Phi(t_2)\, y_0 - \pi\Psi(t_2)\, x_0 + \left(1 - \frac{1}{\alpha_1}\right)\left[\pi\Phi(t_2)\, y_0\right. \\ &\quad \left. + \int_0^{t_2} \pi\Phi(t_2 - t)\, v(t)\, dt\right] - \int_0^{t_2} \Psi(t_2 - t)\,\omega_2^0(t)\, dt \\ &\quad = \left(1 - \frac{1}{\alpha_1}\right)\pi y(t_2).\end{aligned} \tag{29}$$

Since, by Assumption 8, $1 < \alpha_1 \le R/(R-\ell)$ and $y(t_2) \in D \subset RS$, (29) implies that

$$\begin{aligned}&-m + \pi y(t_2) - \pi x(t_2) = \left(1 - \frac{1}{\alpha_1}\right)\pi y(t_2) \\ &\quad \in \left(1 - \frac{1}{\alpha_1}\right) RS \subset \ell S.\end{aligned} \tag{30}$$

Hence,

$$\pi y(t_2) - \pi x(t_2) \in M_1. \tag{31}$$

Let us turn to case (ii). By Assumption 6, for any point $x_0 \in R^n$, there is time $r_2 = r_2(x_0) > 0$ such that inclusion (19) is satisfied at $r_1 = r_2$. The same reasoning as that in the proof of Theorem 7 applies to conclude that $x(r_2) = x_* \in D$. If now $t = r_2$ is taken as the initial time for the game and set $x_0 = x(r_2) = x_*$, $y_0 = y(r_2)$, then we arrive at case (i), and so there exists $t_2 > 0$ such that $\pi y(t_2) - \pi x(t_2) \in M_1$. Note that, in case (ii), in order to complete the game, the pursuer has to spend time $r_2 + t_2$.

Thus, it has been proven that control (28) guarantees completion of pursuit in game (1)-(2) at $r_2 + t_2$, which proves the theorem. □

Admissibility of pursuit control (28) can be obtained in much the same way as in the proof of Theorem 7.

From Theorems 7 and 9, one can easily obtain the following statements, respectively.

Corollary 10. *Let, for point* (x_0, y_0), $y_0 - x_0 \notin M$, $x_0, y_0 \in D$, *there exists time* $t_3 = t_3(x_0, y_0) > 0$ *such that Assumptions 4 and 5 are satisfied at* $t = t_3$, $x_* = x_0$, $y = y_0$. *Then, pursuit can be completed from point* (x_0, y_0) *at time* t_3.

Corollary 11. *Let, for point* (x_0, y_0), $y_0 - x_0 \notin M$, $x_0, y_0 \in D$, *there exists time* $t_4 = t_4(x_0, y_0) > 0$ *such that Assumption 8 is satisfied at* $t = t_4$, $x_* = x_0$, $y = y_0$. *Then, pursuit can be completed from point* (x_0, y_0) *at time* t_4.

Thus, Corollaries 10 and 11 enable us to draw conclusion that if the pursuer is in set D at the initial time, then completion of pursuit is guaranteed without Assumption 6.

Example 12. Consider a simple motion differential game:

$$\begin{aligned} \dot{x} &= u, \\ \dot{y} &= v, \end{aligned} \tag{32}$$

where $x, y, u, v \in R^n$, $n \geq 1$, pursuit control function is a measurable function subject to integral constraint:

$$\int_0^\infty |u(t)|^2 \, dt \leq \rho^2 \tag{33}$$

and evasion control function is a measurable function subject to geometric constraint:

$$|v| \leq \sigma. \tag{34}$$

A phase constraint is imposed to the state of the evader y

$$y \in RS \subset R^n. \tag{35}$$

Differential game (32)–(34) is considered completed if $y - x \in \ell S$, $\ell > 0$; that is, $M = \ell S \subset R^n$.

It is not difficult to verify that if

$$\rho > 2\sqrt{\sigma (R - \ell)}, \tag{36}$$

then, for game (32) with different type constraints (33)–(35), all the hypotheses of Assumptions 4–8 are satisfied. Therefore, Theorems 7 and 9 can be applied and they give the same result, namely, if inequality (36) is satisfied, then pursuit is completed in game (32) with constraints (33)–(35) from all initial points $y_0 - x_0 \notin M$, $y_0 \in RS$, for a finite time. Note that if there is not a state constraint for the evader, then pursuit can be completed in game (32)–(34) only from some points of the phase space.

4. Conclusion

We have proposed a technique to solve pursuit problem which consists of two steps: first-step state of the pursuer is brought to a given bounded convex set, regardless of the behavior of evading player and then, in the second step, pursuit is completed.

New sufficient conditions of completion of pursuit from all initial positions for a finite time have been obtained. Moreover, results have been illustrated on a model example.

Note that Assumptions 4, 5, and 8 depend on linear measurable function $F(t, \tau) : R^n \to R^n$ of τ, $0 \leq \tau \leq t$, to a considerable extent. Therefore, future investigations can be carried out towards the choice of this function to weaken Assumptions 4, 5, and 8.

Competing Interests

The authors declare that there are no competing interests regarding the publication of this paper.

References

[1] A. A. Azamov, A. Sh. Kuchkarov, and B. B. Samatov, "The relation between problems of pursuit, controllability and stability in the large in linear systems with different types of constraints," *Prikladnaya Matematika i Mekhanika*, vol. 71, no. 2, pp. 259–263, 2007.

[2] A. A. Azamov, "On the problem of kind for the simple motion game with restriction," *Serdika: Bulgarsko Matematichesko Spisanie*, vol. 12, pp. 38–43, 1986.

[3] A. A. Azamov, "On the evasion problem for a given curve," *Applied Mathematics and Mechanics*, no. 4, pp. 694–697, 1982.

[4] A. Raxmanov and G. Ibragimov, "Linear discrete pursuit game with phase constraints," *Scientific World Journal*, vol. 2014, Article ID 435103, 5 pages, 2014.

[5] A. Raxmonov and G. I. Ibragimov, "An approach for solving discrete game problems with total constraints on controls," *Abstract and Applied Analysis*, vol. 2014, Article ID 674651, 6 pages, 2014.

[6] A. F. Filippov, "On some problems of theory of optimal regulation," *Vestnik Moskovskogo Universiteta, Seriya Matematiki, Mekhaniki*, no. 2, pp. 25–32, 1959.

[7] G. I. Ibragimov, "A game problem on a closed convex set," *Siberian Advances in Mathematics*, vol. 12, no. 3, pp. 16–31, 2002.

[8] G. I. Ibragimov, "On the optimal pursuit game of several pursuers and one evader," *Prikladnaya Matematika i Mekhanika*, vol. 62, no. 2, pp. 199–205, 1998.

[9] G. I. Ibragimov, A. A. Azamov, and M. Khakestari, "Solution of a linear pursuit-evasion game with integral constraints," *ANZIAM Journal*, vol. 52, pp. E59–E75, 2010.

[10] R. P. Ivanov, "Simple pursuit-evasion on a compact convex set," *Doklady Akademii Nauk SSSR*, vol. 254, no. 6, pp. 1318–1321, 1980.

[11] N. N. Krasovskii, *Control of Dynamic Systems*, Nauka, Moscow, Russia, 1985.

[12] A. S. Kuchkarov, G. I. Ibragimov, and M. Khakestari, "On a linear differential game of optimal approach of many pursuers with one evader," *Journal of Dynamical and Control Systems*, vol. 19, no. 1, pp. 1–15, 2013.

[13] A. S. Kuchkarov, "On a differential game with integral and phase constraints," *Automation and Remote Control*, vol. 74, no. 1, pp. 12–25, 2013.

[14] M. S. Nikol'skii, "A direct method of solution of linear differential pursuit-evasion games," *Mathematical Notes of the Academy of Sciences of the USSR*, vol. 33, no. 6, pp. 455–458, 1983.

[15] A. H. Nishanov and A. T. Rakhmanov, "On a method of prosecution under state constraints on the state of the evader," *European Applied Sciences*, no. 6, pp. 48–51, 2013.

[16] L. S. Pontryagin, *Selected Works*, Nauka, Moscow, Russia, 1988.

[17] B. N. Pshenichnii, A. A. Chikrii, and J. S. Rappoport, "Pursuit by several controlled objects in the presence of phase constraints," *Doklady Akademii Nauk SSSR*, vol. 259, no. 4, pp. 138–141, 1981.

[18] L. A. Petrosyan, "On a family of differential games of survival in space," *Doklady Sciences of the USSR*, vol. 161, no. 1, pp. 52–54, 1965.

[19] A. T. Rakhmanov, "Linear pursuit differential game under phase constraint on the state of evader," in *Proceedings of the 7th International Conference on Priority Directions in Science and Technology in the* XX*I-th Century*, vol. 2, pp. 123–127, Tashkent, Uzbekistan, 2014.

[20] A. T. Rahmanov, "On a pursuit method in linear differential games with integral constraints on controls," *Differential Equations*, vol. 25, no. 5, pp. 785–790, 1989.

[21] N. Yu. Satimov, *Methods of Solution of Pursuit Problems in the Theory of Differential Games*, NUUz Press, Tashkent, Uzbekistan, 2003.

[22] B. T. Samatov, "The differential game with 'a survival zone' with different classes of admissible control functions," in *Game Theory and Applications*, vol. 13, pp. 143–150, Nova Science, Hauppauge, NY, USA, 2008.

[23] B. T. Samatov, "The pursuit-evasion problem under integral-geometric constraints on pursuer controls," *Automation and Remote Control*, vol. 74, no. 7, pp. 1072–1081, 2013.

[24] L. P. Yugay, "On differential games with constraints on phase state and controls of players," *Doklady Academy of Sciences of USSSR*, no. 4, pp. 5–6, 1977.

Hindawi Publishing Corporation
Discrete Dynamics in Nature and Society
Volume 2016, Article ID 4275372, 14 pages
http://dx.doi.org/10.1155/2016/4275372

Research Article

Dynamic Complexities in 2-Dimensional Discrete-Time Predator-Prey Systems with Allee Effect in the Prey

Jie Yan,[1,2] Chunli Li,[1] Xueli Chen,[1,2] and Lishun Ren[1]

[1]*Department of Mathematics and Statistics, Zhoukou Normal University, Zhoukou, Henan 466000, China*
[2]*Department of Mathematics and Statistics, Zhengzhou University, Zhengzhou, Henan 450001, China*

Correspondence should be addressed to Lishun Ren; 9236rls@sina.com

Received 6 June 2016; Accepted 18 July 2016

Academic Editor: Massimiliano Ferrara

Copyright © 2016 Jie Yan et al. This is an open access article distributed under the Creative Commons Attribution License, which permits unrestricted use, distribution, and reproduction in any medium, provided the original work is properly cited.

The Allee effect is incorporated into a predator-prey model with linear functional response. Compared with the predator-prey which only takes the crowding effect and predator partially dependent on prey into consideration, it is found that the Allee effect of the prey species would increase the extinction risk of both the prey and predator. Moreover, by using a center manifold theorem and bifurcation theory, it is shown that the model with Allee effect undergoes the flip bifurcation and Hopf bifurcation in the interior of R_+^2 with different Allee effect values. In the two bifurcations, we can come to the conclusion that different Allee effect will have different bifurcation value and the increasing of the Allee effect will increase the value of bifurcation, respectively.

1. Introduction

The predator-prey interaction is a topic of great interest for many ecologists and mathematics. Such interactions have motivated various models of phenotypic coevolution in prey-predator communities. Many researchers have studied the dynamical behavior of the predator-prey system in ecology and contributed to growth of continuous models for large size population [1–13]. Also, a number of researchers have established the discrete-time models which are more appropriate and provided more efficient results as compared to the continuous models for small size population.

In [14], the author has investigated the stability and bifurcation of discrete-time predator-prey system with crowding effect of predator where predator is partially dependent on prey, this can be described by the following system (3). By analyzing, the author got the following conclusion: the systems undergoes flip bifurcation and Hopf bifurcation at fixed points under specific conditions when δ varies in small neighborhood. And numerical simulations of the model display cascade of period-doubling bifurcation in orbits of periods 2, 4, 8, chaotic sets and stable window of period 9 orbit in case of flip bifurcation, and smooth invariant circles in case of Hopf bifurcation. In biology, it means that the predator coexists with prey at period-n orbits and smooth invariant circle.

Now, on the basis of previous systems, we make an improvement in it. We assume the prey with Allee effect and use center manifold theorem and bifurcation theory to study the system with Allee effect.

The concept of Allee effect originates from observations made by an American ecologist Allee in the 1930s [15]. In the 1930s, Allee found that factors affecting the growth rate of single group include the resources space constraints and density of the initial population density. When the initial density of the population is lower than a certain critical value, population will eventually become extinct because of the restriction of the conditions or other conditions of the population reproduction, which is called Allee effect. This effect is probably one of the most exciting concepts in ecology, a concept that has long been neglected but now has attracted renewed interest. The most usual continuous growth function considering Allee effect is expressed by [16–19]

$$\frac{dx}{dt} = rx\left(1 - \frac{x}{k}\right)(x - m), \tag{1}$$

where x denotes the population density; k denotes the carrying capacity; r denotes the intrinsic per capita growth

rate of the population. In (1), when $m > 0$, it is the strong Allee effect. when $-k < m \leq 0$, it is the weak Allee effect. Weak Allee effect growth function always remains positive, while in the strong Allee effect, there is a threshold population level m below which the growth is negative and the species will become extinct.

Other mathematical forms have been proposed to model the Allee effect [16, 20–23] and most of them are topologically equivalent [24]. For instance, in [25, 26] the following equation is proposed:

$$\frac{dx}{dt} = r\left(1 - \frac{x}{k} - \frac{n}{x+b}\right), \tag{2}$$

which has been called additive Allee effect; (2) allows the modelling of multiple Allee effect [20]. Here, n and b are Allee effect parameter.

In our paper, we consider the following system:

$$\begin{aligned} \dot{x}(t) &= ax\left(1 - \frac{x}{k}\right) - \frac{bxy}{x+l}, \\ \dot{y}(t) &= cy + \frac{mbxy}{x+l} - dy^2, \end{aligned} \tag{3}$$

where all the parameters are positive. $x(t)$ and $y(t)$ represent the densities of prey and predator population, respectively; a, b denote the intrinsic growth rate of prey and predator, respectively; c denotes the growth rate of predator due to alternative resources. Again, d denotes competition among individuals of predator species due to overcrowding; l denotes the half saturation constant; m denotes the conversion rate for predator; and k denotes carrying capacity of the prey in a particular habitat.

In this prey-predator system, due to the impact of their own breeding process or because of the prey itself, the prey population will have the Allee effect. By observing some signs, single species of plant and animal which are influenced by Allee effect are very wide. Many facts point out the fact that the prey of the growth rate with Allee effect will fall to very low but remain positive. So, Allee effect provides an important basis for the management of endangered species. Without the Allee effect, the evolution of the system is a sublimate situation, the time to reach the p point of the system is less than that of the system without Allee system which is not conducive to the evolution of biological, under the influence of the Allee effect, and the evolution of the system will reach a state of equilibrium. In our paper, it is shown that Allee effect of the prey species has a significant effect on the dynamics of the predator-prey system with linear functional response. Many studies have demonstrated the potential importance of Allee effect for dynamics of small population, range expansion, community composition, and biological invasion. It is widely accepted that Allee effect may increase the extinction risk of low density populations.

Because of the difficulties in finding mates when the prey population density becomes low, the Allee effect may occur in the prey species. So, in this paper, we consider the following Allee effect [27]. For example, this might correspond to the density below which it is so difficult to find a mate that reproduction does not compensate for mortality. Let $f(x)$ be the fertility of a species that has x adults in an isolated patch; then the fertility increases with the population density, which is described by

$$f(x) = \frac{ax}{A_1 + x}, \tag{4}$$

where a is the maximum per capita birth rate of the species, $x/(A_1 + x)$ is the per capita fertilization probability of the species, and A_1 is the Allee effect constant of the species. Here, if $A_1 > 0$, it is strong Allee effect; the fertility of the species will be therefore zero when x is zero and approaches to a when x becomes very large. Then, $f(x)$ increases with x, which depends on the parameter A_1. Biologically, A_1 is the population density at which a species reaches half its maximum fertility. If $A_1 < 0$, it is the weak Allee effect. When $A_1 = 0$, the fertility is density independent with $f(x) = a$.

Now, we apply forward Euler's scheme to the system of (3); we choose a time step size $\delta > 0$. For any $t \geq 0$, let $x_t = x(t)$, $y_t = y(t)$, $x_{t+1} = x(t+\delta)$, and $y_{t+1} = y(t+\delta)$, since

$$\begin{aligned} \dot{x} &= \lim_{\delta \to 0} \frac{x_{t+1} - x_t}{\delta}, \\ \dot{y} &= \lim_{\delta \to 0} \frac{y_{t+1} - y_t}{\delta}. \end{aligned} \tag{5}$$

We can assume that for small enough $\delta > 0$

$$\begin{aligned} \dot{x} &= \frac{x_{t+1} - x_t}{\delta}, \\ \dot{y} &= \frac{y_{t+1} - y_t}{\delta}. \end{aligned} \tag{6}$$

Thus, from system (1), we get the discrete-time system as

$$\begin{aligned} x &\longrightarrow x + \delta\left[ax\left(1 - \frac{x}{k}\right) - \frac{bxy}{x+l}\right], \\ y &\longrightarrow y + \delta\left(cy + \frac{mbxy}{x+l} - dy^2\right), \end{aligned} \tag{7}$$

where δ is the step size. Shrinking the step size in Euler's method will yield numerical solutions that more accurately approximate the true solution.

So, when the prey species is subject to Allee effect

$$f(x) = \frac{ax}{A_1 + x}, \tag{8}$$

the system of (7) can transform the following system:

$$\begin{aligned} x &\longrightarrow x + \delta x\left[\left(1 - \frac{x}{k}\right)\frac{ax}{A_1 + x} - \frac{by}{x+l}\right], \\ y &\longrightarrow y + \delta y\left(c + \frac{mbx}{x+l} - dy\right), \end{aligned} \tag{9}$$

where A_1 is Allee effect threshold value, if $A_1 > 0$, the Allee effect will be strong, and if $A_1 < 0$, the Allee effect will be weak. Here A_1 is a positive parameter denoting Allee

effect imposed on the prey population. Next, we investigate model (9) by way of mathematical analysis and numerical simulations.

Keeping in view of the literature, the rest of the paper is organized as follows: Section 2 deals with the stability criterion of the system at different fixed points in interior of R_+^2. In Section 3, we obtain the specific conditions of existence of flip bifurcation and Hopf bifurcation. Numerical simulations are presented to support our analytical findings in Section 4, especially for the period doubling bifurcation and chaotic behavior. Finally a brief conclusion is given in the last section.

2. Stability of Fixed Points

The fixed points of system (9) are $p_0(0,0)$, $p_1(k,0)$, $p_2(0,c/d)$, and $p_3(x^*,y^*)$, where x^*, y^* satisfy

$$a\left(1-\frac{x^*}{k}\right)\frac{x^*}{A_1+x^*}-\frac{by^*}{x^*+l}=0,$$
$$c+\frac{mbx^*}{x^*+l}-dy^*=0. \tag{10}$$

The Jacobian matrix of (9) at the fixed point (x,y) is written as

$$J=\begin{pmatrix} 1+\delta\left[\dfrac{ax^2+2A_1ax}{(A_1+x)^2}-\dfrac{2ax^3+3A_1ax^2}{k(A_1+x)^2}-\dfrac{bly}{(x+l)^2}\right] & -\dfrac{\delta bx}{x+l} \\ \dfrac{\delta mbly}{(x+l)^2} & 1+\delta\left(c+\dfrac{mbx}{x+l}-2dy\right)\end{pmatrix}. \tag{11}$$

The characteristic equation of the Jacobian matrix is given by

$$\lambda^2+p(x,y)\lambda+q(x,y)=0, \tag{12}$$

where

$$\begin{aligned} p(x,y) &= -\operatorname{tr}J=-2-\delta\left[\frac{ax^2+2A_1ax}{(A_1+x)^2}\right.\\ &\quad\left.-\frac{2ax^3+3A_1ax^2}{k(A_1+x)^2}-\frac{bly}{(x+l)^2}+c+\frac{mbx}{x+l}-2dy\right],\\ q(x,y) &= \det J=1+\delta\left[\frac{ax^2+2A_1ax}{(A_1+x)^2}\right.\\ &\quad\left.-\frac{2ax^3+3A_1ax^2}{k(A_1+x)^2}-\frac{bly}{(x+l)^2}\right]\left[1\right.\\ &\quad\left.+\delta\left(c+\frac{mbx}{x+l}-2dy\right)\right]+\frac{\delta^2mb^2lxy}{(x+l)^3}. \end{aligned} \tag{13}$$

Clearly, we can see the Jacobian matrix of (9) at the point $p_0(0,0)$ is

$$J=\begin{pmatrix}1 & 0\\ 0 & 1+\delta c\end{pmatrix}. \tag{14}$$

So, $\lambda_1=1$, $\lambda_2=1+\delta c$; then $p_0(0,0)$ is unstable.

Now, we state a definition and a lemma same as in [28, 29].

Definition 1. A fixed point (x,y) is called

(i) sink if $|\lambda_1|<1$ and $|\lambda_2|<1$, and it is asymptotically stable;

(ii) source if $|\lambda_1|>1$ and $|\lambda_2|>1$, and it is locally unstable;

(iii) saddle if $|\lambda_1|>1$ and $|\lambda_2|<1$ (or $|\lambda_1|<1$ and $|\lambda_2|>1$);

(iv) nonhyperbolic if either $|\lambda_1|=1$ or $|\lambda_2|=1$.

Lemma 2. *Let $F(\lambda)=\lambda^2+P\lambda+Q$. Suppose that $F(1)>0$ and λ_1,λ_2 are roots of $F(\lambda)=0$. Then, one has the following:*

(i) *$|\lambda_1|<1$ and $|\lambda_2|<1$ if and only if $F(-1)>0$ and $Q<1$;*

(ii) *$|\lambda_1|<1$ and $|\lambda_2|>1$ (or $|\lambda_1|>1$ and $|\lambda_2|<1$) if and only if $F(-1)<0$;*

(iii) *$|\lambda_1|>1$ and $|\lambda_2|>1$ if and only if $F(-1)>0$ and $Q>1$;*

(iv) *$\lambda_1=-1$ and $|\lambda_2|\neq 1$ if and only if $F(-1)=0$ and $P\neq 0,2$;*

(v) *$|\lambda_1|$ and $|\lambda_2|$ are complex and $|\lambda_1|=-1$, $|\lambda_2|=-1$ if and only if $P^2-4Q<0$ and $Q=1$.*

Proposition 3. *The fixed point $p_1(k,0)$ is source if $\delta>2/a+2A_1/ak$, saddle if $0<\delta<2/a+2A_1/ak$, and nonhyperbolic if $\delta=2/a+2A_1/ak$. In this condition, we assume $A_1>-k$. That is, if $-k<A_1<0$, it is weak Allee effect, and if $A_1>0$, it is strong Allee effect.*

One can see that when $\delta=2/a+2A_1/ak$, one of the eigen values of fixed point $p_1(k,0)$ is -1 and magnitude of other is not equal to 1. Thus the flip bifurcation occurs when a parameter changes in small neighborhood of $\delta=2/a+2A_1/ak$.

Proposition 4. *There exist different topological types of $p_2(0,c/d)$ for possible parameters.*

(i) *$p_2(0,c/d)$ is sink if $0<\delta<\min\{2/c,2dl/bc\}$.*

(ii) *$p_2(0,c/d)$ is source if $\delta>\max\{2/c,2dl/bc\}$.*

(iii) *$p_2(0,c/d)$ is nonhyperbolic if $\delta=2/c$ or $\delta=2dl/bc$.*

(iv) $p_2(0, c/d)$ *is saddle for all value of the parameters, except for values which lie in (i) to (iii).*

In this condition, we can see that the system at p_2 is not affected by the Allee effect threshold value; that is, bifurcation parameter δ has nothing to do with A_1.

The term (iii) of Proposition 4 implies that the parameters lie in the set

$$F_A = \left\{ (a, b, c, d, k, l, m, \delta, A_1),\ \delta = \frac{2}{c},\ \delta \neq \frac{2dl}{bc},\ a, b, c, d, k, l, m, \delta, A_1 > 0 \right\}. \tag{15}$$

If the term (iii) of Proposition 4 holds, then one of the eigen values of fixed points $p_2(0, c/d)$ is -1 and the magnitude of the other is not equal to 1. The point $p_2(0, c/d)$ undergoes flip bifurcation when the parameter changes in small neighborhood of F_A.

Last condition, the characteristic equation of the Jacobian matrix J of system (9) at the fixed point $p_3(x^*, y^*)$ is written as

$$\lambda^2 + p(x^*, y^*)\lambda + q(x^*, y^*) = 0, \tag{16}$$

where

$$\begin{aligned} p(x^*, y^*) &= -2 - G\delta, \\ q(x^*, y^*) &= 1 + G\delta + H\delta^2, \\ G &= \frac{ax^{*2} + 2A_1 ax^*}{(A_1 + x^*)^2} - \frac{2ax^{*3} + 3A_1 ax^{*2}}{k(A_1 + x^*)^2} \\ &\quad - \frac{bly^*}{(x^* + l)^2} + c + \frac{mbx^*}{x^* + l} - 2dy^*, \\ H &= \left[\frac{ax^{*2} + 2A_1 ax^*}{(A_1 + x^*)^2} - \frac{2ax^{*3} + 3A_1 ax^{*2}}{k(A_1 + x^*)^2} \right. \\ &\quad \left. - \frac{bly^*}{(x^* + l)^2} \right] \left[c + \frac{mbx^*}{x^* + l} - 2dy^* \right] + \frac{mb^2 lx^* y^*}{(x^* + l)^3}. \end{aligned} \tag{17}$$

Now

$$F(\lambda) = \lambda^2 - (2 + G\delta)\lambda + \left(1 + G\delta + H\delta^2\right). \tag{18}$$

Therefore

$$\begin{aligned} F(1) &= H\delta^2, \\ F(-1) &= 4 + 2G\delta + H\delta^2. \end{aligned} \tag{19}$$

Using Lemma 2, we get the following proposition.

Proposition 5. *There exist different topological types of $p_3(x^*, y^*)$ for all possible parameters.*

(i) $p_3(x^*, y^*)$ *is a sink if either condition (1) or (2) holds:*

(1) $G^2 - 4H \geq 0$ *and* $0 < \delta < (-G - \sqrt{G^2 - 4H})/H$,
(2) $G^2 - 4H < 0$ *and* $0 < \delta < -G/H$.

(ii) $p_3(x^*, y^*)$ *is a source if either condition (1) or (2) holds:*

(1) $G^2 - 4H \geq 0$ *and* $\delta > (-G + \sqrt{G^2 - 4H})/H$,
(2) $G^2 - 4H < 0$ *and* $\delta > -G/H$.

(iii) $p_3(x^*, y^*)$ *is nonhyperbolic if either condition (1) or (2) holds:*

(1) $G^2 - 4H \geq 0$ *and* $\delta = (-G \pm \sqrt{G^2 - 4H})/H$,
(2) $G^2 - 4H < 0$ *and* $\delta = -G/H$.

(iv) $p_3(x^*, y^*)$ *is saddle for all values of the parameters, except for values which lie in (i) to (iii).*

If the term (1) in (iii) of Proposition 5 holds, then one of the eigen values of the fixed point $p_3(x^*, y^*)$ is -1 and the magnitude of the other is not equal to 1. The term (1) in (iii) of Proposition 5 may be written as follows:

$$\begin{aligned} F_{B1} &= \left\{ (a, b, c, d, k, l, m, \delta, A_1) : \delta \right. \\ &\quad = \frac{-G - \sqrt{G^2 - 4H}}{H},\ G^2 - 4H \\ &\quad \left. \geq 0, a, b, c, d, k, l, m, \delta, A_1 > 0 \right\}, \\ F_{B2} &= \left\{ (a, b, c, d, k, l, m, \delta, A_1) : \delta \right. \\ &\quad = \frac{-G + \sqrt{G^2 - 4H}}{H},\ G^2 - 4H \\ &\quad \left. \geq 0, a, b, c, d, k, l, m, \delta, A_1 > 0 \right\}. \end{aligned} \tag{20}$$

Then a flip bifurcation will occur in the neighborhood of F_{B1} or F_{B2}.

If the term (2) in (iii) of Proposition 5 holds, then the eigen values of the fixed point $p_3(x^*, y^*)$ are a pair of complex conjugate numbers with modulus 1. The term (2) in (iii) of Proposition 5 may be written as follows:

$$H_B = \left\{ (a, b, c, d, k, l, m, \delta, A_1) : \delta = -\frac{G}{H},\ G^2 - 4H < 0, a, b, c, d, k, l, m, \delta, A_1 > 0 \right\}. \tag{21}$$

One can see that a Hopf bifurcation will occur in the neighborhood of H_B.

3. Bifurcation Behavior

In this section, we study the flip bifurcation and Hopf bifurcation at the fixed point $p_3(x^*, y^*)$.

3.1. Flip Bifurcation. We consider system (9) with arbitrary parameter $(a, b, c, d, k, l, m, \delta_1, A_1) \in F_{B1}$, which is described as follows:

$$\begin{aligned} x &\longrightarrow x + \delta_1 x\left[\left(1-\frac{x}{k}\right)\frac{ax}{A_1+x} - \frac{by}{x+l}\right], \\ y &\longrightarrow y + \delta_1 y\left(c + \frac{mbx}{x+l} - dy\right), \end{aligned} \tag{22}$$

$p_3(x^*, y^*)$ is fixed point of system (22), where x^*, y^* are given by (9), and

$$\delta_1 = \frac{-G - \sqrt{G^2 - 4H}}{H}. \tag{23}$$

The eigen values of $p_3(x^*, y^*)$ are $\lambda_1 = -1$, $\lambda_2 = 3 + G\delta_1$, with $|\lambda_2| \neq 1$ by Proposition 5.

Consider the perturbation of (22) as below:

$$\begin{aligned} x &\longrightarrow x + (\delta_1 + \delta^*) x\left[\left(1-\frac{x}{k}\right)\frac{ax}{A_1+x} - \frac{by}{x+l}\right], \\ y &\longrightarrow y + (\delta_1 + \delta^*) y\left(c + \frac{mbx}{x+l} - dy\right), \end{aligned} \tag{24}$$

where $|\delta^*| \ll 1$ is a limited perturbation parameter.

Let $u = x - x^*$ and $v = y - y^*$.

After the transformation of the fixed point $p_3(x^*, y^*)$ of system (24) to the point $(0, 0)$, we obtain

$$\begin{pmatrix} u \\ v \end{pmatrix} \longrightarrow \begin{pmatrix} a_{11}u + a_{12}v + a_{13}u^2 + a_{14}uv + b_{11}\delta^* u + b_{12}\delta^* v + b_{13}\delta^* u^2 + b_{14}\delta^* uv + O\left(|u|, |v|, |\delta^*|\right)^3 \\ a_{21}u + a_{22}v + a_{23}u^2 + a_{24}uv + a_{25}v^2 + b_{21}\delta^* u + b_{22}\delta^* v + b_{23}\delta^* u^2 + b_{24}\delta^* uv + b_{25}\delta^* v^2 + O\left(|u|, |v|, |\delta^*|\right)^3 \end{pmatrix}, \tag{25}$$

where

$$\begin{aligned} a_{11} &= 1 + \delta_1\left[\frac{\left(2A_1 + x^*\right)ax^*}{\left(A_1 + x^*\right)^2} - \frac{\left(3A_1x^{*2} + 2x^{*3}\right)a}{k\left(A_1 + x^*\right)^2} - \frac{by^*}{x^*+l} + \frac{bx^*y^*}{\left(x^*+l\right)^2}\right], \\ a_{12} &= -\frac{\delta_1 bx^*}{x^*+l}, \\ a_{13} &= \delta_1\left[\frac{aA_1^2}{\left(A_1+x^*\right)^3} - \frac{\left(ax^{*3} + 3A_1x^* + 3A_1^2x^*\right)}{k\left(A_1+x^*\right)^3} + \frac{by^*}{\left(x^*+l\right)^2} - \frac{bx^*y^*}{\left(x^*+l\right)^3}\right], \\ a_{14} &= \delta_1\left[\frac{bx^*}{\left(x^*+l\right)^2} - \frac{b}{x^*+l}\right], \\ b_{11} &= \frac{\left(2A_1 + x^*\right)ax^*}{\left(A_1 + x^*\right)^2} - \frac{\left(3A_1x^{*2} + 2x^{*3}\right)a}{k\left(A_1 + x^*\right)^2} - \frac{by^*}{x^*+l} + \frac{bx^*y^*}{\left(x^*+l\right)^2}, \\ b_{12} &= -\frac{bx^*}{x^*+l}, \\ b_{13} &= \frac{aA_1^2}{\left(A_1+x^*\right)^3} - \frac{ax^{*3} + 3A_1x^* + 3A_1^2x^*}{k\left(A_1+x^*\right)^3} + \frac{by^*}{\left(x^*+l\right)^2} - \frac{bx^*y^*}{\left(x^*+l\right)^3}, \\ b_{14} &= \frac{bx^*}{\left(x^*+l\right)^2} - \frac{b}{x^*+l}, \\ a_{21} &= \frac{\delta_1 mbly^*}{\left(x^*+l\right)^2}, \\ a_{22} &= 1 - \delta_1 dy^*, \\ a_{23} &= -\frac{\delta_1 mbly^*}{\left(x^*+l\right)^3}, \\ a_{24} &= \frac{\delta_1 mbl}{\left(x^*+l\right)^2}, \\ a_{25} &= -\delta_1 d, \\ b_{21} &= \frac{mbly^*}{\left(x^*+l\right)^2}, \\ b_{22} &= -dy^*, \\ b_{23} &= -\frac{mbly^*}{\left(x^*+l\right)^3}, \\ b_{24} &= \frac{mbl}{\left(x^*+l\right)^2}, \\ b_{25} &= -d. \end{aligned} \tag{26}$$

Consider the following translation:

$$\begin{pmatrix} u \\ v \end{pmatrix} = T\begin{pmatrix} \widetilde{x} \\ \widetilde{y} \end{pmatrix}, \tag{27}$$

where

$$T = \begin{pmatrix} a_{11} & a_{12} \\ -1-a_{11} & \lambda_2 - a_{11} \end{pmatrix},$$

$$T^{-1} = \begin{pmatrix} \dfrac{\lambda_2 - a_{11}}{a_{12}(\lambda_2+1)} & -\dfrac{1}{\lambda_2+1} \\ \dfrac{1+a_{11}}{a_{12}(\lambda_2+1)} & \dfrac{1}{\lambda_2+1} \end{pmatrix}, \tag{28}$$

$$\begin{pmatrix} u \\ v \end{pmatrix} = T \begin{pmatrix} \widetilde{x} \\ \widetilde{y} \end{pmatrix} = \begin{pmatrix} a_{11} & a_{12} \\ -1-a_{11} & \lambda_2 - a_{11} \end{pmatrix} \begin{pmatrix} \widetilde{x} \\ \widetilde{y} \end{pmatrix}.$$

Taking T^{-1} on both sides of (16), we get

$$\begin{pmatrix} \widetilde{x} \\ \widetilde{y} \end{pmatrix} \longrightarrow \begin{pmatrix} -1 & 0 \\ 0 & \lambda_2 \end{pmatrix} \begin{pmatrix} \widetilde{x} \\ \widetilde{y} \end{pmatrix} + \begin{pmatrix} f(u,v,\delta^*) \\ g(u,v,\delta^*) \end{pmatrix}, \tag{29}$$

where

$$\begin{aligned} f(u,v,\delta^*) = {} & \frac{[a_{13}(\lambda_2 - a_{11}) - a_{12}a_{23}]u^2}{a_{12}(\lambda_2+1)} \\ & + \frac{[a_{14}(\lambda_2 - a_{11}) - a_{12}a_{24}]uv}{a_{12}(\lambda_2+1)} \\ & - \frac{a_{12}a_{25}v^2}{a_{12}(\lambda_2+1)} \\ & + \frac{[b_{11}(\lambda_2 - a_{11}) - a_{12}b_{21}]\delta^* u}{a_{12}(\lambda_2+1)} \\ & + \frac{[b_{12}(\lambda_2 - a_{11}) - a_{12}b_{22}]\delta^* v}{a_{12}(\lambda_2+1)} \\ & + \frac{[b_{13}(\lambda_2 - a_{11}) - a_{12}b_{23}]\delta^* u^2}{a_{12}(\lambda_2+1)} \\ & + \frac{[b_{14}(\lambda_2 - a_{11}) - a_{12}b_{24}]\delta^* uv}{a_{12}(\lambda_2+1)} \\ & - \frac{a_{12}b_{25}\delta^* v^2}{a_{12}(\lambda_2+1)} + 0\left(|u|, |v|, |\delta^*|\right)^3, \end{aligned} \tag{30}$$

$$\begin{aligned} g(u,v,\delta^*) = {} & \frac{[a_{13}(1+a_{11}) + a_{12}a_{23}]u^2}{a_{12}(\lambda_2+1)} \\ & + \frac{[a_{14}(1+a_{11}) + a_{12}a_{24}]uv}{a_{12}(\lambda_2+1)} \\ & + \frac{a_{12}a_{25}v^2}{a_{12}(\lambda_2+1)} \\ & + \frac{[b_{11}(1+a_{11}) + a_{12}b_{21}]\delta^* u}{a_{12}(\lambda_2+1)} \\ & + \frac{[b_{12}(1+a_{11}) + a_{12}b_{22}]\delta^* v}{a_{12}(\lambda_2+1)} \\ & + \frac{[b_{13}(1+a_{11}) + a_{12}b_{23}]\delta^* u^2}{a_{12}(\lambda_2+1)} \\ & + \frac{[b_{14}(1+a_{11}) + a_{12}b_{24}]\delta^* uv}{a_{12}(\lambda_2+1)} \\ & + \frac{a_{12}b_{25}\delta^* v^2}{a_{12}(\lambda_2+1)} + 0\left(|u|, |v|, |\delta^*|\right)^3, \end{aligned} \tag{31}$$

$$u = a_{12}(\widetilde{x} + \widetilde{y}),$$

$$v = -(1+a_{11})\widetilde{x} + (\lambda_2 - a_{11})\widetilde{y}.$$

Apply the center manifold theorem to (22) at the origin in the limited neighborhood of $\delta^* = 0$. The center manifold $W^c(0,0)$ can be approximately presented as

$$\begin{aligned} W^c(0,0) = {} & \left\{(\widetilde{x}, \widetilde{y}) : \widetilde{y} = a_0\delta^* + a_1\widetilde{x}^2 + a_2\widetilde{x}\delta^* \right. \\ & \left. + a_3\delta^{*2} + O\left(\left(|\widetilde{x}| + |\delta^*|\right)^3\right)\right\}, \end{aligned} \tag{32}$$

where $O(|\widetilde{x}| + |\delta^*|)^3$ is a function with at least third orders in variables $(\widetilde{x}, \delta^*)$.

By simple calculations for center manifold, we have

$$\begin{aligned} a_0 &= 0, \\ a_1 &= \frac{[a_{13}(1+a_{11}) + a_{12}a_{23}]a_{12} - [a_{14}(1+a_{11}) + a_{12}a_{24}](1+a_{11}) + a_{25}(1+a_{11})^2}{1-\lambda_2^2}, \\ a_2 &= -\frac{[b_{11}(1+a_{11}) + a_{12}b_{21}]a_{12} + [b_{12}(1+a_{11}) + a_{12}b_{22}](1+a_{11})}{a_{12}(1+\lambda_2)^2}, \\ a_3 &= 0. \end{aligned} \tag{33}$$

Now, consider the map restricted to the center manifold $W^c(0,0)$ as below:

$$f:\tilde{x}\longrightarrow -\tilde{x}+h_1\tilde{x}^2+h_2\tilde{x}\delta^*+h_3\tilde{x}^2\delta^*+h_4\tilde{x}\left(\delta^*\right)^2 +h_5\tilde{x}^3+O\left(\left(|\tilde{x}|+|\delta^*|\right)^4\right), \tag{34}$$

where

$$\begin{aligned}
h_1 &= \frac{\left[a_{13}\left(\lambda_2-a_{11}\right)-a_{12}a_{23}\right]a_{12}}{\lambda_2+1} \\
&\quad -\frac{\left[a_{14}\left(\lambda_2-a_{11}\right)-a_{12}a_{24}\right]\left(1+a_{11}\right)}{\lambda_2+1} \\
&\quad -\frac{a_{12}a_{25}\left(1+a_{11}\right)^2}{a_{12}\left(\lambda_2+1\right)}, \\
h_2 &= \frac{\left[b_{11}\left(\lambda_2-a_{11}\right)-a_{12}b_{21}\right]}{\lambda_2+1} \\
&\quad -\frac{\left[b_{12}\left(\lambda_2-a_{11}\right)-a_{12}b_{22}\right]\left(1+a_{11}\right)}{\left(\lambda_2+1\right)a_{12}}, \\
h_3 &= \frac{\left[a_{13}\left(\lambda_2-a_{11}\right)-a_{12}a_{23}\right]2a_2a_{12}}{\lambda_2+1} \\
&\quad +\frac{\left[a_{14}\left(\lambda_2-a_{11}\right)-a_{12}a_{24}\right]\left(\lambda_2-2a_{11}-1\right)a_2}{\lambda_2+1} \\
&\quad +\frac{2a_{25}\left(1+a_{11}\right)\left(\lambda_2-a_{11}\right)a_2}{\lambda_2+1} \\
&\quad +\frac{\left[b_{11}\left(\lambda_2-a_{11}\right)-a_{12}b_{21}\right]a_1}{\lambda_2+1} \\
&\quad +\frac{\left[b_{12}\left(\lambda_2-a_{11}\right)-a_{12}b_{22}\right]\left(\lambda_2-a_{11}\right)a_1}{a_{12}\left(\lambda_2+1\right)} \\
&\quad +\frac{\left[b_{13}\left(\lambda_2-a_{11}\right)-a_{12}b_{23}\right]a_{12}}{\lambda_2+1} \\
&\quad -\frac{\left[b_{14}\left(\lambda_2-a_{11}\right)-a_{12}b_{24}\right]\left(1+a_{11}\right)}{\lambda_2+1} \\
&\quad -\frac{b_{25}\left(1+a_{11}\right)^2}{\lambda_2+1}, \\
h_4 &= \frac{\left[b_{11}\left(\lambda_2-a_{11}\right)-a_{12}b_{21}\right]a_2}{\lambda_2+1} \\
&\quad +\frac{\left[b_{12}\left(\lambda_2-a_{11}\right)-a_{12}b_{22}\right]\left(\lambda_2-a_{11}\right)a_2}{a_{12}\left(\lambda_2+1\right)}, \\
h_5 &= \frac{\left[a_{13}\left(\lambda_2-a_{11}\right)-a_{12}a_{23}\right]2a_{12}a_1}{\lambda_2+1} \\
&\quad +\frac{\left[a_{14}\left(\lambda_2-a_{11}\right)-a_{12}a_{24}\right]\left(\lambda_2-2a_{11}-1\right)a_1}{\lambda_2+1} \\
&\quad +\frac{2a_{25}\left(1+a_{11}\right)\left(\lambda_2-a_{11}\right)a_1}{\lambda_2+1}.
\end{aligned} \tag{35}$$

According to flip bifurcation, the discriminatory quantities γ_1 and γ_2 are given by

$$\begin{aligned}
\gamma_1 &= \left(\frac{\partial^2 f}{\partial\tilde{x}\partial\delta^*}+\frac{1}{2}\frac{\partial f}{\partial\delta^*}\frac{\partial^2 f}{\partial\tilde{x}^2}\right)\Bigg|_{(0,0)}, \\
\gamma_2 &= \left(\frac{1}{6}\frac{\partial^3 f}{\partial\tilde{x}^3}+\left(\frac{1}{2}\frac{\partial^2 f}{\partial\tilde{x}^2}\right)^2\right)\Bigg|_{(0,0)}.
\end{aligned} \tag{36}$$

After simple calculations, we obtain $\gamma_1 = h_2$ and $\gamma_2 = h_5 + h_1^2$.

Analyzing above and the flip bifurcation conditions discussed in [30], we write the following theorem.

Theorem 6. *If $\gamma_2 \neq 0$ and parameter δ^* alters in the limiting region of the point $(0,0)$, then system (10) passes through flip bifurcation at the point $p_3(x^*, y^*)$. Also, the period-2 points that bifurcations from fixed point $p_3(x^*, y^*)$ are stable (resp., unstable) if $\gamma_2 > 0$ (resp., $\gamma_2 < 0$).*

3.2. Hopf Bifurcation. Consider system (7) with arbitrary parameter $(a, b, c, k, l, m, \delta_2, A_1) \in H_B$. This is described as follows:

$$\begin{aligned}
x &\longrightarrow x+\delta_2 x\left[\left(1-\frac{x}{k}\right)\frac{ax}{A_1+x}-\frac{by}{x+l}\right], \\
y &\longrightarrow y+\delta_2 y\left(c+\frac{mbx}{x+l}-dy\right).
\end{aligned} \tag{37}$$

$p_3(x^*, y^*)$ is the fixed point of system (37), where x^*, y^* are given by (3) and $\delta_2 = -G/H$.

Consider the perturbation of (37) as given below:

$$\begin{aligned}
x &\longrightarrow x+\left(\delta_2+\delta\right)x\left[\left(1-\frac{x}{k}\right)\frac{ax}{A_1+x}-\frac{by}{x+l}\right], \\
y &\longrightarrow y+\left(\delta_2+\delta\right)y\left(c+\frac{mbx}{x+l}-dy\right),
\end{aligned} \tag{38}$$

where $|\delta| \ll 1$ is limited perturbation parameter.

The characteristic equation of map (38) at $p_3(x^*, y^*)$ is given by $\lambda^2 + p(\delta)\lambda + q(\delta) = 0$, where

$$\begin{aligned}
p(\delta) &= -2-G\delta, \\
q(\delta) &= 1+G\delta+H\delta^2.
\end{aligned} \tag{39}$$

Since the parameter $(a, b, c, k, l, m, \delta_2, A_1) \in H_B$, the eigen values of $p_3(x^*, y^*)$ are a pair of complex conjugate numbers $\overline{\lambda}$ and λ with modulus 1 by Proposition 5, where

$$\overline{\lambda}, \lambda = \frac{-p(\delta) \mp i\sqrt{4q(\delta)-p^2(\delta)}}{2}. \tag{40}$$

Therefore

$$\overline{\lambda}, \lambda = 1+\frac{G\left(\delta_2+\delta\right)}{2} \mp \frac{i\left(\delta_2+\delta\right)\sqrt{4H-G^2}}{2}. \tag{41}$$

Now we have

$$|\lambda| = q(\delta)^{1/2},$$
$$l = \left.\frac{d|\lambda|}{d\delta}\right|_{\delta=0} = -\frac{G}{2} > 0. \tag{42}$$

When δ varies in limited neighborhood of $\delta = 0$, then $\overline{\lambda}, \lambda = \alpha \pm i\beta$, where

$$\alpha = 1 + \frac{\delta_2 G}{2},$$
$$\beta = \frac{\delta_2\sqrt{4H - G^2}}{2}. \tag{43}$$

Hopf bifurcation requires that when $\delta = 0$, then $\overline{\lambda^n}, \lambda^n \neq 1$ $(n = 1, 2, 3, 4)$ which is equivalent to $p(0) \neq -2, 0, 1, 2$.

Since the parameter $(a, b, c, d, l, m, \delta_2, A_1) \in H_B$. therefore $p(0) \neq -2, 2$. It is the only requirement that $p(0) \neq 0, 1$, which follows that $G^2 \neq 2H, 3H$. Let $u = x - x^*$ and $v = y - y^*$.

After the transformation of the fixed points $p_3(x^*, y^*)$ of system (38) to the points $(0, 0)$, we have

$$\begin{pmatrix} u \\ v \end{pmatrix} \longrightarrow \begin{pmatrix} a_{11}u + a_{12}v + a_{13}u^2 + a_{14}uv + 0(|u|, |v|)^3 \\ a_{21}u + a_{22}v + a_{23}u^2 + a_{24}uv + a_{25}v^2 + 0(|u|, |v|)^3 \end{pmatrix}, \tag{44}$$

where $a_{11}, a_{12}, a_{13}, a_{21}, a_{22}, a_{23}, a_{24}, a_{25}$ are given in (26) by substituting δ_2 for $\delta_2 + \delta$.

Now, we discuss the normal form of (44) when $\delta = 0$.

Consider the translation as below:

$$\begin{pmatrix} u \\ v \end{pmatrix} = T\begin{pmatrix} \widetilde{x} \\ \widetilde{y} \end{pmatrix}, \tag{45}$$

where

$$T = \begin{pmatrix} a_{12} & 0 \\ \alpha - a_{11} & -\beta \end{pmatrix},$$
$$T^{-1} = \begin{pmatrix} \dfrac{1}{a_{12}} & 0 \\ \dfrac{\alpha - a_{11}}{\beta a_{12}} & -\dfrac{1}{\beta} \end{pmatrix}, \tag{46}$$
$$\begin{pmatrix} u \\ v \end{pmatrix} = T\begin{pmatrix} \widetilde{x} \\ \widetilde{y} \end{pmatrix} = \begin{pmatrix} a_{12} & 0 \\ \alpha - a_{11} & -\beta \end{pmatrix}\begin{pmatrix} \widetilde{x} \\ \widetilde{y} \end{pmatrix}.$$

Taking T^{-1} on both sides of (44), we get

$$\begin{pmatrix} \widetilde{x} \\ \widetilde{y} \end{pmatrix} \longrightarrow \begin{pmatrix} \alpha & -\beta \\ \beta & \alpha \end{pmatrix}\begin{pmatrix} \widetilde{x} \\ \widetilde{y} \end{pmatrix} + \begin{pmatrix} \widetilde{f}(\widetilde{x}, \widetilde{y}) \\ \widetilde{g}(\widetilde{x}, \widetilde{y}) \end{pmatrix}, \tag{47}$$

where

$$\widetilde{f}(\widetilde{x}, \widetilde{y}) = \frac{a_{13}}{a_{12}}u^2 + \frac{a_{14}}{a_{12}uv} + O(|u|, |v|)^3,$$
$$\widetilde{g}(\widetilde{x}, \widetilde{y}) = \frac{[a_{13}(\alpha - a_{11}) - a_{12}a_{23}]}{a_{12}\beta}u^2 + \frac{[a_{14}(\alpha - a_{11}) - a_{12}a_{24}]}{a_{12}\beta}uv - \frac{a_{25}}{\beta}v^2 + O(|u|, |v|)^3, \tag{48}$$
$$u = a_{12}\widetilde{x},$$
$$v = (\alpha - a_{11})\widetilde{x} - \beta\widetilde{y}.$$

Now

$$\widetilde{f}_{\widetilde{x}\widetilde{x}} = 2a_{12}a_{13} + 2a_{14}(\alpha - a_{11}),$$
$$\widetilde{f}_{\widetilde{x}\widetilde{y}} = -a_{14}\beta,$$
$$\widetilde{f}_{\widetilde{y}\widetilde{y}} = 0,$$
$$\widetilde{f}_{\widetilde{x}\widetilde{x}\widetilde{x}} = 0,$$
$$\widetilde{f}_{\widetilde{x}\widetilde{x}\widetilde{y}} = 0,$$
$$\widetilde{f}_{\widetilde{x}\widetilde{y}\widetilde{y}} = 0,$$
$$\widetilde{f}_{\widetilde{y}\widetilde{y}\widetilde{y}} = 0,$$
$$\widetilde{g}_{\widetilde{x}\widetilde{x}} = \frac{2a_{12}}{\beta}[a_{13}(\alpha - a_{11}) - a_{12}a_{23}] + \frac{2(\alpha - a_{11})}{\beta}[a_{14}(\alpha - a_{11}) - a_{12}a_{24}] - \frac{2a_{25}}{\beta}(\alpha - a_{11})^2, \tag{49}$$
$$\widetilde{g}_{\widetilde{x}\widetilde{y}} = -[a_{14}(\alpha - a_{11}) - a_{12}a_{24}] + 2a_{25}(\alpha - a_{11}),$$
$$\widetilde{g}_{\widetilde{y}\widetilde{y}} = -2a_{25}\beta,$$
$$\widetilde{g}_{\widetilde{x}\widetilde{x}\widetilde{x}} = 0,$$
$$\widetilde{g}_{\widetilde{x}\widetilde{x}\widetilde{y}} = 0,$$
$$\widetilde{g}_{\widetilde{x}\widetilde{y}\widetilde{y}} = 0,$$
$$\widetilde{g}_{\widetilde{y}\widetilde{y}\widetilde{y}} = 0.$$

According to Hopf bifurcation, the discriminatory quantity s is given by

$$s = -\operatorname{Re}\left[\frac{(1 - 2\overline{\lambda})\overline{\lambda}^2}{1 - \lambda}\varphi_{11}\varphi_{20}\right] - \frac{1}{2}\|\varphi_{11}\|^2 - \|\varphi_{02}\|^2 + \operatorname{Re}(\overline{\lambda}\varphi_{21}), \tag{50}$$

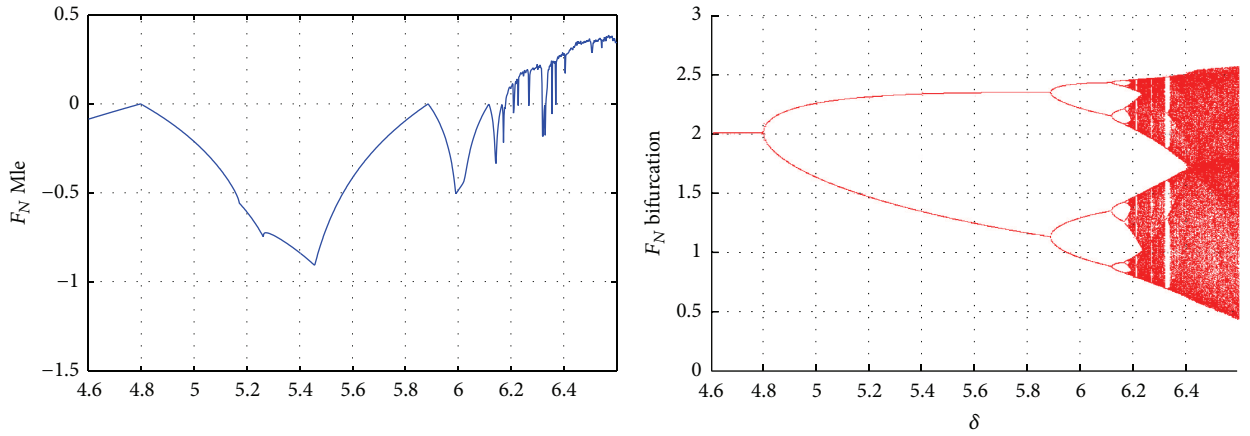

FIGURE 1: Largest Lyapunov exponents and bifurcation diagram of system (25) for $a = 0.8$, $b = 0.8$, $c = 0.4$, $d = 0.2$, $k = 5$, $l = 2$, and $A_1 = 0.18$ with the initial value of $(x, y) = (1, 1)$ and δ covering $[4.6, 6.6]$.

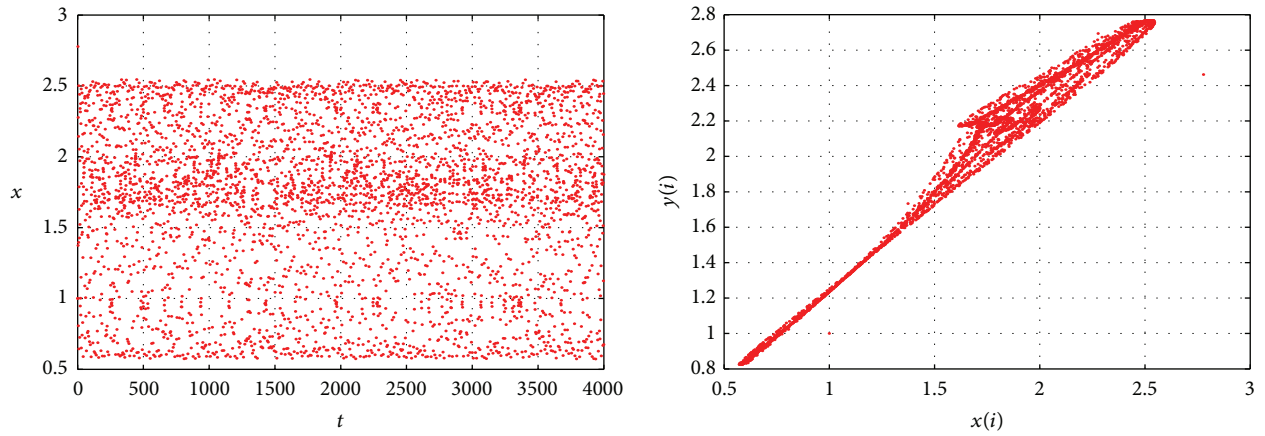

FIGURE 2: The portraits for several values of $A_1 = 0.18$, $\delta = 6.45$.

where

$$\begin{aligned}
\varphi_{20} &= \frac{1}{8}\left[\left(\tilde{f}_{\bar{x}\bar{x}} - \tilde{f}_{\bar{y}\bar{y}} + 2\tilde{g}_{\bar{x}\bar{y}}\right)\right. \\
&\quad \left. + i\left(\tilde{g}_{\bar{x}\bar{x}} - \tilde{g}_{\bar{y}\bar{y}} - 2\tilde{f}_{\bar{x}\bar{y}}\right)\right], \\
\varphi_{11} &= \frac{1}{4}\left[\left(\tilde{f}_{\bar{x}\bar{x}} + \tilde{f}_{\bar{y}\bar{y}}\right) + i\left(\tilde{g}_{\bar{x}\bar{x}} + \tilde{g}_{\bar{y}\bar{y}}\right)\right], \\
\varphi_{02} &= \frac{1}{8}\left[\left(\tilde{f}_{\bar{x}\bar{x}} - \tilde{f}_{\bar{y}\bar{y}} - 2\tilde{g}_{\bar{x}\bar{y}}\right)\right. \\
&\quad \left. + i\left(\tilde{g}_{\bar{x}\bar{x}} - \tilde{g}_{\bar{y}\bar{y}} + 2\tilde{f}_{\bar{x}\bar{y}}\right)\right], \\
\varphi_{21} &= \frac{1}{16}\left[\left(\tilde{f}_{\bar{x}\bar{x}\bar{x}} + \tilde{f}_{\bar{x}\bar{y}\bar{y}} + \tilde{g}_{\bar{x}\bar{x}\bar{y}} + \tilde{g}_{\bar{y}\bar{y}\bar{y}}\right)\right. \\
&\quad \left. + i\left(\tilde{g}_{\bar{x}\bar{x}\bar{x}} - \tilde{g}_{\bar{x}\bar{y}\bar{y}} - \tilde{f}_{\bar{x}\bar{x}\bar{y}} - \tilde{f}_{\bar{y}\bar{y}\bar{y}}\right)\right].
\end{aligned} \tag{51}$$

Analyzing above and Hopf bifurcation conditions discussed in [30], we write the theorem as below.

Theorem 7. *If the condition (38) holds, $s \neq 0$, and the parameter δ alters in the limited region of the point $(0, 0)$, then system (38) passes through a Hopf bifurcation at the point $p_3(x^*, y^*)$. Moreover, if $s < 0$ (resp., $s < 0$), then an attracting (resp., repelling) invariant closed curve bifurcates from the fixed point $p_3(x^*, y^*)$ for $\delta > 0$ (resp., $\delta < 0$).*

4. Numerical Simulations

To verify the theoretical analysis, we draw the bifurcation diagrams, largest Lyapunov exponents, and phase portraits for system (22). These diagrams show the complete dynamical behavior and the global stability of the system at the fixed points. The bifurcation behavior of system (22) is discussed in the following cases.

Case 1. On the one hand, if we take $a = 0.8$, $b = 0.8$, $c = 0.4$, $d = 0.2$, $k = 5$, $l = 2$, $m = 0.1$, and $A_1 = 0.18$ with the initial value of $(x, y) = (1, 1)$ and δ covering $[4.6, 6.6]$, then, we observe that at the fixed point $(2.0126, 2.2006)$ a flip bifurcation appears at $\delta = 4.792$. In this case $\gamma_1 = -0.3528$, $\gamma_2 = 2.857$ (see Figure 1).

From Figure 2, we can see that the fixed point of system (9) is stable for $\delta < 4.792$ and loses its stability at $\delta = 4.792$ and there appears period doubling bifurcation for $\delta > 4.792$.

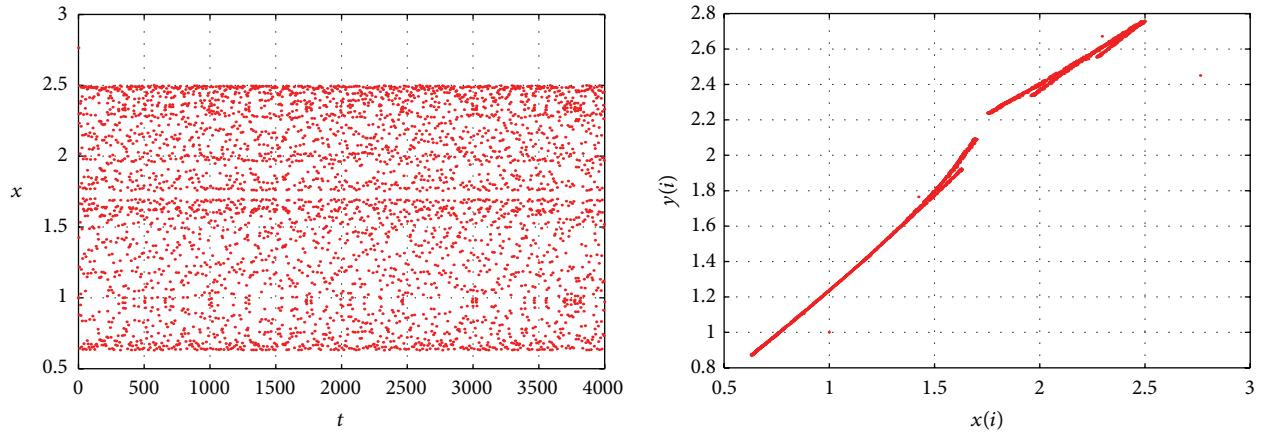

Figure 3: The portraits for several values of $A_1 = 0.18$, $\delta = 6.4$.

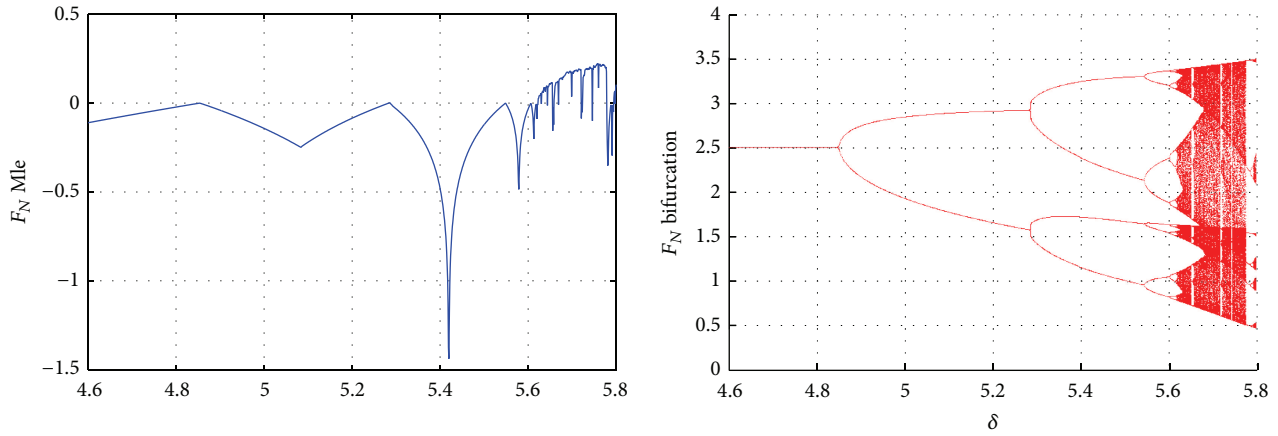

Figure 4: Largest Lyapunov exponents and bifurcation diagram of system (25) for $a = 0.8$, $b = 0.8$, $c = 0.4$, $d = 0.2$, $k = 5$, $l = 2$, and $A_1 = 0.03$ with the initial value of $(x, y) = (1, 1)$ and δ covering $[4.6, 5.8]$.

The phase portraits show that there are orbits of periods 2, 4, 8 for $\delta \in [5, 6.15]$ and chaotic sets at $\delta = 6.45$ and $\delta = 6.4$ (see Figures 2 and 3).

On the other hand, if we take $a = 0.8$, $b = 0.8$, $c = 0.4$, $d = 0.2$, $k = 5$, $l = 2$, $m = 0.1$, and $A_1 = 0.03$ with the initial value of $(x, y) = (1, 1)$ and δ covering $[4.6, 5.8]$, then, we observe that at the fixed point $(2.5025, 2.2223)$ a flip bifurcation appears at $\delta = 4.846$. In this case $\gamma_1 = -0.175$, $\gamma_2 = 2.2893$ (see Figure 4).

From Figure 5, we can see that the fixed point of system (9) is stable for $\delta < 4.846$ and loses its stability at $\delta = 4.846$ and there appears period doubling bifurcation for $\delta > 4.846$. The phase portraits show that there are orbits of periods 2, 4, 8 for $\delta \in [5, 5.6]$ and chaotic sets at $\delta = 5.7$ and $\delta = 5.75$.

But, from the former paper in [17], we know when $\delta = 4.87985$ loses its stability without Allee effect. So, we can see Allee effect changes the value of δ.

Case 2. First, we take $a = 0.8$, $b = 0.8$, $c = 0.4$, $d = 0.2$, $k = 5$, $l = 3$, $m = 0.1$, and $A_1 = 0.18$ with initial value of $(x, y) = (1, 1)$ and δ covering $[5.3, 5.37]$ (see Figure 6). We can see that at the fixed point $(3.0927, 2.203)$ a Hopf bifurcation emerges at $\delta = 5.335$. We can see that the fixed point of system (9) is stable $\delta < 5.335$ and loses its stability at $\delta = 5.335$, and an invariant circle appears at $\delta > 5.335$ (see Figures 7 and 8). Here $\alpha = -0.8171$, $\beta = 0.37345$, and $s = -0.911$.

Second, we take $a = 0.8$, $b = 0.8$, $c = 0.4$, $d = 0.2$, $k = 5$, $l = 3$, $m = 0.1$, and $A_1 = 0.03$ with initial value of $(x, y) = (1, 1)$ and δ covering $[4.87, 4.95]$ (see Figure 9). We can see that at the fixed point $(3.206, 2.207)$ a Hopf bifurcation emerges at $\delta = 4.8795$. We can see that the fixed point of system (9) is stable $\delta < 4.8795$ and loses its stability at $\delta = 4.8795$, and an invariant circle appears at $\delta > 4.8795$ (see Figures 10 and 11). Here $\alpha = -0.9523$, $\beta = 0.3096$, and $s = -0.9172$.

5. Conclusions

In recent years, the Allee effect has drawn considerable attention in almost every aspect of ecology and conservation. The consequences of Allee effect become more and more significant. In this paper, based on the discrete-time predator-prey system with predator partially dependent on prey and crowding effect of predator, we investigated the impact of Allee

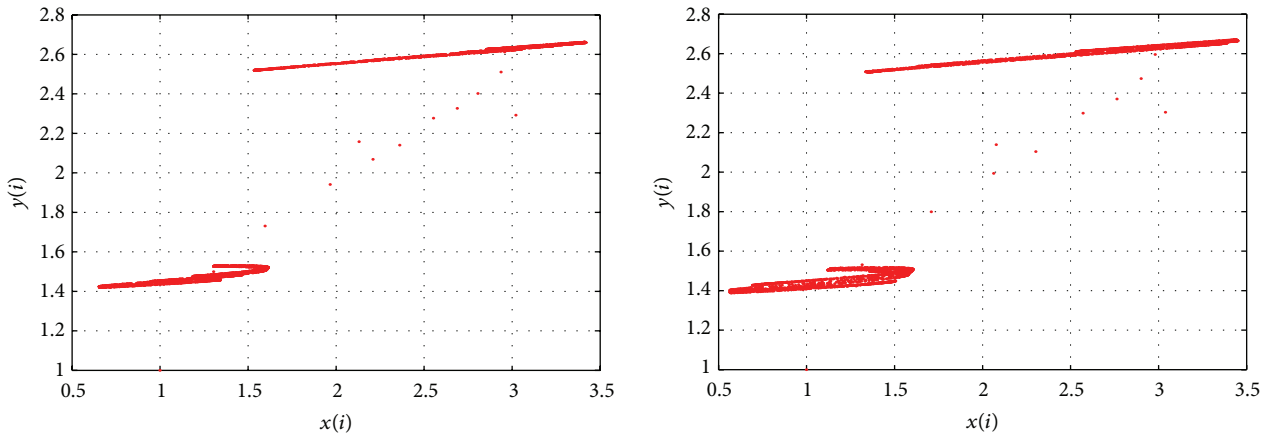

Figure 5: The portraits for several values of $A_1 = 0.03$, $\delta = 5.7$, and $\delta = 5.75$.

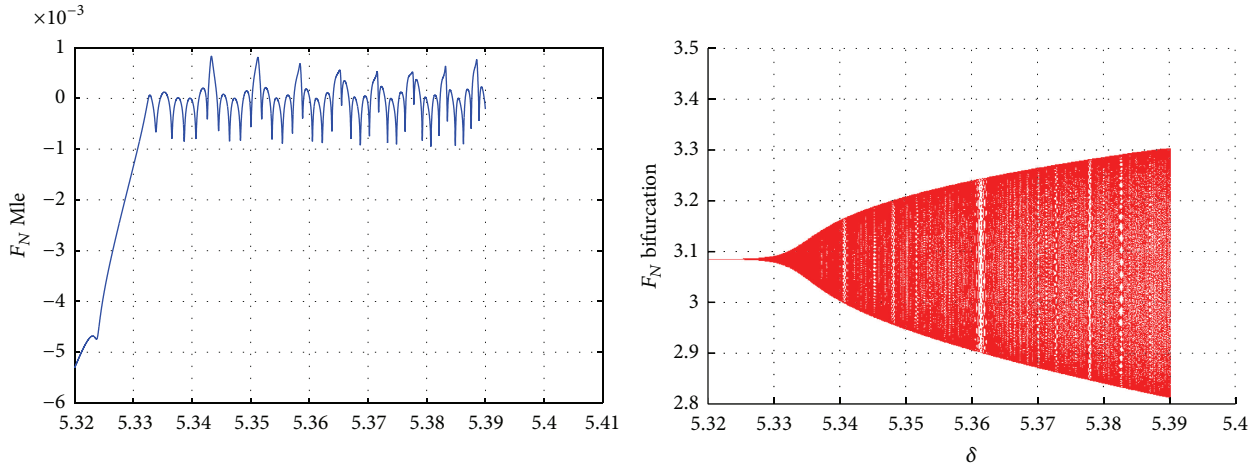

Figure 6: Largest Lyapunov exponents and bifurcation diagram of system (25) for $a = 0.8$, $b = 0.8$, $c = 0.4$, $d = 0.2$, $k = 5$, $l = 3$, and $A_1 = 0.18$ with the initial value of $(x, y) = (1, 1)$ and δ covering $[5.32, 5.39]$.

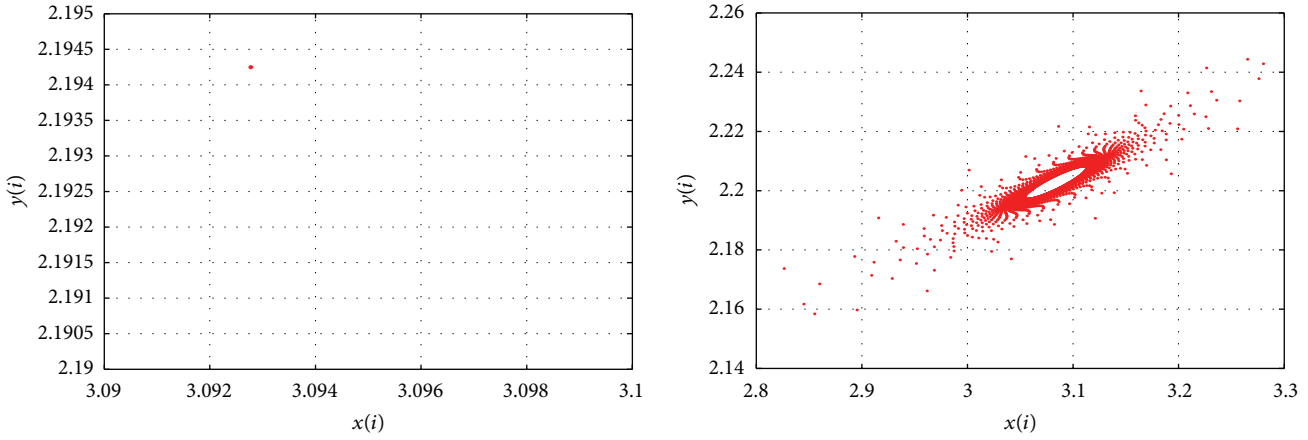

Figure 7: The portraits for several values of $A_1 = 0.18$, $\delta = 5.3$, and $\delta = 5.335$.

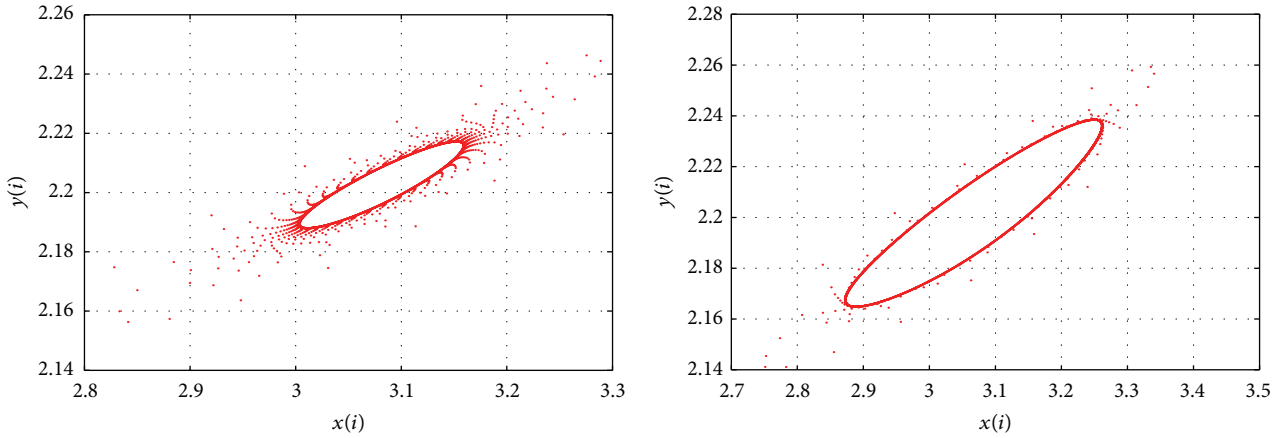

Figure 8: The portraits for several values of $A_1 = 0.18$, $\delta = 5.34$, and $\delta = 5.37$.

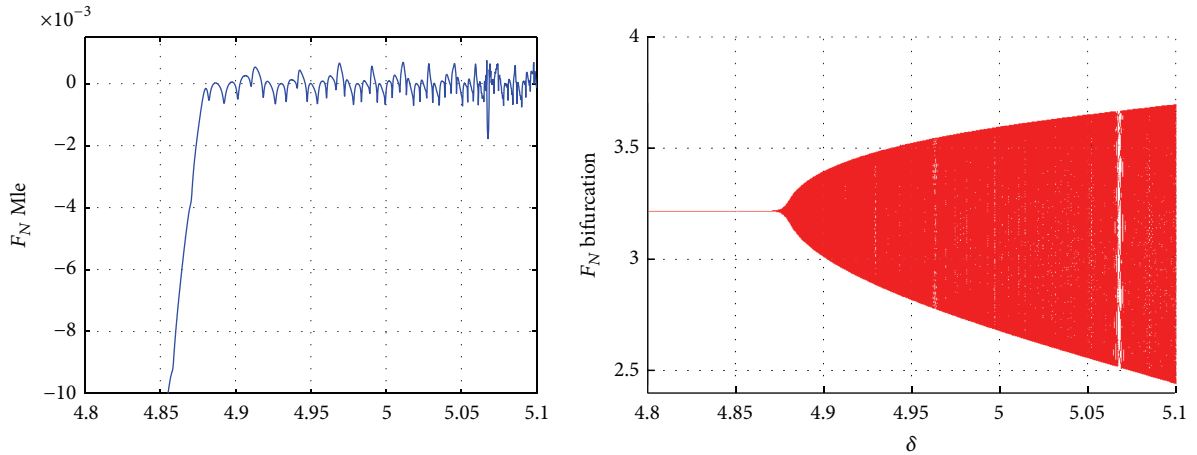

Figure 9: Largest Lyapunov exponents and bifurcation diagram of system (25) for $a = 0.8$, $b = 0.8$, $c = 0.4$, $d = 0.2$, $k = 5$, $l = 3$, and $A_1 = 0.03$ with the initial value of $(x, y) = (1, 1)$ and δ covering $[4.8, 5.1]$.

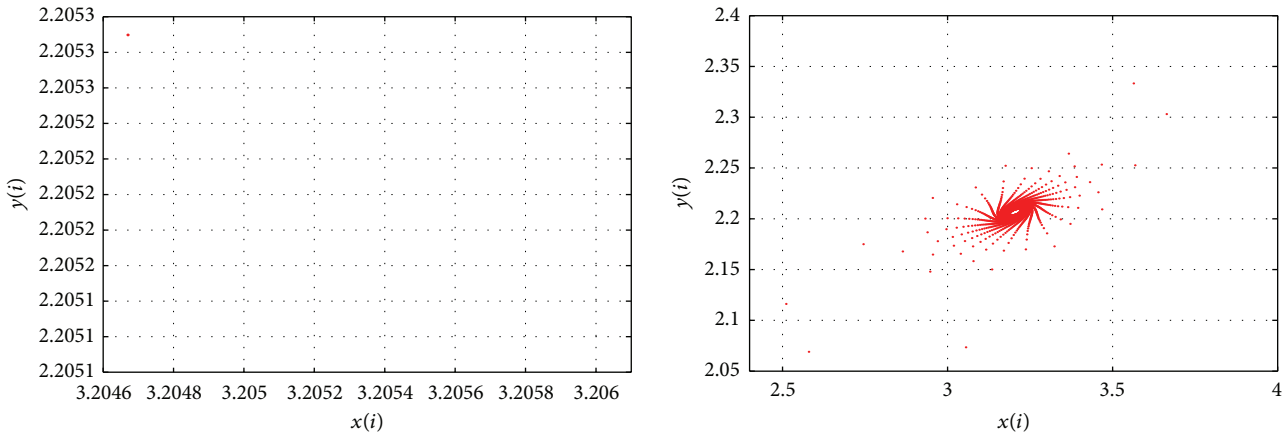

Figure 10: The portraits for several values of $A_1 = 0.03$, $\delta = 4.875$, and $\delta = 4.8795$.

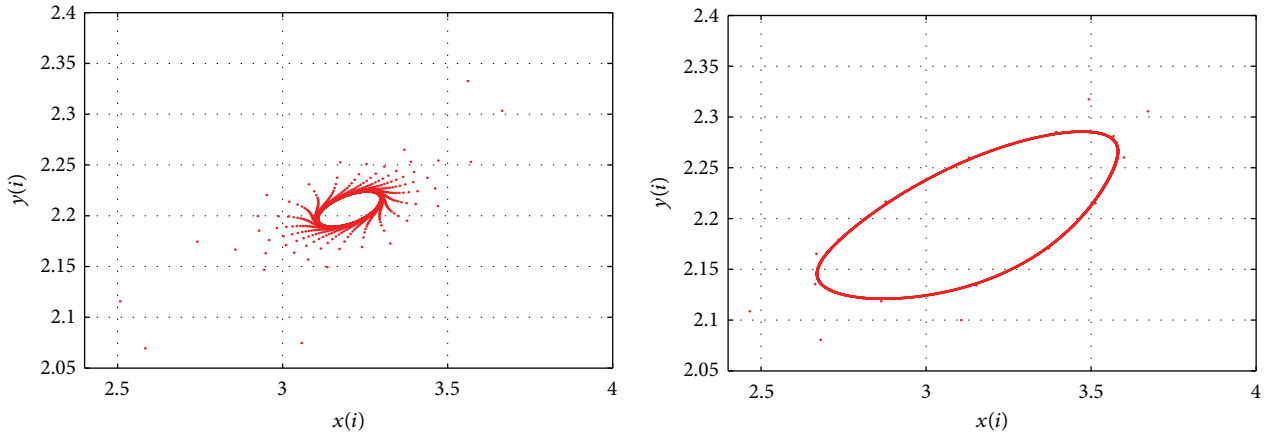

FIGURE 11: The portraits for several values of $A_1 = 0.03$, $\delta = 4.885$, and $\delta = 5$.

effect on the stability of a predator-prey system when the species is subject to Allee effect in the closed first quadrant R_+^2.

By analyzing system (9), we found that the system is asymptotically stable at the $p_2(0, c/d)$, $p_3(x^*, y^*)$ at the interior of the first quadrant for any parameter values. Ecologically speaking, this means that there only exists predator at $p_2(0, c/d)$, in which δ satisfies $0 < \delta < \min\{2/c, 2dl/bc\}$, and the prey and predator species coexist at $p_3(x^*, y^*)$, which should satisfy either condition (1): $G^2 - 4H \geq 0$ and $0 < \delta < (-G - \sqrt{G^2 - 4H})/H$ or condition (2): $G^2 - 4H < 0$ and $0 < \delta < -G/H$.

It is shown that system (9) with Allee effect can go through flip bifurcation and Hopf bifurcation at the neighborhood of the equilibrium point. Because one of the eigen values of fixed point $p_1(k, 0)$ is -1 and magnitude of other is not equal to 1 when $\delta = 2/a + 2A_1/ak$, a flip bifurcation occurs when a parameter changes in small neighborhood of $\delta = 2/a + 2A_1/ak$. The point $p_2(0, c/d)$ undergoes flip bifurcation when the parameter changes in small neighborhood of $F_A = \{(a, b, c, d, k, l, m, \delta, A_1), \delta = 2/c, \delta \neq 2dl/bc, a, b, c, d, k, l, m, \delta, A_1 > 0\}$. Finally, at the positive equilibrium point $p_3(x^*, y^*)$, by our analysing a flip bifurcation will occur in the neighborhood of $F_{B1} = \{(a, b, c, d, k, l, m, \delta, A_1) : \delta = (-G - \sqrt{G^2 - 4H})/H, G^2 - 4H \geq 0$ and $a, b, c, d, k, l, m, \delta, A_1 > 0\}$ or $F_{B2} = \{(a, b, c, d, k, l, m, \delta, A_1) : \delta = (-G + \sqrt{G^2 - 4H})/H, G^2 - 4H \geq 0$ and $a, b, c, d, k, l, m, \delta, A_1 > 0\}$. In contrast, the system will get through a Hopf bifurcation at the neighborhood of $H_B = \{(a, b, c, d, k, l, m, \delta, A_1) : \delta = -G/H, G^2 - 4H < 0$ and $a, b, c, d, k, l, m, \delta, A_1 > 0\}$.

In the paper, we assume the parameter $A_1 > 0$; that is, we only consider the strong Allee effect. When $A_1 < 0$, it is the weak Allee effect, and it is not the same as the $A_1 > 0$. This is the situation we have to consider in the future.

Competing Interests

The authors declare that there is no conflict of interests regarding the publication of this paper.

Acknowledgments

This work was supported by the National Natural Science Foundation of Henan Education committee (Grant no. 201113110034) and Science and Technology Program of Henan Province (Grant no. 162102310604).

References

[1] A. A. Berryman, "The origins and evolution of predator-prey theory," *Ecology*, vol. 73, no. 5, pp. 1530–1535, 1992.

[2] J. Dhar, "A prey-predator model with diffusion and a supplementary resource for the prey in a two-patch environment," *Mathematical Modelling and Analysis*, vol. 9, no. 1, pp. 9–24, 2004.

[3] J. Dhar and K. S. Jatav, "Mathematical analysis of a delayed stage-structured predator-prey model with impulsive diffusion between two predators territories," *Ecological Complexity*, vol. 16, pp. 59–67, 2013.

[4] B. Dubey, "A prey-predator model with a reserved area," *Nonlinear Analysis: Modelling and Control*, vol. 12, no. 4, pp. 479–494, 2007.

[5] H. Freedman, *Deterministic Mathematical Models in Population Ecology*, HIFR Consulting, Edmonton, Canada, 1980.

[6] J. M. Jeschke, M. Kopp, and R. Tollrian, "Predator functional responses: discriminating between handling and digesting prey," *Ecological Monographs*, vol. 72, no. 1, pp. 95–112, 2002.

[7] R. E. Kooij and A. Zegeling, "A predator-prey model with Ivlev's functional response," *Journal of Mathematical Analysis and Applications*, vol. 198, no. 2, pp. 473–489, 1996.

[8] A. J. Lotka, Scientific Books: Elements of Physical Biology, vol. 66, pp. 281–282, 1927.

[9] W. Ma and Y. Takeuchi, "Stability analysis on a predator-prey system with distributed delays," *Journal of Computational and Applied Mathematics*, vol. 88, no. 1, pp. 79–94, 1998.

[10] R. M. May, *Stability and Complexity in Model Ecosystems*, vol. 6, Princeton University Press, 2001.

[11] M. Sen, M. Banerjee, and A. Morozov, "Bifurcation analysis of a ratio-dependent prey-predator model with the Allee effect," *Ecological Complexity*, vol. 11, pp. 12–27, 2012.

[12] S. Sinha, O. P. Misra, and J. Dhar, "Modelling a predator-prey system with infected prey in polluted environment," *Applied Mathematical Modelling*, vol. 34, no. 7, pp. 1861–1872, 2010.

[13] V. Volterra, "Fluctuations in the abundance of a species considered mathematically," *Nature*, vol. 118, no. 2972, pp. 558–560, 1926.

[14] J. Dhar, H. Singh, and H. S. Bhatti, "Discrete-time dynamics of a system with crowding effect and predator partially dependent on prey," *Applied Mathematics and Computation*, vol. 252, pp. 324–335, 2015.

[15] W. Allee, *Animal Aggregations: A Study in General Sociology*, University of Chicago Press, Chicago, Ill, USA, 1931.

[16] E. D. Conway and J. A. Smoller, "Global analysis of a system of predator-prey equations," *SIAM Journal on Applied Mathematics*, vol. 46, no. 4, pp. 630–642, 1986.

[17] A. D. Bazykin, *Nonlinear Dynamics of Interacting Populations*, vol. 11 of *World Scientific Series on Nonlinear Science Series A*, World Scientific, River Edge, NJ, USA, 1998.

[18] E. González-Olivares, J. Mena-Lorca, A. Rojas-Palma, and J. D. Flores, "Dynamical complexities in the Leslie-Gower predator-prey model as consequences of the Allee effect on prey," *Applied Mathematical Modelling*, vol. 35, no. 1, pp. 366–381, 2011.

[19] P. J. Pal and P. K. Mandal, "Bifurcation analysis of a modified Leslie-Gower predator-prey model with Beddington-DeAngelis functional response and strong Allee effect," *Mathematics and Computers in Simulation*, vol. 97, pp. 123–146, 2014.

[20] L. Berec, E. Angulo, and F. Courchamp, "Multiple Allee effects and population management," *Trends in Ecology and Evolution*, vol. 22, no. 4, pp. 185–191, 2007.

[21] D. S. Boukal and L. Berec, "Single-species models of the Allee effect: extinction boundaries, sex ratios and mate encounters," *Journal of Theoretical Biology*, vol. 218, no. 3, pp. 375–394, 2002.

[22] D. S. Boukal, M. W. Sabelis, and L. Berec, "How predator functional responses and Allee effects in prey affect the paradox of enrichment and population collapses," *Theoretical Population Biology*, vol. 72, no. 1, pp. 136–147, 2007.

[23] G. Wang, X.-G. Liang, and F.-Z. Wang, "The competitive dynamics of populations subject to an Allee effect," *Ecological Modelling*, vol. 124, no. 2-3, pp. 183–192, 1999.

[24] E. González-Olivares, B. González-Yañez, J. Mena-Lorca, and R. Ramos-Jiliberto, "Modelling the Allee effect: are the different mathematical forms proposed equivalents?" in *Proceedings of the International Symposium on Mathematical and Computational Biology*, R. Mondaini, Ed., pp. 53–71, E-Papers Serviços Editoriais Ltda, Rio de Janeiro, Brazil, 2007.

[25] F. Courchamp, T. Clutton-Brock, and B. Grenfell, "Inverse density dependence and the Allee effect," *Trends in Ecology and Evolution*, vol. 14, no. 10, pp. 405–410, 1999.

[26] P. A. Stephens and W. J. Sutherland, "Consequences of the Allee effect for behaviour, ecology and conservation," *Trends in Ecology and Evolution*, vol. 14, no. 10, pp. 401–405, 1999.

[27] J. Zu, "Global qualitative analysis of a predator-prey system with Allee effect on the prey species," *Mathematics and Computers in Simulation*, vol. 94, pp. 33–54, 2013.

[28] X. Liu and D. Xiao, "Complex dynamic behaviors of a discrete-time predator-prey system," *Chaos, Solitons & Fractals*, vol. 32, no. 1, pp. 80–94, 2007.

[29] Z. He and X. Lai, "Bifurcation and chaotic behavior of a discrete-time predator-prey system," *Nonlinear Analysis: Real World Applications*, vol. 12, no. 1, pp. 403–417, 2011.

[30] J. Guckenheimer and P. Holmes, *Nonlinear Oscillations, Dynamical Systems, and Bifurcations of Vector Fields*, vol. 42 of *Applied Mathematical Sciences*, Springer, New York, NY, USA, 1983.

Hindawi Publishing Corporation
Discrete Dynamics in Nature and Society
Volume 2016, Article ID 1026726, 7 pages
http://dx.doi.org/10.1155/2016/1026726

Research Article

Existence of Nonoscillatory Solutions of Higher-Order Neutral Differential Equations with Distributed Coefficients and Delays

Youjun Liu,[1] Huanhuan Zhao,[1] and Jurang Yan[2]

[1]*College of Mathematics and Computer Sciences, Shanxi Datong University, Datong, Shanxi 037009, China*
[2]*School of Mathematical Sciences, Shanxi University, Taiyuan, Shanxi 030006, China*

Correspondence should be addressed to Youjun Liu; lyj9791@126.com

Received 23 May 2016; Revised 11 July 2016; Accepted 12 July 2016

Academic Editor: Massimiliano Ferrara

Copyright © 2016 Youjun Liu et al. This is an open access article distributed under the Creative Commons Attribution License, which permits unrestricted use, distribution, and reproduction in any medium, provided the original work is properly cited.

We consider the existence of nonoscillatory solutions of higher-order neutral differential equations with distributed coefficients. We use the *Banach* contraction principle to obtain new sufficient condition for the existence of nonoscillatory solutions.

1. Introduction

In this paper, we consider the higher-order nonlinear neutral differential equation with distributed deviating arguments:

$$\left[\Phi\left[r(t)\,x(t)+\int_a^b p(t,\theta)\,x(t-\theta)\,d\theta\right]\right]^{(n)} + \int_c^d q_1(t,\tau)\,g_1(x(t-\tau))\,d\tau - \int_e^f q_2(t,\sigma)\,g_2(x(t-\sigma))\,d\sigma = h(t). \tag{1}$$

Throughout this paper, the following conditions are assumed to hold:

(1) where $n \geq 1$ is a positive integer, $r \in C([t_0, \infty), R^+)$, $0 < a < b$, $0 < c < d$, $0 < e < f$;

(2) $p \in C([t_0,\infty) \times [a,b], R)$, $q_1 \in C([t_0,\infty) \times [c,d], R^+)$, $q_2 \in C([t_0,\infty) \times [e,f], R^+)$, $h \in C([t_0,\infty), R)$;

(3) $\Phi(u)$ are continuously increasing real odd function with respect to u defined on R, and $\Phi^{-1}(u)$ satisfy the local *Lipschitz* condition;

(4) $g_i \in C(R,R)$, $g_i(u)$ satisfy the local *Lipschitz* condition and $ug_i(u) > 0$, $i = 1, 2$, for $u \neq 0$.

Recently there have been a lot of activities concerning the existence of nonoscillatory solutions for neutral differential equations with positive and negative coefficient. In 2002, Zhou and Zhang [1] studied higher-order linear neutral delay differential equation:

$$\frac{d^n}{dt^n}[x(t)+cx(t-\tau)] + (-1)^{n+1}[P(t)\,x(t-\sigma) - Q(t)\,x(t-\delta)] = 0. \tag{2}$$

In 2005, the existence of nonoscillatory solutions of first-order linear neutral delay differential equations of the form

$$\frac{d}{dt}[x(t)+P(t)\,x(t-\tau)] + Q_1(t)\,x(t-\sigma_1) - Q_2(t)\,x(t-\sigma_2) = 0 \tag{3}$$

was investigated by Zhang et al. [2] and, in the same year, Yu and Wang [3] studied nonoscillatory solutions of second-order nonlinear neutral differential equations of the form

$$\left[r(t)\left[x(t)+P(t)\,x(t-\tau)\right]'\right]' + Q_1(t)\,f(x(t-\sigma_1)) - Q_2(t)\,g(x(t-\sigma_2)) = 0. \tag{4}$$

In 2010, Candan and Dahiya [4] studied nonoscillatory solutions of first-order and second-order nonlinear neutral differential equations with positive and negative coefficients:

$$\frac{d^k}{dt^k}[x(t)+P(t)\,x(t-\tau)] + \int_a^b q_1(t,\xi)\,x(t-\xi)\,d\xi - \int_c^d q_2(t,\mu)\,x(t-\mu)\,d\mu = 0, \quad k = 1, 2. \tag{5}$$

In 2012, Candan [5] study higher-order nonlinear differential equation:

$$\left[r(t)\left[x(t)+P(t)x(t-\tau)\right]^{(n-1)}\right]' + (-1)^n \cdot \left[Q_1(t)g_1\left(x\left(t-\sigma_1\right)\right) - Q_2(t)g_2\left(x\left(t-\mu\right)\right) - f(t)\right] = 0. \tag{6}$$

In 2015, Liu et al. [6] study higher-order neutral differential equation with distributed deviating arguments:

$$\left[r(t)x(t)+P(t)x(t-\theta)\right]^{(n)} + \int_c^d q_1(t,\tau)g_1(x(t-\tau))\,d\tau - \int_e^f q_2(t,\sigma)g_2(x(t-\sigma))\,d\sigma = f(t). \tag{7}$$

As can be seen from the development process of the above equations, the delay of neutral part in the discussed differential equations was all constant delays, and the main thought in the employed verification method also kept the same in which the coefficient neutral part in the neutral was all discussed in four cases, that is, $(-\infty,-1)$, $(-1,0)$, $(0,1)$, and $(1,+\infty)$, and then was verified by constructing the corresponding operator. However, the case for distributed deviating arguments is rather rare. In 2013, Candan [7] studied first-order neutral differential equation with distributed deviating arguments:

$$\left[\left[x(t)-\int_a^b p_2(t,\xi)x(t-\xi)\,d\xi\right]^{\gamma}\right]' + \int_c^d Q_2(t,\xi)G(x(t-\xi))\,d\xi = 0, \tag{8}$$

where γ is a ratio of odd positive integers; however the discussion only covered the condition for coefficient being $0 < \int_a^b p_2(t,\xi)d\xi < 1$, while being without the other three conditions, which might be caused by the difficulty in establishing feasible operator. In view of the above, here, in this paper, the difficulty of operator establishment was settled and sufficient condition for the existence of nonoscillatory solutions of differential equation with coefficient of $\int_a^b p_2(t,\xi)d\xi$ in the four cases was obtained. Thus, this paper may present its theoretical value as well as practical application value. For related work, we refer the reader to the references [8–12].

As usual, a solution of (1) is said to be oscillatory if it has arbitrarily large zeros. Otherwise the solution is said to be nonoscillatory.

A solution of (1) is a continuous function $x(t)$ defined on $[t_1-\mu,\infty)$, for some $t_1 > t_0$, such that $\Phi(r(t)x(t) + \int_a^b p(t,\theta)x(t-\theta)d\theta)$ is n times continuously differentiable and (1) holds for all $n \geq 1$. Here, $\mu = \max\{b,d,f\}$.

Let L_i, $i = 1,2$ denote the *Lipschitz* constants of functions g_i, $i = 1,2$ on the set A, K denote the *Lipschitz* constants of functions $\Phi^{-1}(u)$, respectively, and $L = \max\{L_1,L_2\}$, $\beta_i = \max_{x\in A} g_i(x)$, $i = 1,2$.

2. The Main Results

Theorem 1. *Assume that* $0 \leq \int_a^b p(t,\theta)d\theta \leq p_1 < 1$, $1 \leq r(t) \leq 1/p_1$, *and*

$$\int_t^\infty s^{n-1}\int_c^d q_1(s,\tau)\,d\tau\,ds < \infty,\quad \int_t^\infty s^{n-1}\int_e^f q_2(s,\sigma)\,d\sigma\,ds < \infty,\quad \int_t^\infty s^{n-1}h(s)\,ds < \infty. \tag{9}$$

Then (1) has a bounded nonoscillatory solution.

Proof. Let Λ be the set of all continuous and bounded functions on $[t_0,\infty)$ and the norm be $\|x(t)\| = \sup_{t_0\leq t<+\infty} x(t)$. Set $A = \{x \in \Lambda,\ M_1 \leq x(t) \leq M_2,\ t \geq t_0\}$, where M_1, M_2 are two positive constants such that $p_1M_2 + M_1/p_1 < \alpha < M_2$. From (9), one can choose $t_1 \geq t_0 + \mu$ and sufficiently large $t \geq t_1$ such that

$$\int_t^\infty \frac{(s-t)^{n-1}}{(n-1)!}\left[\beta_1\int_c^d q_1(s,\tau)\,d\tau + |h(s)|\right]ds \leq \Phi(M_2) - \Phi(\alpha), \tag{10}$$

$$\int_t^\infty \frac{(s-t)^{n-1}}{(n-1)!}\left[\beta_2\int_e^f q_2(s,\sigma)\,d\sigma + |h(s)|\right]ds \leq \Phi(\alpha) - \Phi\left(p_1M_2 + \frac{M_1}{p_1}\right), \tag{11}$$

$$\int_t^\infty \frac{(s-t)^{n-1}}{(n-1)!}\left[\int_c^d q_1(s,\tau)\,d\tau + \int_e^f q_2(s,\sigma)\,d\sigma\right]ds \leq \frac{1-p_1}{KL}, \tag{12}$$

and define an operator T on A as follows:

$$(Tx)(t) = \begin{cases} \dfrac{1}{r(t)}\left\{-\displaystyle\int_a^b p(t,\theta)x(t-\theta)\,d\theta + \Phi^{-1}\left[\Phi(\alpha) + \int_t^\infty \frac{(s-t)^{n-1}}{(n-1)!}\left[\int_c^d q_1(s,\tau)g_1(x(s-\tau))\,d\tau - \int_e^f q_2(s,\sigma)g_2(x(s-\sigma))\,d\sigma - h(s)\right]ds\right]\right\}, & t \geq t_1, \\ (Tx)(t_1), & t_0 \leq t \leq t_1. \end{cases} \tag{13}$$

It is easy to see that T is continuous, for $t \geq t_1$, $x \in A$. By using (10), we have

$$\begin{aligned}(Tx)(t) &\leq \frac{1}{r(t)}\left\{\Phi^{-1}\left[\Phi(\alpha)\right.\right.\\ &\quad\left.\left.+\int_t^{\infty}\frac{(s-t)^{n-1}}{(n-1)!}\left[\int_c^d q_1(s,\tau)\,g_1(x(s-\tau))\,d\tau - h(s)\right]ds\right]\right\}\\ &\leq \Phi^{-1}\left[\Phi(\alpha)\right.\\ &\quad\left.+\int_t^{\infty}\frac{(s-t)^{n-1}}{(n-1)!}\left(\beta_1\int_c^d q_1(s,\tau)\,d\tau + |h(s)|\right)ds\right]\\ &\leq \Phi^{-1}\left[\Phi(\alpha)+\Phi(M_2)-\Phi(\alpha)\right] = M_2,\end{aligned} \tag{14}$$

and, taking (11) into account, we have

$$\begin{aligned}(Tx)(t) &\geq \frac{1}{r(t)}\left\{-\int_a^b p(t,\theta)\,x(t-\theta)\,d\theta - \Phi^{-1}\left[\Phi(\alpha)\right.\right.\\ &\quad\left.\left.-\int_t^{\infty}\frac{(s-t)^{n-1}}{(n-1)!}\left[\int_e^f q_2(s,\sigma)\,g_2(x(s-\sigma))\,d\sigma + h(s)\right]ds\right]\right\}\\ &\geq p_1\left\{-p_1M_2+\Phi^{-1}\left[\Phi(\alpha)\right.\right.\\ &\quad\left.\left.-\int_t^{\infty}\frac{(s-t)^{n-1}}{(n-1)!}\left(\beta_2\int_e^f q_2(s,\sigma)\,d\sigma + |h(s)|\right)ds\right]\right\}\\ &\geq p_1\left\{-p_1M_2+\Phi^{-1}\left[\Phi(\alpha)-\Phi(\alpha)+\Phi\left(p_1M_2+\frac{M_1}{p_1}\right)\right]\right\}\\ &= M_1.\end{aligned} \tag{15}$$

These show that $TA \subset A$. Since A is bounded, close, convex subset of Λ, in order to apply the contraction principle we have to show that T is a contraction mapping on A. For $\forall x_1, x_2 \in A$, and $t \geq t_1$,

$$\begin{aligned}\left|(Tx_1)(t)-(Tx_2)(t)\right| &\leq \frac{1}{r(t)}\left\{\int_a^b p(t,\theta)\left|x_1(t-\theta)-x_2(t-\theta)\right|d\theta + \Phi^{-1}\left[\Phi(\alpha)\right.\right.\\ &\quad+\int_t^{\infty}\frac{(s-t)^{n-1}}{(n-1)!}\left|\int_c^d q_1(s,\tau)\,g_1\left(x_1(s-\tau)\right)d\tau - \int_e^f q_2(s,\sigma)\,g_2\left(x_1(s-\sigma)\right)d\sigma - h(s)\right|ds\Big] - \Phi^{-1}\Big[\Phi(\alpha)\\ &\quad\left.+\int_t^{\infty}\frac{(s-t)^{n-1}}{(n-1)!}\left|\int_c^d q_1(s,\tau)\,g_1\left(x_2(s-\tau)\right)d\tau - \int_e^f q_2(s,\sigma)\,g_2\left(x_2(s-\sigma)\right)d\sigma - h(s)\right|ds\right]\right\} \leq \frac{1}{r(t)}\left\{p_1\left|x_1-x_2\right|\right.\\ &\quad+K\int_t^{\infty}\frac{(s-t)^{n-1}}{(n-1)!}\left[\int_c^d q_1(s,\tau)\left|g_1\left(x_1(s-\tau)\right)-g_1\left(x_2(s-\tau)\right)\right|d\tau\right.\\ &\quad\left.\left.+\int_e^f q_2(s,\sigma)\left|g_2\left(x_1(s-\sigma)\right)-g_2\left(x_2(s-\sigma)\right)\right|d\sigma\right]ds\right\}.\end{aligned} \tag{16}$$

Using (12),

$$\begin{aligned}\left|(Tx_1)(t)-(Tx_2)(t)\right| &\leq \left|x_1-x_2\right|\left(p_1\right.\\ &\quad+KL\int_t^{\infty}\frac{(s-t)^{n-1}}{(n-1)!}\left[\int_c^d q_1(s,\tau)\,d\tau\right.\\ &\quad\left.\left.+\int_e^f q_2(s,\sigma)\,d\sigma\right]ds\right) < \rho\left|x_1-x_2\right|.\end{aligned} \tag{17}$$

This implies with the sup norm that

$$\left\|Tx_1-Tx_2\right\| < \rho\left\|x_1-x_2\right\|, \tag{18}$$

where $\rho = 1$, which shows that T is a contraction mapping on A and therefore there exists a unique solution, obviously a bounded positive solution of (1) $x \in A$, such that $Tx = x$. The proof is complete. □

Theorem 2. *Assume that* $1 < p_3 \leq \int_a^b p(t,\theta)d\theta \leq p_2 < 2p_3 < +\infty$, $2p_3 \leq r(t) \leq 2p_2$ *and that (9) holds.*

Then (1) has a bounded nonoscillatory solution.

Proof. Let Λ be the set of all continuous and bounded functions on $[t_0,\infty)$ and the norm be $\|x(t)\| = \sup_{t_0\leq t<+\infty}x(t)$. Set $A = \{x \in \Lambda,\ M_3 \leq x(t) \leq M_4,\ t \geq t_0\}$, where M_3, M_4 are two positive constants such that $p_2M_4+2p_2M_3 < \alpha < 2p_3M_4$. From (9), one can choose $t_1 \geq t_0 + \mu$ and sufficiently large $t \geq t_1$ such that

$$\begin{aligned}&\int_t^{\infty}\frac{(s-t)^{n-1}}{(n-1)!}\left[\beta_1\int_c^d q_1(s,\tau)\,d\tau + |h(s)|\right]ds\\ &\quad\leq \Phi\left(2p_3M_4\right)-\Phi(\alpha),\end{aligned} \tag{19}$$

$$\begin{aligned}&\int_t^{\infty}\frac{(s-t)^{n-1}}{(n-1)!}\left[\beta_2\int_e^f q_2(s,\sigma)\,d\sigma + |h(s)|\right]ds\\ &\quad\leq \Phi(\alpha)-\Phi\left(p_2M_4-2p_2M_3\right),\end{aligned} \tag{20}$$

$$\begin{aligned}&\int_t^{\infty}\frac{(s-t)^{n-1}}{(n-1)!}\left[\int_c^d q_1(s,\tau)\,d\tau + \int_e^f q_2(s,\sigma)\,d\sigma\right]ds\\ &\quad\leq \frac{2p_3-p_2}{KL},\end{aligned} \tag{21}$$

and define an operator T on A as follows:

$$(Tx)(t) = \begin{cases} \dfrac{1}{r(t)}\left\{-\displaystyle\int_a^b p(t,\theta)\,x(t-\theta)\,d\theta + \Phi^{-1}\left[\Phi(\alpha) + \int_t^\infty \frac{(s-t)^{n-1}}{(n-1)!}\left[\int_c^d q_1(s,\tau)\,g_1(x(s-\tau))\,d\tau - \int_e^f q_2(s,\sigma)\,g_2(x(s-\sigma))\,d\sigma - h(s)\right]ds\right]\right\}, & t \ge t_1, \\ (Tx)(t_1), & t_0 \le t \le t_1. \end{cases} \tag{22}$$

It is easy to see that T is continuous, for $t \ge t_1$, $x \in A$. By using (19), we have

$$\begin{aligned} (Tx)(t) &\le \frac{1}{r(t)}\left\{\Phi^{-1}\left[\Phi(\alpha) + \int_t^\infty \frac{(s-t)^{n-1}}{(n-1)!}\left[\int_c^d q_1(s,\tau)\,g_1(x(s-\tau))\,d\tau - h(s)\right]ds\right]\right\} \\ &\le \frac{1}{2p_3}\left\{\Phi^{-1}\left[\Phi(\alpha) + \int_t^\infty \frac{(s-t)^{n-1}}{(n-1)!}\left[\beta_1\int_c^d q_1(s,\tau)\,d\tau + |h(s)|\right]ds\right]\right\} \le M_4, \end{aligned} \tag{23}$$

and, taking (20) into account, we have

$$\begin{aligned} (Tx)(t) &\ge \frac{1}{r(t)}\left\{-\int_a^b p(t,\theta)\,x(t-\theta)\,d\theta + \Phi^{-1}\left[\Phi(\alpha) - \int_t^\infty \frac{(s-t)^{n-1}}{(n-1)!}\left[\int_e^f q_2(s,\sigma)\,g_2(x(s-\sigma))\,d\sigma + h(s)\right]ds\right]\right\} \\ &\ge \frac{1}{2p_2}\left\{-p_2M_4 + \Phi^{-1}\left[\Phi(\alpha) - \int_t^\infty \frac{(s-t)^{n-1}}{(n-1)!}\left(\beta_2\int_e^f q_2(s,\sigma)\,d\sigma + |h(s)|\right)ds\right]\right\} \ge M_3. \end{aligned} \tag{24}$$

These show that $TA \subset A$. Since A is bounded, close, convex subset of Λ, in order to apply the contraction principle, we have to show that T is a contraction mapping on A. For $\forall x_1, x_2 \in A$, and $t \ge t_1$,

$$\begin{aligned} \left|(Tx_1)(t) - (Tx_2)(t)\right| &\le \frac{1}{r(t)}\left\{\int_a^b p(t,\theta)\left|x_1(t-\theta) - x_2(t-\theta)\right|d\theta + \Phi^{-1}\left[\Phi(\alpha)\right.\right. \\ &+ \int_t^\infty \frac{(s-t)^{n-1}}{(n-1)!}\left|\int_c^d q_1(s,\tau)\,g_1\left(x_1(s-\tau)\right)d\tau - \int_e^f q_2(s,\sigma)\,g_2\left(x_1(s-\sigma)\right)d\sigma - h(s)\right|ds\Big] - \Phi^{-1}\left[\Phi(\alpha)\right. \\ &\left.\left.+ \int_t^\infty \frac{(s-t)^{n-1}}{(n-1)!}\left|\int_c^d q_1(s,\tau)\,g_1\left(x_2(s-\tau)\right)d\tau - \int_e^f q_2(s,\sigma)\,g_2\left(x_2(s-\sigma)\right)d\sigma - h(s)\right|ds\right]\right\} \le \frac{1}{r(t)}\left\{p_2\left|x_1 - x_2\right|\right. \\ &+ K\int_t^\infty \frac{(s-t)^{n-1}}{(n-1)!}\left[\int_c^d q_1(s,\tau)\left|g_1\left(x_1(s-\tau)\right) - g_1\left(x_2(s-\tau)\right)\right|d\tau\right. \\ &\left.\left.+ \int_e^f q_2(s,\sigma)\left|g_2\left(x_1(s-\sigma)\right) - g_2\left(x_2(s-\sigma)\right)\right|d\sigma\right]ds\right\}. \end{aligned} \tag{25}$$

Or, using (21),

$$\begin{aligned} \left|(Tx_1)(t) - (Tx_2)(t)\right| &\le \left|x_1 - x_2\right|\frac{1}{2p_3}\left\{p_2\right. \\ &+ KL\int_t^\infty \frac{(s-t)^{n-1}}{(n-1)!}\left[\int_c^d q_1(s,\tau)\,d\tau\right. \\ &\left.\left.+ \int_e^f q_2(s,\sigma)\,d\sigma\right]ds\right\} < \rho\left|x_1 - x_2\right|. \end{aligned} \tag{26}$$

This implies with the sup norm that

$$\left\|Tx_1 - Tx_2\right\| < \rho\left\|x_1 - x_2\right\|, \tag{27}$$

where $\rho = 1$, which shows that T is a contraction mapping on A and therefore there exists a unique solution, obviously a bounded positive solution of (1) $x \in A$, such that $Tx = x$. The proof is complete. □

Theorem 3. *Assume that* $-1 < p_4 \le \int_a^b p(t,\theta)d\theta \le 0, 1 \le r(t) \le 1/-p_4$ *and that (9) holds.*

Then (1) has a bounded nonoscillatory solution.

Proof. Let Λ be the set of all continuous and bounded functions on $[t_0, \infty)$ and the norm be $\|x(t)\| = \sup_{t_0 \le t < +\infty} x(t)$. Set $A = \{x \in \Lambda,\ M_5 \le x(t) \le M_6,\ t \ge t_0\}$, where M_5, M_6 are two positive constants such that $M_5/-p_4 < \alpha < (1+p_4)M_6$.

From (9), one can choose $t_1 \geq t_0 + \mu$ and sufficiently large $t \geq t_1$ such that

$$\begin{aligned}
&\int_t^\infty \frac{(s-t)^{n-1}}{(n-1)!}\left[\beta_1 \int_c^d q_1(s,\tau)\,d\tau + |h(s)|\right] ds \\
&\quad \leq \Phi\left(\left(1+p_4\right) M_6\right) - \Phi(\alpha), \\
&\int_t^\infty \frac{(s-t)^{n-1}}{(n-1)!}\left[\beta_2 \int_e^f q_2(s,\sigma)\,d\sigma + |h(s)|\right] ds \\
&\quad \leq \Phi(\alpha) - \Phi\left(-\frac{M_5}{p_4}\right),
\end{aligned} \tag{28}$$

$$\int_t^\infty \frac{(s-t)^{n-1}}{(n-1)!}\left[\int_c^d q_1(s,\tau)\,d\tau + \int_e^f q_2(s,\sigma)\,d\sigma\right] ds \leq \frac{1+p_4}{KL}. \tag{29}$$

and define an operator T on A as follows:

$$(Tx)(t) = \begin{cases} \dfrac{1}{r(t)}\left\{-\displaystyle\int_a^b p(t,\theta)\,x(t-\theta)\,d\theta + \Phi^{-1}\left[\Phi(\alpha) + \int_t^\infty \frac{(s-t)^{n-1}}{(n-1)!}\left[\int_c^d q_1(s,\tau)\,g_1(x(s-\tau))\,d\tau - \int_e^f q_2(s,\sigma)\,g_2(x(s-\sigma))\,d\sigma - h(s)\right] ds\right]\right\}, & t \geq t_1, \\ (Tx)(t_1), & t_0 \leq t \leq t_1. \end{cases} \tag{31}$$

It is easy to see that T is continuous, for $t \geq t_1$, $x \in A$. By using (28), we have

$$\begin{aligned}
(Tx)(t) &\leq \frac{1}{r(t)}\left\{-\int_a^b p(t,\theta)\,x(t-\theta)\,d\theta + \Phi^{-1}\left[\Phi(\alpha)\right.\right. \\
&\quad \left.\left. + \int_t^\infty \frac{(s-t)^{n-1}}{(n-1)!}\left[\int_c^d q_1(s,\tau)\,g_1(x(s-\tau))\,d\tau - h(s)\right] ds\right]\right\} \\
&\leq -p_4 M_6 + \Phi^{-1}\left[\Phi(\alpha)\right. \\
&\quad \left. + \int_t^\infty \frac{(s-t)^{n-1}}{(n-1)!}\left[\beta_1 \int_c^d q_1(s,\tau)\,d\tau + |h(s)|\right] ds\right] \leq M_6,
\end{aligned} \tag{32}$$

and, taking (29) into account, we have

$$\begin{aligned}
(Tx)(t) &\geq \frac{1}{r(t)}\left\{-\int_a^b p(t,\theta)\,x(t-\theta)\,d\theta + \Phi^{-1}\left[\Phi(\alpha)\right.\right. \\
&\quad \left.\left. - \int_t^\infty \frac{(s-t)^{n-1}}{(n-1)!}\left[\int_e^f q_2(s,\sigma)\,g_2(x(s-\sigma))\,d\sigma + h(s)\right] ds\right]\right\} \\
&\geq -p_4\left\{\Phi^{-1}\left[\Phi(\alpha)\right.\right. \\
&\quad \left.\left. - \int_t^\infty \frac{(s-t)^{n-1}}{(n-1)!}\left[\beta_2 \int_e^f q_2(s,\sigma)\,d\sigma + |h(s)|\right] ds\right]\right\} \\
&\geq -p_4\left\{\Phi^{-1}\left[\Phi(\alpha) - \Phi(\alpha) + \Phi\left(-\frac{M_5}{p_4}\right)\right]\right\} = M_5.
\end{aligned} \tag{33}$$

These show that $TA \subset A$. Since A is bounded, close, convex subset of Λ, in order to apply the contraction principle, we have to show that T is a contraction mapping on A. For $\forall x_1, x_2 \in A$, and $t \geq t_1$,

$$\begin{aligned}
\left|(Tx_1)(t) - (Tx_2)(t)\right| &\leq \frac{1}{r(t)}\left\{\int_a^b p(t,\theta)\left|x_1(t-\theta) - x_2(t-\theta)\right| d\theta + \Phi^{-1}\left[\Phi(\alpha)\right.\right. \\
&\quad + \int_t^\infty \frac{(s-t)^{n-1}}{(n-1)!}\left|\int_c^d q_1(s,\tau)\,g_1\left(x_1(s-\tau)\right) d\tau - \int_e^f q_2(s,\sigma)\,g_2\left(x_1(s-\sigma)\right) d\sigma - h(s)\right| ds\Big] - \Phi^{-1}\left[\Phi(\alpha)\right. \\
&\quad \left.\left. + \int_t^\infty \frac{(s-t)^{n-1}}{(n-1)!}\left|\int_c^d q_1(s,\tau)\,g_1\left(x_2(s-\tau)\right) d\tau - \int_e^f q_2(s,\sigma)\,g_2\left(x_2(s-\sigma)\right) d\sigma - h(s)\right| ds\right]\right\} \leq \frac{1}{r(t)}\left\{-p_4\left|x_1 - x_2\right|\right. \\
&\quad + K\int_t^\infty \frac{(s-t)^{n-1}}{(n-1)!}\left[\int_c^d q_1(s,\tau)\left|g_1\left(x_1(s-\tau)\right) - g_1\left(x_2(s-\tau)\right)\right| d\tau\right. \\
&\quad \left.\left. + \int_e^f q_2(s,\sigma)\left|g_2\left(x_1(s-\sigma)\right) - g_2\left(x_2(s-\sigma)\right)\right| d\sigma\right] ds\right\}.
\end{aligned} \tag{34}$$

Or, using (30),

$$\begin{aligned}
\left|(Tx_1)(t) - (Tx_2)(t)\right| &\leq \left|x_1 - x_2\right|\left(-p_4\right. \\
&\quad \left. + KL\int_t^\infty \frac{(s-t)^{n-1}}{(n-1)!}\left[\int_c^d q_1(s,\tau)\,d\tau\right.\right. \\
&\quad \left.\left. + \int_e^f q_2(s,\sigma)\,d\sigma\right] ds\right) < \rho\left|x_1 - x_2\right|.
\end{aligned} \tag{35}$$

This implies with the sup norm that

$$\left\|Tx_1 - Tx_2\right\| < \rho\left\|x_1 - x_2\right\|, \tag{36}$$

where $\rho = 1$, which shows that T is a contraction mapping on A and therefore there exists a unique solution, obviously a bounded positive solution of (1) $x \in A$, such that $Tx = x$. The proof is complete. □

Theorem 4. *Assume that* $-\infty < 2p_5 < p_6 \le \int_a^b p(t,\theta)d\theta \le p_5 < -1$, $-2p_5 < r(t) < -2p_6$ *and that (9) holds.*

Then (1) has a bounded nonoscillatory solution.

Proof. Let Λ be the set of all continuous and bounded functions on $[t_0, \infty)$ and the norm be $\|x(t)\| = \sup_{t_0 \le t < +\infty} x(t)$. Set $A = \{x \in \Lambda,\ M_7 \le x(t) \le M_8,\ t \ge t_0\}$, where M_7, M_8 are two positive constants such that $-2p_6M_7 < \alpha < (-2p_5 + p_6)M_8$. From (9), one can choose $t_1 \ge t_0 + \mu$ and sufficiently large $t \ge t_1$ such that

$$\int_t^\infty \frac{(s-t)^{n-1}}{(n-1)!}\left[\beta_1 \int_c^d q_1(s,\tau)\,d\tau + |h(s)|\right] ds \le \Phi\left(-2p_5M_8 + p_6M_8\right) - \Phi(\alpha), \tag{37}$$

$$\int_t^\infty \frac{(s-t)^{n-1}}{(n-1)!}\left[\beta_2 \int_e^f q_2(s,\sigma)\,d\sigma + |h(s)|\right] ds \le \Phi(\alpha) - \Phi\left(-2p_6M_7\right), \tag{38}$$

$$\int_t^\infty \frac{(s-t)^{n-1}}{(n-1)!}\left[\int_c^d q_1(s,\tau)\,d\tau + \int_e^f q_2(s,\sigma)\,d\sigma\right] ds \le \frac{p_6 - 2p_5}{KL}, \tag{39}$$

and define an operator T on A as follows:

$$(Tx)(t) = \begin{cases} \dfrac{1}{r(t)}\left\{-\displaystyle\int_a^b p(t,\theta)\,x(t-\theta)\,d\theta + \Phi^{-1}\left[\Phi(\alpha) + \int_t^\infty \frac{(s-t)^{n-1}}{(n-1)!}\left[\int_c^d q_1(s,\tau)\,g_1(x(s-\tau))\,d\tau - \int_e^f q_2(s,\sigma)\,g_2(x(s-\sigma))\,d\sigma - h(s)\right] ds\right]\right\}, & t \ge t_1, \\ (Tx)(t_1), & t_0 \le t \le t_1. \end{cases} \tag{40}$$

It is easy to see that T is continuous, for $t \ge t_1$, $x \in A$. By using (37), we have

$$\begin{aligned} (Tx)(t) &\le \frac{1}{r(t)}\left\{-\int_a^b p(t,\theta)\,x(t-\theta)\,d\theta + \Phi^{-1}\left[\Phi(\alpha) + \int_t^\infty \frac{(s-t)^{n-1}}{(n-1)!}\left[\int_c^d q_1(s,\tau)\,g_1(x(s-\tau))\,d\tau - h(s)\right] ds\right]\right\} \\ &\le \frac{1}{-2p_5}\left\{-p_6M_8 + \Phi^{-1}\left[\Phi(\alpha) + \int_t^\infty \frac{(s-t)^{n-1}}{(n-1)!}\left[\beta_1\int_c^d q_1(s,\tau)\,d\tau + |h(s)|\right] ds\right]\right\} \le M_8, \end{aligned} \tag{41}$$

and, taking (38) into account, we have

$$\begin{aligned} (Tx)(t) &\ge \frac{1}{r(t)}\left\{\Phi^{-1}\left[\Phi(\alpha) - \int_t^\infty \frac{(s-t)^{n-1}}{(n-1)!}\left[\int_e^f q_2(s,\sigma)\,g_2(x(s-\sigma))\,d\sigma + h(s)\right] ds\right]\right\} \\ &\ge \frac{1}{-2p_6}\left\{\Phi^{-1}\left[\Phi(\alpha) - \int_t^\infty \frac{(s-t)^{n-1}}{(n-1)!}\left[\beta_2\int_e^f q_2(s,\sigma)\,d\sigma + |h(s)|\right] ds\right]\right\} \ge M_7. \end{aligned} \tag{42}$$

These show that $TA \subset A$. Since A is bounded, close, convex subset of Λ, in order to apply the contraction principle, we have to show that T is a contraction mapping on A. For $\forall x_1, x_2 \in A$, and $t \ge t_1$,

$$\begin{aligned} \left|(Tx_1)(t) - (Tx_2)(t)\right| &\le \frac{1}{r(t)}\left\{\int_a^b p(t,\theta)\left|x_1(t-\theta) - x_2(t-\theta)\right| d\theta + \Phi^{-1}\left[\Phi(\alpha) + \int_t^\infty \frac{(s-t)^{n-1}}{(n-1)!}\left|\int_c^d q_1(s,\tau)\,g_1(x_1(s-\tau))\,d\tau - \int_e^f q_2(s,\sigma)\,g_2(x_1(s-\sigma))\,d\sigma - h(s)\right| ds\right] - \Phi^{-1}\left[\Phi(\alpha) + \int_t^\infty \frac{(s-t)^{n-1}}{(n-1)!}\left|\int_c^d q_1(s,\tau)\,g_1(x_2(s-\tau))\,d\tau - \int_e^f q_2(s,\sigma)\,g_2(x_2(s-\sigma))\,d\sigma - h(s)\right| ds\right]\right\} \le \frac{1}{r(t)}\left\{-p_6\left|x_1 - x_2\right|\right. \\ &\quad + K\int_t^\infty \frac{(s-t)^{n-1}}{(n-1)!}\left[\int_c^d q_1(s,\tau)\left|g_1(x_1(s-\tau)) - g_1(x_2(s-\tau))\right| d\tau \right. \\ &\quad \left.\left. + \int_e^f q_2(s,\sigma)\left|g_2(x_1(s-\sigma)) - g_2(x_2(s-\sigma))\right| d\sigma\right] ds\right\}. \end{aligned} \tag{43}$$

Or, using (39),

$$\begin{aligned}\left|(Tx_1)(t)-(Tx_2)(t)\right| &\le \left|x_1-x_2\right|\frac{1}{-2p_5}\left\{-p_6\right.\\ &+KL\int_t^{\infty}\frac{(s-t)^{n-1}}{(n-1)!}\left[\int_c^d q_1(s,\tau)\,d\tau\right.\\ &\left.\left.+\int_e^f q_2(s,\sigma)\,d\sigma\right]ds\right\}<\rho\left|x_1-x_2\right|.\end{aligned}\tag{44}$$

This implies with the sup norm that

$$\left\|Tx_1-Tx_2\right\|<\rho\left\|x_1-x_2\right\|,\tag{45}$$

where $\rho = 1$, which shows that T is a contraction mapping on A and therefore there exists a unique solution, obviously a bounded positive solution of (1) $x \in A$, such that $Tx = x$. The proof is complete. □

3. Remark

We note that when $n = 1$, $r(t) \equiv 1$, $\Phi(u) = u^{\gamma}$, $q_2(t,\sigma) = 0$, and $h(t) = 0$, we obtain (8). Thus, this paper great achievement was further obtained compared to that of [7].

4. Example

Example 1. Consider high-order neutral differential equation with distributed deviating arguments:

$$\begin{aligned}&\left[\left(\frac{3}{2+\sin t}x(t)+\int_{\pi/2}^{\pi}e^{-t}x(t-\theta)\,d\theta\right)^3\right]''\\ &+36\int_{\pi}^{3\pi/2}\tau e^{-t}x(t-\tau)\,d\tau\\ &-72\int_{\pi/2}^{\pi}\sigma e^{-2t}x(t-\sigma)\,d\sigma=e^{-3t}\left(15\cos^3 t\right.\\ &-30\sin^3 t+63\pi\sin^2 t-18\pi\cos^2 t\\ &+\frac{1}{2}\sin 2t\left(15\cos t-27\sin^2 t+33\pi\right)\\ &\left.+6\pi^2(\cos t-7\sin t)+9\pi^3\right)+18e^{-2t}\left(8\pi\cos t\right.\\ &\left.+\cos 2t-\sin 2t+4\sin t-4\cos t-3\pi^2\right)\\ &+9e^{-t}\left(4\pi\cos t-6\pi\sin t+5\pi^2+2\pi\right).\end{aligned}\tag{46}$$

Here, $n = 2$, $r(t) = 3/(2+\sin t)$, $P(t,\theta) = e^{-t}$, $q_1(t,\tau) = 36\tau e^{-t}$, $q_2(t,\sigma) = 72\sigma e^{-2t}$, $\Phi(u) = u^3$, $g_1(u) = g_2(u) = u$, $a = e = \pi/2$, $b = c = f = \pi$, $d = 3\pi/2$. $1 < r(t) = 3/(2+\sin t) < 3$, $\int_{\pi/2}^{\pi} e^{-t}d\theta = (\pi/2)e^{-t} < 1$, $\int_{t_0}^{\infty}\int_{3\pi/2}^{\pi} 36\tau s e^{-s}d\tau\,ds < \infty$, $\int_{t_0}^{\infty}\int_{\pi/2}^{\pi}\sigma s e^{-2s}d\sigma\,ds < \infty$, $\int_{t_0}^{\infty} e^{-3s}|15\cos^3 s - 30\sin^3 s + 63\pi\sin^2 s - 18\pi\cos^2 s + (1/2)\sin 2s(15\cos s - 27\sin^2 s + 33\pi) + 6\pi^2(\cos s - 7\sin s) + 9\pi^3| + 18e^{-2s}|8\pi\cos s + \cos 2s - \sin 2s + 4\sin s - 4\cos s - 3\pi^2| + 9e^{-s}|4\pi\cos s - 6\pi\sin s + 5\pi^2 + 2\pi|ds < \infty$.

Then it is easy to see that all the conditions of Theorem 1 are satisfied. In fact, $x(t) = 2+\sin t$ is a nonoscillatory solution of (46).

Competing Interests

The authors declare that they have no competing interests.

Acknowledgments

This research is supported by Scientific Research Project Shanxi Datong University (no. 2011K3) and Scientific Research Startup Funding of Doctor of Shanxi Datong University (2015-B-07).

References

[1] Y. Zhou and B. G. Zhang, "Existence of nonoscillatory solutions of higher-order neutral differential equations with positive and negative coefficients," *Applied Mathematics Letters*, vol. 15, no. 7, pp. 867–874, 2002.

[2] W. Zhang, W. Feng, J. Yan, and J. Song, "Existence of nonoscillatory solutions of first-order linear neutral delay differential equations," *Computers & Mathematics with Applications*, vol. 49, no. 7-8, pp. 1021–1027, 2005.

[3] Y. Yu and H. Wang, "Nonoscillatory solution of second-order nonlinear neutral delay equtions," *Journal of Mathematical Analysis and Applications*, vol. 311, pp. 445–456, 2005.

[4] T. Candan and R. S. Dahiya, "Existence of nonoscillatory solutions of first and second order neutral differential equations with distributed deviating arguments," *Journal of the Franklin Institute*, vol. 347, no. 7, pp. 1309–1316, 2010.

[5] T. Candan, "The existence of nonoscillatory solutions of higher order nonlinear neutral equations," *Applied Mathematics Letters*, vol. 25, no. 3, pp. 412–416, 2012.

[6] Y. J. Liu, J. W. Zhang, and J. R. Yan, "Existence of nonoscillatory solutions of higher order neutral differential equations with distributed deviating arguments," *Acta Mathematicae Applicatae Sinica*, vol. 38, no. 2, pp. 235–243, 2015 (Chinese).

[7] T. Candan, "Existence of nonoscillatory solutions of first-order nonlinear neutral differential equations," *Applied Mathematics Letters*, vol. 26, no. 12, pp. 1182–1186, 2013.

[8] T. Candan, "Existence of nonoscillatory solutions for system of higher order neutral differential equations," *Mathematical and Computer Modelling*, vol. 57, no. 3-4, pp. 375–381, 2013.

[9] Y. Liu, J. Zhang, and J. Yan, "Existence of nonoscillatory solutions for system of higher-order neutral differential equations with distributed deviating arguments," *Discrete Dynamics in Nature and Society*, vol. 2013, Article ID 391973, 8 pages, 2013.

[10] M. R. Kulenović and S. Hadžiomerspahić, "Existence of nonoscillatory solution of second order linear neutral delay equation," *Journal of Mathematical Analysis and Applications*, vol. 228, no. 2, pp. 436–448, 1998.

[11] Ö. Öcalan, "Oscillation of neutral differential equation with positive and negative coefficients," *Journal of Mathematical Analysis and Applications*, vol. 331, no. 1, pp. 644–654, 2007.

[12] I. Györi and G. Ladas, *Oscillation Theory of Delay Differential Equations with Applications*, Clarendon Press, Oxford, UK, 1991.

Hindawi Publishing Corporation
Discrete Dynamics in Nature and Society
Volume 2016, Article ID 1386242, 8 pages
http://dx.doi.org/10.1155/2016/1386242

Research Article

Simple Motion Pursuit and Evasion Differential Games with Many Pursuers on Manifolds with Euclidean Metric

Atamurat Kuchkarov,[1] Gafurjan Ibragimov,[2] and Massimiliano Ferrara[3,4]

[1] *Institute of Mathematics, National University of Uzbekistan, 100125 Tashkent, Uzbekistan*
[2] *Department of Mathematics & Institute for Mathematical Research, Universiti Putra Malaysia, 43400 Serdang, Malaysia*
[3] *Department of Law and Economics, Mediterranea University of Reggio Calabria, 89127 Reggio Calabria, Italy*
[4] *ICRIOS-Bocconi University, 20123 Milan, Italy*

Correspondence should be addressed to Massimiliano Ferrara; massimiliano.ferrara@unirc.it

Received 17 May 2016; Accepted 4 July 2016

Academic Editor: Filippo Cacace

Copyright © 2016 Atamurat Kuchkarov et al. This is an open access article distributed under the Creative Commons Attribution License, which permits unrestricted use, distribution, and reproduction in any medium, provided the original work is properly cited.

We consider pursuit and evasion differential games of a group of m pursuers and one evader on manifolds with Euclidean metric. The motions of all players are simple, and maximal speeds of all players are equal. If the state of a pursuer coincides with that of the evader at some time, we say that pursuit is completed. We establish that each of the differential games (pursuit or evasion) is equivalent to a differential game of m groups of countably many pursuers and one group of countably many evaders in Euclidean space. All the players in any of these groups are controlled by one controlled parameter. We find a condition under which pursuit can be completed, and if this condition is not satisfied, then evasion is possible. We construct strategies for the pursuers in pursuit game which ensure completion the game for a finite time and give a formula for this time. In the case of evasion game, we construct a strategy for the evader.

1. Introduction

Multiplayer differential games are natural extension of two-person differential games. New methods of solution for the games of many players were proposed in many works such as [1–7]. The main problem for such games is to find conditions of evasion or completion of pursuit and construct strategies of players as well.

Pursuit and evasion differential games of many players attract attention of many researchers. The case when all players have equal dynamic possibilities [8] proved to be an alternative: if the initial position of the evader belongs to the interior of convex hull of the initial positions of the pursuers, then pursuit problem is solvable; else evasion problem is solvable. This work was extended by many researchers such as [2, 3, 6, 9]. It should be noted that one of the main methods for solving differential games of many pursuers and one evader is the method of resolving functions developed by Pshenichnii et al. [6].

In the evasion game with many pursuers studied by Chernous'ko [1], it was shown that an evader whose speed is bounded by 1 can, by remaining in a neighborhood of a given motion, avoid an exact contact with any finite number of pursuers whose speeds are bounded by a number less than 1. Later on, this result was extended by Zak [10]. The work [11] presented a sufficient condition of existence of evasion strategy in the game of many pursuers in the plane.

In differential games of many pursuers studied by Ivanov and Ledyaev [12], Ibragimov [13], Ibragimov and Rikhsiev [14], Ibragimov and Salimi [15], and Ibragimov et al. [16], optimal strategies of players were constructed.

In the real control systems, the state constraints occur and they are given usually in the form of equalities and inequalities. For example, the works [17, 18] study control problems with state constraints of equality type and [19] does properties of shortest curves in the domain described by equality and inequality type of constraints.

In differential games, mainly two types of state constraints are considered. According to the first constraint a player moves within a given set, and according to the second one it moves along a submanifold of the state space.

In pursuit-evasion differential games, the state constraint can be imposed on the states of pursuers or evaders separately. In the papers [20, 21], the Isaacs method was applied to study the simple motion pursuit differential games of one pursuer and one evader on two-dimensional Riemannian manifolds. In [22], the problem of evasion of one evader from many pursuers was studied on a hypersurface in $\mathbb{R}^n$.

In the works [23–25] devoted to generalized "Lion and Man" differential game of Rado, the evader moves along a given absolutely continuous curve and the pursuer moves in the space. In the case where the evader's speed is greater than that of the pursuer, an evasion strategy was constructed, which enables us to estimate from below the distance between players. If the maximal speeds of the players are equal and the curve does not intersect itself, necessary and sufficient conditions of completion of pursuit from a given initial position as well as from all the initial positions [25] were obtained.

Simple motion pursuit and evasion differential games studied in [26] occur in a ball of the Riemannian manifold, and all players have the same dynamic possibilities. The pursuers move in the ball, and with respect to the motion of the evader two cases were considered: in the first case, the evader moves on the sphere of the ball, and in the second case, the evader also moves in the ball. For each case, sufficient conditions of both completion of pursuit and evasion were obtained.

In the games of many pursuers and many evaders studied in [5, 7, 27], all of the evaders are controlled by one controlled parameter, but pursuers have different control parameters. By definition, game is said to be completed if the state of a pursuer coincides with that of an evader at some time. In these papers, sufficient conditions of completion of pursuit were obtained. In the work [28], a simple motion evasion game of many pursuers and many evaders was studied under integral constraints on controls of players.

In the present paper, we deal with the manifolds, each point of which has a neighborhood isometric to a region of Euclidean space; in other words, the Riemannian metric at each point of the manifold, in a local coordinate system, is expressed as Euclidean one. Such manifolds are called ones with Euclidean metric or ones locally isometric to Euclidean space [29, 30]. For example, two-dimensional manifolds locally isometric to Euclidean space are only plane, cylinder, torus, Mobius strip, and the Klein bottle. Note that a differential game of optimal approach [31] was studied on such manifolds, where duration of the game is fixed, and payoff of the game is distance between the players when the game is terminated. We will study, however, pursuit and evasion differential games of many pursuers and one evader on manifolds with Euclidean metric. Maximal speeds of all players are assumed to be identical. We find a condition on initial positions of players under which pursuit problem is solvable. If this condition is not satisfied, then we show that evasion problem is solvable.

To solve the pursuit or evasion differential game of m pursuers and one evader on manifold M with Euclidean metric, we first reduce the game to an equivalent one in Euclidean space $\mathbb{R}^n$, where a group of countably many pursuers $x_i^1, x_i^2, \ldots \in \mathbb{R}^n$, $i = 1, 2, \ldots, m$, and group of countably many evaders $y^1, y^2, \ldots \in \mathbb{R}^n$ correspond to each pursuer $x_i \in M$ and evader $y \in M$, respectively. Each group of players is controlled by one control parameter. In the new game in $\mathbb{R}^n$, if $x_i^j(\tau) = y^k(\tau)$ at some $i \in \{1, 2, \ldots, m\}$, $j, k \in \mathbb{N}$ and $\tau > 0$, then game is completed; otherwise evasion is possible. At first glance, the condition $y_0^k \in \operatorname{int} \operatorname{conv}\{x_{i0}^j, i = 1, \ldots, m; j = 1, 2, \ldots\}$ seems to be the condition for completing pursuit. It turns out that this condition does not guarantee that pursuit can be completed in the game on M. We obtain another condition (see Theorem 10), which is necessary and sufficient condition of completion of pursuit on manifolds with local Euclidean metric.

2. Statement of Problem

Let M be n, $n \geq 2$, dimensional manifold with positive defined symmetric bilinear form $\langle \cdot, \cdot \rangle_x$ on the tangent space TM_x at the point $x \in M$, and let $\| \cdot \|_x$ be the norm defined by

$$\begin{aligned} \langle a, b \rangle_x &= \langle G(x)\, a, b \rangle, \\ \|a\|_x &= \langle a, a \rangle_x, \\ & \qquad x \in M,\ a, b \in TM_x, \end{aligned} \tag{1}$$

where $\langle \cdot, \cdot \rangle$ is inner product in $\mathbb{R}^n$; the matrix $G(\cdot)$, called metric tensor, defines the Riemannian metric on the manifold M, which becomes identity matrix at each point of the manifold in a local coordinate system; that is, M is a manifold with local Euclidean metric.

The motion of a group of pursuers $\{P_1, P_2, \ldots, P_m\}$ and one evader E are described on the manifold M by the following equations:

$$\begin{aligned} P_i\colon &\quad \dot{x}_i = u_i, \\ &\quad x_i(0) = x_{i0}, \\ E\colon &\quad \dot{y} = v, \\ &\quad y(0) = y_0, \\ &\quad y_0 \neq x_{i0}, \end{aligned} \tag{2}$$

where $x_i, y \in M$, $u_i \in TM_{x_i}$, $v \in TM_y$, and u_i, v are control parameters, $i = 1, 2, \ldots, m$.

Definition 1. Borel measurable functions $v(t)$ and $u_i(t)$, $t \geq 0$, are called controls of the evader E and pursuer P_i, $i = 1, 2, \ldots, m$, respectively, if for the solutions $y(t)$ and $x_i(t)$ of initial value problems,

$$\begin{aligned} \dot{y} &= v(t), \quad y(0) = y_0, \\ \dot{x}_i &= u_i(t), \quad x_i(0) = x_{i0}, \end{aligned} \tag{3}$$

the following inequalities,

$$\begin{aligned} \|v(t)\|_{y(t)} &\le 1, \\ \|u_i(t)\|_{x_i(t)} &\le 1, \end{aligned} \tag{4}$$

and inclusions,

$$\begin{aligned} v(t) &\in M_{y(t)}, \\ u_i(t) &\in M_{x_i(t)}, \end{aligned} \tag{5}$$

hold true for almost all t, $t \ge 0$.

In the tangent space TM_z, denote the ball $\{w \in TM_z \mid |z - w| \le \rho\}$ of radius ρ centered at z by $B_*(z, \rho)$.

Definition 2. A function $U = (U_1, U_2, \ldots, U_m)$, $U_i = U_i(t, x_1, x_2, \ldots, x_m, y, v)$,

$$U_i : [0, \infty) \times M^{m+1} \times B_*(y, 1) \longrightarrow B_*(x_i, 1), \tag{6}$$

is called a strategy of the group of the pursuers $\{P_1, P_2, \ldots, P_m\}$ if for any control of the evader the following initial value problem,

$$\begin{aligned} \dot{y} &= v(t), \quad y(0) = y_0, \\ \dot{x}_i(t) &= U_i\left(t, x_1, x_2, \ldots, x_m, y, v(t)\right), \\ x_i(0) &= x_{i0}, \ i = 1, 2, \ldots, m, \end{aligned} \tag{7}$$

has a unique absolutely continuous solution $(x_1(\cdot), x_2(\cdot), \ldots, x_m(\cdot), y(\cdot))$ on $[0, \infty)$. The function $x_i(\cdot)$ is referred to as the trajectory of the pursuer P_i generated by the triple: the strategy U, initial position $(x_{10}, x_{20}, \ldots, x_{m0}, y_0)$, and control $v(\cdot)$.

Definition 3. A function $V(t, x_1, x_2, \ldots, x_m, y), V : [0, \infty) \times M^{m+1} \to B_*(y, 1)$ is called a strategy of the evader E.

Let $\Delta = \{t_0 = 0, t_1, \ldots\}$ be a partition of the interval $[0, \infty)$. The trajectory $y(\cdot)$ of the evader E generated by the controls of pursuers $u_1(\cdot), u_2(\cdot), \ldots, u_m(\cdot)$, a strategy of the evader V, initial position $(x_{10}, x_{20}, \ldots, x_{m0}, y_0)$, and partition Δ is defined as follows:

(1) At each time t_k, we define a unit vector,

$$\begin{aligned} v_k &= V\left(t, x_1(t_k), x_2(t_k), \ldots, x_m(t_k), y(t_k)\right), \\ v_k &\in B_*\left(y(t_k), 1\right), \end{aligned} \tag{8}$$

and construct a geodesic $\gamma_k : [0, t_{k+1} - t_k] \to M$ such that

$$\begin{aligned} \gamma_k'(0) &= v_k, \\ \gamma_k(0) &= y(t_i), \\ \left|\gamma_i'(s)\right| &= 1, \\ s &\in [0, t_{k+1} - t_k], \ k = 1, 2, \ldots \end{aligned} \tag{9}$$

(note that such a geodesic exists and is unique [29]).

(2) The trajectory $y(\cdot)$ is defined as the solution of initial value problem

$$\begin{aligned} \dot{y} &= \gamma_i'(t - t_i), \\ t &\in [t_i, t_{i+1}), \ i = 1, 2, \ldots, \ y(0) = y_0. \end{aligned} \tag{10}$$

Thus, strategy of the group of pursuers is defined as a contrstrategy, and corresponding motion is the solution of the initial value problem, whereas strategy of the evader is defined as a positional (closed loop) strategy, and corresponding to it trajectory of the evader is defined as a stepwise motion [32].

The problems of the players are as follows.

Problem 4 (pursuit problem). For each initial position $(x_{10}, x_{20}, \ldots, x_{m0}, y_0)$, find a number T and function (strategy) U such that pursuit can be completed for time T; that is, for any control $v(\cdot)$ of the evader E, solution of system (7) satisfies the equation $x_i(t) = y(t)$ at some $t \in [0, T]$ and $i \in \{1, 2, \ldots, m\}$.

Problem 5 (evasion problem). For any initial position $(x_{10}, x_{20}, \ldots, x_{m0}, y_0)$, $y_0 \ne x_{i0}$, construct a function (strategy) V and find a partition Δ such that evasion is possible; that is, for any controls $u_1(\cdot), u_2(\cdot), \ldots, u_m(\cdot)$ of the pursuers $P_1, P_2, \ldots, P_m$, the trajectories $x_1(\cdot), x_2(\cdot), \ldots, x_m(\cdot), y(\cdot)$ generated by the controls $u_1(\cdot), u_2(\cdot), \ldots, u_m(\cdot)$, strategy V, partition Δ, and initial position $(x_{10}, x_{20}, \ldots, x_{m0}, y_0)$ satisfy the inequality $x_i(t) \ne y(t)$ for all $t \ge 0$ and $i \in \{1, 2, \ldots m\}$.

3. An Equivalent Game in Euclidean Space

We first reduce game (2), (4), (5), (7), and (10) on manifold M to a specific one in Euclidean space $\mathbb{R}^n$ by unfolding M in $\mathbb{R}^n$ [29, 30]. Such unfolding can be conducted by the multivalued mapping which is inverse to the universal covering $\pi : \mathbb{R}^n \to M$ that is local isometry. If M itself is not Euclidean space and $z \in M$, then the set of its preimages $\pi^{-1}(z)$ consists of the class of denumerable points equivalent to each other: $z^1, z^2, \ldots \in \mathbb{R}^n$.

Thus, game (2), (4), (5), (7), and (10) is reduced to a game in Euclidean space $\mathbb{R}^n$ in which m groups of pursuers $\pi^{-1}(x_i) = \{x_i^1, x_i^2, \ldots\}$, $i = 1, 2, \ldots, m$, consisting of countably many pursuers try to capture the group of the evaders $\pi^{-1}(y) = \{y^1, y^2, \ldots\}$. All members of each group have the same control parameter.

Dynamics of the groups of pursuers and evaders are described by the following equations:

$$\begin{aligned} \dot{x}_i^j &= \overline{u}_i, \quad x_i^j(0) = x_{i0}^j, \ i = 1, 2, \ldots, m, \\ \dot{y}^j &= \overline{v}, \quad y^j(0) = y_0^j, \ j = 1, 2, \ldots, \end{aligned} \tag{11}$$

where $x_i^j, y^j, \overline{u}_i, \overline{v} \in \mathbb{R}^n$; $x_{i0}^j \ne y_0^k$ for all $i \in \{1, 2, \ldots, m\}$, $j, k \in \{1, 2, \ldots\}$; $\overline{u}_1, \overline{u}_2, \ldots, \overline{u}_m$ and $\overline{v}$ are the control parameters of the groups of pursuers and group of evaders, respectively, which satisfy the constraints

$$\begin{aligned} \left|\overline{u}_i\right| &\le 1, \\ |\overline{v}| &\le 1. \end{aligned} \tag{12}$$

Controls, strategies of the groups of pursuers and group of evaders, trajectories generated by the initial position, strategies of pursuers, and control of evaders (or vice versa) are defined as in Definitions 2 and 3.

We say that pursuit can be completed if

$$x_i^j(t) = y^k(t) \quad \text{at some } i \in \{1,2,\ldots,m\},\ j,k \in \{1,2,\ldots\},\ t > 0. \tag{13}$$

In the differential game (11)-(12), the task of groups of pursuers is to assure equality (13) and that of the group of evaders is the opposite.

Show that games (2), (4), (5), (7), (10), and (11)-(12) are equivalent. Let $y(t), t \geq 0$ be a trajectory of the evader on M corresponding to some control function $v(t), t \geq 0$. Then $\pi^{-1}(y(t)), t \geq 0$, is a family of trajectories in $\mathbb{R}^n$. Since π is a local isometry and $|\dot{y}(t)| = |v(t)| \leq 1$, then $|dy^i(t)/dt| \leq 1, i = 1,2,\ldots$. Also note that $dy^1(t)/dt = dy^2(t)/dt = dy^3(t)/dt = \cdots$. Hence, for given $v(t) \in M_{y(t)}$, $|v(t)| \leq 1$, there is a unique vector $\overline{v}(t) \in \mathbb{R}^n$, $|\overline{v}(t)| \leq 1$, such that $dy^i(t)/dt = \overline{v}(t), i = 1,2,\ldots$. The same conclusion can be drawn for the pursuers.

Note that (13) is equivalent to the equation $\pi^{-1}(x_i(t)) = \pi^{-1}(y(t))$ in $\mathbb{R}^n$, and, hence, it is equivalent to the equation $x_i(t) = y(t)$ on manifold M. Thus, differential game (2), (4), (5), (7), and (10) of pursuers $x_1,\ldots,x_m$ and evader y on manifold M is equivalent to game (11)-(12) of groups of countably many pursuers $\pi^{-1}(x_i) = \{x_i^1, x_i^2, \ldots\}$, $i = 1,2,\ldots,m$, and a group of countably many evaders $\pi^{-1}(y) = \{y^1, y^2, \ldots\}$ in $\mathbb{R}^n$, where each group is controlled by one control parameter.

4. Properties of the Multivalued Mapping

The multivalued mapping $\pi^{-1} : M \to \mathbb{R}^n$ has the following properties [29, 30]:

(1) π^{-1} maps the straight lines (i.e., geodesics) on manifold M to a family of parallel straight lines in $\mathbb{R}^n$.

(2) If $\pi^{-1}(z) = \{z^1, z^2, \ldots\}, z \in M$, then

$$z^i + \left(z^j - z^k\right) \in \pi^{-1}(z) \quad \forall i,j,k = 1,2,\ldots. \tag{14}$$

(3) There exists a positive number h such that

$$\left|z^i - z^j\right| > h, \quad i \neq j. \tag{15}$$

Let

$$N(M) = \operatorname{conv}\left\{z^j - z^k \mid z^j \in \pi^{-1}(z),\ z^k \in \pi^{-1}(z),\ z \in M\right\}. \tag{16}$$

Then the properties of mapping π^{-1} mentioned above imply the following statement.

Lemma 6. *The following statements hold true:*

(1) *For any $z \in M$ and $z_* \in \pi^{-1}(z)$, inclusion $\pi^{-1}(z) \subset z_* + N(M)$ holds.*

(2) *There exists a number $r > 0$ such that, for any $a \in N(M)$, the ball $\{x \mid |x-a| \leq r,\ x \in N(M)\}$, contains at least one point of the set $\pi^{-1}(z), z \in M$.*

(3) *$N(M)$ is a subspace of $\mathbb{R}^n$. Moreover, if M is a compact set, then $N(M) = \mathbb{R}^n$.*

Proof. (1) Let $z \in M$ and $z_* \in \pi^{-1}(z)$. Then, for any $z^* \in \pi^{-1}(z)$, we obtain from (16) that $z^* - z_* \in N(M)$; that is, $z^* \in z_* + N(M)$. Therefore $\pi^{-1}(z) \subset z_* + N(M)$.

(2) Without loss of generality, we assume that $z^1 = 0$ and $\dim \operatorname{conv} \pi^{-1}(z) = k$. Then $\pi^{-1}(z)$ contains a linearly independent set of k vectors, say $\{z^2, z^3, \ldots, z^{k+1}\}$. Denote the k-dimensional prism constructed on the vectors $z^2, z^3, \ldots, z^{k+1}$ by P. Since $z^1 = 0$, therefore by (14) and (16) we obtain $\operatorname{conv} \pi^{-1}(z) = N(M)$. Cover the set $\operatorname{conv} \pi^{-1}(z)$ by P and prisms that can be obtained by parallel translation of P. In view of (16), vertices of these prisms belong to $\pi^{-1}(z)$. This implies, in particular, that $N(M)$ is a k-dimensional subspace of $\mathbb{R}^n$. To prove part (2) of lemma it suffices to put $r = \operatorname{diam} P$.

(3) If M is a compact set, then there is a bounded set $M_0 \subset \mathbb{R}^n$ of nonempty interior such that $\pi : M_0 \to M$ is one-to-one [29]. Since $\mathbb{R}^n$ can be represented as a union of M_0 and the bounded sets, $M_1, M_2, \ldots$, which can be obtained by parallel translation of M_0 and whose interiors are disjoint [29], therefore, for any $z \in M$, each of the compact sets $M_i, i = 0,1,\ldots$, contains only one element of $\pi^{-1}(z)$. This implies that $\dim \operatorname{conv} \pi^{-1}(z) = n$, which is the desired conclusion. □

We now study some examples to illustrate the set $N(M)$.

Example 7. Let M be a plane. Then, clearly, $N(M) = \{0\}$.

Example 8. Let

$$M = \left\{z = \left(z^{(1)}, z^{(2)}, z^{(3)}\right) \in \mathbb{R}^3 \mid \left(z^{(1)}\right)^2 + \left(z^{(2)}\right)^2 = 1\right\}; \tag{17}$$

that is, M is two-dimensional cylinder in $\mathbb{R}^3$. Then [30], for some $a, a \in [0, 2\pi]$,

$$\pi^{-1}(z) = \left\{x = \left(x^{(1)}, x^{(2)}\right) \in \mathbb{R}^2 \mid x^{(2)} = z^{(3)},\ x^{(1)} = a + 2\pi n,\ n \in \mathbb{Z}\right\},\quad z \in M, \tag{18}$$

where $\mathbb{Z}$ is the set of integers. It is obvious that the set $N(M) = \{z = (x^{(1)}, x^{(2)}) \in \mathbb{R}^2 \mid x^{(2)} = 0\}$ is a straight line. Here, the number r mentioned in Lemma 6 can be any number not less than 2π.

Example 9. Let now M be two-dimensional torus $M = S^1 \times S^1$, where S^1 is a unit circle; then [30]

$$\pi^{-1}(z) = \left\{x = \left(x^{(1)}, x^{(2)}\right) \in \mathbb{R}^2 : x^{(1)} = a + 2\pi n,\ x^{(2)} = b + 2\pi k,\ n,k \in \mathbb{Z}\right\},\quad z \in M, \tag{19}$$

where a and b are some numbers in $[0, 2\pi]$. Therefore, $N(M)$ is a plane and the number r mentioned in Lemma 6 can be, for example, $\pi\sqrt{2}$.

5. Main Result

We now formulate the main result of the present paper.

Theorem 10. *(i) If there exist points,*

$$z_1, z_2, \ldots, z_m \in \mathbb{R}^n \quad \text{with } z_i \in \pi^{-1}(x_{i0}) = \left\{x_{i0}^1, x_{i0}^2, \ldots\right\},\ i = 1, 2, \ldots, m, \tag{20}$$

and number $j \in \{1, 2, \ldots\}$ such that

$$y_0^j \in \operatorname{int} \operatorname{conv}\{z_1, z_2, \ldots, z_m\}, \tag{21}$$

then pursuit can be completed in game (11)-(12) (and hence in game (2), (4), (5), (7), and (10)) for the time:

$$T = \frac{1}{A}\sum_{i=1}^{m} \left|z_i - y_0^j\right|; \qquad A = \min_{|\nu|=1} \sum_{i=1}^{m} \left(\left|\langle e_i, \nu\rangle\right| - \langle e_i, \nu\rangle\right), \tag{22}$$

where

$$\left\{y_0^1, y_0^2, \ldots\right\} = \pi^{-1}(y_0), \qquad e_i = \frac{\left(y_0^j - z_i\right)}{\left|y_0^j - z_i\right|}, \quad i = 1, 2, \ldots, m. \tag{23}$$

(ii) If for any set $\{z_1, z_2, \ldots, z_m\}$ with $z_i \in \pi^{-1}(x_{i0})$, $i = 1, 2, \ldots, m$, and for any number $j \in \{1, 2, \ldots\}$, inclusion (21) fails to hold; then evasion is possible in game (11)-(12) (and hence in game (2), (4), (5), (7), and (10)).

It should be noted that condition (21) implies that $m > n$ and $A > 0$.

Proof.

Part I. It follows from condition (14) that if for a number $j \in \{1, 2, \ldots\}$ there exists a set $\{z_1, z_2, \ldots, z_m\}$ to satisfy (21), then for each $j \in \{1, 2, \ldots\}$ such a set exists as well. Therefore, from now on, one writes y_0 and $y(t)$ instead of y_0^j and $y^j(t)$, respectively. This means that the group of evaders consists of only one evader.

Assume that there exists a set $\{z_1, z_2, \ldots, z_m\}$ with $z_i \in \pi^{-1}(x_{i0})$, $i = 1, 2, \ldots, m$, satisfying inclusion (21). Without loss of generality, we may assume that $z_i = x_{i0}^1$, $i = 1, \ldots, m$.

Let $v(\cdot)$ be an arbitrary control of the evader. Let the pursuers use the strategy of parallel approach [33]:

$$U_i(v) = v + \lambda_i(v)\, e_i; \qquad \lambda_i(v) = -\langle v, e_i\rangle + \sqrt{1 - |v|^2 + \langle v, e_i\rangle^2}. \tag{24}$$

Analysis similar to [8] shows that pursuit can be completed for time T.

Part II. We now turn to the case, where there is no set $\{z_1, z_2, \ldots, z_m\}$ with $z_i \in \pi^{-1}(x_{i0})$, $i = 1, 2, \ldots, m$, to satisfy (21). We need to consider the following two cases.

Case 1 ($m \le n$). In this case, observe that $\operatorname{int} \operatorname{conv}\{z_1, z_2, \ldots, z_m\} = \emptyset$ and inclusion (21) fails to hold for any set $\{z_1, z_2, \ldots, z_m\}$; $z_i \in \pi^{-1}(x_{i0})$, $i = 1, 2, \ldots, m$.

For simplicity of notation, we denote the $(m+1)$-tuple $(\pi^{-1}(x_1), \pi^{-1}(x_2), \ldots, \pi^{-1}(x_m), y)$ by w. Set

$$W(w) = \left\{x_i^j \mid \left|x_i^j - y\right| \le \frac{h}{2} \text{ at some } i \in \{1, 2, \ldots, m\},\ j \in \{1, 2, \ldots\}\right\}. \tag{25}$$

From now on, we assume that the number $h > 0$ satisfies inequalities (15) for all $z = z_i$, $i = 1, \ldots, m$. It follows from inequality (15) that, for each $i \in \{1, \ldots, m\}$, the set $W(w)$ contains not more than one element of the set $\pi^{-1}(x_i)$. Therefore, for any w, the number of elements of the set $W(w)$ does not exceed m.

Let the partition Δ be defined by numbers $t_k = kh/4$, $k = 0, 1, \ldots$. Define the strategy $V(w)$ of the evader by requiring conditions

$$\min_{|\nu|=1} \max_{x_i^j \in W(w)} \left\langle \frac{x_i^j - y}{\left|x_i^j - y\right|}, \nu \right\rangle = \max_{x_i^j \in W(w)} \left\langle \frac{x_i^j - y}{\left|x_i^j - y\right|}, V(w) \right\rangle, \quad |V(w)| = 1. \tag{26}$$

Since the set $W(w)$ is finite, max in (26) attains. In view of $m \le n$, we conclude that $V(w)$ must satisfy inequality

$$\max_{x_i^j \in G(w)} \left\langle \frac{x_i^j - y}{\left|x_i^j - y\right|}, V(w) \right\rangle \le 0. \tag{27}$$

Let $\overline{u}_1(\cdot), \overline{u}_2(\cdot), \ldots, \overline{u}_m(\cdot)$ be any controls of the groups of pursuers, and let $y(\cdot), x_i^j(\cdot)$, $j = 1, 2, \ldots$, $i = 1, 2, \ldots, m$, be the trajectories generated by these controls, initial positions, strategy $V(w)$, and partition Δ. We shall have established the theorem if we prove the following statement: if the inequalities $x_i^j(t) \ne y(t)$, $i = 1, 2, \ldots, m$, $j = 1, 2, \ldots$, hold for all $t \in [t_{k-1}, t_k]$, then they hold true for all $t \in [t_k, t_{k+1}]$, $k = 1, 2, \ldots$, as well (recall $t_0 = 0$). Then, clearly, $x_i^j(t) \ne y(t)$, for all $i = 1, 2, \ldots, m$, $j = 1, 2, \ldots$, and $t \ge 0$.

Let $x_1^1(t_k) \in W(w(t_k))$. Then (27) implies that

$$\left\langle \frac{x_1^1(t_k) - y(t_k)}{\left|x_1^1(t_k) - y(t_k)\right|}, V(w(t_k)) \right\rangle \le 0, \tag{28}$$

and so the greatest (nonacute) angle of the triangle with vertices $y(t) = y(t_k) + (t - t_k)V(w(t_k))$, $x_1^1(t_k)$, and $y(t_k)$ is at the vertex $y(t_k)$. Therefore,

$$\left|x_1^1(t_k) - y(t)\right| > \left|(t - t_k)\, V(w(t_k))\right| = t - t_k, \quad t \in [t_k, t_{k+1}]. \tag{29}$$

This inequality and (12) now give

$$\begin{aligned}\left|x_1^1(t) - y(t)\right| &\geq \left|x_1^1(t_k) - y(t)\right| - \left|x_1^1(t) - x_1^1(t_k)\right| \\ &> t - t_k - \left|\int_{t_k}^{t} \overline{u}_1(\tau)\, d\tau\right| \\ &\geq t - t_k - \int_{t_k}^{t} \left|\overline{u}_1(\tau)\right| d\tau \geq 0, \\ &\qquad t_k \leq t \leq t_{k+1}.\end{aligned} \tag{30}$$

We can now turn to the case $x_1^1(t_k) \notin W(w(t_k))$. For $t_k \leq t \leq t_{k+1}$, first using the triangle inequality and then (12), (25), and (26), we get

$$\begin{aligned}&\left|x_1^1(t) - y(t)\right| \\ &= \left|x_1^1(t_k) + \int_{t_k}^{t} \overline{u}_1(\tau)\, d\tau - y(t_k) - \int_{t_k}^{t} V(w(t_k))\, d\tau\right| \\ &\geq \left|x_1^1(t_k) - y(t_k)\right| - \left|\int_{t_k}^{t} \overline{u}_1(\tau)\, d\tau\right| \\ &\quad - \left|\int_{t_k}^{t} V(w(t_k))\, d\tau\right| \\ &> \frac{h}{2} - \int_{t_k}^{t} \left|\overline{u}_1(\tau)\right| d\tau - (t - t_k) \geq \frac{h}{2} - (t - t_k) - \frac{h}{4} \\ &\geq \frac{h}{2} - \frac{h}{4} - \frac{h}{4} = 0.\end{aligned} \tag{31}$$

Inequalities (30) and (31) show that for any location of $w(t_k)$ the inequality $x_1^1(t) \neq y(t)$, $t \in [t_k, t_{k+1}]$ holds. In a similar way, one can prove that $x_i^j(t) \neq y(t)$, $i = 1, 2, \ldots, m$, $j = 1, 2, \ldots$, for all $t \in [t_k, t_{k+1}]$. This is our assertion in the case $m \leq n$.

Case 2 ($m > n$). Let $N = N(M)$ (see (16)). If $m > n$ and $\dim N = n$, then it is not difficult to verify using the second statement of Lemma 6 that there exists a set,

$$\{z_1, z_2, \ldots, z_m\}, \quad z_i \in \left\{x_{i0}^1, x_{i0}^2, \ldots\right\}, \; i = 1, 2, \ldots, m, \tag{32}$$

to satisfy inclusion (21). Therefore, if $m > n$ and $y_0 \notin \operatorname{int}\operatorname{conv}\{z_1, z_2, \ldots, z_m\}$ for any set $\{z_1, z_2, \ldots, z_m\}$ with $z_i \in \{x_{i0}^1, x_{i0}^2, \ldots\}$, $i = 1, 2, \ldots, m$, then necessarily $\dim N < n$. Thus, it remains to study the case where $m > n$ and $\dim N < n$.

Denote by $N^{\perp}$ the orthogonal complement of the subspace N and by $F, F : \mathbb{R}^n \to N^{\perp}$ the orthogonal projection operator. Then, clearly, $F : N \to \{0\}$ and it follows from (14) that the set $F\pi^{-1}(z)$, $z \in M$, consists of a unique point. Therefore, we denote

$$\begin{aligned}&F\pi^{-1}(y_0) = b, \\ &F\pi^{-1}(x_{i0}) = a_i, \quad i = 1, 2, \ldots, m.\end{aligned} \tag{33}$$

Show that the following inclusion,

$$b \in \operatorname{int}\operatorname{conv}\{a_1, a_2, \ldots, a_m\}, \tag{34}$$

fails to hold in the subspace $N^{\perp}$, where the operations int and conv act on the subspace $N^{\perp}$. Assume the contrary; let (34) hold.

It follows from condition (14) that if for a number $j \in \{1, 2, \ldots\}$ there exists a set $\{z_1, z_2, \ldots, z_m\}$ to satisfy (21), then for each $j \in \{1, 2, \ldots\}$ also such a set exists. Therefore, from now on, one writes $y_0 = b = 0$ and $y(t)$ instead of y_0^j and $y^j(t)$, respectively. This means that group of evaders consists of only one evader.

Since $m > n$ and $\dim N^{\perp} < n$, then in view of (34) the point $b = 0$ belongs to convex hull of some n points from $a_1, a_2, \ldots, a_m$. Without loss of generality, we assume that

$$0 \in \operatorname{conv}\{a_1, a_2, \ldots, a_n\}, \tag{35}$$

in the subspace $N^{\perp}$.

Next, let $p \in N$ be a unit vector, and let A be a positive number. Choose linearly independent set of vectors $z_i \in \pi^{-1}(x_{i0})$, $i = 1, 2, \ldots, n$, so that $\langle z_i, p\rangle > A$. Construct the cone

$$\begin{aligned}K = \{z \in \mathbb{R}^n : z = \alpha_1 z_1 + \alpha_2 z_2 + \cdots + \alpha_n z_n, \; \alpha_i \geq 0, \; i \\ = 1, 2, \ldots, n\}\end{aligned} \tag{36}$$

and its conjugate

$$\begin{aligned}K^* = \{z \in \mathbb{R}^n : z = \alpha_1 z_1 + \alpha_2 z_2 + \cdots + \alpha_n z_n, \; \alpha_i \\ \leq 0, \; i = 1, 2, \ldots, n\}.\end{aligned} \tag{37}$$

Since the set of vectors $\{z_1, z_2, \ldots, z_n\}$ is linearly independent, therefore these cones have nonempty interiors. Observe that $p \in K$ and $-p \in K^*$. It follows from inclusions $-p \in K^*$, $p \in N$, and statement (2) of Lemma 6 that the set

$$\operatorname{int} K^* \cap \pi^{-1}(x_{n+1}) \tag{38}$$

has infinitely many elements. Choose a vector z_{n+1} from this set. Then by construction of the cones K and K^* in view of (35) we have

$$0 \in \operatorname{int}\operatorname{conv}\{z_1, z_2, \ldots, z_{n+1}\}. \tag{39}$$

By hypothesis of the theorem there is no set $\{z_1, z_2, \ldots, z_m\}$ with $z_i \in \pi^{-1}(x_{i0})$, $i = 1, 2, \ldots, m$, to satisfy (21), a contradiction.

Thus, (34) does not hold, and so

$$0 \bar{\in} \operatorname{int}\operatorname{conv}\{a_1, a_2, \ldots, a_m\}. \tag{40}$$

From this it follows that there exists a unit vector $V_0 \in N^{\perp}$ such that

$$\begin{aligned}\left\langle V_0, x_{i0}^j - y_0 \right\rangle &= \left\langle V_0, F\pi^{-1}\left(x_{i0}\right) - F\pi^{-1}\left(y_0\right)\right\rangle \\ &= \left\langle V_0, a_i \right\rangle \le 0, \\ &\qquad i = 1, 2, \ldots, m, \;\; j = 1, 2, \ldots.\end{aligned} \tag{41}$$

Let the evader use the constant control $V(w) = V_0$, $t \ge 0$. We conclude from (41) that, for any $i \in \{1, 2, \ldots, m\}$, $j \in \{1, 2, \ldots\}$, and $t \ge 0$, the greatest angle of the triangle with vertices x_{i0}^j, y_0, and $y(t) = y_0 + V_0 t$ is at the vertex y_0. This gives

$$\left|y(t) - x_{i0}^j\right| > \left|y(t) - y_0\right| = t. \tag{42}$$

Next, by the restriction $|u_i(\cdot)| \le 1$, we obtain

$$\left|x_i^j(t) - x_{i0}^j\right| = \left|\int_0^t \overline{u}_i(s)\, ds\right| \le \int_0^t \left|\overline{u}_i(s)\right| ds \le t. \tag{43}$$

From the last two relations we obtain $y(t) \ne x_i^j(t)$ for all $i = 1, 2, \ldots, m$, $j = 1, 2, \ldots$, and $t \ge 0$, and the proof is complete. □

Remark 11. Obviously, if $m \le n$, inclusion (21) fails to hold. In this case, by Theorem 10, evasion is possible from any initial points. In addition, in the proof of this statement, we have used only inequality (15), and other properties of multivalued mapping $\pi^{-1} : M \to \mathbb{R}^n$ have not been used. Therefore, if $m \le n$, then evasion is possible in the game of type (11)-(12) from any initial points that satisfy (15).

It should be noted that condition (21) of Theorem 10 is fairly easy to check. In the following example, we give conditions which are equivalent to condition (21).

Example 12. Let M be the cylinder given in Example 8. Then in view of (18) one can verify that condition (21) is equivalent to the following inequalities:

$$\min_{1\le i\le m} x_{i0}^{(3)} < y_0^{(3)} < \max_{1\le i\le m} x_{i0}^{(3)}, \quad m \ge 3. \tag{44}$$

Next, in the case where the set M is compact, $\dim N(M) = n$ by Lemma 6, and there exists a number r such that each ball of radius r in $\mathbb{R}^n$ contains at least one point of the set $\pi^{-1}(x)$, $x \in M$. Therefore, if $m > n$, inclusion (21) holds. According to this property, we obtain the following corollary of Theorem 10:

Corollary 13. *If M is a compact set and $m > n$, then, for any initial position of the players $(x_{10}, x_{20}, \ldots, x_{m0}, y_0)$, $x_{i0} \ne y_0$, $i = 1, \ldots, m$, there exists a positive number $T = T(x_{10}, x_{20}, \ldots, x_{m0}, y_0)$ such that pursuit can be completed for time T.*

Remark 14. Condition (21) is equivalent to the following one: there exist geodesics $\gamma_i : [0, \alpha_i] \to M$ such that $\gamma_i(0) = y_0, \gamma_i(\alpha_i) = x_{i0}$, $i = 1, 2, \ldots, m$, and the inclusion

$$0 \in \operatorname{int} \operatorname{conv}\left\{\gamma_1'(0), \gamma_2'(0), \ldots, \gamma_m'(0)\right\} \tag{45}$$

holds in the tangent space TM_{y_0}. Note that such geodesics, in general, are not unique.

6. Conclusion

We have studied pursuit and evasion differential games of m pursuers and one evader on manifolds with Euclidean metric. The following are our main contributions:

(1) We have proposed a method of reduction of simple motion differential game with many pursuers and one evader on a class of manifolds (e.g., cylinder and torus) to an equivalent differential game in $\mathbb{R}^n$, which contains m groups of countably many pursuers, $x_i^1, x_i^2, \ldots$, $i = 1, \ldots, m$, and one group of countably many evaders, $y^1, y^2, \ldots$.

(2) We have obtained necessary and sufficient condition of evasion in the equivalent game. It should be noted that even though the condition $y_0^l \in \{x_{i0}^j,\ i = 1, \ldots, m;\ j = 1, 2, \ldots\}$, for some positive integer l, is more similar to the condition of Pshenichnii [8] than condition (21), it is not sufficient for completion of pursuit in the game.

(3) If condition (21) is not satisfied, we have constructed an evasion strategy and proved that evasion is possible. Note that many researchers (see, e.g., Pshenichnii [8] and Grigorenko [3]) suggested to the evader a constant velocity depending on initial positions of players, which guarantees the evasion in $\mathbb{R}^n$. In the game we studied, evasion using constant velocity does not work. In general, the evader will be captured if it moves with constant velocity. Evasion strategy used in the present paper depends on current positions of players and requires a specific construction.

Competing Interests

The authors declare that they have no competing interests.

References

[1] F. L. Chernous'ko, "A problem of evasion of several pursuers," *Journal of Applied Mathematics and Mechanics*, vol. 40, no. 1, pp. 14–24, 1976.

[2] A. Chikrii, *Conflict-Controlled Processes*, vol. 405 of *Mathematics and Its Applications*, Springer Science & Business Media, Dordrecht, The Netherlands, 1997.

[3] N. L. Grigorenko, "On the problem of group pursuit," *Proceedings of the Steklov Institute of Mathematics*, vol. 2, pp. 73–81, 1990.

[4] E. F. Mishchenko, M. S. Nikol'skii, and N. Yu. Satimov, "Evoidance encounter problem in differential games of many persons," *Trudy MIAN USSR*, vol. 143, pp. 105–128, 1977.

[5] N. N. Petrov, "Simple pursuit of rigidly linked evaders," *Avtomatika i Telemekhanika*, no. 12, pp. 89–96, 1997, English Translation in *Automation and Remote Control*, vol. 58, no. 12, pp. 1914–1919, 1998.

[6] B. N. Pshenichnii, A. A. Chikrii, and I. S. Rappoport, "Effective method of solving differential games with many pursuers," *Doklady Akademii Nauk SSSR*, vol. 256, no. 3, pp. 530–535, 1981.

[7] N. Yu. Satimov and M. Sh. Mamatov, "The pursuit-evasion problem in differential games between the groups of pursuers and evaders," *Differentsialnie Uravneniya*, vol. 26, no. 9, pp. 1541–1551, 1990.

[8] B. N. Pshenichnii, "Simple pursuit by several objects," *Kibernetika*, vol. 3, pp. 145–146, 1976.

[9] P. V. Prokopovich and A. A. Chikrii, "A linear evasion problem for interacting groups of objects," *Journal of Applied Mathematics and Mechanics*, vol. 58, no. 4, pp. 583–591, 1994.

[10] V. L. Zak, "On a problem of evading many pursuers," *Journal of Applied Mathematics and Mechanics*, vol. 43, no. 3, pp. 492–501, 1978.

[11] P. Borówko and W. Rzymowski, "Avoidance of many pursuers in the simple motion case," *Journal of Mathematical Analysis and Applications*, vol. 111, no. 2, pp. 535–546, 1985.

[12] R. P. Ivanov and Y. S. Ledyaev, "Optimality of pursuit time in simple motion differential game of many objects," *Trudy Matematicheskogo Instituta imeni VA Steklova*, vol. 158, pp. 87–97, 1981.

[13] G. I. Ibragimov, "Optimal pursuit with countably many pursuers and one evader," *Differential Equations*, vol. 41, no. 5, pp. 627–635, 2005.

[14] G. I. Ibragimov and B. B. Rikhsiev, "On some sufficient conditions for optimality of the pursuit time in the differential game with multiple pursuers," *Automation and Remote Control*, vol. 67, no. 4, pp. 529–537, 2006.

[15] G. I. Ibragimov and M. Salimi, "Pursuit-evasion differential game with many inertial players," *Mathematical Problems in Engineering*, vol. 2009, Article ID 653723, 15 pages, 2009.

[16] G. Ibragimov, N. Abd Rasid, A. Kuchkarov, and F. Ismail, "Multi pursuer differential game of optimal approach with integral constraints on controls of players," *Taiwanese Journal of Mathematics*, vol. 19, no. 3, pp. 963–976, 2015.

[17] A. V. Arutyunov and D. Y. Karamzin, "Maximum principle in an optimal control problem with equality state constraints," *Differential Equations*, vol. 51, no. 1, pp. 33–46, 2015.

[18] A. V. Arutyunov and D. Y. Karamzin, "Non-degenerate necessary optimality conditions for the optimal control problem with equality-type state constraints," *Journal of Global Optimization*, vol. 64, no. 4, pp. 623–647, 2016.

[19] A. V. Davydova and D. Y. Karamzin, "On some properties of the shortest curve in a compound domain," *Differential Equations*, vol. 51, no. 12, pp. 1626–1636, 2015.

[20] A. A. Melikyan and N. V. Ovakimyan, "A differential game of simple approach on manifolds," *Journal of Applied Mathematics and Mechanics*, vol. 57, no. 1, pp. 41–51, 1993.

[21] A. A. Melikyan, N. V. Ovakimyan, and L. L. Harutiunian, "Games of simple pursuit and approach on a two-dimensional cone," *Journal of Optimization Theory and Applications*, vol. 98, no. 3, pp. 515–543, 1998.

[22] N. Yu. Satimov and A. Sh. Kuchkarov, "Deviation from encounter with several pursuers on a surface," *Uzbekskii Matematicheskii Zhurnal*, vol. 1, pp. 51–55, 2001.

[23] A. A. Azamov, "On a problem of escape along a prescribed curve," *Journal of Applied Mathematics and Mechanics*, vol. 46, no. 4, pp. 553–555, 1982.

[24] A. A. Azamov and A. S. Kuchkarov, "Generalized 'Lion & Man' Game of R. Rado," *Contributions to Game Theory and Management*, vol. 2, pp. 8–20, 2009.

[25] A. S. Kuchkarov, "Solution of simple pursuit-evasion problem when evader moves on a given curve," *International Game Theory Review*, vol. 12, no. 3, pp. 223–238, 2010.

[26] A. Sh. Kuchkarov, "A simple pursuit-evasion problem on a ball of a Riemannian manifold," *Mathematical Notes*, vol. 85, no. 2, pp. 190–197, 2009.

[27] D. Vagin and N. Petrov, "The problem of the pursuit of a group of rigidly coordinated evaders," *Journal of Computer and Systems Sciences International*, vol. 40, no. 5, pp. 749–753, 2001.

[28] I. A. Alias, G. Ibragimov, and A. Rakhmanov, "Evasion differential game of infinitely many evaders from infinitely many pursuers in Hilbert space," *Dynamic Games and Applications*, vol. 6, no. 2, pp. 1–13, 2016.

[29] E. Cartan, "Sur une classe remarkable despaces de Riemann," *Bulletin de la Société Mathématique de France*, vol. 54, pp. 214–216, 1926.

[30] V. V. Nikulin and I. R. Shafarevich, *Geometriya i Gruppy*, Nauka, Moscow, Russia, 1983.

[31] A. Sh. Kuchkarov, "The problem of optimal approach in locally Euclidean spaces," *Automation and Remote Control*, vol. 68, no. 6, pp. 974–978, 2007.

[32] A. I. Subbotin and A. G. Chentsov, *Guaranteed Optimization in Control Problems*, Nauka, Moscow, Russia, 1981 (Russian).

[33] L. A. Petrosjan, *Differential Games of Pursuit*, World Scientific, New York, NY, USA, 1993.

Hindawi Publishing Corporation
Discrete Dynamics in Nature and Society
Volume 2016, Article ID 6142501, 8 pages
http://dx.doi.org/10.1155/2016/6142501

Research Article

Modeling and Nonlinear Response of the Cam-Follower Oblique-Impact System

Yong-Feng Yang,[1] Yu Lu,[1] Ting-Dong Jiang,[1,2] and Na Lu[1]

[1]*Institute of Vibration Engineering, Northwestern Polytechnical University, Xi'an 710072, China*
[2]*Guizhou Aero-Engine Research Institute, Guiyang 550081, China*

Correspondence should be addressed to Yong-Feng Yang; yyf@nwpu.edu.cn

Received 4 May 2016; Accepted 20 June 2016

Academic Editor: Massimiliano Ferrara

Copyright © 2016 Yong-Feng Yang et al. This is an open access article distributed under the Creative Commons Attribution License, which permits unrestricted use, distribution, and reproduction in any medium, provided the original work is properly cited.

In order to quickly and accurately analyze the complex behavior of cam-follower oblique-impact system, a mathematical model which can describe separation, impact, and contact was established in this paper. The transient impact hypothesis was extended, and the oblique collision model was established by considering the tangential slip. Moreau time-stepping method was employed to solve the linear complementarity problem which transformed by the oblique-impact equations. The simulation results show that the cam and follower kept permanent contact when the cam rotational speed was low. With the increase of the cam rotational speed, the cam and follower would be separated and then impact under the gravity action. The system performance shows very complex nonlinear characteristics.

1. Introduction

Cam-follower devices are important classical impacting systems which are used in a wide range of applications. The rotation of the cam at some constant speed provides the force to operate the follower. The most common example is valve trains of internal combustion engines, where the cam rotation imparts through the follower the proper motion to the engine valves while a spring provides the restoring force necessary to maintain contact between the components [1]. The impact of cam-follower is a typical oblique impact. In analyses using nonsmooth dynamics, oblique impact of rough bodies in an unsymmetrical configuration can result in self-locking or "jam" at the sliding contact if the coefficient of friction is sufficiently large: this has been termed Painleve's paradox [2]. Because of this, the follower may exhibit very complex behavior including bifurcations and chaos.

Alzate et al. [3] show that a sudden transition to chaos is observed in an experimental cam-follower. In their mathematical model, the tangential friction effect is ignored. Considering the effect of tangential friction, Sundar et al. [4] study the linear response of a cam-follower. But they do not discuss the nonlinear characteristic. Some researches studied the beam's analysis and experimental methods that are similar and can be used in our study. For example, Ding et al. [5, 6] investigates the convergence of the Galerkin method for the dynamic response of an elastic beam resting on a nonlinear foundation with viscous damping subject to a moving concentrated load. Zhang et al. [7] present experimental verifications of vibration suppression for a cantilever beam bond with a piezoelectric actuator by an adaptive controller. In our research, the transient impact hypothesis is extended, and the oblique collision model is established by considering the tangential slip. Moreau time-stepping method is employed to solve the linear complementarity problem which transforms by the oblique-impact equations. The complex behavior including bifurcations and chaos is shown by the simulation.

2. Linear Complementarity Problem

A linear complementarity problem (LCP) is a problem of the form $\mathbf{y} = \mathbf{M}\mathbf{x} + \mathbf{b}$, $\mathbf{y} \geq 0$, $\mathbf{x} \geq 0$, and $\mathbf{y}^T\mathbf{x} = 0$, where $\mathbf{M}$ is an $n \times n$ matrix and $\mathbf{x}$, $\mathbf{y}$, and $\mathbf{b}$ are an n-dimensional vector [8].

LCP equations may have unique solution, no solution, or multiple solutions. Many problems in scientific computing and engineering applications may lead to solutions of LCP.

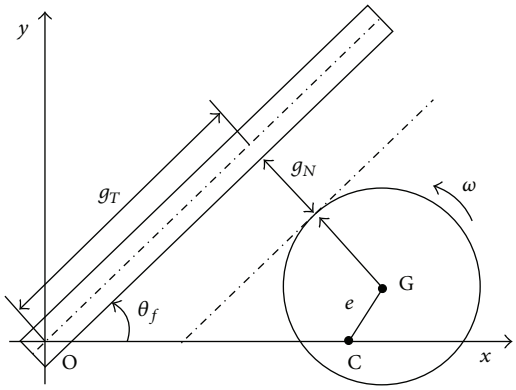

Figure 1: Sketch of cam-follower oblique-impact model.

For example, the LCP may arise from application problems such as the linear and quadratic programming, the economies with institutional restrictions upon prices, the optimal stopping in Markov chain, and the free boundary problems. Several computational methods have been developed for solving LCPs. The two basic functions of the LCP are Upr function and Sgn function:

$$\text{Upr} = \begin{cases} \{0\} & x > 0 \\ (-\infty, 0] & x = 0 \\ \varnothing & x < 0, \end{cases}$$
$$\text{Sgn} = \partial |x| = \begin{cases} \{1\} & x > 0 \\ [-1, 1] & x = 0 \\ \{-1\} & x < 0. \end{cases} \tag{1}$$

In mechanics, Upr function is used to simulate geometry and dynamics of unilateral constraint, and Sgn function is used to simulate various kinds of dry friction.

3. Oblique-Impact Model

A cam-follower with oblique-impact on the contact point is studied in Figure 1. The summary of the general notations used in Figure 1 is shown in Notations. By extending the transient impact hypothesis and considering the tangential slip, the oblique collision model is established.

In the present work, the normal contact between rigid bodies is characterized by a set-valued force law called Signorini's condition [9]. Figure 2 shows two convex rigid bodies apart from each other by a relative normal gap or distance denoted by g_N. The relative normal gap is nonnegative due to bodies' impenetrability condition, being the two bodies in contact with each other when $g_N = 0$. According to Signorini's condition, the normal contact conditions are

$$\begin{aligned} &g_N = 0 \wedge \lambda_N \geq 0 \quad \text{(closed contact)}, \\ &g_N > 0 \wedge \lambda_N = 0 \quad \text{(open contact)}. \end{aligned} \tag{2}$$

Equation (2) represents a complementarity behavior; always zero is the product of the relative normal gap and normal contact force; that is, $g_N \lambda_N = 0$.

The classical Coulomb friction law is another typical example that can be considered as a set-valued force law [9]. For the two conditions sliding and sticking, the tangential forces are

$$\begin{aligned} &-\lambda_T = \mu \lambda_N \text{Sgn}(\gamma_T), \quad \gamma_T \neq 0 \ \text{(sliding)}, \\ &-\mu\lambda_N \leq \lambda_T \leq \mu\lambda_N \quad \text{(sticking)}, \end{aligned} \tag{3}$$

where μ is the friction coefficient; λ_N is the normal contact force; and γ_T is the relative tangential velocity. These two conditions can be summarized by a set-valued force law as [9]

$$-\lambda_T \in \mu \lambda_N \text{Sgn}(\gamma_T). \tag{4}$$

Tangential Coulomb's contact states can be expressed by Sgn function. It also represents a complementarity behavior.

4. Dynamics Equations of the Follower

For the model shown in Figure 1, the dynamics of follower under different speed conditions are considered. There are three states of the follower and cam: separate, contact, and impact. The dynamic equations of the follower can be expressed as [10]

$$M\dot{u} + h = 0 \quad \text{separate}, \tag{5}$$
$$M\dot{u} + h - w_N \lambda_N - w_T \lambda_T = 0 \quad \text{contact}, \tag{6}$$
$$M(u^+ - u^-) - w_N \Lambda_N - w_T \Lambda_T = 0 \quad \text{impact}, \tag{7}$$

where u is generalized velocity and here is the follower's angular velocity $\dot{\theta}_f$; $M = J_o = ml^2/3 + mr^2/4$ is the follower's moment of inertia; $h = mgl\cos(\theta_f)/2$ is the follower's external force; w is the generalized coefficient in contact point; Λ is the force of the follower, and u^+ and u^- are the velocity before and after the impact point, respectively. Notice that λ_N is a continuous boundary parameter when there is no impact. λ_T is a noncontinuous parameter when there is viscous-to-slip transition or change in the direction of relative speed. N denotes normal direction and T denotes tangential direction.

The relationship between w_N, w_T and contact point's relative speeds is

$$\gamma_N = w_N u + \frac{\partial w_N}{\partial t}, \qquad \gamma_T = w_T u + \frac{\partial w_T}{\partial t}. \tag{8}$$

In order to get the unknown parameters w_N and w_T, we need to calculate the distance function in Figure 1:

$$\begin{aligned} g_N &= [x_0 + e\cos(\theta_c)]\sin(\theta_f) - e\sin(\theta_c)\cos(\theta_f) \\ &\quad - r - R, \\ g_T &= [x_0 + e\cos(\theta_c)]\cos(\theta_f) + e\sin(\theta_c)\sin(\theta_f). \end{aligned} \tag{9}$$

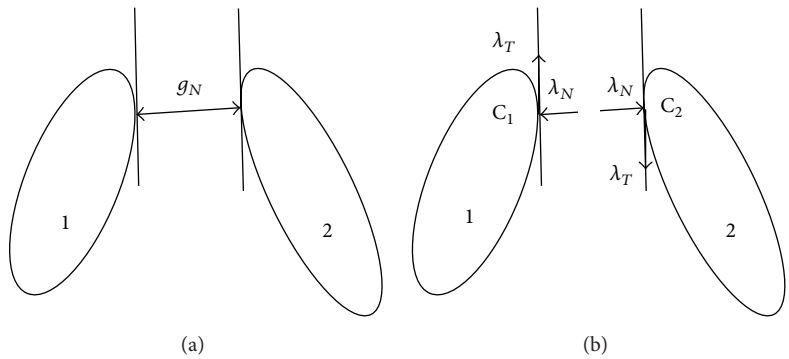

FIGURE 2: Sketch of rigid body contact: (a) normal distance g_N and (b) tangential and normal force.

According to the results of [11],

$$\dot{g} = w\dot{q} + \frac{\partial w}{\partial t}. \tag{10}$$

Therefore,

$$\begin{aligned} w_N &= \left(x_0 + e\cos\left(\theta_c\right)\right)\cos\left(\theta_f\right) + e\sin\left(\theta_c\right)\sin\left(\theta_f\right), \\ w_T &= -\left(x_0 + e\cos\left(\theta_c\right)\right)\sin\left(\theta_f\right) \\ &\quad + e\sin\left(\theta_c\right)\cos\left(\theta_f\right). \end{aligned} \tag{11}$$

There are three equations for the cam-follower impact system. In order to quickly and accurately analyze the complex behavior of cam-follower oblique-impact system, it is better to establish one mathematical equation which can describe separation, impact, and contact motion. Equation measure is introduced here. Equation (6) is multiplied by the Lebesgue measure dt and (7) is multiplied by the atoms measure $d\eta$. Then add the two equations:

$$\begin{aligned} &M\left[\dot{u}dt + \left(u^+ - u^-\right)d\eta\right] + hdt - w_N\left(\lambda_N dt + \Lambda_N d\eta\right) \\ &\quad - w_T\left(\lambda_T dt + \Lambda_T d\eta\right) = 0. \end{aligned} \tag{12}$$

This equation can be abbreviated as

$$Mdu + hdt - w_N dP_N - w_T dP_T = 0, \tag{13}$$

where $du = \dot{u}dt + (u^+ - u^-)d\eta$ is velocity measure. It contains two parts: one is the continuous part, Lebesgue measure $\dot{u}dt$; the other is the noncontinuous part, Dirac measure. When the cam-follower is in the nonimpact state, the velocity measure $du = \dot{u}dt$. The impact measure which relates to the Lagrange multiplier also contains two parts: $dP = \lambda dt + \Lambda d\eta$. The separation, impact, and contact equations are expressed as the unified form in (13) [10].

Moreau time-stepping method [10] is employed to discretize (13). We can get

$$M_M\left(u_E - u_A\right) + h_M\Delta t - w_{NM}p_N - w_{TM}p_T = 0, \tag{14}$$

where A and E represent starting and ending time. M is the middle time of A and E. For the normal impact parameter p_N, apply the Upr function:

$$-p_N \in \mathrm{Upr}\left(\xi_N\right) \Longleftrightarrow p_N \geq 0,\ \xi_N \geq 0,\ p_N\xi_N = 0, \tag{15}$$

where $\xi_N = \gamma_N^+ + \varepsilon_N\gamma_N^-$.

In order to get the expectation LCP condition, we need to separate Sgn function to two Upr functions. For the tangential impact parameter p_T, we can get

$$\begin{aligned} &-p_T \in \mu p_N \mathrm{Sgn}\left(\xi_T\right) \Longleftrightarrow \exists \xi_R, \xi_L \\ &\text{s.t.} \quad \mu p_N + p_T \geq 0,\ \xi_R \geq 0,\ \left(\mu p_N + p_T\right)\xi_R = 0 \\ &\qquad \mu p_N - p_T \geq 0,\ \xi_L \geq 0,\ \left(\mu p_N - p_T\right)\xi_L = 0 \\ &\qquad \xi_T = \xi_R - \xi_L. \end{aligned} \tag{16}$$

For the sake of brevity, we define $p_R \coloneqq \mu p_N + p_T$ and $p_L \coloneqq \mu p_N - p_T$, where "$\coloneqq$" means "is defined as." The second and third expressions of (16) are $P_R \geq 0,\ \xi_R \geq 0,\ P_R\xi_R = 0$ and $P_L \geq 0,\ \xi_L \geq 0,\ P_L\xi_L = 0$. The LCP condition is

$$0 \leq \begin{pmatrix} \xi_N \\ \xi_R \\ p_L \end{pmatrix} \perp \begin{pmatrix} p_N \\ p_R \\ \xi_L \end{pmatrix} \geq 0. \tag{17}$$

The full LCP equation of follower can be expressed as

$$\begin{aligned} &\begin{pmatrix} \xi_N \\ \xi_R \\ p_L \end{pmatrix} \\ &= \begin{pmatrix} w_{NM}M_M^{-1}\left(w_{NM} - w_{TM}\mu\right) & w_{NM}M_M^{-1}w_{TM} & 0 \\ w_{TM}M_M^{-1}\left(w_{NM} - w_{TM}\mu\right) & w_{NM}M_M^{-1}w_{TM} & 1 \\ 2\mu & -1 & 0 \end{pmatrix}\begin{pmatrix} p_N \\ p_R \\ \xi_L \end{pmatrix} \\ &\quad + \begin{pmatrix} w_{NM}M_M^{-1}h_M\Delta t + \left(1+\varepsilon_N\right)\gamma_{NA} \\ w_{TM}M_M^{-1}h_M\Delta t + \left(1+\varepsilon_N\right)\gamma_{TA} \\ 0 \end{pmatrix}. \end{aligned} \tag{18}$$

From the solution of (17) and (18), we can get p_N and p_R. Then the generalized velocity can be calculated by

$$\begin{aligned} u_E &= M_M^{-1}\left(w_{NM} - w_{TM}\mu\right)p_N + M_M^{-1}w_{TM}p_R \\ &\quad + M_M^{-1}h_M\Delta t + u_A \end{aligned} \tag{19}$$

and the generalized displacement can be gotten by the definition of Moreau time time-stepping method.

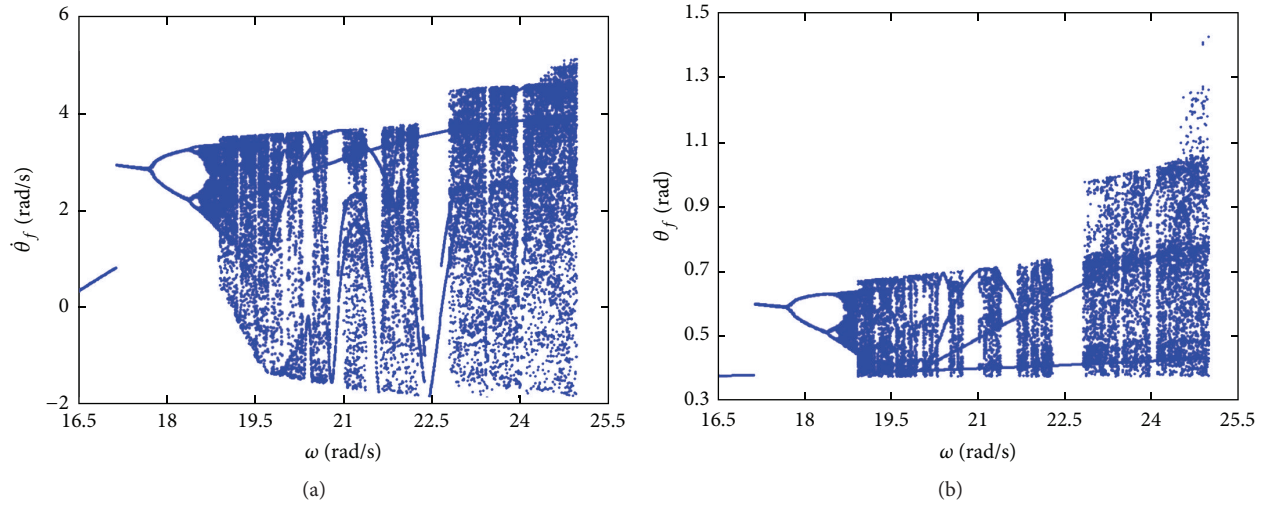

Figure 3: Bifurcation diagram with the change of cam speed: (a) angular velocity and (b) angular displacement.

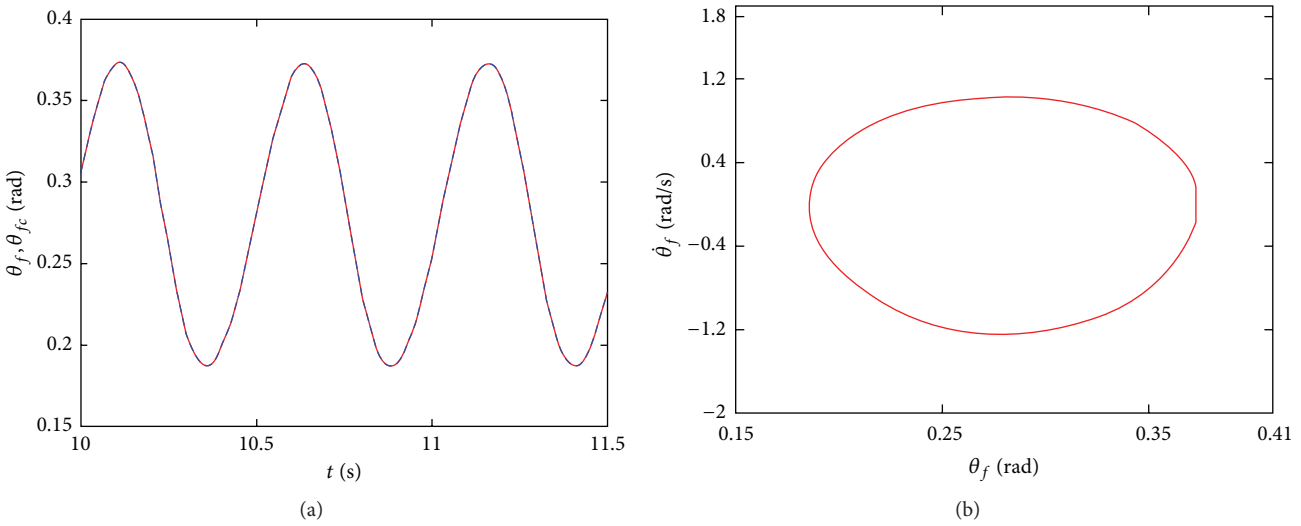

Figure 4: Cam and follower permanent contact when $\omega = 12$ rad/s: (a) time history of θ_f (solid line) and θ_{fc} (dashed line) and (b) phase diagram.

5. Simulation of the Dynamics Response

MATLAB is employed for simulation of the equations. In order to get a proper accuracy, the time step of Moreau midpoint method must be very small. We choose 0.0002 s as the time step, and the values of other parameters can be found in Table 1.

With the increasing of the cam rotational speed, the state of the cam-follower is transformed from the initial permanent contact to the separation and impact. The system performs very complex nonlinear characteristics, such as period, quasiperiod, and chaos response. The bifurcation diagrams are shown in Figure 3.

5.1. Permanent Contact. When the cam rotational speed is low, the constraining force between cam and follower is less than the follower's restoring force. Therefore, the cam and follower keep in contact. The angular displacement of time history diagram and phase diagram is shown in Figure 4 when $\omega = 12$ rad/s. The motion of cam and follower remained the same (there are a solid line and a dashed line in Figure 4(a)), and the phase plane shows a smooth circle.

5.2. Period Motion. With the increasing of the cam speed, the cam and follower would be separated. When the cam and follower impact, there are minor collisions after the first impact, and then follower would contact the cam's surface until the next separation. As shown in Figure 5, the motion of the follower is periodic 1 or the orbit is $P(\infty, 1)$.

When the cam speed goes higher, as shown in Figures 6 and 7, the responses are $P(1,1), P(2,2), P(4,4), \ldots$. From the time history of these $P(n,n)$ responses, the common point is that there is only 1 impact in each cam period.

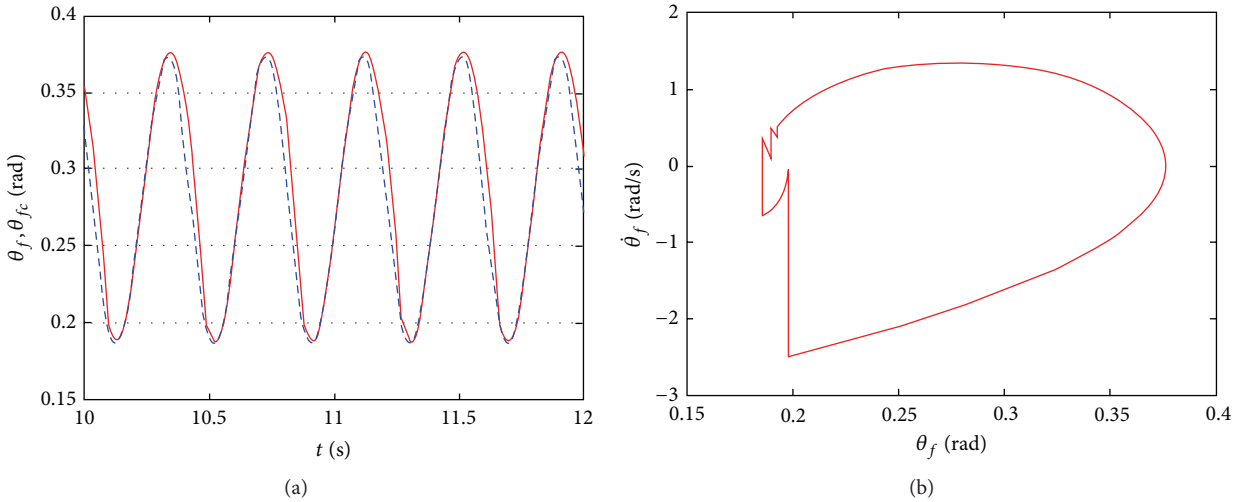

FIGURE 5: $P(\infty, 1)$ motion when $\omega = 16$ rad/s: (a) time history of θ_f (solid line) and θ_{fc} (dashed line) and (b) phase diagram.

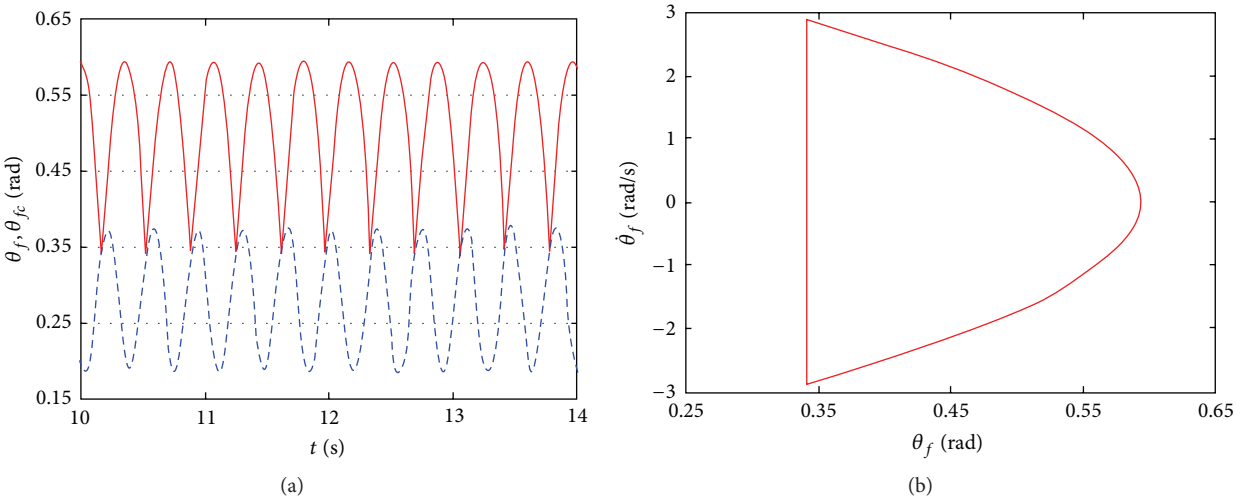

FIGURE 6: $P(1, 1)$ motion when $\omega = 17.4$ rad/s: (a) time history of θ_f (solid line) and θ_{fc} (dashed line) and (b) phase diagram.

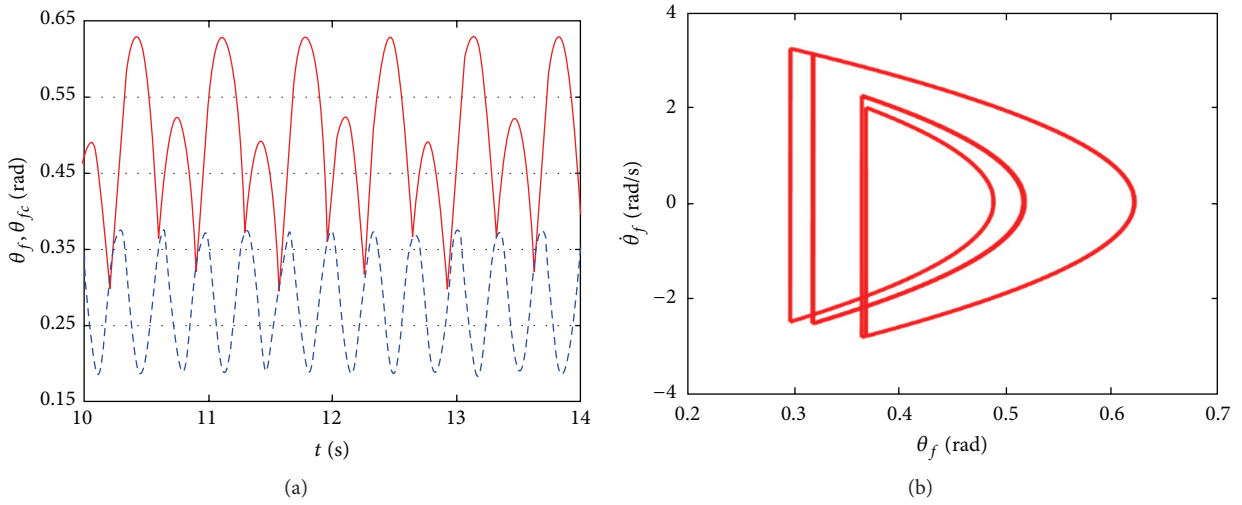

FIGURE 7: $P(4, 4)$ motion when $\omega = 18.5$ rad/s: (a) time history of θ_f (solid line) and θ_{fc} (dashed line) and (b) phase diagram.

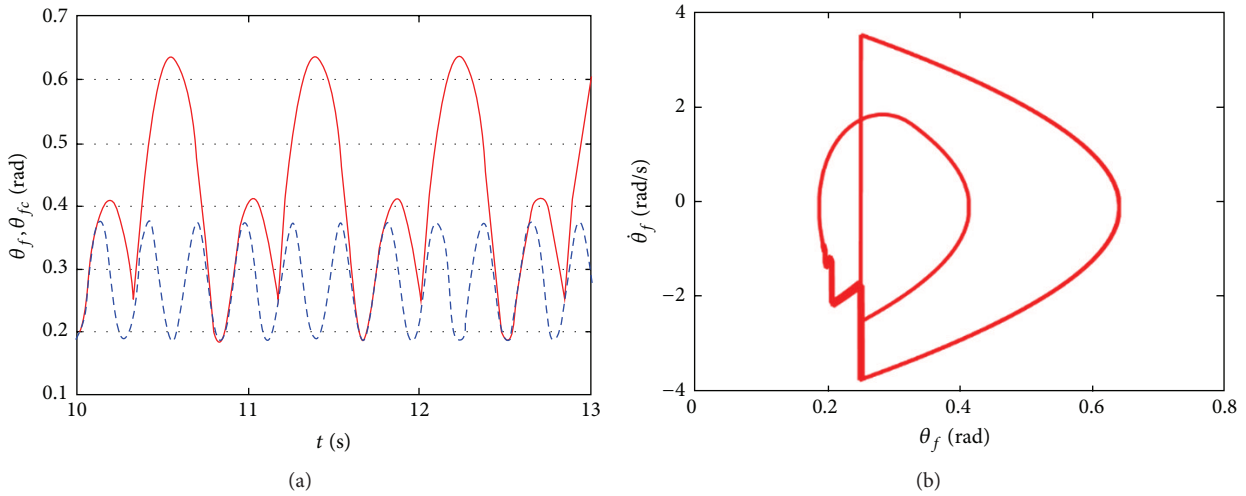

FIGURE 8: $P(\infty, 2)$ motion when $\omega = 22.5$ rad/s: (a) time history of θ_f (solid line) and θ_{fc} (dashed line) and (b) phase diagram.

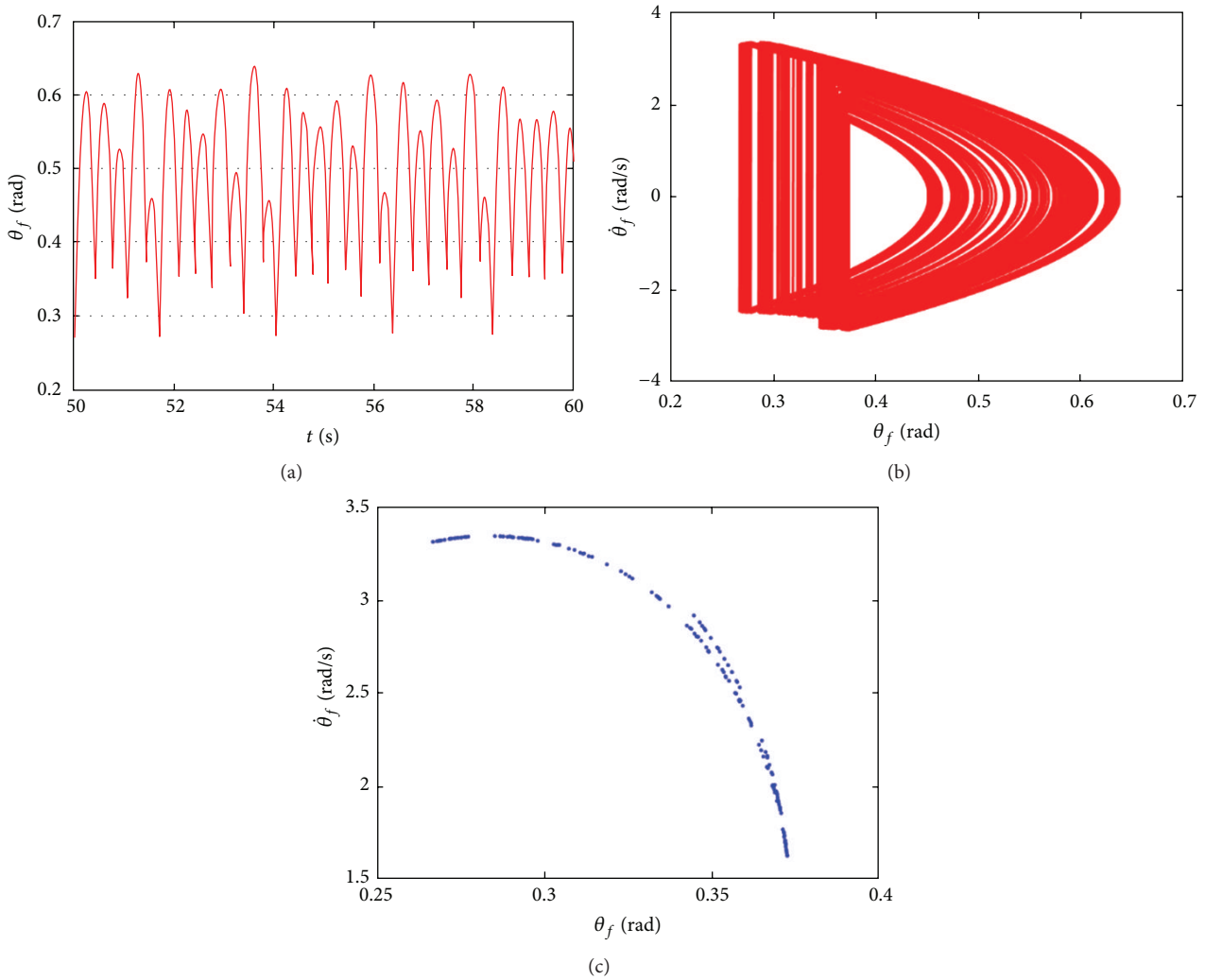

FIGURE 9: Chaos motion when $\omega = 18.84$ rad/s: (a) time history; (b) phase diagram; and (c) Poincaré map.

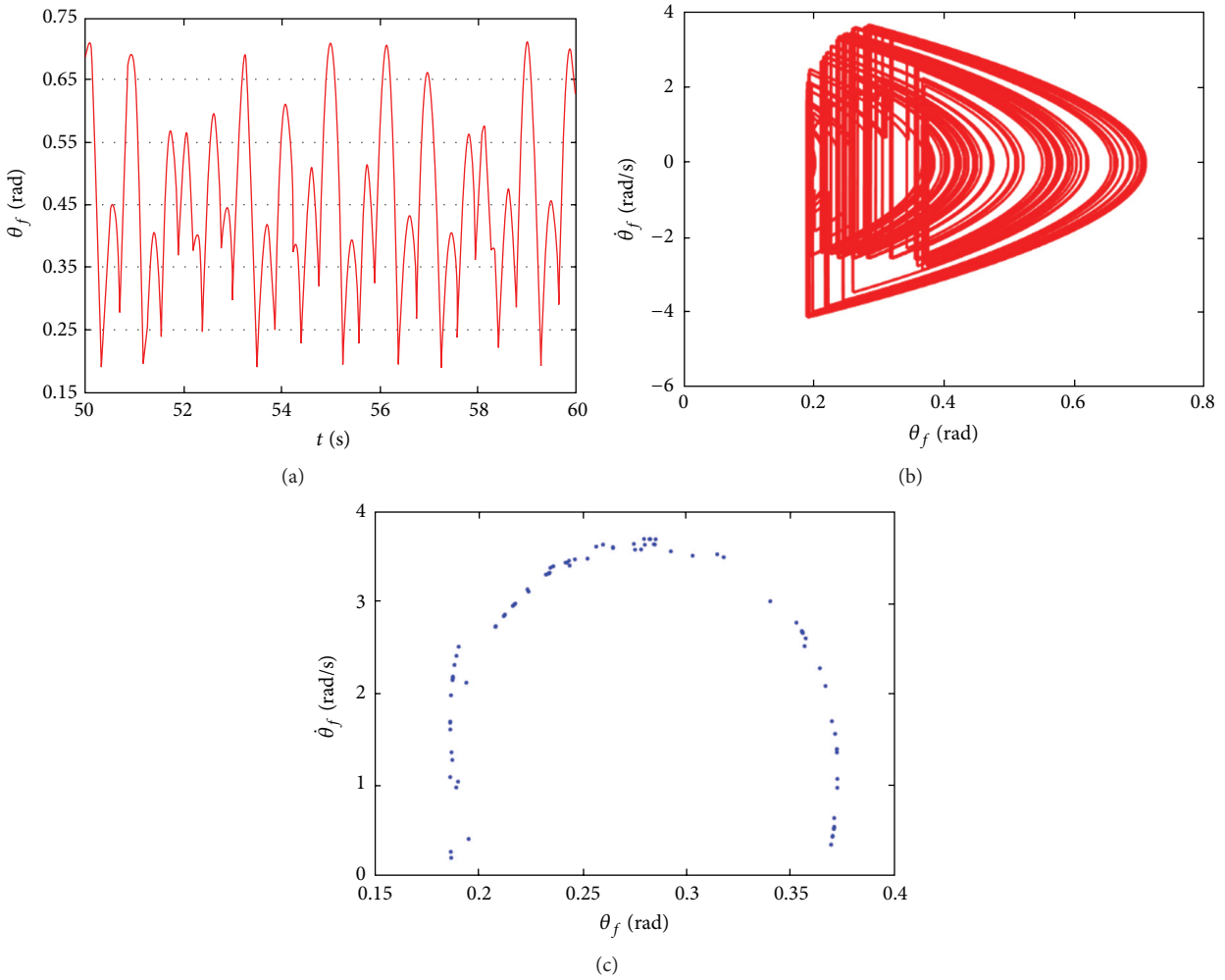

Figure 10: Chaos motion when $\omega = 21.7$ rad/s: (a) time history; (b) phase diagram; and (c) Poincaré map.

Table 1: Cam-follower oblique-impact numerical simulation parameters.

Parameter	Value
Length of the follower, L	0.8 m
Radius of the follower, r	0.01 m
Mass of the follower, m	1.975 kg
Eccentricity of the cam, e	0.036 m
Radius of the cam, R	0.1 m
Coefficient of restitution in normal direction	0.42
Coefficient of restitution in tangential direction	0.4
Friction coefficient, μ	0.2
Distance between bear fix point of the follower and rotation center of the cam, x_0	0.4 m
Initial angular position of the cam, θ_0	0 rad

There also exist $P(\infty, n)$ motions. The rotation speeds of these motions are between two chaos areas in Figure 3. Figure 8 shows the $P(\infty, 2)$ motion. For these motions, the period of impact is greater than the cam. When the collision occurs, the normal velocity of cam and follower is close. Therefore, collision could not change the follower's angular velocity direction.

5.3. Chaos Motion. Generally, for vibroimpact system, there are two ways for Poincaré section selection: (1) to select the fixed phase section of trajectory as Poincaré and (2) to select the collision surface as Poincaré section. In this paper, the collision surface is used:

$$\Sigma = \left\{\left(\theta, \dot{\theta}, t\right) \in R^2 \times R^+ \mid \xi_N = 0,\ \gamma_{NA} < 0\right\}. \tag{20}$$

$\xi_N = 0$ represents the collision point, and the mirror collision can be excluded by $\gamma_{NA} < 0$.

Figure 9 shows the response when $\omega = 18.84$ rad/s. The collision does not follow the periodic variation and became chaotic. Figure 10 shows the response when $\omega = 21.7$ rad/s. Compared with Figure 9, the chaos response shows more characteristics of slip phenomenon with 21.7 rad/s.

6. Conclusions

The cam and follower oblique collision model is established in this paper. In order to simulate the response, the equations of the separation, impact, and contact motion are transformed to a linear complementarity problem. The main conclusions are as follows:

(1) The contact and tangential impact law represent a complementarity behavior. LCP equation method could be used to solve the oblique collision problem.

(2) The system performs very complex nonlinear characteristics, such as period, quasiperiod, and chaos response. For every motion, there is a special collision phenomenon.

Notations

r: Radius of the follower
O: Bear fix point of the follower
L: Length of the follower
θ_f: Angular position of follower with counterclockwise sense of rotation
θ_c: Angular position of cam with counterclockwise sense of rotation
e: Eccentricity of the cam
ω: Rotation speed of the cam
C: Rotation center of the cam
G: Geometric center of the cam
θ_0: Initial angular position of the cam
g_N: Displacement between cam and follower
g_T: Displacement between follower's fix point and the point which is nearest to the cam.

Competing Interests

The authors declare that they have no competing interests.

Acknowledgments

This work was supported by the National Natural Science Foundation of China (Grants nos. 11272257 and 11672251) and NPU Aoxiang New Star.

References

[1] R. Alzate, M. Di Bernardo, U. Montanaro, and S. Santini, "Experimental and numerical verification of bifurcations and chaos in cam-follower impacting systems," *Nonlinear Dynamics*, vol. 50, no. 3, pp. 409–429, 2007.

[2] Y. Shen and W. J. Stronge, "Painleve paradox during oblique impact with friction," *European Journal of Mechanics. A. Solids*, vol. 30, no. 4, pp. 457–467, 2011.

[3] R. Alzate, P. T. Piiroinen, and M. Di Bernardo, "From complete to incomplete chattering: a novel route to chaos in impacting cam-follower systems," *International Journal of Bifurcation and Chaos*, vol. 22, no. 5, Article ID 1250102, 2012.

[4] S. Sundar, J. T. Dreyer, and R. Singh, "Rotational sliding contact dynamics in a non-linear cam-follower system as excited by a periodic motion," *Journal of Sound and Vibration*, vol. 332, no. 18, pp. 4280–4295, 2013.

[5] H. Ding, L.-Q. Chen, and S.-P. Yang, "Convergence of Galerkin truncation for dynamic response of finite beams on nonlinear foundations under a moving load," *Journal of Sound and Vibration*, vol. 331, no. 10, pp. 2426–2442, 2012.

[6] H. Ding and L.-Q. Chen, "Galerkin methods for natural frequencies of high-speed axially moving beams," *Journal of Sound and Vibration*, vol. 329, no. 17, pp. 3484–3494, 2010.

[7] T. Zhang, H. G. Li, Z. Y. Zhong, and G. P. Cai, "Hysteresis model and adaptive vibration suppression for a smart beam with time delay," *Journal of Sound and Vibration*, vol. 358, pp. 35–47, 2015.

[8] M. B. Meingast, M. Legrand, and C. Pierre, "A linear complementarity problem formulation for periodic solutions to unilateral contact problems," *International Journal of Non-Linear Mechanics*, vol. 66, pp. 18–27, 2014.

[9] R. I. Leine and C. Glocker, "A set-valued force law for spatial Coulomb-Contensou friction," *European Journal of Mechanics—A/Solids*, vol. 22, no. 2, pp. 193–216, 2003.

[10] P. Flores, R. Leine, and C. Glocker, "Application of the nonsmooth dynamics approach to model and analysis of the contact-impact events in cam-follower systems," *Nonlinear Dynamics*, vol. 69, no. 4, pp. 2117–2133, 2012.

[11] C. Glocker, "On frictionless impact models in rigid-body systems," *Philosophical Transactions of the Royal Society of London B: Biological Sciences*, vol. 359, no. 1789, pp. 2385–2404, 2001.

Hindawi Publishing Corporation
Discrete Dynamics in Nature and Society
Volume 2016, Article ID 9031351, 8 pages
http://dx.doi.org/10.1155/2016/9031351

Research Article

Risk-Averse Evolutionary Game Model of Aviation Joint Emergency Response

Wei Pan,[1] Ying Guo,[1] and Shujie Liao[2]

[1]*School of Economics and Management, Wuhan University, Wuhan 430072, China*
[2]*Cancer Biology Research Center, Tongji Hospital, Tongji Medical College, Huazhong University of Science and Technology, Wuhan, Hubei 430030, China*

Correspondence should be addressed to Shujie Liao; sjliao@tjh.tjmu.edu.cn

Received 8 March 2016; Revised 27 April 2016; Accepted 28 April 2016

Academic Editor: Massimiliano Ferrara

Copyright © 2016 Wei Pan et al. This is an open access article distributed under the Creative Commons Attribution License, which permits unrestricted use, distribution, and reproduction in any medium, provided the original work is properly cited.

We study effects of risk-averse attitude of both participators in aviation joint emergency response on the coevolution of cooperation mechanisms and individual preferences between airport and nonprofit organization. First, based on the current aviation joint emergency mechanism in China, we put forward two mechanisms to select the joint nonprofit organization, including reputation cooperation and bidding competition. Meanwhile, we consider two preferences including altruism and selfishness. Then we build replicator dynamics equations using the theory of conditional value-at-risk (CVaR) taking risk aversion attitude into account. Finally, we introduce the factor of government and give all participators some suggestions. We show that the risk-averse attitude of the other game participator affects the one participator's decision and the effects subject to some parameters.

1. Introduction

Emergencies happen suddenly, and they are likely to cause significant casualties, property losses, and other serious social problems [1]. Airports always have a higher disaster probability than other accidental locations. Recently, aviation joint emergency response mechanisms have been studied and reach some academic achievements [2, 3]. Generally, airports are profit organizations to maximize their expected return in emergencies, including increasing reputation and decreasing compensation to victims. Hospitals and firefighters are nonprofit organizations to realize their responsibility and social value by saving life and property. Governments are the third departments to stabilize the society by supporting and supervising relief organizations. Now, Chinese aviation joint emergency mechanisms are mainly guided by airports. Airports buy the service from nonprofit organizations, schedule the emergency plans, and coordinate with nonprofit organizations.

In aviation joint emergency mechanisms, Zhu and Luo [2] put forward the solutions that the joint emergency response system to aviation calamities should work under command of emergency headquarters of aviation authorities at all levels, employ virtual network organization, and put participators' responsibilities in order, making sense in quick response and coordination. Disaster response center in the north of Salt Lake City, Utah, USA, has handled several air crashes successfully coordinating with polices, firefighters, and other relief organizations [3]. De-Sheng and Wei-An [4] build a random matching game model to analyze the influence of contracting cost on the interaction between formal contracts and informal contracts. Abbasi [5] studies the mechanisms of emergency response network evolution by examining the link formation pattern among participators involved in a real emergency collaboration network.

In cooperation, some researches focus on the evolution of cooperation among altruistic preference and selfish individuals [6]. Nowak et al. study evolutionary game dynamics and specify the conditions required for natural selection to favor the emergence of cooperation and define evolutionary stability in finite populations [7]. Faraj and Xiao investigate the coordination practices of a medical trauma center and develop a coordination-practice perspective that emphasizes expertise coordination and dialogic coordination

[8]. Kapucu analyzes the cooperation among public and nonprofit organizations to achieve public service goals in emergencies and examines the factors that contribute to successful public-nonprofit partnerships [9]. Gürerk et al. provide new empirical insights into Tiebout's intuition by showing that self-selection in open heterogeneous communities can significantly foster communities' success [10].

Perc and Szolnoki reviewed recent works on evolutionary games incorporating coevolutionary rules and describe many factors in evolutionary process. This mini review on coevolutionary games gives us a clear line about research on evolutionary games incorporating coevolutionary rules [11]. Szabó and Szolnoki studied spatial evolutionary games as a personal character is tuned from selfishness to other regarding preferences via fraternity. The paper gives a utility function of its income and others' payoff with a weight factor [12]. Buesser et al. presented a systematic numerical investigation of standard evolutionary games on weighted networks, which extends previous work on unweighted networks, and they found that taking the weights into account only changes the results slightly with respect to the unweighted network [13]. Carlsen et al. studied future robot systems for civil protection based on a coevolutionary scenario approach and the development of different evolutionary paths, and they considered opportunities, threats, and ethical aspects in the domestic security and safety sector and discussed the above aspects in the context of different scenarios of different future societies [14].

In the applications of game theory in emergency management, Dehai and Lijuan put forward two city demolition modes and analyze the emergencies of equilibrium evolution learned by Akihiko's model about evolutionary analysis of game equilibrium with interaction between different cultures [15]. Feng and Wu use game theory model to find the retailers' optimal order quantity by the conditional value-at-risk as a risk measure and considering emergencies leads to the decision makers risk aversion [1]. Li et al. investigate the evolution of cooperation on supply networks focusing on the impacts of network topologies in emergency management and offer a useful insight into understanding complex strategy behaviors in supply networks [16]. Abbasi et al. show actors' interconnectedness in an emergency response operation [17].

Since 2002, CVaR is introduced by Roekafller and Uryasev [18, 19] and used widely from risky assets to any risky decisions, including logistics [20–22] and disasters [23–25]. Chen et al. studied the collective-risk social dilemma with risky assets in well-mixed and structured populations. They found that in low-risk situations bounded rational allocation of assets works the best, while in high-risk situations the simplest uniform distribution of assets among all the groups is optimal, which indicate that prosocial behavior depends sensitively on the potential losses [26]. Chen et al. studied "problems of the commons" with group performance dependent risk levels, and they showed that stronger feedback between group performance and risk level is in general more favorable for the successful evolution of public cooperation [27]. Xia et al. studied dynamic instability of cooperation due to diverse activity patterns in evolutionary social dilemmas, and they showed that if the interaction network is not strongly heterogeneous, the overall failure of cooperation evolution is not impaired, which may be because inactivity negatively affects the potency of low-degree defectors [28]. From above, we can see that there are many researches which have been done in terms of risk aversion in evolutionary games. However, in those works with risk aversion in evolutionary games, there are few studies using the tool of CVaR to express the evolutionary process. At present, there are many papers on relationship of governments and nonprofit organizations [29–32]. But few papers are about the relationship between airports and nonprofit organizations in emergency management and evolutionary game in emergency management taking participators' risk preferences into account. Therefore, this paper is to study the coevolution of cooperation mechanisms and risk preferences among airports and nonprofit organizations. It is not difficult to imagine that players, including airport and nonprofit organizations, are risk-averse under emergency situations. Inspired by the conditional value-at-risk (CVaR) [20–22], we use CVaR instead of expected return and construct replicator dynamics equations.

The rest of this paper is organized as follows: Section 2 presents evolutionary game between airport and nonprofit organization for analyzing the replicator dynamics equations with risk-averse attitude. Section 3 shows the effect of government on the evolutionary equilibrium and gives some suggestions for actors. Section 4 concludes a brief discussion of theoretical and practical implications. At last, it presents the future researches.

2. Evolutionary Game of Aviation Joint Emergency Mechanisms

2.1. The Null Hypothesis. As we all know, there are some nonprofit organizations, such as hospitals, that operate for both nonprofit and profit purpose, and more and more international governments buy service from nonprofit organizations by bidding. In China, many airports cooperate with nonprofit organizations directly who have bigger size and higher reputation, increasing airports' reputation and cognitive safety for travelers. Hence, the assumption that airport selects the joint organizations by either reputation cooperation mechanism or bidding competition mechanism is reasonable and practical. Some nonprofit organizations pursue loyalty and social value. They are altruistic. On the other hand, some organizations prefer power and position. They are selfish individuals. Altruism always takes actions for high degree of coordination and obeys the airports' commands. However, selfish individuals always make decisions without authorization for saving life and property. So the assumption that nonprofit organization has two preferences is reasonable and practical.

In order to simplify the analysis, we have some hypotheses as follows. (1) Airports take two joint mechanisms that are reputation cooperation and bidding competition. Reputation cooperation mechanism prefers sharing value and codetermination. Bidding competition mechanism prefers leadership and command. (2) Nonprofit organization has

two preferences that are altruism and selfishness. Altruism prefers loyalty and social value. Selfishness prefers power and important position. (3) Altruism always has a sense of disloyalty under bidding competition mechanism, which makes altruism produce subjective cost. Selfish individuals always gain more extra payoff from mechanism of reputation cooperation. (4) Airport must take cost to supervise and manage joint organizations to support the bidding competition mechanism. Cost for selfishness is larger than altruism. (5) Demand of an accident about coordination is a constant d. It will affect airport payoff directly. (6) The risk-averse degree of airport is η_1 and the risk-averse degree of nonprofit organization is η_2. The random payoff deals with 0-1 variable. x, y represent the random selection variable of airport and nonprofit organization, respectively.

2.2. Evolutionary Game between Airport and Nonprofit Organization. We use the following notations throughout this paper:

H: the same payoff for both airport and nonprofit organization when nonprofit organization prefers altruism,

L: the same payoff for both airport and nonprofit organization when nonprofit organization prefers selfishness,

d: the constant demand of an accident for degree of coordination,

λ: the speculative extra payoff of nonprofit organization when airport adopts reputation cooperation mechanism,

λ_1: airport's management cost for altruism,

λ_2: airport's management cost for selfishness,

C: altruism's subjective cost for disloyalty.

$\lambda_1 \le \lambda_2 \le \lambda$, $H \le L + \lambda$, $H - C \ge L$, and $\lambda \le \lambda_2 + (1/M)\lambda_1$, noting that the speculative extra payoff λ would not be much too bigger, and M is a quite big number. Coevolution of cooperation mechanisms and preferences are presented in Table 1.

2.3. Analysis of the Evolutionary Process with Risk-Averse. We note that the probability of adopting reputation cooperation mechanism is p. Accordingly, the probability of adopting bidding competition mechanism is $1 - p$. We note that the portion of altruism is q and the portion of selfishness is $1 - q$. Taking advantage of the tool of risk management in financial, conditional value-at-risk (CVaR) [20–22], we consider the risk attitudes of actors. The analysis is as follows.

(1) Analysis of Evolutionary Process for Airport. The CVaR of reputation cooperation mechanism is represented by

$$\begin{aligned}
\mathrm{CVaR}_{11} &= \max\left\{r_{11} - \frac{1}{1-\eta_1}E\left(r_{11} - \pi_{11}(y)\right)^+\right\},\\
F_{11} &= r_{11} - \frac{1}{1-\eta_1}E\left(r_{11} - \pi_{11}(y)\right)^+\\
&= r_{11} - \frac{q}{1-\eta_1}\left(r_{11} - H + d\right)^+\\
&\quad - \frac{1-q}{1-\eta_1}\left(r_{11} - L + d + \lambda\right)^+,\\
\mathrm{CVaR}_{11} &= L - d - \lambda \quad \text{when } q \le \eta_1,\\
\mathrm{CVaR}_{11} &= H - d - \frac{1-q}{1-\eta_1}(H - L + \lambda) \quad \text{when } q > \eta_1.
\end{aligned} \tag{1}$$

The CVaR of bidding competition mechanism is represented by

$$\begin{aligned}
\mathrm{CVaR}_{12} &= \max\left\{r_{12} - \frac{1}{1-\eta_1}E\left(r_{12} - \pi_{12}(y)\right)^+\right\},\\
F_{12} &= r_{12} - \frac{q}{1-\eta_1}\left(r_{12} - H + d + \lambda_1\right)^+\\
&\quad - \frac{1-q}{1-\eta_1}\left(r_{12} - L + d + \lambda_2\right)^+,\\
\mathrm{CVaR}_{12} &= L - d - \lambda_2 \quad \text{when } q \le \eta_1,\\
\mathrm{CVaR}_{12} &= H - d - \lambda_1 - \frac{1-q}{1-\eta_1}\left(H - L - \lambda_1 + \lambda_2\right)\\
&\qquad \text{when } q > \eta_1.
\end{aligned} \tag{2}$$

The CVaR of reputation cooperation and bidding competition mechanism is represented by

$$\begin{aligned}
\mathrm{CVaR}_1 &= \max\left\{r_1 - \frac{1}{1-\eta_1}E\left(r_1 - \pi_1(x,y)\right)^+\right\},\\
F_1 &= r_1 - \frac{p}{1-\eta_1}\left(r_1 - \mathrm{CVaR}_{11}\right)^+\\
&\quad - \frac{1-p}{1-\eta_1}\left(r_1 - \mathrm{CVaR}_{12}\right)^+,\\
\mathrm{CVaR}_1 &= L - d - \lambda_2 - \frac{p}{1-\eta_1}\left(\lambda - \lambda_2\right)\\
&\qquad \text{when } q \le \eta_1,\ p \le 1 - \eta_1,
\end{aligned} \tag{3}$$

$$\begin{aligned}
\mathrm{CVaR}_1 &= L - d - \lambda \quad \text{when } q \le \eta_1,\ p > 1 - \eta_1,\\
\mathrm{CVaR}_1 &= H - d - \lambda_1 - \frac{1-q}{1-\eta_1}\left(H - L - \lambda_1 + \lambda_2\right)\\
&\qquad \text{when } q > \eta_1,\ p \le \eta_1,\\
\mathrm{CVaR}_1 &= \frac{q-\eta_1}{1-\eta_1}\lambda_1 - \frac{1-q}{1-\eta_1}\left(\lambda - \lambda_2\right)\\
&\qquad \text{when } q > \eta_1,\ p > \eta_1.
\end{aligned}$$

The replicator dynamics equation of reputation cooperation mechanism for airport is represented by

$$G(p) = \frac{dp}{dt} = p * \left(\mathrm{CVaR}_{11} - \mathrm{CVaR}_1\right). \tag{4}$$

Table 1: Coevolution of cooperation mechanisms and preferences.

(Airport, nonprofit organization)	Altruistic preference (q)	Selfish preference ($1-q$)
Reputation cooperation (p)	$(H-d, H)$	$(L-d-\lambda, L+\lambda)$
Bidding competition ($1-p$)	$(H-d-\lambda_1, H-C)$	$(L-d-\lambda_2, L)$

$G(p) = dp/dt = 0$ means that the evolutionary game reaches a stable state.

When $q \le \eta_1$ and $p \le 1-\eta_1$, $p^* = 0$, $p^* = 1-\eta_1$. We have $G(p) < 0$, $G'(0) > 0$, $G'(1-\eta_1) < 0$; then $p^* = 1-\eta_1$ is the evolutionary stable strategy (ESS).

When $q \le \eta_1$ and $p > 1-\eta_1$, $G(p) = 0$, $G'(p) = 0$.

When $q > \eta_1$ and $p \le \eta_1$, $p^* = 0$, $q^* = (\lambda+\eta_1\lambda_1-\lambda_2)/(\lambda+\lambda_1-\lambda_2) > \eta_1$. If $q \le q^*$, then $G(p) < 0$, $G'(0) < 0$, and $p^* = 0$ is the ESS. If $q > q^*$, then $G(p) > 0$, $G'(0) > 0$, and $p^* = 0$ is not the ESS.

When $q > \eta_1$ and $p > \eta_1$, $p^* = 1$, $q^* = (\lambda+\eta_1\lambda_1-\lambda_2)/(\lambda+\lambda_1-\lambda_2) > \eta_1$. If $q \le q^*$, then $G(p) < 0$, $G'(1) > 0$, and $p^* = 1$ is not the ESS. If $q > q^*$, then $G(p) > 0$, $G'(1) < 0$, and $p^* = 1$ is the ESS.

(2) Analysis of Evolutionary Process for Nonprofit Organization. The CVaR of altruism is represented by

$$\begin{aligned}
\mathrm{CVaR}_{21} &= \max\left\{r_{21} - \frac{1}{1-\eta_2}E\left(r_{21}-\pi_{21}(x)\right)^+\right\},\\
F_{21} &= r_{21} - \frac{p}{1-\eta_2}\left(r_{21}-H\right)^+\\
&\quad - \frac{1-p}{1-\eta_2}\left(r_{21}-H+C\right)^+,\\
\mathrm{CVaR}_{21} &= H-C \quad \text{when } p \le \eta_2,\\
\mathrm{CVaR}_{21} &= H - \frac{1-p}{1-\eta_2}C \quad \text{when } p > \eta_2.
\end{aligned} \tag{5}$$

The CVaR of selfishness is represented by

$$\begin{aligned}
\mathrm{CVaR}_{22} &= L \quad \text{when } p \le \eta_2,\\
\mathrm{CVaR}_{22} &= L + \frac{p-\eta_2}{1-\eta_2}\lambda \quad \text{when } p > \eta_2.
\end{aligned} \tag{6}$$

The CVaR of altruism and selfishness is represented by

$$\begin{aligned}
\mathrm{CVaR}_2 &= \max\left\{r_2 - \frac{1}{1-\eta_2}E\left(r_2-\pi_2(x,y)\right)^+\right\},\\
\mathrm{CVaR}_2 &= L \quad \text{when } p \le \eta_2,\ q \le \eta_2,\\
\mathrm{CVaR}_2 &= \frac{q-\eta_2}{1-\eta_2}(H-C) + \frac{1-q}{1-\eta_2}L\\
&\qquad \text{when } p \le \eta_2,\ q > \eta_2,\\
\mathrm{CVaR}_2 &= \frac{q-\eta_2}{1-\eta_2}\left(L + \frac{p-\eta_2}{1-\eta_2}\lambda\right)\\
&\quad - \frac{1-q}{1-\eta_2}\left(H - \frac{1-p}{1-\eta_2}C\right)\\
&\qquad \text{when } p > \eta_2,\ q \le 1-\eta_2,\\
\mathrm{CVaR}_2 &= H - \frac{1-p}{1-\eta_2}C \quad \text{when } p > \eta_2,\ q > 1-\eta_2.
\end{aligned} \tag{7}$$

The replicator dynamics equation of altruism preference for nonprofit organization is represented by

$$G(q) = \frac{dq}{dt} = q * \left(\mathrm{CVaR}_{21} - \mathrm{CVaR}_2\right). \tag{8}$$

When $p \le \eta_2$ and $q \le \eta_2$, $q^* = 0$. We have $G(q) > 0$, $G'(0) > 0$; then $q^* = 0$ is not the ESS.

When $p \le \eta_2$ and $q > \eta_2$, $q^* = 1$, $G(q) > 0$, and $G'(1) < 0$; then $q^* = 1$ is the ESS.

When $p > \eta_2$ and $q \le 1-\eta_2$, $q^* = 0$, $q^* = 1-\eta_2$, and $p^* = 1-((L+\lambda-H)/(\lambda-C))(1-\eta_2) > \eta_2$. If $p \le p^*$, then $G(q) > 0$, $G'(0) > 0$, and $q^* = 0$ is not the ESS. If $p > p^*$, then $G(p) < 0$, $G'(1-\eta_2) < 0$, and $q^* = 1-\eta_2$ is the ESS.

When $p > \eta_2$ and $q > 1-\eta_2$, $G(q) = 0$, $G'(q) = 0$.

(3) The Stability of Evolutionary Game as a Whole. When $\eta_1 < 1-((\lambda+\lambda_1-\lambda_2)/\lambda_1)\eta_2 < 1-\eta_2$ and $\eta_2 < \lambda_1/(\lambda+\lambda_1-\lambda_2)$, ESS is $p^* = 1-((L+\lambda-H)/(\lambda-C))(1-\eta_2)$, $q^* = (\lambda+\eta_1\lambda_1-\lambda_2)/(\lambda+\lambda_1-\lambda_2)$.

With the exception of above situations, there does not exist an ESS as a whole. Actor prejudges the opponent's strategy using its experience and makes the optimum reaction. This learning and evolution process will be dynamic and would not reach a stable state, so the ESS would not exist for the wrong learning paths.

2.4. Results and Discussion. (1) Based on expected theory, the ESS is $\tilde{p}^* = (H-C-L)/(\lambda-C)$, $\tilde{q}^* = (\lambda-\lambda_2)/(\lambda+\lambda_1-\lambda_2)$. When $\eta_1 < 1-((\lambda+\lambda_1-\lambda_2)/\lambda_1)\eta_2 < 1-\eta_2$ and $\eta_2 < \lambda_1/(\lambda+\lambda_1-\lambda_2)$, that is, the risk attitudes of airport and nonprofit organizations are confided by parameters, we have $p^* \ge \tilde{p}^*$ and $q^* \ge \tilde{q}^*$, meaning that the risk attitudes affect the evolutionary game. We can conclude that they may not reach ESS, and if the risk attitudes of airport and emergency organizations meet the constraint conditions, the evolution can reach ESS. If the risk attitude of airport and the risk attitude of emergency organizations are higher simultaneously, the ESS is more likely to be the strategies (reputation cooperation and altruism behavior), but the strategies (reputation cooperation and altruism behavior)

could not be reached completely. This can explain why it is reasonable in practice that reputation cooperation can coexist with bidding competition and altruism behaviors can coexist with selfish behaviors.

(2) The evolutionary strategy is affected not only by risk-averse attitude of itself but also by the risk-averse attitude of the game rival. From the expression of ESS, we can see that the airport's selection for reputation cooperation is more likely with the greater risk-averse attitude of emergency organizations and the emergency organizations' selection for altruism behaviors is more likely with the greater risk-averse attitude of airport. The explanations are as follows. (1) The replicator dynamics equation describes the logical relationship of mechanisms and preferences. Meanwhile, the adoptive fitness of mechanism is affected by the proportion distribution of preference and the adoptive fitness of preference is affected by the probability distribution of mechanism. (2) The reputation cooperation mechanism means the airport prefers to share value and codetermination [33]. If emergency organizations have higher risk-averse attitudes, the reputation cooperation mechanism is selected by airport based on the incentive theory to meet emergency organizations' psychological requirement. (3) The evolution of preference is driven by loyalty, social value, responsibility and power, and influence. If the airport has higher risk-averse attitude, the emergency organizations will be more inclined to altruism behavior to realize their intrinsic value and social responsibility. On the other hand, emergency organizations will deem that the airport has more strict supervise with higher risk-averse attitude, and they will prefer altruism behaviors to avoid penalties.

(3) From the whole ESS equation, if the supervised and managerial cost of airport is higher, the ESS is more easy to reach just for the enlarged initial feasible region of risk-averse degree. At the same time, q^* is smaller, which means the proportion of altruism is less. The possible reason is that the altruism prefers loyalty. The higher supervised and managerial cost mean stronger effort in supervising the nonprofit organization. When the speculative extra payoff λ is higher, the ESS is impossibly reach that p^* is smaller and q^* is larger. The possible reason is that the payoff of altruism is higher than selfish individual when airport adopts the bidding competition mechanism. Airport is more likely to adopt the bidding competition mechanism when the speculative extra payoff is higher.

(4) The evolutionary state strategies are affected by parameters of payoff and risk-averse attitude. For airport, it can reveal risk-averse attitude of itself and decrease supervised and managerial cost by increasing professional management to affect other emergency organizations' behaviors. For nonprofit emergency organizations, they can make use of their professional rescue skill and more free behavior mechanism to create more chance to participate in the emergency decisions, which will speed the evolution process of codetermination. However, for government, it can change payoffs of both sides of the evolutionary game to affect the evolutionary process.

2.5. Numerical Analysis. We assume the parameters equal to value as in Table 2.

Table 2: Parameters values.

H	d	L	λ	λ_1	λ_2	C
10	2	8	3	1	3	1

Based on the above theory analysis, we can get the final decisions from both participators with different risk-averse attitudes like Table 3. In Table 3, the first column represents the values of η_1, the first line represents the values of η_2, and the values in middle represent the ESS (p^*, q^*).

From Table 3, we can see that the results of the numerical analysis are consistent with the above results of theory analysis (1), (2), (3), and (4) in Section 2.4. Different from our intuition, the risk-averse attitude of one participator affects the other participator's decision.

3. Evolutionary Game with Governmental Intervention

3.1. Evolutionary Game Model. If we cannot get the equilibrium or $q^* \ll 0.5$, the government should subsidize the altruism for the high coordination degree. Because the reputation cooperation mechanism faces a higher risk for a selfish individual, government should subsidize airports who adopt reputation cooperation mechanism [34–36]. The combination of strategies is presented in Table 4.

When $\lambda - \lambda_2 < S < \lambda_1 < \lambda_2 < \lambda$ and $0 \le S < L + \lambda - H$, if S feasible zone is nonnull, the unique ESS is $p^* = 1 - (1 - \eta_2)(L + \lambda - H - S)/(\lambda - C), q^* = (\lambda + \eta_1\lambda_1 - \lambda_2 + (1 - \eta_1)S)/(\lambda + \lambda_1 - \lambda_2)$. Otherwise, the evolutionary game would not reach the evolutionary stability.

The improvement of governmental subsidy increases the probability of reputation cooperation mechanism and the proportion of altruistic preference. However, the evolutionary game cannot reach the stable state $p^* = 1, q^* = 1$ unless $\eta_1 = 1, \eta_2 = 1$. This result certainly explains that it is reasonable to adopt both reputation cooperation and bidding competition mechanisms for airports. Meanwhile, it is reasonable for nonprofit organization preferring the combination of altruism and selfishness. The risk attitude and governmental intervention affect the participators' strategy. This can help managers to make decisions.

From the above analysis, we can see that government can change payoffs of both sides of the evolutionary game to affect the evolutionary process. And the decisions of governmental subsidy need to meet some constraint conditions, which require the government to make decisions seriously; otherwise this will lead to negative effectiveness.

3.2. Numerical Analysis. We continue using the values in Section 2.5, and we can get the ESS as Table 5. From Table 5, we can see that when S is larger, p^* is larger and q^* is larger; that is, the airport prefers selecting reputation cooperation mechanism and nonprofit organizations prefer altruism behaviors, which leads to a more efficient and harmonious result.

Table 3: The ESS with different risk-averse attitudes.

(p^*, q^*)	0.1	0.2	0.3	0.4	0.5	0.6	0.7	0.8	0.9
0.1	0.55, 0.1	0.6, 0.1	0.65, 0.1	0.7, 0.1	0.75, 0.1	0.8, 0.1	0.85, 0.1	0.9, 0.1	0.95, 0.1
0.2	0.55, 0.2	0.6, 0.2	0.65, 0.2	0.7, 0.2	0.75, 0.2	0.8, 0.2	0.85, 0.2	0.9, 0.2	Null
0.3	0.55, 0.3	0.6, 0.3	0.65, 0.3	0.7, 0.3	0.75, 0.3	0.8, 0.3	0.85, 0.3	Null	Null
0.4	0.55, 0.4	0.6, 0.4	0.65, 0.4	0.7, 0.4	0.75, 0.4	0.8, 0.4	Null	Null	Null
0.5	0.55, 0.5	0.6, 0.5	0.65, 0.5	0.7, 0.5	0.75, 0.5	Null	Null	Null	Null
0.6	0.55, 0.6	0.6, 0.6	0.65, 0.6	0.7, 0.6	Null	Null	Null	Null	Null
0.7	0.55, 0.7	0.6, 0.7	0.65, 0.7	Null	Null	Null	Null	Null	Null
0.8	0.55, 0.8	0.6, 0.8	Null	Null	Null	Null	Null	Null	Null
0.9	0.55, 0.9	Null	Null	Null	Null	Null	Null	Null	Null

Table 4: Coevolution of cooperation mechanisms and preferences with government.

(Airport, nonprofit organization)	Altruistic preference (q)	Selfish preference ($1 - q$)
Reputation cooperation (p)	$(H - d + S, H + S)$	$(L - d - \lambda + S, L + \lambda)$
Bidding competition ($1 - p$)	$(H - d - \lambda_1, H - C + S)$	$(L - d - \lambda_2, L)$

Table 5: The ESS with different risk-averse attitudes.

(a) When $S = 0.2$

(p^*, q^*)	0.2	0.5	0.8
0.2	0.68, 0.36	0.8, 0.36	0.92, 0.36
0.5	0.68, 0.6	0.8, 0.6	Null
0.8	0.68, 0.84	Null	Null

(b) When $S = 0.5$

(p^*, q^*)	0.2	0.5	0.8
0.2	0.8, 0.6	0.875, 0.6	0.95, 0.6
0.5	0.8, 0.75	0.875, 0.75	Null
0.8	0.8, 0.9	Null	Null

(c) When $S = 0.8$

(p^*, q^*)	0.2	0.5	0.8
0.2	0.92, 0.84	0.95, 0.84	0.98, 0.84
0.5	0.92, 0.9	0.95, 0.9	Null
0.8	0.92, 0.96	Null	Null

3.3. Advises for Actors. Currently, in Chinese aviation joint emergency response, airport emergency management institution generally takes a leader role. It makes emergency plans and arranges work for joint nonprofit organizations. The government supervises and supports the emergency management. Nash equilibrium represents the Pareto state and harmonious coordination represents the better rescue management.

Firstly, the government should evaluate the risk-averse degree for participators. According to the result, it may determine the quantity of subsidy to attain the Pareto state. Meanwhile, in order to quickly obtain the expected evolutionary result, government can make rules. For example, some nonprofit organizations directly participate in the joint emergency response system without bidding to restrict inefficient self-learning. On the other hand, government should punish the speculative extra payoff of selfishness when airport adopts the reputation cooperation mechanism. Secondly, the airport emergency management institution should decrease supervised and managerial cost under bidding competition mechanism by using managerial skills and methods. Moreover, airport can sign an agreement with joint organizations to increase the risk-averse degree of them. For example, they can decrease punishment for bad coordination or increase their responsibility and social role. Thirdly, nonprofit organizations can make use of their special superiority and mechanism advantage. They can promote their reputation, power, and right to speak. Meanwhile, they also can decrease the speculative extra payoff and increase the probability of reputation cooperation mechanism. All above suggestions can help realize the Pareto state and harmonious coordination.

4. Conclusions

We study effects of risk-averse degree of participators in aviation joint emergency response considering the coevolution of cooperation mechanisms and individual preferences between airport and nonprofit organization. We put forward two mechanisms to select the joint nonprofit organization on the current aviation joint emergency mechanism in China and two preferences. We build replicator dynamics equations taking risk aversion attitude into account. Moreover, we introduce the factor of government. The results show that the larger the risk-averse degree is, the larger the probabilities of reputation cooperation mechanism and altruistic preference are. It can make the emergency environment more harmonious. Hence, government should make rules or subside actors for guiding and speeding up the harmonious evolution.

In theory aspect, this paper develops the evolutionary game between airport and nonprofit organization in aviation joint emergency response system. Meanwhile, it enlarges the research applications between public or private sector and nonprofit organizations. Moreover, we also introduce risk attitude factor to the evolutionary process. According

to it, we compute the replicator dynamics equations by the conditional value-at-risk (CVaR) and study the effect of government intervention on evolution. It enriches relative researches on evolution of joint mechanism and emergency management. In practice aspect, this work can help actors to make decisions more accurately and efficiently. Moreover, it can instruct leaders to speed up evolutionary process for realizing Pareto state. In order to achieve the better management effect about disaster emergencies, we should pay more attention to risk attitudes and make sense of the effects on joint emergency response mechanisms.

However, in real environment, much information is uncertainty [37–40]. According to this situation, the randomness of effect scale in an aviation accident means the demand for coordination is stochastic. So, the random demand will be studied in the future. In this study, we consider risk-averse attitude for both actors. However, it is not difficult to image that the actors may be risk-taking. The risk attitude is related with accident probability. We will further research these problems in the future.

Competing Interests

The authors declare that they have no competing interests.

Acknowledgments

This work is partially supported by Grants from the National Science Foundation of China (NSFC nos. U1333115, 71373188, 90924024, 91224001, and 81372804), the Fundamental Research Funds for the Central Universities (no. 1101012), Post-1970 Young Scholars in Humanities and Social Sciences from Wuhan University, Training Program of High Level International Journal Articles in Humanities and Social Sciences from Wuhan University, the Huibei Province Science Foundation (2011CDB191), and the Central University Basic Science Research Fund (2012QN188).

References

[1] Y.-G. Feng and J. Wu, "Risk-averse newsvendor game model under emergency situations," *System Engineering Theory and Practice*, vol. 35, no. 3, pp. 598–607, 2015.

[2] X.-Y. Zhu and F. Luo, "Study on mechanism optimization of joint emergency response to aviation calamities in China," *China Safety Science Journal*, vol. 17, no. 6, pp. 5–11, 2007.

[3] T. Debbie, "Hazmat clean-up firm opens regional response center in North Salt Lake," *Enterprise/Salt Lake City*, vol. 36, no. 4, pp. 1–6, 2006.

[4] W. U. De-Sheng and L. I. Wei-An, "Interaction between formal contracts and informal contracts under random matching game," *Journal of Management Science in China*, vol. 13, no. 12, pp. 76–85, 2010.

[5] A. Abbasi, "Link formation pattern during emergency response network dynamics," *Natural Hazards*, vol. 71, no. 3, pp. 1957–1969, 2014.

[6] J. M. Smith and G. R. Price, "The logic of animal conflict," *Nature*, vol. 246, no. 5427, pp. 15–18, 1973.

[7] M. A. Nowak, A. Sasaki, C. Taylor, and D. Fudenherg, "Emergence of cooperation and evolutionary stability in finite populations," *Nature*, vol. 428, no. 6983, pp. 646–650, 2004.

[8] S. Faraj and Y. Xiao, "Coordination in fast-response organizations," *Management Science*, vol. 52, no. 8, pp. 1155–1169, 2006.

[9] N. Kapucu, "Public-nonprofit partnerships for collective action in dynamic contexts of emergencies," *Public Administration*, vol. 84, no. 1, pp. 205–220, 2006.

[10] Ö. Gürerk, B. Irlenbusch, and B. Rockenbach, "On cooperation in open communities," *Journal of Public Economics*, vol. 120, pp. 220–230, 2014.

[11] M. Perc and A. Szolnoki, "Co-evolutionary games—a mini review," *BioSystems*, vol. 99, no. 2, pp. 109–125, 2010.

[12] G. Szabó and A. Szolnoki, "Selfishness, fraternity, and other-regarding preference in spatial evolutionary games," *Journal of Theoretical Biology*, vol. 299, pp. 81–87, 2012.

[13] P. Buesser, J. Peña, E. Pestelacci, and M. Tomassini, "The influence of tie strength on evolutionary games on networks: an empirical investigation," *Physica A: Statistical Mechanics and Its Applications*, vol. 390, no. 23-24, pp. 4502–4513, 2011.

[14] H. Carlsen, L. Johansson, P. Wikman-Svahn, and K. H. Dreborg, "Co-evolutionary scenarios for creative prototyping of future robot systems for civil protection," *Technological Forecasting and Social Change*, vol. 84, pp. 93–100, 2014.

[15] L. Dehai and Y. Lijuan, "Equilibrium evolutionary analysis about city demolition emergency based scenario analysis," *Management Review*, vol. 24, no. 5, pp. 154–159, 2012.

[16] G. Li, Y.-G. Gu, and Z.-H. Song, "Evolution of cooperation on heterogeneous supply networks," *International Journal of Production Research*, vol. 51, no. 13, pp. 3894–3902, 2013.

[17] A. Abbasi, C. Owen, L. Hossain, and J. Hamra, "Social connectedness and adaptive team coordination during fire events," *Fire Safety Journal*, vol. 59, pp. 30–36, 2013.

[18] T. R. Roekaflller and S. Uryasev, "Optimization of conditional value-at-risk," *Journal of Risk*, vol. 2, no. 3, pp. 21–41, 2000.

[19] R. T. Rockafellar and S. Uryasev, "Conditional value-at-risk for general loss distributions," *Journal of Banking and Finance*, vol. 26, no. 7, pp. 1443–1471, 2002.

[20] W. Jammernegg and P. Kischka, "Risk-averse and risk-taking newsvendors: a conditional expected value approach," *Review of Managerial Science*, vol. 1, no. 1, pp. 93–110, 2007.

[21] W. Jammernegg and P. Kischka, "Risk preferences and robust inventory decisions," *International Journal of Production Economics*, vol. 118, no. 1, pp. 269–274, 2009.

[22] W. Jammernegg and P. Kischka, "Risk preferences of a newsvendor with service and loss constraints," *International Journal of Production Economics*, vol. 143, no. 2, pp. 410–415, 2013.

[23] F. Wex, G. Schryen, S. Feuerriegel, and D. Neumann, "Emergency response in natural disaster management: allocation and scheduling of rescue units," *European Journal of Operational Research*, vol. 235, no. 3, pp. 697–708, 2014.

[24] R. Abounacer, M. Rekik, and J. Renaud, "An exact solution approach for multi-objective location-transportation problem for disaster response," *Computers and Operations Research*, vol. 41, no. 1, pp. 83–93, 2014.

[25] A. Bozorgi-Amiri, M. S. Jabalameli, and S. M. Mirzapour Al-e-Hashem, "A multi-objective robust stochastic programming model for disaster relief logistics under uncertainty," *OR Spectrum*, vol. 35, no. 4, pp. 905–933, 2013.

[26] X. Chen, Y. Zhang, T.-Z. Huang, and M. Perc, "Solving the collective-risk social dilemma with risky assets in well-mixed

and structured populations," *Physical Review E*, vol. 90, no. 5, Article ID 052823, 2014.

[27] X. Chen, A. Szolnoki, and M. Perc, "Averting group failures in collective-risk social dilemmas," *EPL*, vol. 99, pp. 1–6, 2012.

[28] C.-Y. Xia, S. M. Meloni, M. Perc, and Y. Moreno, "Dynamic instability of cooperation due to diverse activity patterns in evolutionary social dilemmas," *Europhysics Letters*, vol. 109, no. 5, Article ID 58002, pp. 1–6, 2015.

[29] H. Herlin and A. Pazirandeh, "Nonprofit organizations shaping the market of supplies," *International Journal of Production Economics*, vol. 139, no. 2, pp. 411–421, 2012.

[30] I. M. Nolte, E. C. Martin, and S. Boenigk, "Cross-sectoral coordination of disaster relief," *Public Management Review*, vol. 14, no. 6, pp. 707–730, 2012.

[31] W. L. Waugh Jr. and G. Straib, "Collaboration and leadership for effective emergency management," *Public Administration Review*, vol. 66, no. 1, pp. 131–140, 2006.

[32] J. M. Brinkerhoff, "Government-nonprofit partnership: a defining framework," *Public Administration and Development*, vol. 22, no. 1, pp. 19–30, 2002.

[33] K. Huang, "Co-evolution between individual preference and mechanisms: a new approach," *Research on institutional Economics*, no. 1, pp. 1–27, 2014.

[34] Y.-L. Liu, X.-X. Mei, and F. Sun, "Evolution path on the change of enterprises' international operational pattern based evolutionary game," *Xitong Gongcheng Lilun yu Shijian/System Engineering Theory and Practice*, vol. 35, no. 3, pp. 763–770, 2015.

[35] Y. Xu, B. Hu, and R. Qian, "Analysis on stability of strategic alliances based on stochastic evolutionary game including simulations," *System Engineering Theory and Practice*, vol. 31, no. 5, pp. 920–926, 2011.

[36] M. A. Nowak, "Five rules for the evolution of cooperation," *Science*, vol. 314, no. 5805, pp. 1560–1563, 2006.

[37] W. Pan, S. Liu, Y. Guo, and F. Wang, "Fuzzy multi-objective model for supplier selection considering multiple products in low carbon supply chain," *Environmental Engineering and Management Journal*, vol. 14, no. 8, 2015.

[38] W. Pan, F. Wang, Y. Guo, and S. Liu, "A fuzzy multiobjective model for supplier selection under considering stochastic demand in a supply chain," *Mathematical Problems in Engineering*, vol. 2015, Article ID 174585, 8 pages, 2015.

[39] W. Pan, L. Yu, S. Wang, and X. Wang, "A fuzzy multi-objective model for provider selection in data communication services with different QoS levels," *International Journal of Production Economics*, vol. 147, pp. 689–696, 2014.

[40] W. Pan, X. Wang, Y.-G. Zhong et al., "A fuzzy multi-objective model for capacity allocation and pricing policy of provider in data communication service with different QoS levels," *International Journal of Systems Science*, vol. 43, no. 6, pp. 1054–1063, 2012.